Peptide Deamination

Thesis

PEPTIDE DEAMINATION

A thesis presented by

NEILL HUGH CARMAN

in partial fulfilment of the requirements

for the degree of

DOCTOR OF PHILOSOPHY

of the

OPEN UNIVERSITY

Date of submission: 12 June 1992
Date of award: 26 October 1992

Department of Chemistry
The Open University

May 1992

ProQuest LLC.
789 East Eisenhower Parkway
P.O. Box 1346
Ann Arbor, MI 48106 – 1346

for my

Mum and Dad.

Thanks.

ACKNOWLEDGEMENTS

I would like to express my gratitude to my supervisor Professor Brian Challis for his encouragement and guidance throughout the course of this work. I would also like to thank Dr. Jim Iley for many stimulating conversations, his active interest in the work and for carrying out the molecular modelling experiments for me. Thanks are also due to Dr. Judy Challis for supplying the mass spectra and her expertise and help in interpreting them and elucidating the structures of many of the reaction products.

I am grateful to Derek Hillbeck of Hoechst UK who carried out the accurate mass measurements on the diazo compounds. I would also like to thank the technical staff of The Open University for all their help, in particular Gordon Howell, who obtained the nmr spectra and a special thanks to Graham Jeffs for all his helpful advice on chromatography. Many thanks too, to Sue Hegarty for typing this thesis.

I must also thank my colleagues, in particular Pam Bradley, Steve Lowes and Graham Ruecroft for providing some light relief from research.

Finally, a special thanks to Deirdre, not just for all her help during the preparation of this thesis, but, also for the support and understanding she showed during the three years research preceding it.

I am grateful to the SERC for a grant allowing me to carry out this research.

ABBREVIATIONS

Ac	Acetyl
AcOH	Acetic acid
Asn	Asparagine
AsnOMe	Asparagine methyl ester
Asp	Aspartic acid
Aspartame	Aspartylphenylalanine methyl ester
CI	Chemical ionisation
COSY	Correlation spectroscopy
CBZ	Carbobenzyloxy
DCC	Dicyclohexyl carbodiimide
DMF	N,N-Dimethylformamide
DMSO	Dimethylsulphoxide
EI	Electron impact
equiv	Equivalents
FAB	Fast atom bombardment
FT	Fourier transform
glc	Gas liquid chomatography
glc-ms	Gas liquid chomatography-mass spectrometry
Gln	Glutamine
Gly	Glycine
GlyOEt	Glycine ethyl ester
hplc	High performance liquid chromatography
ir	Infra-red
Leu	Leucine
M	$moldm^{-3}$
MeOH	Methanol
mp	Melting point

ms	Mass spectrometry
m/z	Mass/charge ratio
N_2AsnOMe	Methyl-2-diazo-3-carbamoyl propanoate
nmr	Nuclear magnetic resonance
PA	Peak area
Phe	Phenylalanine
TEGDE	Tetraethyleneglycol diethyl ether
tlc	Thin layer chromatography
TMS	Tetramethylsilane
uv	Ultraviolet
w/v	Weight/volume
w/w	Weight/weight
Z	Carbobenzyloxy

Glossary of Mechanistic Terms

A_1	Acid catalysed, unimolecular, bond fission.
A_2	Acid catalysed, bimolecular, bond fission.
$A_{Ac}1$	Acid catalysed, unimolecular, acyl oxygen bond fission.
$A_{Ac}2$	Acid catalysed, bimolecular, acyl oxygen bond fission.
A S_E2	Acid catalysed, bimolecular, electrophilic substitution.
$B_{Al}1$	Base catalysed, unimolecular, alkyl oxygen bond fission.
$B_{Al}2$	Base catalysed, bimolecular, alkyl oxygen bond fission.
$B_{Ac}2$	Base catalysed, bimolecular, acyl oxygen bond fission.

Abstract

The nitrosation of the terminal amino group of peptides and amino acids, the synthesis and properties of diazoamino acids and diazopeptides and their decomposition products, particularly products resulting from intramolecular cyclisations are reviewed and discussed in relation to human cancer. The reactivity of *N*-(1'-methoxycarbonyl-2'-phenyl)ethyloxetan-2-one-4-carboxamide (1) formed from the deamination of L-aspartyl-L-phenylalanine methyl ester (aspartame) is examined from a mechanistic stand-point to determine its potential as an alkylating agent *in-vivo*. The stability of (1) in aqueous solution is investigated. Three hydrolysis mechanisms are observed for the β-lactone ring at differing pH values. Below pH2 the $A_{AC}2$ mechanism dominates and above pH7 the $B_{AC}2$ mechanism is observed. In the physiological pH range (2-7) hydrolysis is independent of pH occuring via the $B_{A1}2$ mechanism and (1) has a half life of 13.5h at 37°C.

The reactivity of (1) to nucleophiles other than water is studied. Alkylation and acylation are both observed depending upon the nucleophile used. Attempts to rationalise this dual reactivity which is also observed for β-butyrolactone and β-propiolactone, two known carcinogens, are made. The implications of the nitrosation of aspartame *in vivo* are discussed briefly.

The formation of cyclic products from the nitrosation of asparagine and glutamine derivatives is described. In aqueous solution intra-molecular cyclisation is observed, occurring on the carboxamide O-atom. The synthesis of new diazocompounds derived from glutamine, asparagine and glutaminyl and asparaginyl dipeptides are described. The stabilities of these compounds in aqueous media are examined and they are found to decompose via an $A\text{-}S_E2$ pathway. Further, they are decomposed thermally in an organic solvent and the formation of a variety of cyclic products is observed. Mechanisms are proposed. Intramolecular cyclisation on the carboxamide side chain

N-atom is not observed. The possible implications of the nitrosation of asparaginyl and glutaminyl compounds are briefly discussed.

CONTENTS

CHAPTER 1 HISTORICAL REVIEW.

1 HISTORICAL REVIEW

1.1 Introduction

There has been much interest in nitrosation as a causal factor in human cancer since many N-nitrosocompounds are carcinogenic.[1,2] Early research focussed on exposure to exogenous N-nitrosocompounds in the workplace and consumer products but recently this has shifted to endogenous formation in the respiratory tract by inhaled nitrogen oxides and in the stomach by ingested nitrite.[2,3]

The stomach, at pH 1-4 and 37°C, provides favourable conditions for nitrosation reactions. In healthy individuals, fasting gastric nitrite concentrations of 5μM[4] are typical, resulting predominantly from bacterial reduction of both ingested and secreted nitrate in the mouth. (It has been estimated that ca 20% of ingested nitrate is ultimately reduced to nitrite in the oral cavity.[5]) However, concentrations in excess of 0.2mM have been found in association with increased pH (6.5-9.0) for patients with clinical conditions such as pernicious anaemia and gastrectomy.[6] This relates to an overgrowth of nitro-reductase bacteria in the high pH stomach.[6] A higher than average level of N-nitrosamines has also been found in the gastric juice of some of these patients.[6]

Thus far, most investigations have been directed towards the *in vivo* nitrosation of secondary amines, amides and urea substrates where the corresponding N-nitroso derivatives have known carcinogenic properties.[1,2] Other studies have shown that sequential ingestion of proline and nitrate leads to the formation of N-nitroso-proline in humans,[7,8,9] although the validity of this procedure to assess endogenous nitrosation reactions has been questioned.[7] The risks posed by the endogenous nitrosation of secondary amines have been questioned on the basis of intake, rate of nitrosation and carcinogenicity and are considered to be negligible, because of the low dietary intake of secondary amines.[10] These assessments, however, also concluded that the endogenous nitrosation of amino acids and peptides posed a greater risk because of

their availability in the diet. Daily intakes of peptides and proteins are of the order of 100-200g together with approximately 1g of amino acids.[10,11]

Ignoring reactive side chains, nitrosation of peptides can occur on either the terminal primary amino group or the peptide N-atom giving the diazo- and N-nitrosopeptides respectively and both reactions have been observed.[12] Nitrosopeptides have been synthesised and shown to be direct-acting mutagens.[13,14] Between pH 1 and 8 at 37°C they have half lives of the order of a few hours, decomposing *via* a deamination pathway to form diazocompounds[12] (Figure 1.1). Diazopeptides are acid labile, decomposing rapidly at normal gastric pH. For this reason, their endogenous

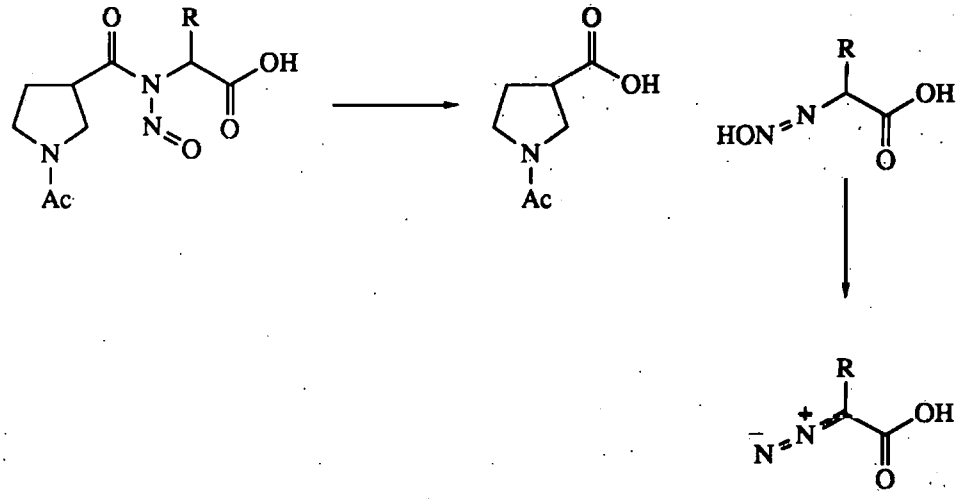

Figure 1.1 Decomposition of N-nitrosopeptides

formation in the stomach may not be biologically significant, other than as a detoxifying process. They have been shown, however, to be carcinogens[15,16] and are relatively stable at blood pH (ca pH 7) and 37°C . The following survey covers various aspects of peptide and amino acid deamination including potential cytotoxic implications .

1.2 Deamination of primary amines

The nitrosation, diazotisation and deamination of aliphatic and aromatic amines can be considered as stages on a common reaction path as shown in Figure 1.2.

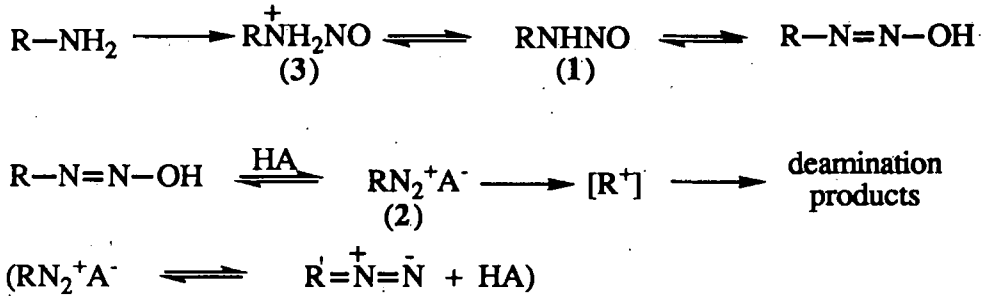

Figure 1.2 Nitrosation, diazotisation and deamination of amines.

With secondary amines, the reaction stops at the N-nitrosamine stage (1); with primary aromatic amines, stable diazonium ions (2) are formed; whilst with primary aliphatic amines, however, the diazonium ion is unstable and subsequent reactions ensue to give a variety of deamination products.

1.2.1 Amine nitrosation

Several generalisations apply to the kinetics of acid-catalysed amine nitrosation and deamination. Firstly, either generation of the nitrosating agent, or its reaction with the amine is rate determining. Secondly, only the unprotonated amine is reactive. Thirdly, nitrous acid itself is unreactive but in aqueous solution it is in equilibrium with a number of species (NOX) which are the effective nitrosating agents (eg. X=NO_2, (dinitrogen trioxide), Cl, (nitrosyl chloride), H_2O, (nitrous acidium ion)). The mechanisms involved have been extensively reviewed[17,18,19,20] and only a brief summary of those relevant to aliphatic amines are given here.

1.2.1.1 Nitrosation at low acidity (pH>2)

A pH of less than 5 is required to generate the various nitrosating agents, but in the region of pH 2-5 the rate of nitrosation is often independent of the amine concentration, obeying equation 1.1. The rate determining step involves the formation of dinitrogen

$$\text{Rate} = k_0 [HNO_2]^2 \qquad \cdots(1.1)$$

trioxide (nitrous anhydride) from two moles of HNO_2, which subsequently reacts rapidly, with the free amine to generate the nitroso ammonium salt (3).

1.2.1.2 Nitrosation at intermediate acidities (pH 1-2)

Increasing the acidity results in a reduction in the concentration of free amine (RNH_2). Reaction of the nitrosating agent with the amine then becomes rate-limiting, and a first-order dependence on $[RNH_2]$ is observed (equation 1.2). Again dinitrogen trioxide has

$$\text{Rate} = k_0 [RNH_2][HNO_2]^2 \quad \cdots(1.2)$$

been implicated as the nitrosating agent. Further increase of acidity invokes a new mechanism involving the nitrous acidium ion (H_2ONO^+), but this process is unimportant for aliphatic amines which are extensively protonated and therefore unreactive at lower pH.

1.2.1.3 Catalysis

Catalysis by halide and thiocyanate ions relates to an increased concentration of NO^+ carriers. The NOX reagents (X=Cl, Br, I, SCN) are usually more reactive than N_2O_3 and rates are therefore faster. The kinetics show a first order dependence on nitrous acid and obey equation 1.3. The dependence upon acid concentration arises from the

$$\text{Rate} = k_0 [RNH_2][H^+][HNO_2][X^-] \quad \ldots(1.3)$$

acid catalysed formation of NOX (Equation 1.4).Nitrosation by NOCl and NOSCN

$$H^+ + HNO_2 + X^- \rightleftharpoons NOX + H_2O \quad \ldots(1.4)$$

will be important reactions in the gastric environment.

1.2.2 The diazonium ion

Except under very special circumstances, reviewed by Bott,[21] aliphatic diazonium ions are too unstable to be isolable. The unprotonated form, however, is well-known and

many aliphatic diazo compounds have been prepared and isolated. The chemistry of diazo compounds has attracted much interest and several excellent reviews exist.[22,23,24]

Several procedures, other than the diazotisation of amines, have been reported for the synthesis of diazoalkanes. These include the Forster reaction[25] (Equation 1.5), oxidation of hydrazones[26] (Equation 1.6), the Bamford-Stevens reaction[27] (Equation 1.7) and deacylation of N-nitrosocarboxamide[28] (Equation 1.8).

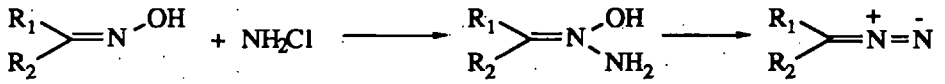
...(1.5)

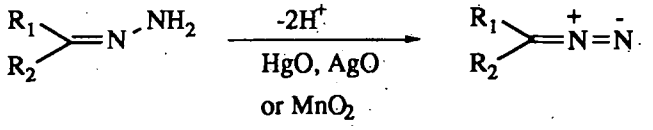
...(1.6)

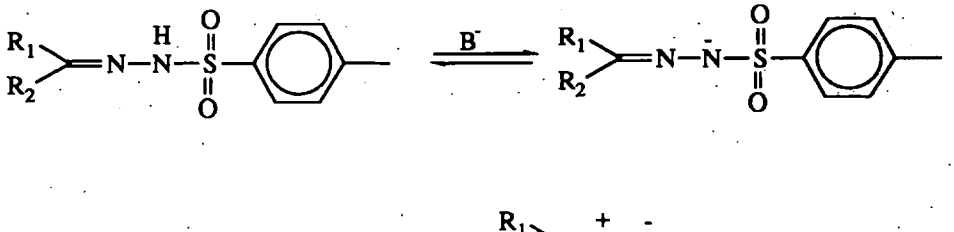
...(1.7)

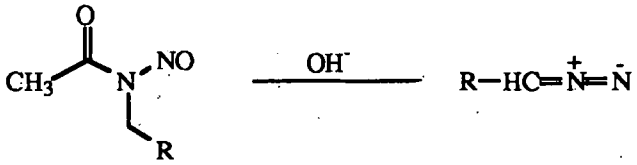
...(1.8)

In general aliphatic diazo compounds have a highly characteristic band in the infrared spectrum at 2100cm^{-1} corresponding to the C=$\overset{+}{N}$=$\overset{-}{N}$ stretching vibration, as well as a strong absorbance in the uv region corresponding to the $\pi \rightarrow \pi^*$ transition. A much weaker absorbance, due to the $n \rightarrow \pi^*$ transition, accounts for their colour.

The diazo group can exist as a resonance hybrid between the three canonical forms (4)-(6) shown in Figure 1.3. The structures (4) and (5) have been confirmed by infra-red spectroscopy.[29] The three hybrid forms account for all the chemistry of diazo

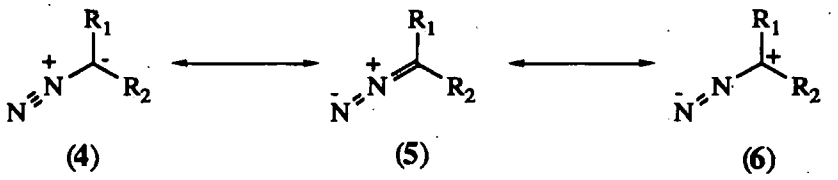

(4) (5) (6)

Figure 1.3 Resonance hybrids of diazo compounds.

compounds. Under appropriate conditions diazoalkanes can behave as acids, bases, electrophiles, nucleophiles, 1,3-dipoles and carbene sources.

Diazoalkanes are generally stable in base but undergo rapid deamination in acid solutions giving a wide number of products (*vide infra*) with either proton transfer, or loss of nitrogen being rate-limiting. Because nitrogen is such a good leaving group, diazoalkanes are powerful, non-discriminatory alkylating agents and should also, therefore, be considered as potentially carcinogenic.

1.2.3 Deamination products

The deamination of aliphatic amines in aqueous media gives a variety of products, derived from substitution, elimination and rearrangement reactions. The mechanism of deamination has been debated at some length. Many aspects of deamination suggest that the reaction proceeds with a unimolecular cleavage of the C-N_2^+ bond (ie. S_N1 reaction). For example, the deamination products of n-butylamine,[30] shown in Figure 1.4, are consistent with the formation of a carbonium ion intermediate (7) which can subsequently react with a nucleophile (8) and (9), rearrange (10) or eliminate a proton (11). Further, racemisation increases with carbonium ion stability and substitution of [1,^{2}H] n-butylamine proceeds with 69% inversion of stereochemistry whereas for 2-aminobutane only 28% inversion is observed.[31] These observations are consistent with an S_N1 type reaction where one side of the carbonium ion is partly shielded by the

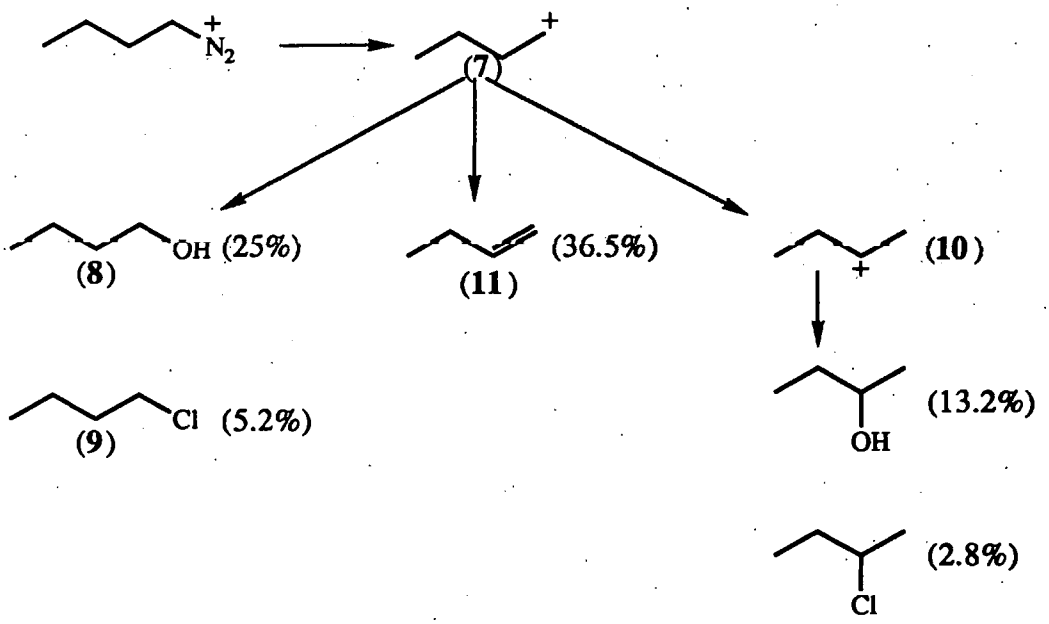

Figure 1.4 Deamination of n-butylamine in aqueous HCl

departing nitrogen.

In solvolytic displacements, known to proceed *via* an S_N1 pathway, however, no rearrangements were detected.[31] Also, the composition of butenes formed from the deamination of 1- and 2- aminobutane did not correspond to those found in the solvolysis of 2-tosylbutane.[31] (Table 1.1). The ratio of butenes in the deamination of butylamine, can be rationalised in terms of ground state control. The products are determined by the relative populations of the different conformations (12), (13) and (14) of the diazonium ion, 2-diazobutane. Only conformations (12) and (13) can

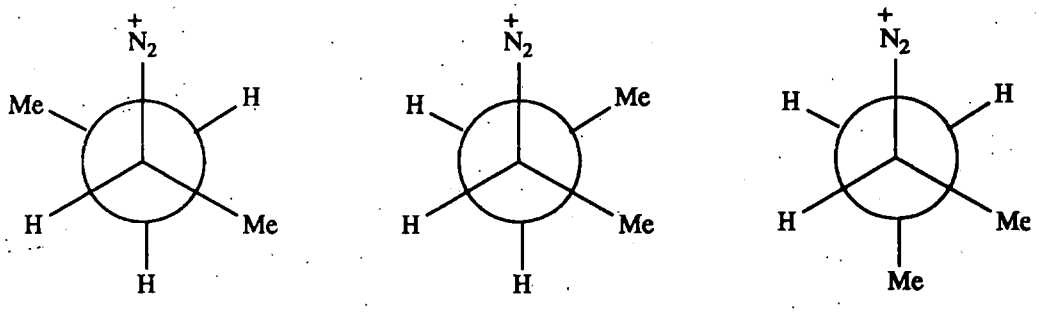

(12) **(13)** **(14)**

undergo anti-periplanar elimination. Conformation (13) will be the least populated hence the major product is the *trans* but-2-ene arising from (12).

Table 1.1 Composition of butenes from solvolysis and amine nitrous acid reactions.[31]

Reaction	Butene composition %			
	1-	2-cis	2-trans	cis/trans ratio
s-BuOTs + AcOH[a]	10.3	43.2	46.5	1.1
s-$BuNH_2$ + HNO_2[b]	25	19	56	2.9
n-$BuNH_2$ + HNO_2[b]	71	9	20	2.2
$Butene_{(g)}$ equilib	2	23	75	3.2

[a] 70°C

[b] room temp

In a study of conformation control of the migrating group in the deamination of 3-phenyl-2-butylamine, Cram and McGarity[32] concluded that the half lives of the carbonium ions, generated by deamination, must be less than the half life of rotation about the carbon-carbon bond. Since this is not usually observed for carbonium ions generated in solvolytic reactions, it was concluded that the decomposition of a diazonium ion to form a carbocation had only a small activation energy. Therefore, the transition state occured early on the reaction coordinate and was reactant-like, hence the energy differences between competing reactions was greatly reduced and a variety of products obtained. Semenow *et al.* observed that allylic deaminations in acetic acid involved less rearrangement than solvolyses of the corresponding halides, and concluded that this was due to a highly reactive 'hot' carbonium ion which reacts with nucleophiles faster than rearrangement can occur.[33] However, as Ridd points out, the involvement of an ion pair between the charged diazonium ion and the acetate ion cannot be ruled out as a possible explanation of the reaction products.[17]

In summary, the deamination of aliphatic amines proceeds *via* an S_N1 pathway with an early, reactant-like transition state. Inversion is observed in substitutions due to partial shielding of one side of the carbonium ion by the departing N_2 group. Elimination and rearrangement reactions are also apparent and are governed by the statistical distribution of the various conformations of the molecule at the reaction temperature.

1.3 Deamination of primary amino acids and peptides

The treatment of α-amino acids with nitrous acid has been used for the synthesis of chiral intermediates in a wide number of syntheses. It is also the basis of the Van-Slyke determination[34] of the number of primary amino groups in biological molecules. There has been comparitively little interest, however, in the effects of nitrosation of the primary amino groups of amino-acids and peptides *in vivo*, and the casual role this may play in the aetiology of cancer.

1.3.1 Nitrosation of the terminal amino group

Peptides are highly functionalised molecules containing a number of groups which may undergo nitrosation. Possible reaction may occur on the nitrogen-containing side chains of arginine, lysine, tryptophan, glutamine and asparagine, the sulphur atom of cysteine or on the aromatic residue of tyrosine, as well as the terminal primary amino group and peptide N-atom. Further, nitrosation of peptides with prolyl N-terminii will lead to N-nitrosamine formation.[8,9] The nitrosation of the side chains of tryptophan, tyrosine, methionine, cystine, arginine and lysine have been reviewed[35,36,37] and will not be discussed further. The nitrosation of proline is also well documented[8,9,38-42] and beyond the scope of this review.

In a study of the reaction rates and products of the nitrosation of simple dipeptides in dilute acid at 37°C, Challis *et al* concluded that the terminal primary amino group is ca 20 fold more reactive than the peptide N-atom.[12] Thus, for small peptides and

proteins, the most likely outcome of gastric nitrosation will be formation of the diazo compound.

There have been few mechanistic studies of the nitrosation of the primary amino group of amino acids and peptides but it is generally accepted that the mechanisms already discussed *(vide supra)* apply. Thus N_2O_3 is the dominating nitrosating agent at high nitrite concentrations (>1mM), whilst NOX (eg X=Cl, SCN) is important at lower nitrite concentrations. The rates of nitrosation of both the side chain and the terminal primary amino groups of isoleucine methyl ester, two dipeptides (isoleucylvaline and valylvaline) as well as the ε-amino groups of α-N-benzoyl-L-lysine, and two polylysyl peptides at pH4 with 0.1-0.01M nitrite show that the N-terminal amino group is considerably more reactive (ca 20-500 fold) than the side chain ε-amino group.[42] This result is consistent with the expected differences in concentration of free amine in solution. An observed kinetic dependence on $[HNO_2]^2$ was indicative of N_2O_3 being the active nitrosating agent. It was also concluded that the rate of reaction was very much dependent on the nature of the environment of the primary amino group in larger peptides.[42]

In dilute HCl under simulated gastric conditions (37°C, pH 1-4, [nitrite]< $20x10^{-6}$M) the nitrosation of simple dipeptides showed a first order nitrite dependence, obeying equation 1.3,[12] consistent with nitrosation by NOCl. This mechanism applied with nitrite concentrations up to 10mM. An additional pathway for the nitrosation of amino acids and small peptides with a free carboxyl group has been observed. In a study of the nitrosation of glycylglycine (glygly) in $HClO_4$ at 37°C a second order kinetic dependence upon [glygly] was observed on increasing the peptide concentration at low nitrite levels (10-100mM). This effect was not observed when the carboxyl group was protected as the ethyl ester and has been attributed to intermolecular nitrosation of the neutral peptide by glycylglycine nitrite ester (15).[12] Similar effects have been observed in the N-nitrosation of sarcosine and proline, this time involving

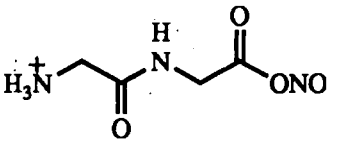

(15)

an intramolecular nitrosation by the nitrite esters (16) and (17) respectively.[43] Although these reactions involve the generation of N-nitrosamines, there is no

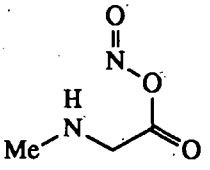

(16)

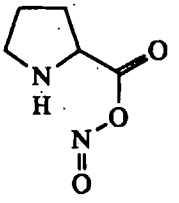

(17)

reason why such an intramolecular reaction should not apply to the nitrosation of other, primary amino acids.

1.3.2 Diazoamino acids and peptides

Diazoamino acids and peptides are elusive compounds. To date only a few have been synthesised and are well known.

1.3.2.1 Synthesis

The first diazopeptide, N-(2-diazoacetyl)triglycine ethyl ester was prepared by Curtius[44] in 1904 from the reaction of sodium nitrite with tetraglycine ethyl ester in acetic acid. Subsequently a number of diazo compounds derived from glycyl peptides were prepared using the same procedure.[45,46,47] In all cases the carboxyl terminus was protected and isolation of the diazopeptide relied upon crystallisation from the reaction solution. A later modification[48] involved a two phase system with the diazopeptide being continually extracted into the organic solvent as it formed, thus limiting the acid catalysed decomposition. The use of nitrous acid, however, is generally inapplicable for the synthesis of non-glycyl amino acids and peptides. Curtius obtained only very low yields of impure diazoamino acid esters on treatment of

the amino acid with acidified nitrite.[49] Other indirect routes for the formation of diazoamino acid derivatives have been reported, including treatment of a nitrosamide with base,[50] pyrolysis of nitrosamide derivatives[51] and acid catalysed decomposition of triazenes,[52] but these methods have not been widely used.

Protected diazoamino acids have been prepared by reaction of the amino acid ester with isoamyl nitrite in the presence of acetic acid,[53,54] but noticeably only those amino acids with non-nucleophilic side chains (eg. alanine, valine, leucine, and protected serine) have been prepared and the method has not been extended for the formation of diazopeptides.[53] The diazo transfer reaction[55] has found some limited use for the synthesis of diazoamino acids and peptides. Thus, treatment of the peptide or amino acid ester with either 4-nitrobenzenediazonium tetrafluoroborate or 2,4-dinitro-benzenediazonium tetrafluoroborate in the presence of base yields the α-diazo-carboxylic acid ester or peptide and the corresponding aniline *via* a base induced cleavage of the triazene intermediate (18), (Figure 1.5). However, the yields of diazopeptides are low.[56,57]

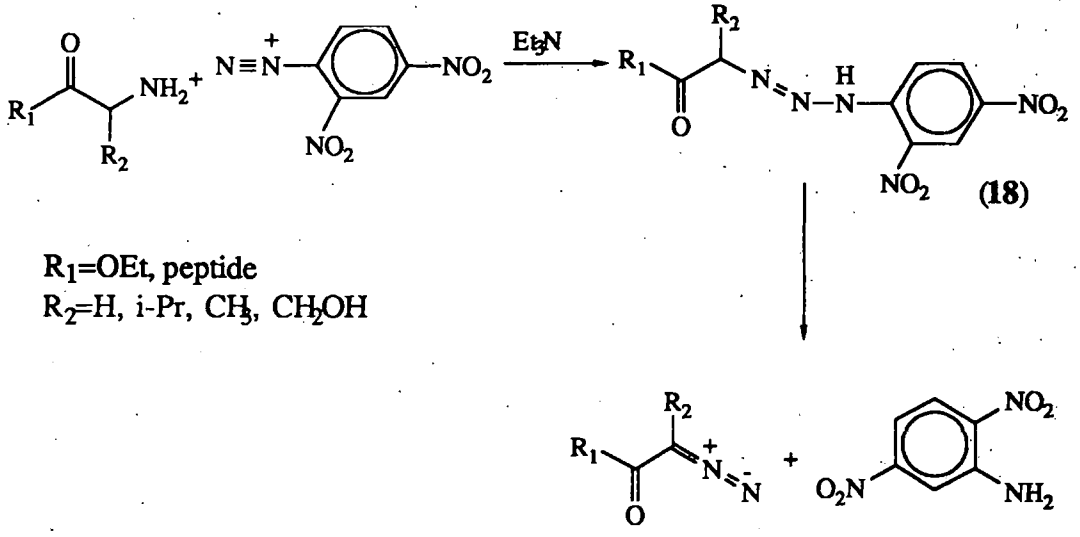

Figure 1.5 Diazotransfer reaction

To date, the most successful method of preparing diazopeptides, including those with a free terminal carboxylic acid moiety, is afforded by diazotisation under mild, neutral

conditions using liquid dinitrogen tetroxide in an aprotic solvent.[58,59] Aprotic diazotisation of the peptide is carried out in CH_2Cl_2 at low temperature (<-40°C) with liquid N_2O_4 in the presence of triethylamine, and anhydrous sodium sulphate, which remove the acid and water liberated during the course of the reaction. Unprotected peptides are solubilised as the tetrabutylammonium salts. Using this procedure the following peptides have been diazotised successfully in yields of ca 40%: leucylglycine ethyl ester; alanylglycine ethyl ester; serylglycine ethyl ester; and threonylglycine ethyl ester.[59] Nitrosation of peptides with a free carboxylic acid C-terminus (glycylclycine, triglycine pentaglycine and alanylglycine) gave lower yields of diazocompound,[59] ca 20%.

1.3.2.2 Reactions of diazoamino acids and peptides

The Wolff rearrangement

The thermal or photolytic decomposition of a diazo compound which has a carbonyl group β to the diazo moiety, does not proceed *via* a simple carbene which can be trapped. The reaction gives rise to rearranged products and is known as the Wolff rearrangement (Figure 1.6). It requires the generation of a singlet carbene which

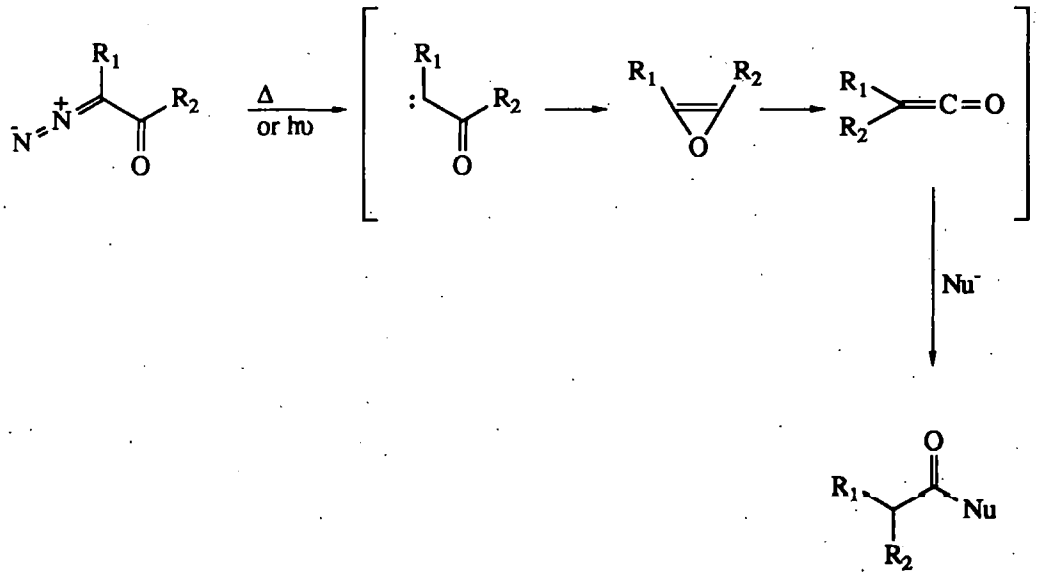

Figure 1.6 The Wolff rearrangement

then rearranges *via* an oxirene forming a ketene. This reactive species undergoes subsequent reactions with nucleophiles present in solution to generate the products. The Wolff rearrangement is commonly observed for diazoketones and these reactions are reviewed elsewhere.[23,60] It has also been observed for ethyl diazoacetate. Photolysis of aqueous or methanolic solutions of ethyl diazoacetate give products formed from two concurrent pathways.[61] One by carbene insertion into the O-H bond of the solvent, and the other proceeding *via* the Wolff rearrangement. This rearrangement may also occur for other diazo amino acid derivatives or diazopeptides but there were no examples available in the literature.

Triazene formation

In basic solutions N-(2-diazoacetyl)glycine derivatives cyclise to triazoles (19) (Figure 1.7).[62,63] For ester derivatives accompanying hydrolysis of the protecting group is observed. The triazoles are stable both in alkaline and acid solution.[63]

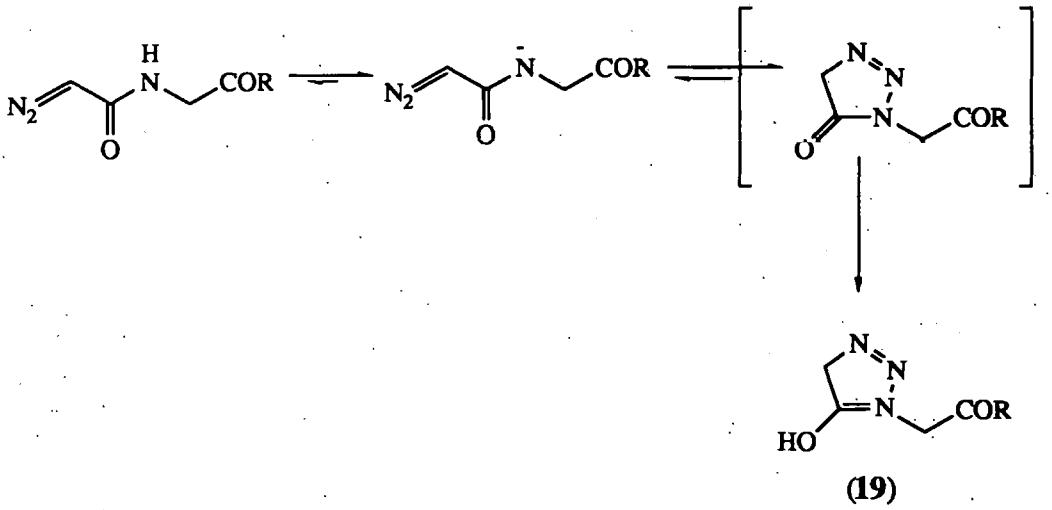

(19)

Figure 1.7 Cyclisation of diazopeptides to triazoles in base

1.3.2.3 Stabilities of diazo peptides and amino acids in aqueous acid

Since few diazoamino acids and diazopeptides have been synthesised little is known about their relative stabilities in aqueous media. The presence of an electron withdrawing carbonyl group α to the carbon bearing the diazo group confers some

stability, over the simple diazoalkanes. Diazopeptides should, therefore, have similar stabilities to diazoamino acids and diazoamino acid esters although additional electronic effects of the side chains may alter their reactivity.

Either one of the two steps in the acid catalysed decomposition of diazoamino acids and peptides may be rate limiting. (Figure 1.8).

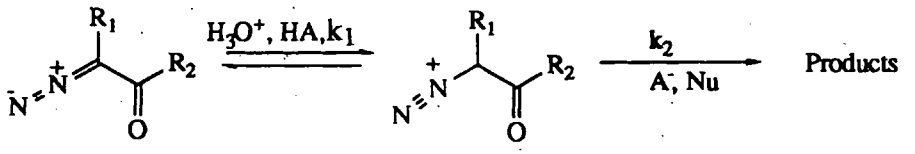

Figure 1.8 Acid-catalysed decomposition of diazo amino acids and peptides

If k_1 is slow and proton transfer rate limiting, the reaction will be subject to general acid catalysis but not to nucleophilic catalysis and a normal deuterium kinetic isotope effect ($k_1(H_3O^+)/k_1(D_3O^+)>1$) will be observed. Such kinetic behaviour has been observed for substituted diazoesters (R_1=CH_2Ph, CH_2OH, $CHCH_3OH$, and $CH_2CH(CH_3)_2$; R_2=OEt)[58] and for ethyl-2-diazopropionate (R_1=CH_3, R_2=OEt).[64] Since protonation is rate limiting information on subsequent steps is inaccessible and it is not known whether decomposition of the diazonium ion is unimolecular (S_N1) or bimolecular (S_N2). Alternatively, k_2 can be rate limiting *via* either an A_1 or A_2 mechanism following a rapid equilibrium protonation of the diazo substrate. Such reactions will show specific hydrogen ion catalysis, an inverse deuterium kinetic isotope effect ($k_2(H_3O^+)/k_2(D_3O^+)$ <1) and may or may not show nucleophilic catalysis. N-2-Diazoacetyl peptides (R_1=H, R_2=$NHCH_2COR_3$) decompose *via* an A-2 pathway in dilute aqueous acid and buffers[58] as does ethyldiazoacetate.[65,66,67] The hydrolysis of the diazoacetate ion is slightly more complicated. In mildly basic and acidic solution it decomposes *via* an A-S_E2 pathway[68] but in strongly basic solutions Kreevoy and Konasewich report decomposition *via* an A-1 mechanism.[68] However, their data is also consistent with an A-2 pathway involving intramolecular nucleophilic catalysis by

the α-carboxylate, as shown in Figure 1.9, which would avoid formation of a primary carbonium ion. The calcium salt of N-(2-diazoacetyl)glycine also follows an

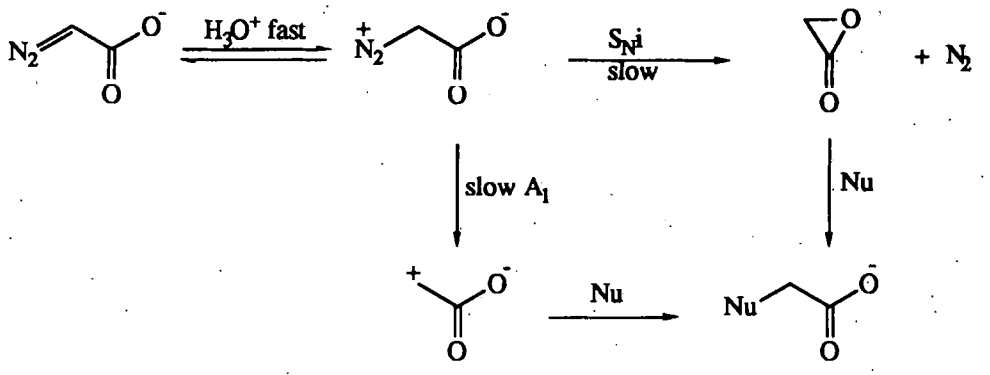

Figure 1.9 Decomposition of ethyl diazoacetate in aqueous solution

A S_E2 pathway at low pH.[69] This can be attributed to intramolecular catalysis by the carboxylate moiety thus proton transfer (k_1) becomes rate limiting. (Figure 1.10). Diketomorpholine (20) has been identified as the reaction product.[69]

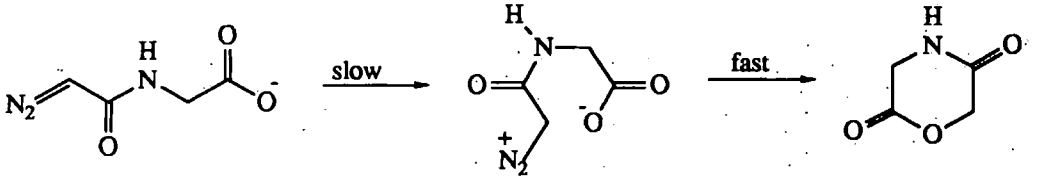

(20)

Figure 1.10 Decomposition of N_2GlyGly

Initial investigations into the relative stabilities of the diazopeptides[69] indicate that the diazoacetyl peptides (R_1 =H) are more stable than those possessing electron donating substituents (eg. R_1=CH_3) adjacent to the diazo group. Since protonation of the diazoacetyl compounds and subsequent cleavage of the C-N bond would generate an unstable primary carbonium ion, C-N bond cleavage is expectedly slow. For other diazopeptides (R_1 ≠H), protonation and C-N bond fission would generate a more stable secondary carbonium ion, hence C-N bond cleavage is faster and protonation rate determining.

All diazopeptides thus far studied are relatively unstable ($t_{1/2}$<1s) at pH<4 but reasonably long lived ($t_{1/2}$ 5-30h) at cellular pH (pH 6-8). The gastric situation may be complicated by incorporation of diazo compounds in lipophilic phases, which protect them from hydrolysis and extend their lifetimes.

1.3.3 Deamination products

As mentioned earlier, products resulting from the nitrosation of the amino acid side chains of peptides as well as the peptide N-atom are reviewed elsewhere[37] and will not be covered here.

The deamination of α-amino acids and peptides with nitrous acid is a useful method of replacing the amino moiety with another functional group. As early as 1848 Piria recorded that treatment of aspartic acid with nitrous acid gave malic acid.[70] Generally, deamination in aqueous media gives 2-hydroxy acids, but in HCl and AcOH varying amounts of the 2-chloro acids[12] and 2-acetoxy compound[12] have been reported for the deamination of glycylglycine. The amino group of 7 amino acids has been replaced by fluoride in yields of 80-98% using nitrite in polyhydrogen fluoride and pyridine.[71] However, yields were noticeably lower (12-60%) for the 5 amino acids investigated which bore a potentially nucleophilic side chain (ie. serine, threonine, aspartic and glutamic acid and glutamine).[71] The reactions of these amino acids will be discussed in some detail later. The deamination of lysine (Figure 1.11) with an equimolar amount of nitrite gave a mixture of 80% (21) and 20% (22)[72] reflecting the greater reactivity of the α-amino group *(vide supra)*, however, with excess nitrite the product was exclusively the dihydroxy acid (23).[72]

There has been considerable interest in the stereochemistry of deamination of the amino acids. With chiral substrates the reaction proceeds with retention of stereochemistry[73] attributed to an interaction between the α-carboxylate moiety and the diazonium ion[74] (Figure 1.12). The resultant α-lactone (24) is ring opened by the incoming nucleophile to give net retention of stereochemistry.

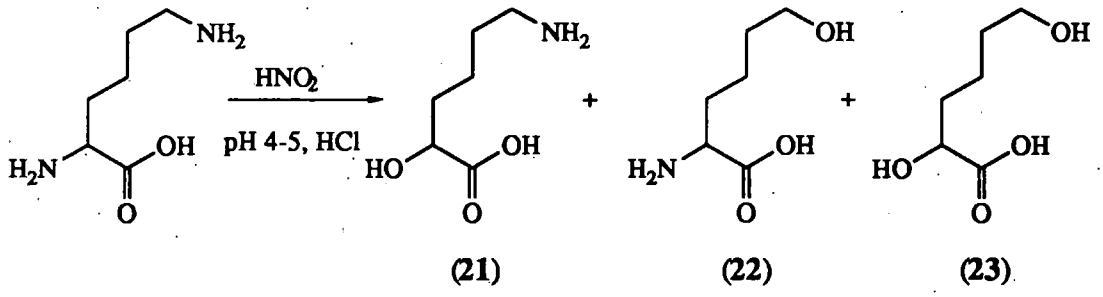

Figure 1.11 Deamination of lysine

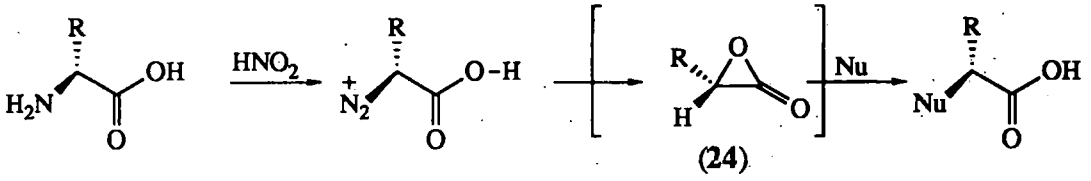

Figure 1.12 Carboxylate neighbouring group effect in deamination of amino acids

Thus deamination of serine gave glyceric acid with retention of stereochemistry[75,76] and similarly deamination of R or S aspartic acid gave the corresponding malic acid with retention in greater than a 94% enantiomeric excess.[75,76,77] Analogously, treatment of L-asparagine under weakly acidic conditions gave L-β-malamidic acid (25).[78]

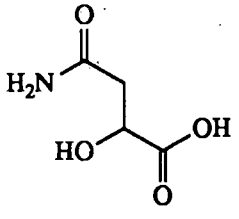

(25)

Deamination of L-phenylalanine in H_2SO_4 gave (S)-α-hydroxybenzene propanoic acid[79] but it was subsequently shown that this reaction was highly dependent on the solvent used. Aryl migration became the major process for deamination in trifluoroacetic acid due to the lower nucleophilicity of the solvent, and 3-(2-phenyl-propanoic acid) trifluoroacetate was formed[80] (Figure 1.13).

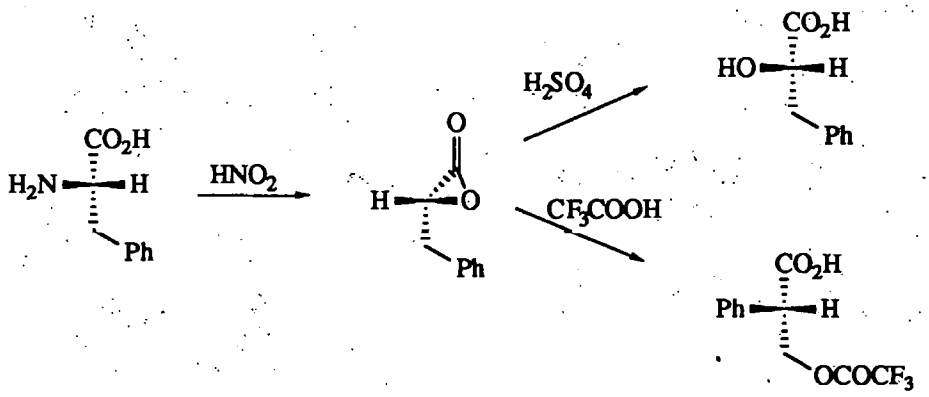

Figure 1.13 Deamination of phenylalanine in H_2SO_4 and CF_3COOH

At high nitrite concentrations several other reactions have been observed. Deamination of glycine gave a mixture of products,[81] shown in Figure 1.14, resulting from trapping of the carbonium ion by nitrite, forming nitroacetic acid (26) which then undergoes a series of reactions as indicated. These reactions at high nitrite levels (saturated solutions), are unique to glycine and glycyl peptides requiring two α-hydrogens, and

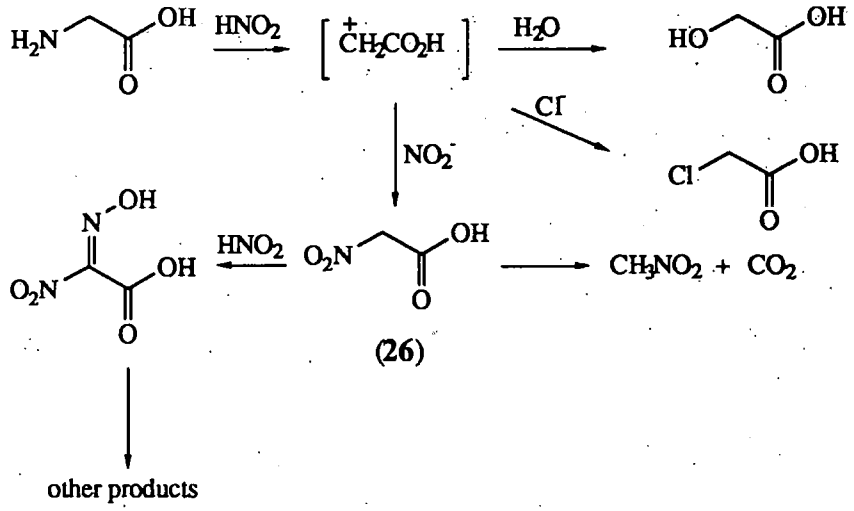

Figure 1.14 Deamination of glycine in AcOH at high nitrite concentration

are responsible for the anomalous behaviour of glycyl compounds in the Van-Slyke determination.

The oxime (27) has been identified as a minor product (10%) in the reaction of glycylglycine with excess nitrite in HCl.[58] In dilute sulphuric acid the nitrile N-oxide

(28) is formed.[63] These are thought to arise from C-nitrosation of the α-carbon atom of the diazopeptide (Figure 1.14).

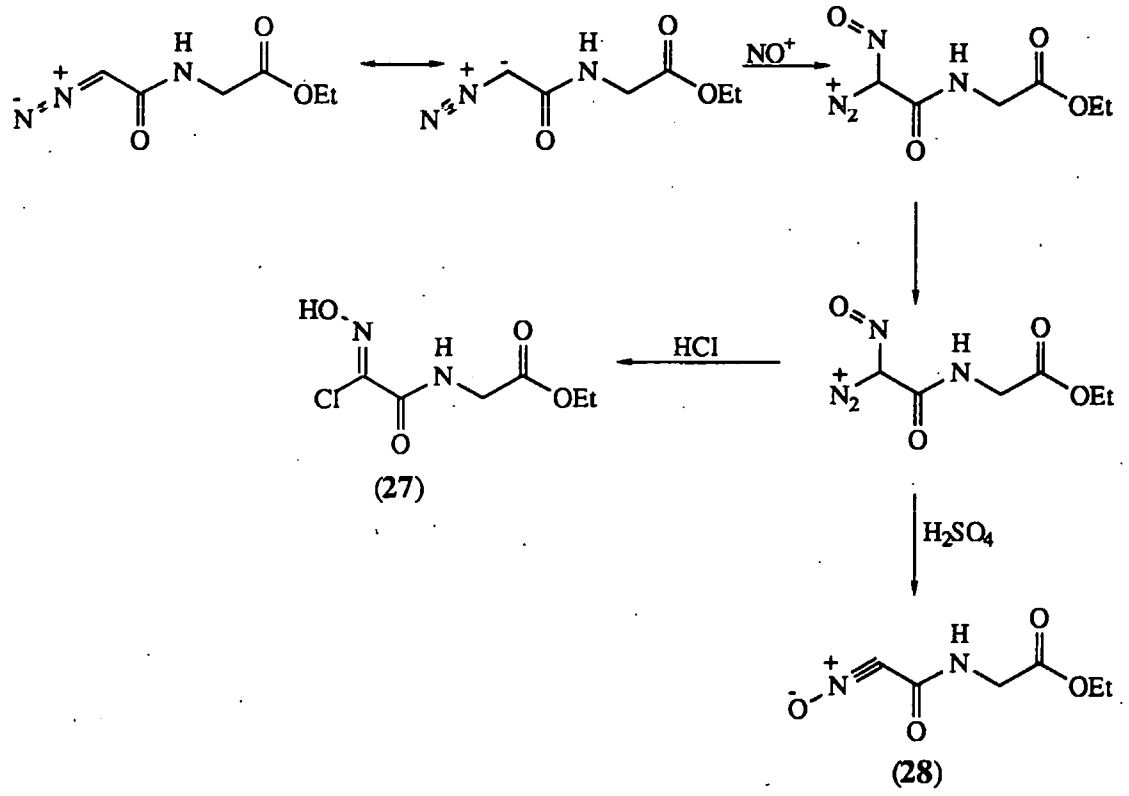

Figure 1.14 Oxime (27) and nitrile oxide (28) formation in deamination of GlyGlyOEt

N-nitrosoimino dialkanoic acids are reported to form on nitrosation of dipeptides at high nitrite concentrations[63,82,83,84] in yields of up to 10-20%.[82] The mechanism is believed to involve the intra-molecular formation of an α-lactam (29) which is subsequently opened by water at the 2-position (Figure 1.15). This reaction is somewhat analogous to the interaction of the α-carboxylate observed on the deamination of α-amino acids. In view of these observations, other intra-molecular reactions may occur between the diazonium ion and suitably nucleophilic groups on the α-side chain.

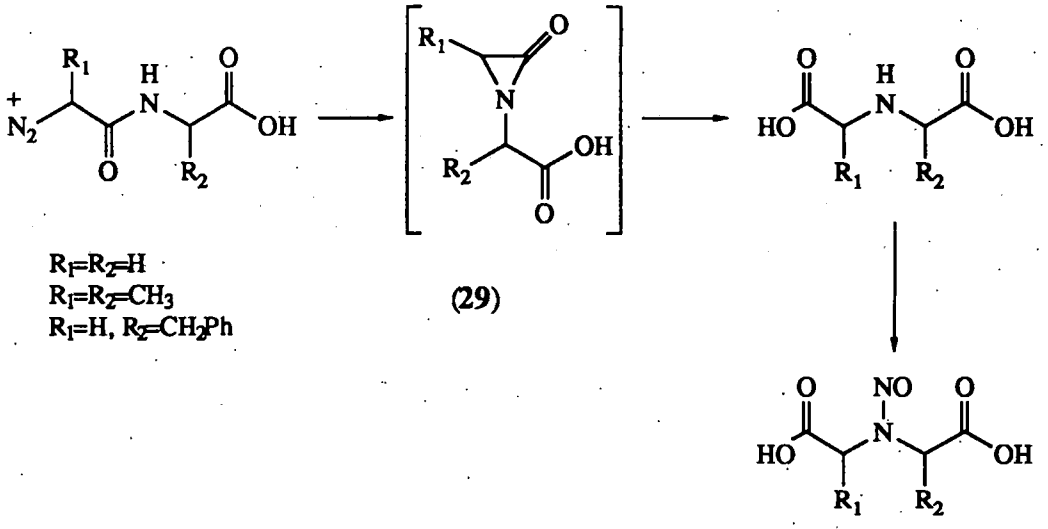

Figure 1.15 Formation of iminodialkanoic acids

1.3.3.1 Cyclic deamination products

The formation of cyclic products from the deamination of a number of amino acids have been reported. Perhaps the best known example is the deamination of glutamic acid to give the γ-lactone (30). It was established by Austin that the reaction proceeded with retention of stereochemistry to give (30) in 93% yield.[85] Thus cyclisation of the γ-carboxylate moiety must be preceded by an S_N2 displacement of the nitrogen by the α-carboxylate moiety[85,86] (Figure 1.16).

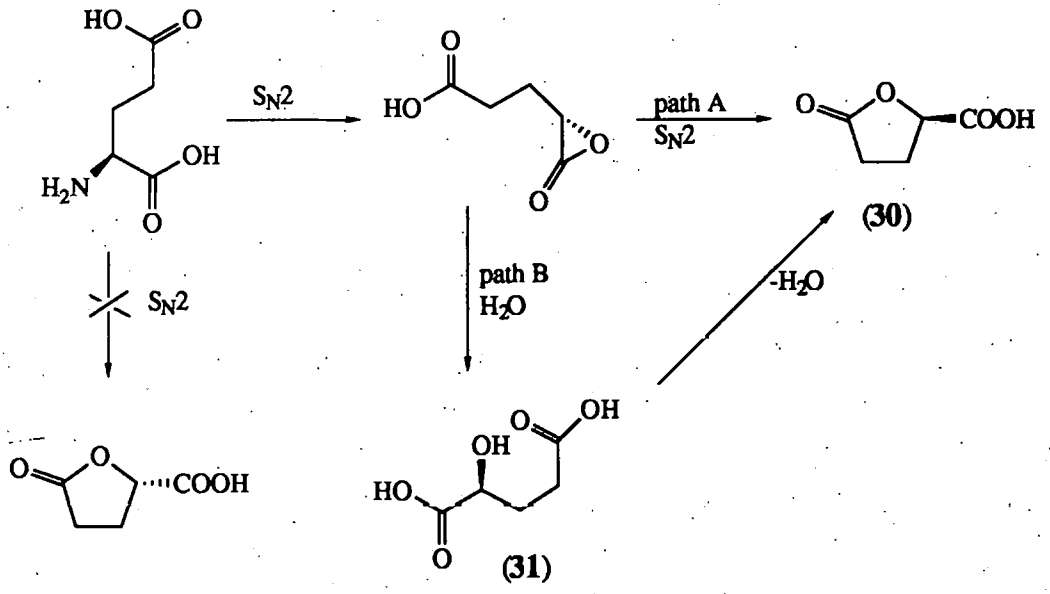

Figure 1.16 γ-lactone formation from L-glutamic acid

Pathway B, involving hydrolysis of the α-lactone to the hydroxydicarboxylic acid (31), followed by lactonisation, was eliminated by Austin who showed the rate of formation of (30) from glutamic acid greatly exceeded the rate of lactonisation of γ-hydroxybutyric acid.[87] Because of the high yield and the stereospecificity of the reaction, it has been widely used to generate (30) which is itself a versatile synthon (for eg. of the uses of (30) see refs. 88-91). The importance of the α-carboxylate was demonstrated by Austin and Howard. On replacing it with either CH_3 (γ-amino valeric acid) or H, (4-aminobutanoic acid) the yields of the corresponding lactones were greatly reduced (25 and 33% respectively).[87] However, with an α-carboxamide group, the yields were not so greatly reduced (46%)[87] indicating that interactions of the type proposed for the formation of imino dialkanoic acids ie. α-lactams *(vide supra)* are not without precedent.

Glutamine, γ-glutaminyl peptides[92] and N-alkylglutamine[93] all give abnormally high amounts of nitrogen (two moles) in the Van-Slyke determination. This has been attributed to the formation of an imidate (32) which subsequently reacts with nitrous acid liberating a second mole of nitrogen[85,92,95] (Figure 1.17). The reaction proceeds with retention of stereochemistry, again implying the formation of an α-lactone intermediate. Thus, treatment of L-glutamine and L-glutamic acid with nitrous acid gave exactly the same product, γ-lactone (30).[85]

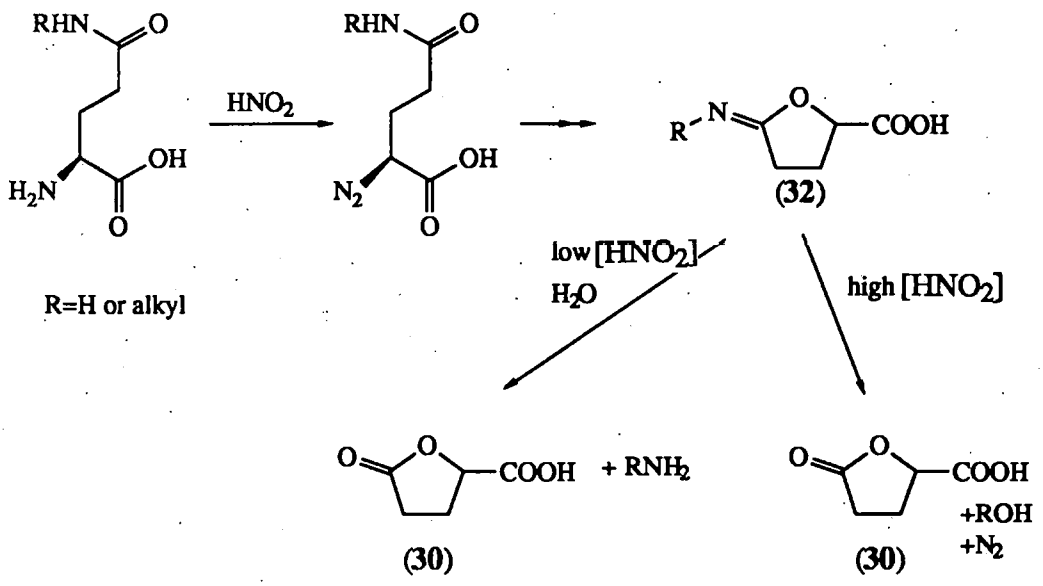

Figure 1.17 Deamination of glutamine

Cyclic products have not been observed for the deamination of asparagine[85] nor aspartic acid[94] which both give the corresponding hydroxy compounds on deamination *(vide supra)*. This is consistent with the formation of a 4-membered ring being more energy demanding than formation of a 5-membered ring. The formation of β-lactones from the nitrous acid deamination of β-amino acids has, however, been observed[96] (Figure 1.18). When both R groups are bulky (eg. R_1=Et, R_2=cyclohexyl) the carboxylic acid and the diazonium ion are forced into close proximity and the yields of

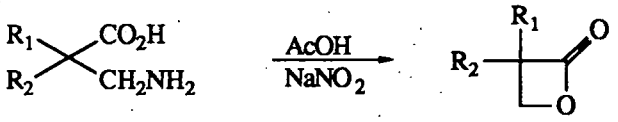

Figure 1.18 β-lactone formation from β-amino acids

the β-lactone are surprisingly high (eg. 59%). More recently the formation of β-lactone (33) on treatment of L-aspartyl phenylalanine methyl ester (aspartame) (34) with HNO_2 has been observed.[97]

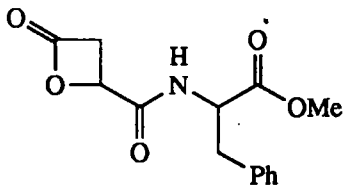

(33)

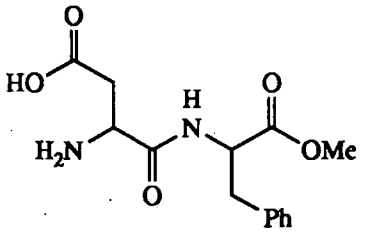

(34)

Although it is generally accepted that nitrosation of cysteine occurs on sulphur, N-nitrosation has been observed resulting in the formation of a thiiran.[72] Treatment of L-cysteine with nitrous acid gave a 3:1 mixture of the (R) and (S) enantiomers of thiiran carboxylic acid (55%).[98,99] The major isomer (R) resulting from ring opening of the α-lactone intermediate by the sulphur whilst the minor (S) isomer resulted from S_N2 displacement of the nitrogen directly by the sulphur. Inversion was observed when the carboxyl group was protected as the methyl ester. Thus, methyl (R)-cysteinate gave methyl (S)-thiiran carboxylate (35) in 47% yield.[98,99] There have been no reports of the formation of an epoxide on deamination of serine or threonine.

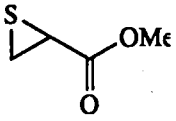

(35)

Cyclic products have also been observed for a number of other amino acids. Thus, arginine and citrulline form the proline derivatives (36) and (37) respectively in yields of 25% and 80%.[72] With a 10 fold excess of nitrite, both amino acids gave N-nitroso

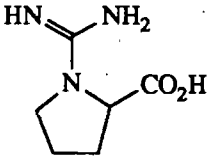

(36)

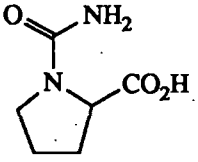

(37)

proline in yields of 0.1% and 27.1% respectively,[100] presumably resulting from nitrosation, deamination and decarboxylation of the above derivatives, followed by N-nitrosation of the resulting proline.

Ornithine, when treated with a 3 fold excess of nitrite gave tetrahydrofuran-2-carboxylic acid in 50% yield but there was no analogous reaction observed for lysine to give the tetrahydropyran-2-carboxylate.[72]

1.4 β-Lactones

Of all the cyclic compounds formed on deamination of the α–amino acids and peptides the β-lactone (33) formed from aspartame[97] is the most interesting since it may have cytotoxic properties.

1.4.1 Hydrolysis of β-lactones

The hydrolysis of β-lactones is well documented in the literature. The two lactones on which the majority of data is available are β-propiolactone (38) and β-butyrolactone (39), both known carcinogens.[101] Some data is also available for β-valerolactone (40).

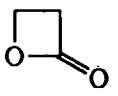

(38)

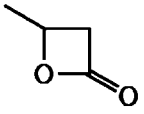

(39)

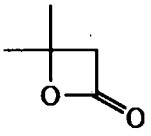

(40)

The hydrolysis of β-lactones is atypical of esters insofar as in addition to the usual acid and base catalysed reactions, β-lactones give an added reaction with water. Using optically active β-butyrolactone (39), it has been shown that this neutral, water reaction involves cleavage of the alkyl-oxygen bond giving inversion of stereochemistry about the chiral centre.[102] Hydrolysis in strong acid and base proceed with the more usual acyl-oxygen bond fission and retention of stereochemistry.[102] Further using O^{18} labelled water in mildly acidic or neutral solutions the label is incorporated in the hydroxyl group, whereas in strong acid or alkaline solutions only minor amounts of incorporation were observed at this site.[103] These observations are consistent with a base catalysed bimolecular alkyl-oxygen fission ($B_{A1}2$) mechanism for hydrolysis in neutral or weakly acidic solutions. This mechanism was also found for β-propiolactone (38)[104] over the pH range 1-7.[104]

The base catalysed cleavage of β-propiolactone[104] and β-butyrolactone has a first order dependence on [OH^-] and follows the base catalysed bimolecular acyl-oxygen fission ($B_{AC}2$) pathway generally observed for esters in basic solution.

Long and Purchase studied the acid catalysed decomposition of β-propiolactone[104] and re-interpreted the original data of Olsen and Miller[102] for β-butyrolactone showing that both reactions were strongly acid catalysed with a kinetic dependence on h_o (the Hammett acidity function) rather than [H_3O^+]. Thus, they concluded that the reaction proceeded *via* a unimolecular acid catalysed acyl-oxygen fission ($A_{Ac}1$) pathway. The unimolecular acid catalysed alkyl-oxygen fission ($A_{A1}1$) mechanism can be discounted since this would involve the formation of a primary carbonium ion ($^+CH_2CH_2COO^-$) from β-propiolactone (38) and would not explain the stereochemical observations of the hydrolysis of β-butyrolactone (39). This pathway, however, has been observed for the acid catalysed decomposition of β-isovalerolactone[105] (40) where alkyl-oxygen bond fission results in a stable tertiary carbonium ion (41). Substantial decarboxylation to form isobutylene (63%) is observed in neutral solution with only 37% hydrolysis of the lactone occuring. The *pseudo* first order rate constant for neutral hydrolysis (k_w) was ca 20 fold greater than that for β-propiolactone (38) and ca 100 fold greater than that of β-butyrolactone (39) (Table 1.2). Electron donating groups would decrease the rate of $B_{A1}2$ hydrolysis rather than increase it and therefore it must be concluded that the reaction proceeds with a prior unimolecular cleavage of the alkyl-oxygen bond even in neutral solution (Figure 1.19).

Table 1.2 Rate constants for hydrolysis of (38) (39) and (40) at 25°C ref. 105

Lactone	$10^5 k_w/s^{-1}$	$k_{OH^-}/M^{-1}s^{-1}$	$10^6 k_H/M^{-1}s^{-1}$
β-propio (38)	5.6	2.2[a]	5.8
β-butyro (39)	1.4	8.2	~2.3
β-valero (40)	135	2.2	2000

[a]Liang and Bartlett[105] quote a value of 1.2 $M^{-1}s^{-1}$ but the original value[104] is 130 M^{-1} min^{-1}, ie. 2.2$M^{-1}s^{-1}$.

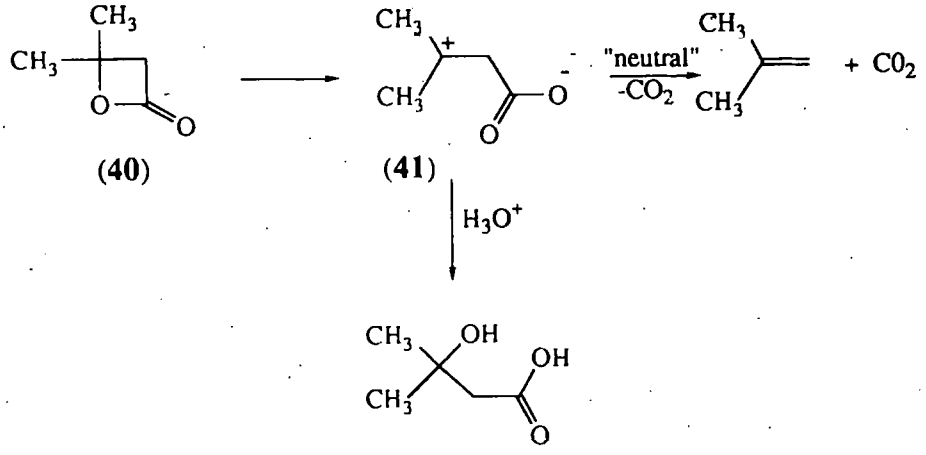

Figure 1.19 Hydrolysis of (40) in acid and neutral solution

β-Lactones can behave as ambident electrophiles, as shown in Figure 1.20, acting either as acylating or alkylating agents. It has been shown that a variety of nucleophilic species are alkylated by β-propiolactone,[106] taking the place of water in the neutral reaction. This reaction is biologically significant if the nucleophile is DNA since alkylation of DNA is widely believed to be responsible for tumour induction. However, it has been shown that acylation of other nucleophilic species occurs.[106] No rationale for this ambident reactivity has been proposed.

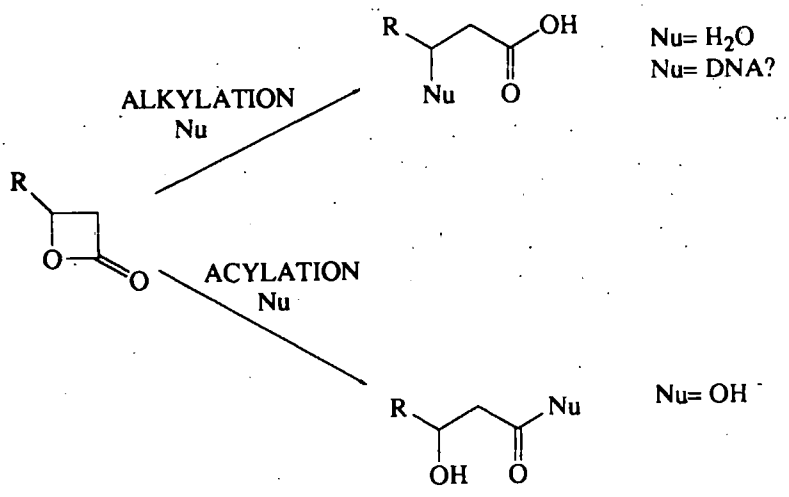

Figure 1.20 Ambident reactivity of β-lactones

1.5 Biological properties of diazopeptides and β-lactones

The biological properties of three diazoacetyl glycine derivatives, N-2-diazoacetyl glycine ethyl ester (42), N-2-diazoacetylglycinamide (43) and N-2-diazoacetylglycine hydrazide (44) have been well studied. All three show similar mutagenic activity

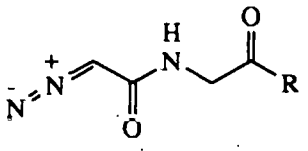

R= OEt **(42)**

R= NH_2 **(43)**

R= $NHNH_2$ **(44)**

in-vivo towards *Salmonella typhimurium* bacteria (Ames test)[15,16] and V79 Chinese hamster cells.[107] They induced various degrees of dose-dependent unscheduled DNA synthesis *in vivo*.[108] Two other diazo compounds, azaserine (45) and 6-diazo-5-oxo-norleucine (DON) (46) induced no detectable DNA damage at equitoxic doses.[109]

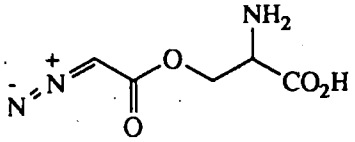

(45)

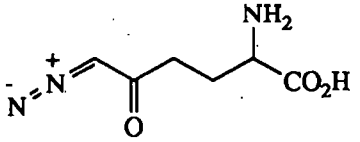

(46)

The amide (43) was found to be 800 and 17000 times more potent than azaserine and DON at equitoxic concentrations for inducing DNA damage. Further, (42), (43) and (44) act as alkylating agents towards 4-(4-nitrobenzyl)pyridine[108] whilst azaserine and DON do not.[109] The amide (43)[107] and the hydrazide (44),[110] administered as interperitoneal injections, have been shown to induce dose-dependent pulmonary adenomas and leukemia in newborn and adult Swiss mice.[111]

A number of diazo compounds have shown antineoplastic properties towards a number of tumours.[112] N-2-Diazoacetylglycylglycinamide and (43) both inhibited the formation of lung metastases[113] but showed no anti-tumourigenic properties against the primary lung tumour implant in mice.[113] DON and azaserine have also been studied for their antineoplastic properties.[114]

More recently three further diazopeptides have been tested. N-2-diazoacetylglycine (47) and N-2-diazoacetylglycylglycine (48), both with free carboxylic acid groups, have been shown to be mutagenic in the Ames test.[69] N-(2-Diazo-4-methylvaleryl) glycine ethyl ester (49), the only diazopeptide to be tested with substitution at the α-carbon atom, was, however, found to be non-mutagenic.[69] Compound (49) is considerably more labile than (43) (ca. 8 fold) and it may be that biological activity is linked to compound stability. Alternatively, factors effecting the transfer across biological membranes may be responsible for differences in biological activity and until more data is available on the structure, stability, toxicity relationships, no conclusions can be drawn.

The cytotoxicity of β-propiolactone and β-butyrolactone are well known. Both are potent slow acting carcinogens, inducing a variety of cancers in all test animals.[107] Substitution in the ring reduces the biological activity and β-propiolactone is more potent than β-butyrolactone. β-propiolactone has been shown to bind to DNA.[115] The only other simple β-lactones for which data is available are 2-carboxy-3-phenyl-3-

hydroxypropionic acid lactone (50) and 2,2-diphenyl-3-hydroxypropionic acid lactone (51) both of which are carcinogenic.[116]

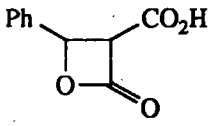

(50)

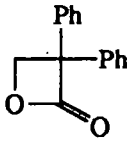

(51)

In view of the known carcinogenicity of some β-lactones the formation of β-lactone (33) may prove to be significant. The dipeptide involved, L-aspartylphenylalanine methyl ester,(34) is the widely used artificial sweetener, aspartame. The reaction was demonstrated to occur under gastric conditions (pH 1.25-3.83, 37°C [NO_2^-] = 1.01mM) with 0.02M aspartame. In 1988, the maximum acceptable daily intake of aspartame was 1-2g.[117] With the current trends for low calorie foodstuffs, intakes of aspartame have undoubtedly increased and may well continue to do so. Clearly, there is a significant chance of aspartame being nitrosated in the stomach and forming the β-lactone (33). β-Lactones have been shown to be carcinogenic *(vide supra)* hence the importance of this reaction. Gouesnard[72] did not observe the formation of (33) in the reaction of aspartame with 1 equivalent of nitrite at pH 4.5 but the reaction solution was left for 8 days before analysis and any β-lactone formed would have hydrolysed over this period.

Although aspartame is one of the most thoroughly tested compounds commercially available today there has been recent controversy about its safety[118] culminating in a government review of testing. Further, it has been shown that treatment of aspartame with nitrous acid forms an unknown alkylating agent,[119] and an unknown mutagen,[120] neither of which can be the diazo compound.

1.6 Summary

Although endogenous nitrosation of secondary amines produces carcinogenic N-nitrosamines, the low levels of dietary secondary amines suggest that these reactions

play a small causal role in human cancer. Similarly, the dietary levels of ureas, amides and guanides are probably too low for their nitrosation to pose a significant health risk. The largest dietary intake of nitrosatable material are the amino acids, peptides and proteins. *In vitro* studies show that the nitrosation of amino acids and small peptides will occur under gastric conditions to yield, initially the corresponding diazo compound. This itself may be carcinogenic as shown for several diazo- derivatives of glycyl compounds. The diazoamino acids and peptides are highly acid labile and may not persist in the gastric environment to undergo interaction with genetically sensitive material. Alternatively, other unknown factors may govern their potency as carcinogens. If a suitable nucleophilic side chain is present, deamination may lead to the formation of cyclic products (eg. thiiran carboxylic acid from cysteine, β-lactone (33) from aspartame). Further, the α-carboxylic group of diazoamino acids forms an α-lactone, which accounts for the stereochemistry of the products. If the side chain of the peptide α-substituent is 2-carbons or less, highly-strained cyclic compounds may form. These compounds would be highly reactive especially towards nucleophiles, and therefore could possibly be cytotoxic acting as stabilised alkylating agents. The possible outcomes of gastric nitrosation of a simple peptide are outlined in Figure 1.21. Elimination and rearrangement reactions reported for diazoalkanes have not been reported for diazoamino acids and diazopeptides, possibly due to their greater stability compared to diazoalkanes.

The work described in this thesis investigates the chemical reactivity of one particular cyclic product, the β-lactone (33), formed from the deamination of aspartame and attempts to assess its potential as an alkylating agent. New diazo compounds, derivatives of asparagine and glutamine, are also synthesised. Their chemical stabilities are investigated together with the formation of cyclic products from their decomposition.

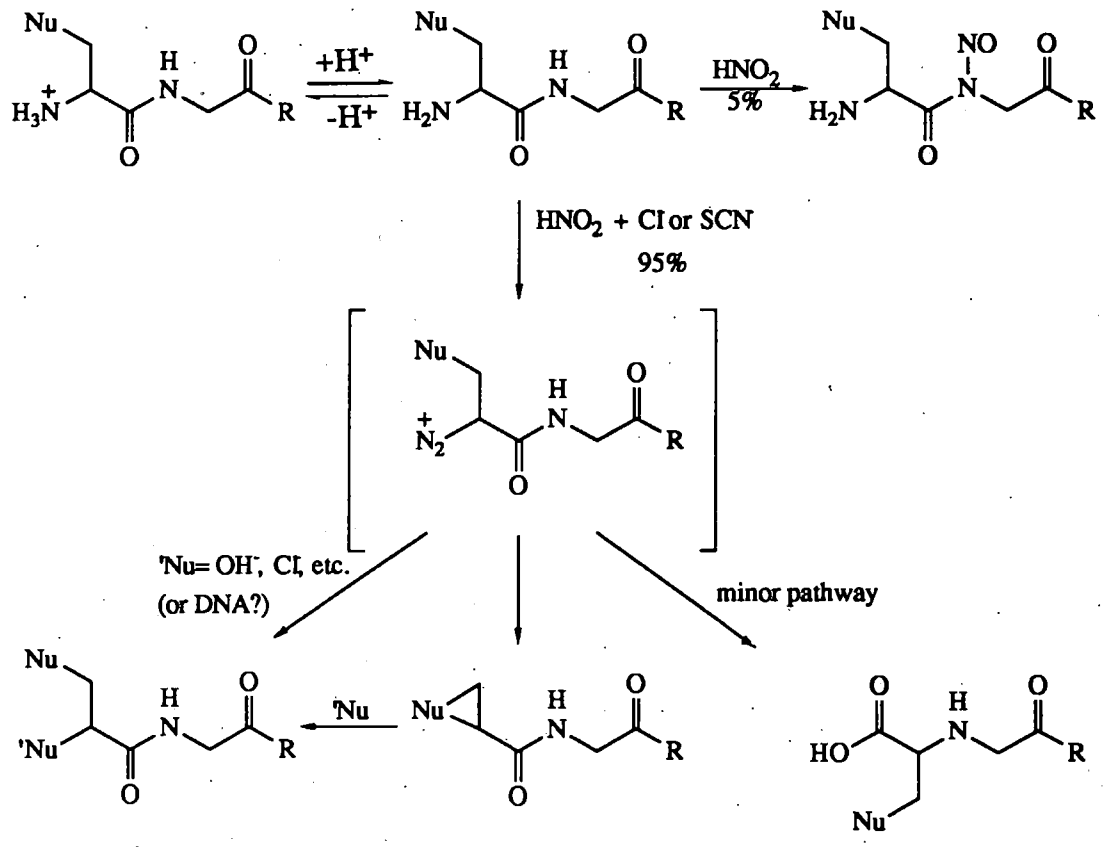

Figure 1.21 Possible reactions resulting from gastric nitrosation of a peptide with a nucleophilic side chain.

CHAPTER 2 REACTIONS OF N-(1'-METHOXYCARBONYL-2'PHENYL) ETHYL OXETAN-2-ONE-4-CARBOXAMIDE

2 REACTIONS OF N-(1'-METHOXYCARBONYL-2'-PHENYL) ETHYL OXETAN-2-ONE-4-CARBOXAMIDE

2.1 Introduction

Shephard *et al.*[119,120] have reported that treatment of L-aspartyl-L-phenylalanine methyl ester (aspartame) with nitrous acid generates an alkylating agent and the reaction mixture is mutagenic towards *S Typhimurium* TA100 (Ames Test).[120] The structures of the alkylating agent and the mutagenic materials are unknown. Sandhu, however, has shown that the nitrosation of aspartame with nitrous acid produces the β-lactone N-(1'-methoxycarbonyl-2'-phenyl)ethyl oxetan-2-one-4-carboxamide (1) in yields of upto 30%.[97] The reaction also proceeds under simulated gastric conditions of (37°C, pH2-4

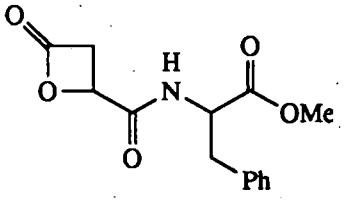

(1)

and $[NO_2^-]$>0.1mM). Since aspartame is a common dietary additive and some β-lactones are known to be carcinogenic,[101] further evaluation of the β-lactone (1) is indicated. The present work was directed towards the stability of the β-lactone (1) and its behaviour as an alkylating agent.

2.2 Synthesis of N-(1'-methoxycarbonyl-2'-phenyl)ethyl oxetan-2-one-4-carboxamide (1)

To further evaluate the properties of (1), a preparative scale synthesis was required. Simple treatment of aspartame with aqueous HNO_2 was not practical because of slow β-lactone formation and its concurrent hydrolysis. The use of an immiscible organic co-solvent into which (1) could migrate was examined but β-lactone (1) formed too slowly for this procedure to have synthetic potential.

The β-lactone (1) was synthesised in an acceptable yield by treatment of aspartame with aqueous HNO_2 at 37°C in the presence of either NaSCN or thiourea catalysts and a bi-phasic aqueous ethyl acetate solvent. NaSCN and thiourea are powerful nitrosation catalysts,[121] forming the highly reactive intermediates (2) and (3), respectively, which act as carriers of the nitrosonium ion (NO^+). This procedure gave (1) in ca 30% yield in under 2hrs. at 37°C and minimising the volume of HCl ensured maximum transfer

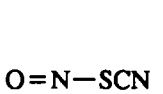

(2)

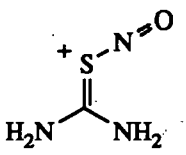

(3)

of (1) into the organic phase. The reaction scheme for the formation of (1) is shown in Figure 2.1.

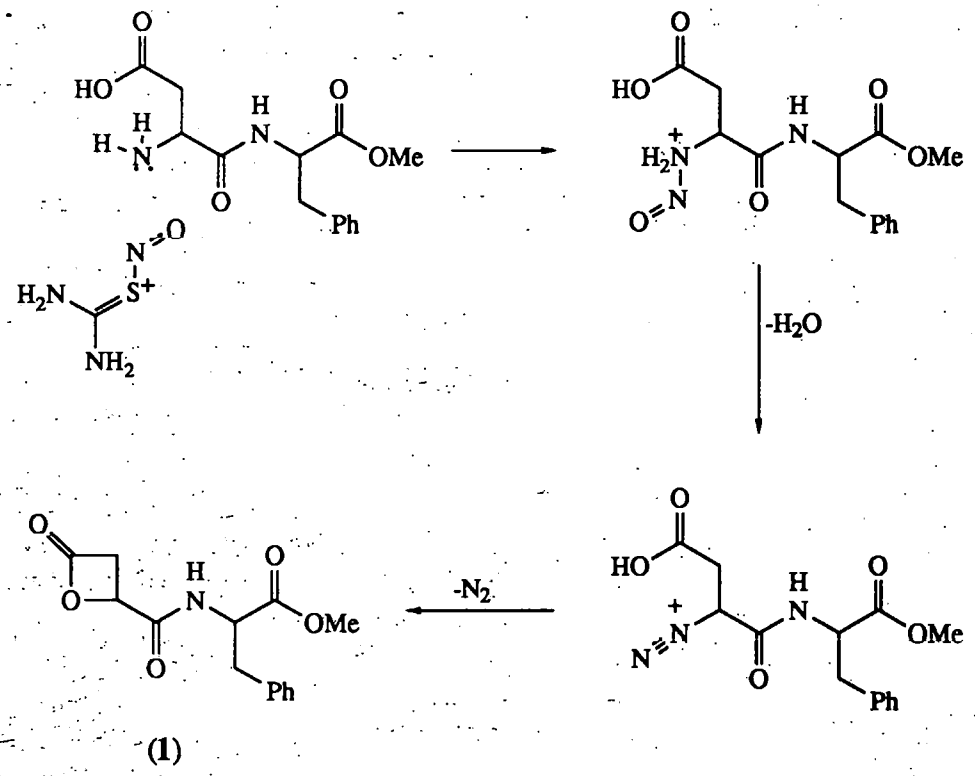

Figure 2.1 – Formation of (1) from L-aspartyl-L-phenylalanine methyl ester and nitrous acid in the presence of thiourea.

The 400MHz ^1H nmr spectrum of (1) (Figure 2.2) shows the presence of two diastereoisomers. The spectral assignments of the major diastereoisomer for the structure illustrated by Figure 2.3 are given in Table 2.1.

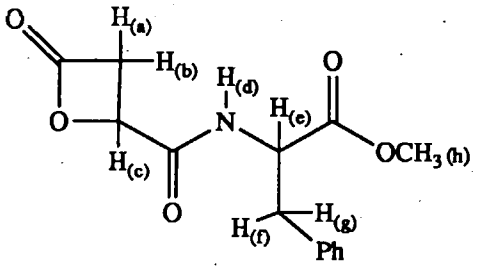

(1)

Figure 2.3 Structure of (1) used for assigning chemical shifts (Table 2.1).

Table 2.1 ^1H nmr spectral assignments of (1)

δ/ppm	Assignment	$J_{(x,y)}$/Hz
7.33	m,p aromatic	
7.16	o aromatic	
6.73	d	
4.87	e	(e,f), 5.66; (e,g), 6.88; (e,d) 8.07
4.81	c	(a,c), 4.66; (b,c), 6.88
3.84	b	(b,c), 6.89; (a,b) 16.80
3.76	h	
3.53	a	(a,c), 4.67; (a,b), 16.81
3.24	f	(e,f), 5.64; (f,g), 13.97
3.12	g	(e,g), 6.86; (f,g), 13.97

From the integrals of the two methyl singlets at δ=3.78 and 3.76 ppm, a ratio of ca

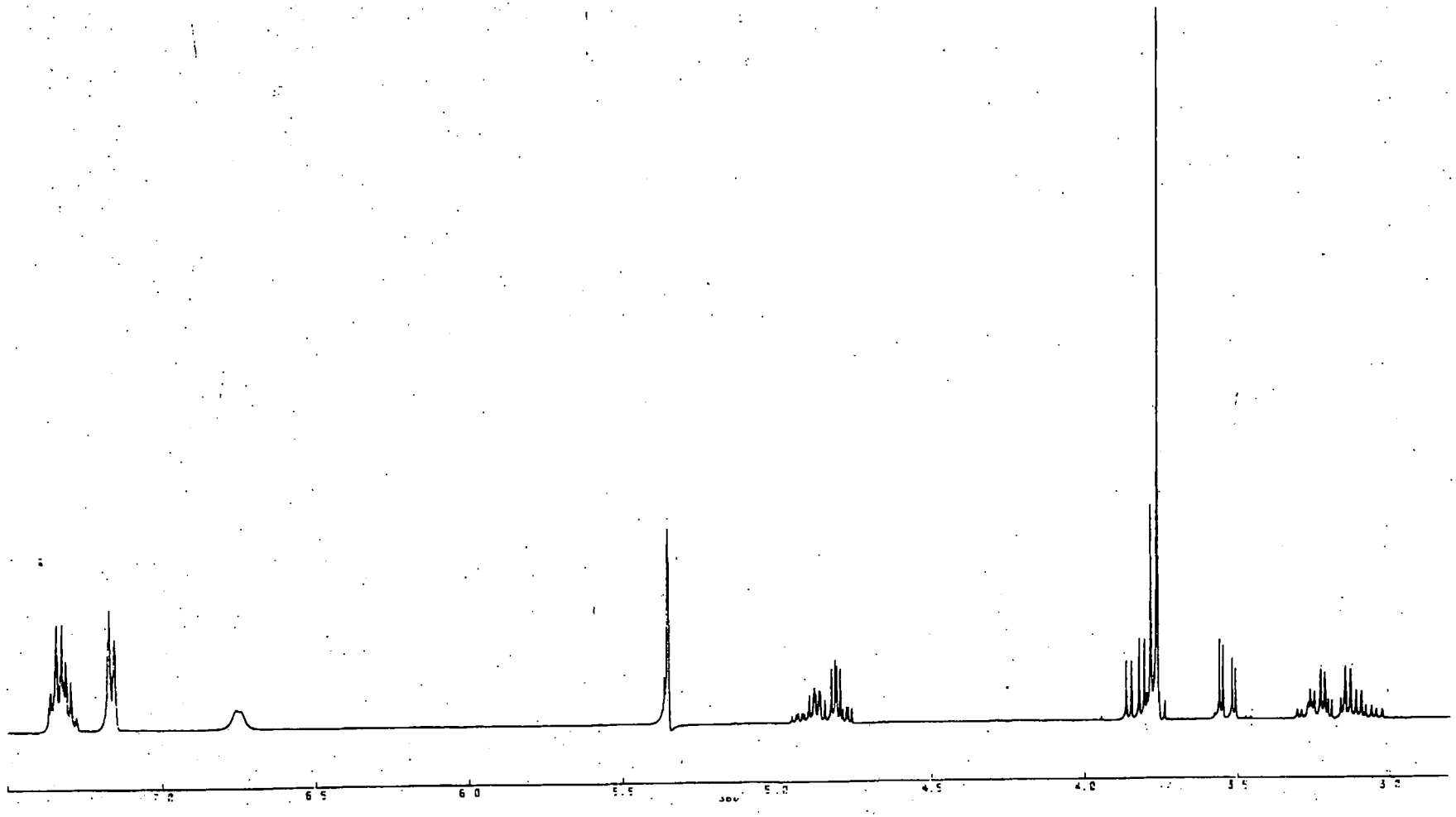

Figure 2.2 *400 MHz ^1H nmr spectrum of β-lactone (1)*

3.3:1 is estimated for the two diastereoisomers. β-Lactone formation therefore proceeds *via* two concurrent pathways (Figure 2.4).

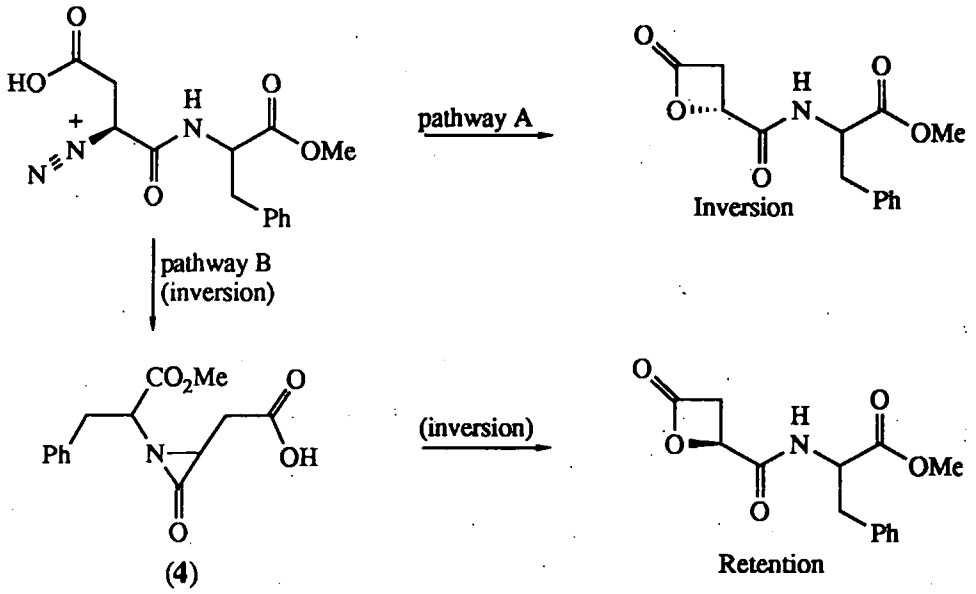

Figure 2.4 Two concurrent pathways for deaminative cyclisation of aspartame

One, (pathway A) involves the reaction of the β-carboxylate moiety directly with the diazonium ion to form the β-lactone and proceeds with inversion. The second (pathway B) is analogous to that observed in the cyclisation of glutamic acid[85] and proceeds *via* an α-lactam intermediate (4) which is subsequently opened by the β-carboxylic acid moiety to give β-lactone (1) with retention of stereochemistry. Pathway B has precedence in the formation of iminodialkanoic acids from diazodipeptides.[82]

2.3 Hydrolysis of (1)

The pH-independent hydrolysis of β-lactones in neutral or weakly acidic solutions with alkyl-oxygen bond fission is relevant to the assessment of their carcinogenic activity. The alkyl-oxygen bond fission generates an alkylating agent and physiological conditions are either neutral (eg blood) or mildly acidic (eg gastric). Thus, alkyl-oxygen bond fission and sufficient stability for absorption intact from the gastric tract into the blood stream are two fundamental requirements for carcinogenic activity by β-lactone (1). The decomposition of the β-lactone (1) was therefore examined in aqueous

media at 37°C with reference to both stability at various pH values and the bond fission. In acidic media, rates were determined from the loss of (1) using the HPLC procedure described in Chapter 7. In basic media (pH >8) rates were determined from the uptake of OH^- by the pH-stat titration technique also described in Chapter 7. In both acidic and basic media, the rates of hydrolysis of the terminal methyl ester of (1) were estimated independently from the rate of hydrolysis of the methyl ester in aspartame. This allowed discrimination between hydrolysis of the β-lactone and the methyl ester of (1). The decomposition of (1) followed *pseudo* first-order kinetics (equation 2.1). The first-order plots were linear over at least 5 half lives and several

$$\text{Rate} = k_O[(1)] \qquad \ldots.(2.1)$$

reactions were monitored to ca 10 half-lives (infinity) by which time (1) was undetectable. For slow reactions ($t_{1/2}$> 6h), infinity values were assumed to be zero on the basis of results from faster reactions.

2.3.1 Hydrolysis of (1) in aqueous buffer solutions

The β-lactone (1) was hydrolysed in a series of aqueous buffers at pH 3.3 to 7.7, 37°C and a constant ionic strength of 0.2 ($NaClO_4$). A typical first-order plot of $\ln(A_t/A_O)$ versus time, where A is the peak area of (1) in the HPLC chromatogram, is shown in Figure 2.5 for the hydrolysis of (1) in 0.05M formic acid buffer at pH 3.32. Values of k_O (equation 2.1) for various aqueous buffers are summarised in Table 2.2.

From these data it is clear that the decomposition of (1) is catalysed by the buffer components (equation 2.2), whose precise nature is discussed in Section 2.5.4.

$$k_O = k_O^i + k_{A^-}[A^-] \qquad \ldots.(2.2)$$

Values of k_O^i and k_{A^-} were obtained from the intercept and slope respectively of plots of k_O against [buffer base], as shown in Figure 2.6 for a series of 1:1 formate buffers at pH 3.36. The intercept (k_O^i) represents the sum of the spontaneous and acid and base

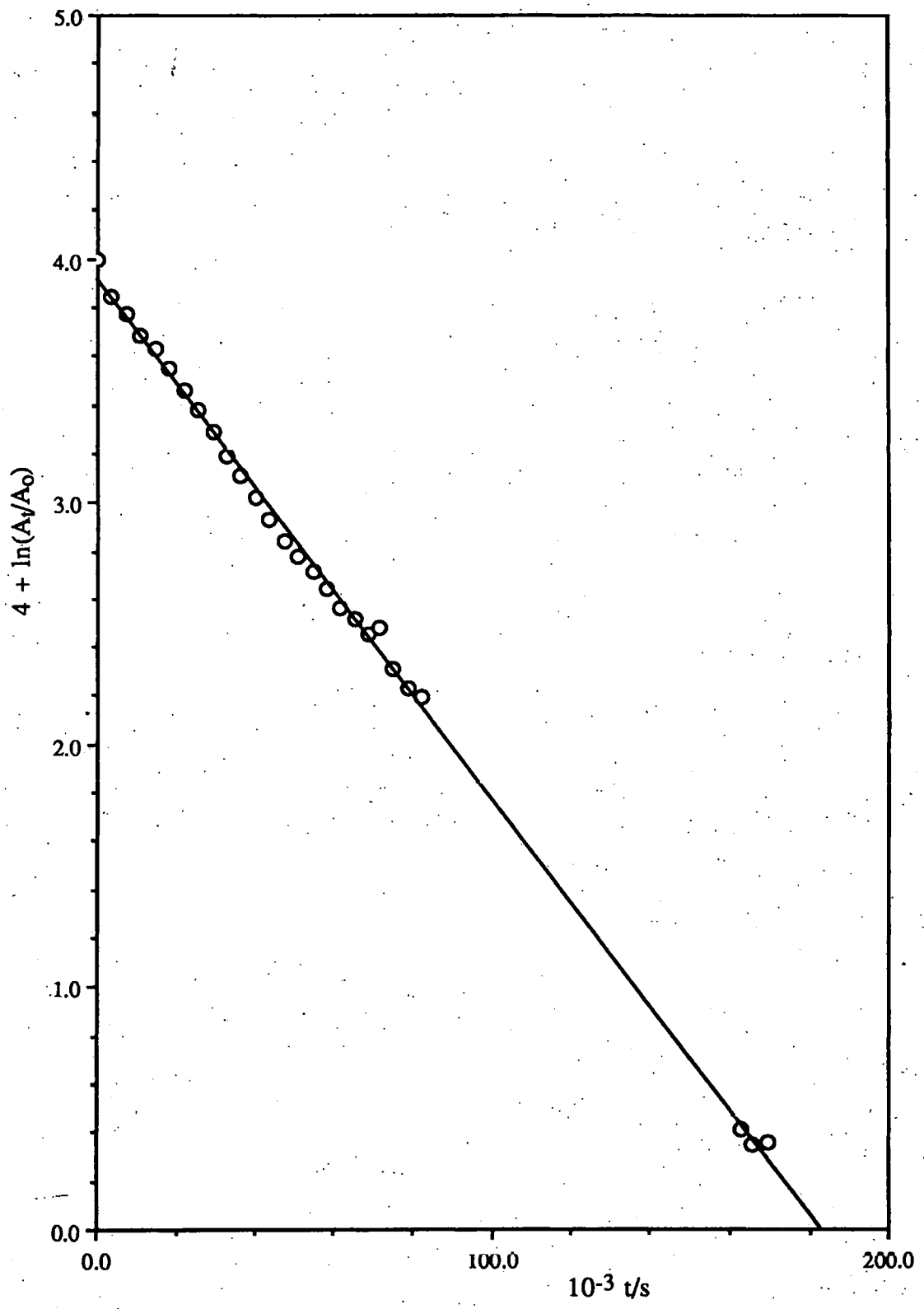

Figure 2.5 First-order plot of $\ln(A_t/A_o)$ against time for the hydrolysis of (1) in 0.05M formic acid buffer at 37°C-pH3.32

Table 2.2 Observed rates of decomposition of (1) in aqueous buffers at 37°C. Initial [(1)] ca 1mM.

Buffer	[HA]/[A⁻]	[A⁻]/M	pH	$10^5 k_o/s^{-1}$
		0.10	3.36	2.69
Formate	1	0.05	3.32	2.13
		0.01	3.40	1.69
Acetate	6	0.10	3.65	4.91
		0.05	3.64	3.21
		0.01	3.72	1.82
		0.10	3.81	4.73
		0.05	3.71	3.05
Acetate	1	0.10	4.60	4.96
		0.05	4.60	2.95
		0.01	4.60	1.69
		0.10	4.63	3.49
		0.05	4.64	2.39
		0.01	4.63	1.59
		0.10	4.63	5.20
		0.05	4.63	3.26
		0.01	4.63	1.79
Acetate	0.278	0.099	5.23	5.33
		0.020	5.12	1.96
		0.009	5.22	1.80
Acetate	0.167	0.20	5.17	9.90
		0.10	5.14	5.69
		0.172	5.54	7.85
		0.129	5.47	6.76
		0.086	5.47	4.68
Borax	-	0.10	7.68	42.8
		0.05	7.27	17.1
		0.07	7.41	9.03

catalysed decomposition of (1) (equation 2.3), although at most pH values one term only will dominate. The slope (k_{A^-}) is the second-order rate coefficient for buffer ion

$$k_o^i = k_H[H_3O^+] + k_B[OH^-] + k_w \qquad \ldots.(2.3)$$

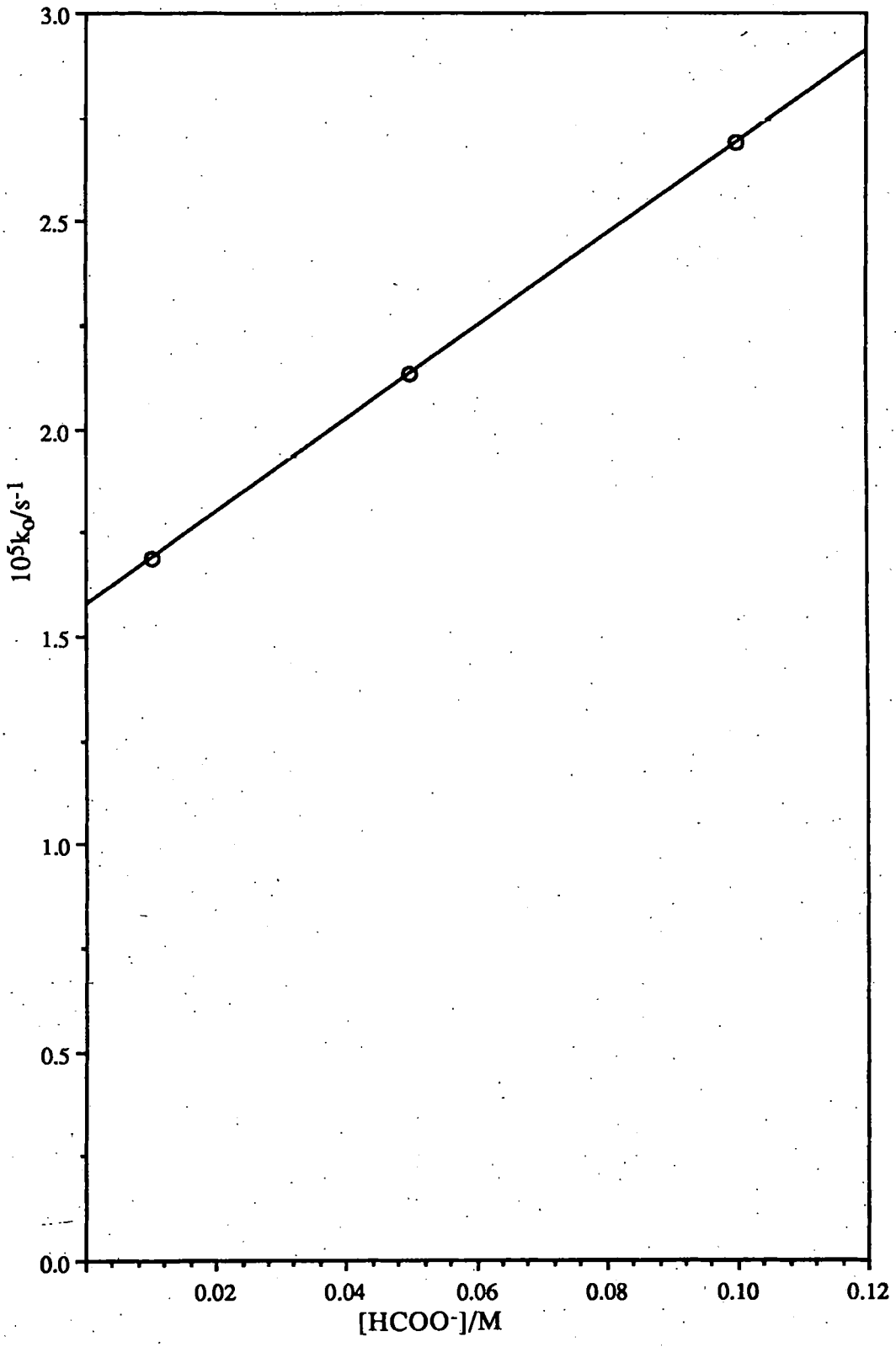

Figure 2.6 *Plot of k_o against [Buffer base] for the hydrolysis of (1) in formate buffers at pH 3.36 and 37°C.*

catalysed decomposition. The values of k_0^i and k_{A^-} obtained are summarised in Table 2.3.

Table 2.3 Values of k_0^i and k_{A^-} for the decomposition of (1) in aqueous buffers at 37°C.

Buffer	pH	$10^5 k_0^i/s^{-1}$	$10^4 k_A/M^{-1}s^{-1}$
Formate	3.36	1.57	1.11
Acetate	3.65	1.48	3.43
	3.80	1.55	3.18 Avg. 3.54
	4.60	1.24	3.68
	4.63	1.30	2.20
	4.63	1.39	3.79
	5.19	1.27	4.08
	5.16	1.48	4.21
	5.49	1.55	3.79
Borax	7.45	1.49	38.3

The average values of k_{A^-} for the acetate ion is 3.54×10^{-4} $M^{-1}s^{-1}$, for formate ion is 1.11×10^{-4} $M^{-1}s^{-1}$ and for the borate ion is 3.83×10^{-3} $M^{-1}s^{-1}$.Over the pH range 3.3 to 7.4, k_0^i is virtually constant with a mean value of $k_0^i = 1.42(\pm 0.22) \times 10^{-5}s^{-1}$. The rate of hydrolysis of (1) is therefore pH independent over this pH range. A detailed study of the hydrolysis mechanism was not made but the pH-independence is consistent with either spontaneous unimolecular cleavage of the neutral β-lactone or bimolecular hydrolysis of the neutral molecule by water. By analogy with other β-lactones, where the pH-independent mechanism of hydrolysis has been studied in detail using isotopically-labelled reactants,[103,104] the consensus is for a bimolecular $B_{A1}2$ mechanism involving alkyl-O fission with water acting as the base (Figure 2.7).

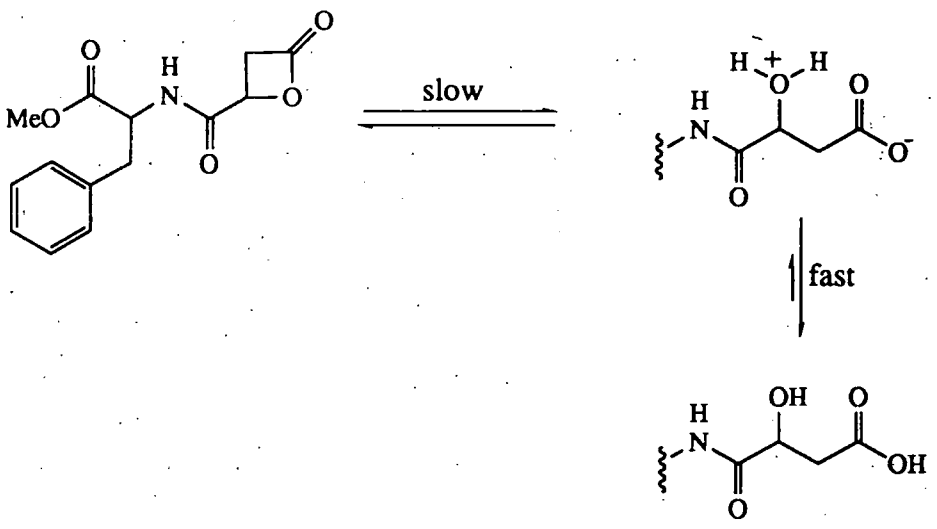

Figure 2.7 $B_{AL}2$ *Hydrolysis of (1)*

It is also difficult to rationalise the alternative unimolecular mechanism with the concurrence of a base-catalysed pathway. For the $B_{A1}2$ pathway the rate of reaction follows equation 2.4 (where k_w is the *pseudo* first order rate coefficient for the neutral

$$\text{Rate} = k_w a_w [(1)] \qquad \ldots.(2.4)$$

hydrolysis of (1) by water and $k_o^i = k_w a_w$). The present reactions were carried out at μ= 0.2 ($NaClO_4$) where a_w = 0.993,which leads to an average value of k_w = 1.43 x $10^{-5}s^{-1}$ at 37°C and a half life of 13.5h. Thus, (1) seems sufficiently stable to remain intact during passage through the gastrointestinal tract provided catalysis by buffer components is negligible. The estimated value of k_w for the hydrolysis of β-propiolactone at 37°C is 2.06 x $10^{-4}s^{-1}$, which corresponds to a half life of 56 min. β-Lactone (1) is ca 15 fold more stable than β-propiolactone presumably because reaction at the C_4 position is retarded by steric hindrance.

2.3.2 Hydolysis of (1) in aqueous $HClO_4$

The decomposition of (1) in aqueous $HClO_4$ also followed *pseudo* first-order kinetics (eqn. 2.1) and, as before, plots of ln (A_t/A_0) were linear over at least 5 half-lives. A typical first-order plot for the hydrolysis of (1) in 2.0M $HClO_4$ at 37°C is shown in Figure 2.8. Values of k_0 increase with increasing acidity (Table 2.4) and they contain a

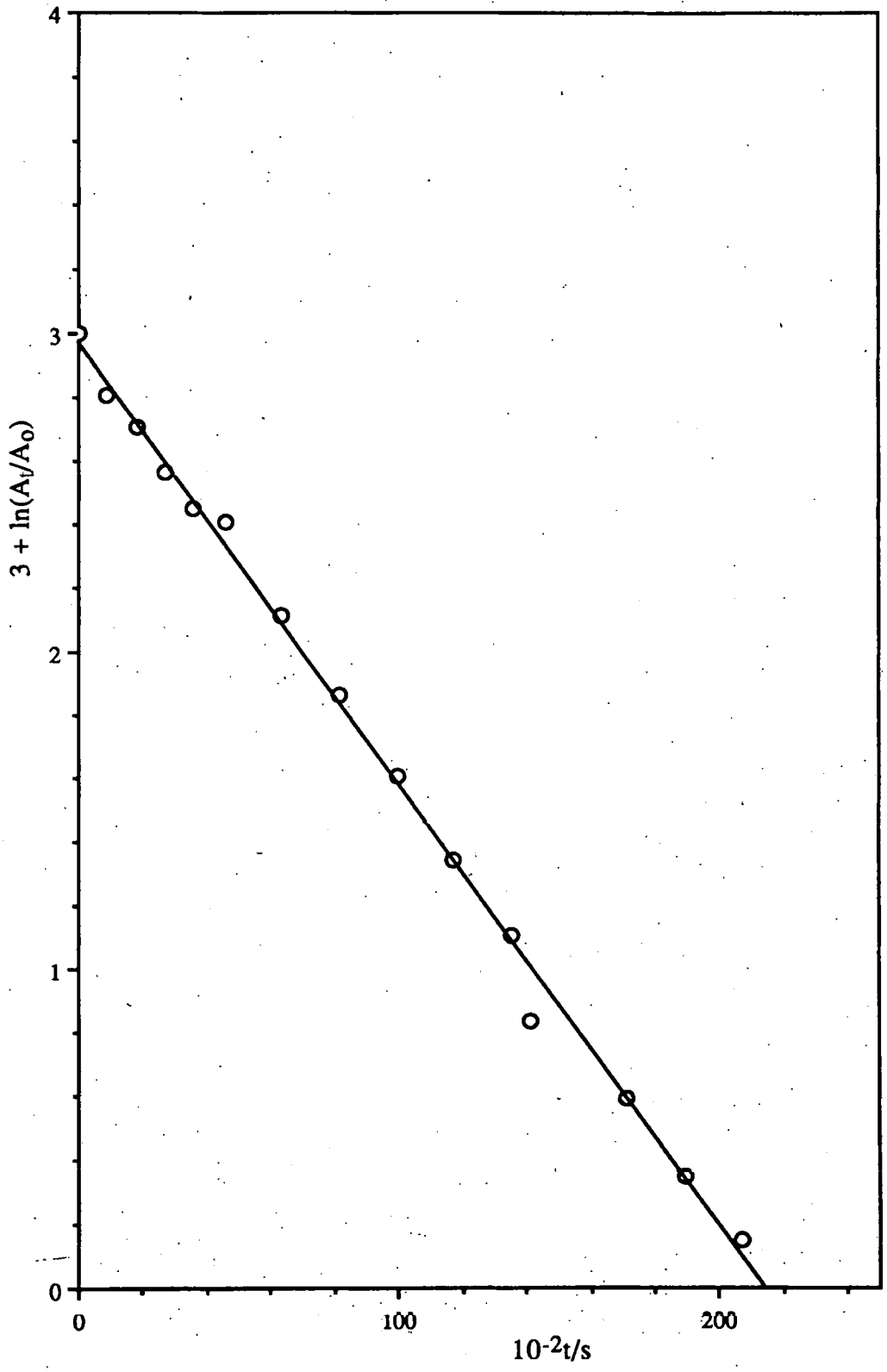

Figure 2.8 *First-order plot of $\ln(A_t/A_o)$ against time for the hydrolysis of (1) in 2.0M $HClO_4$ at 37°C.*

term for an acid catalysed pathway as well as the $B_{A1}2$ pathway for water (eqn. 2.5, where $f(H^+)$ is an unspecified function of the hydrogen ion concentration). The

$$k_o = k_H f(H^+) + k_w a_w \quad \ldots.(2.5)$$

calculated values of a_w and $k_H f(H^+)$ $(= k_o - k_w a_w)$ are also given in Table 2.4.

Table 2.4 Rate coefficients for the hydrolysis of (1) in $HClO_4$ at 37°C. Initial [(1)] = ca 1mM.

$[HClO_4]$	$10^5 k_o/s^{-1}$	a_w[a]	$k_H f(H^+)/s^{-1}$
3.0	18.6	0.859	17.4
2.0	13.1	0.916	12.6
1.0	8.76	0.963	7.38
0.5	4.82	0.982	3.42
0.1	2.54	0.996	1.11

[a] Values of a_w are calculated using equation 2.6 from tabulated values of the molal

$$\ln a_w = \nu m \phi / 55.51 \quad \ldots.(2.6)$$

osmotic coefficient of the solute, ϕ[122] where ν is number of ions formed from 1 mole of electrolyte and m is the molality of the solute. Values of ϕ are tabulated at 25°C but their variation with temperature is only small and ϕ 25°C ~ ϕ 37°C.

Hydrolysis of the β-lactone (1) is more complicated than the hydrolysis of β-propiolactone and β-butyrolactone because of two potential reactive sites, ie. the β-lactone ring and the terminal methyl ester (Figure 2.9). Unfortunately, the method

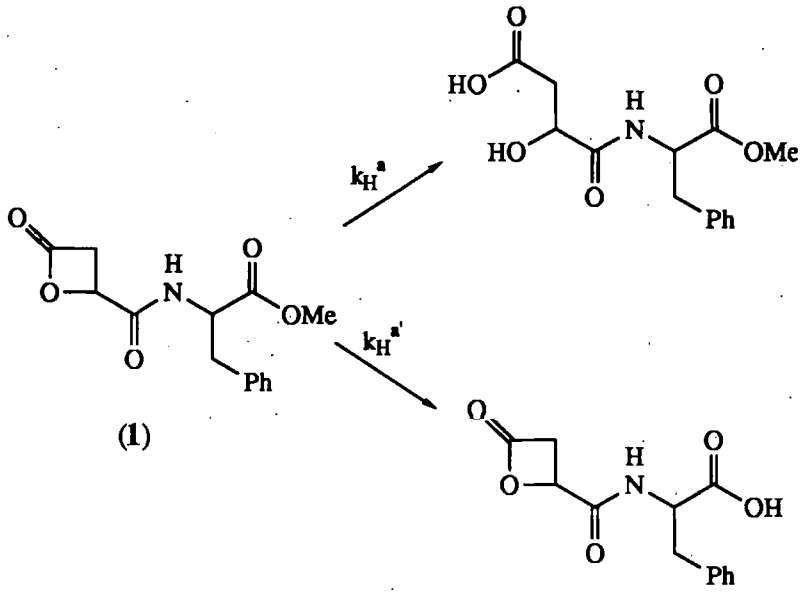

Figure 2.9 Two possible sites in (1) where hydrolysis may occur

of following the decomposition of (1) does not discriminate between these two reactions, and experimental values of k_H are the sum of both (Equation 2.7).

$$k_H = k_H^a + k_H^{a'} \qquad \ldots.(2.7)$$

The potential contribution from $k_H^{a'}$ to the overall rate was estimated from a brief study of the rate of hydrolysis of the methyl ester of aspartame in $HClO_4$ at 37°C using an HPLC procedure to monitor the loss of aspartame. These reactions also followed *pseudo* first-order kinetics (rate = k_o[aspartame]) and values of k_o and $k_H^{a'}$ ($k_H^{a'} = k_o/[HClO_4]$) are summarised in Table 2.5. The value of $k_H^{a'}$ (ca 2.28 x $10^{-5} M^{-1}s^{-1}$) shows that hydrolysis of the terminal methyl ester probably makes a 35% contribution to the overall rate of acid catalysed hydrolysis of (1) in aqueous $HClO_4$ whereas ca 65% is attributable to the β-lactone moiety. Using this

Table 2.5 Acid catalysed hydrolysis of aspartame in aqueous $HClO_4$ at 37°C. Initial [aspartame] = ca 1mM.

$[HClO_4]$/M	$10^5k_o/s^{-1}$	$10^5k_H^{a'}/M^{-1}s^{-1}$
1.0	2.34	2.34
3.0	6.66	2.22

approximation values of $k_Hf(H^+)$, $k_H^af(H^+)$ and $k_H^{a'}[H_3O^+]$ are given in Table 2.6 for the hydrolysis of the β-lactone (1) together with the relevant values of the pH and H_o.

Table 2.6 Variation of $k_H^af(H^+)$ with pH and H_o for the hydrolysis of (1) in aqueous $HClO_4$ at 37°C.

$[HClO_4]$/M	pH	H_o[a]	$10^5k_Hf(H^+)/s^{-1}$	$10^5k_H^{a'}[H_3O^+]/s^{-1}$	$10^5k_H^af(H^+)/s^{-1}$
3.0	-0.477	-1.23	17.4	6.84	10.56
2.0	-0.300	-0.78	12.6	4.56	8.04
1.0	0.000	-0.22	7.38	2.28	5.10
0.5	0.301	0.6 [b]	3.42	1.14	2.28

a) Data from Paul and Long[123]

b) Data from extrapolation of Long's data[104]

From these data it is apparent that the plot of log ($k_H^af(H^+)$) against -pH is reasonably linear with slope = 0.85 (Figure 2.10) whereas the plot against $-H_o$ (Figure 2.11) is also linear but with slope =0.4. It follows that the acid catalysed hydrolysis of the β-lactone moiety of (1) is proportional to $[H_3O^+]$ rather than the H_o acidity function with values of $5.47 \times 10^{-5} M^{-1}s^{-1}$ and $3.19 \times 10^{-5} M^{-1}s^{-1}$ for k_H and k_H^a respectively. This

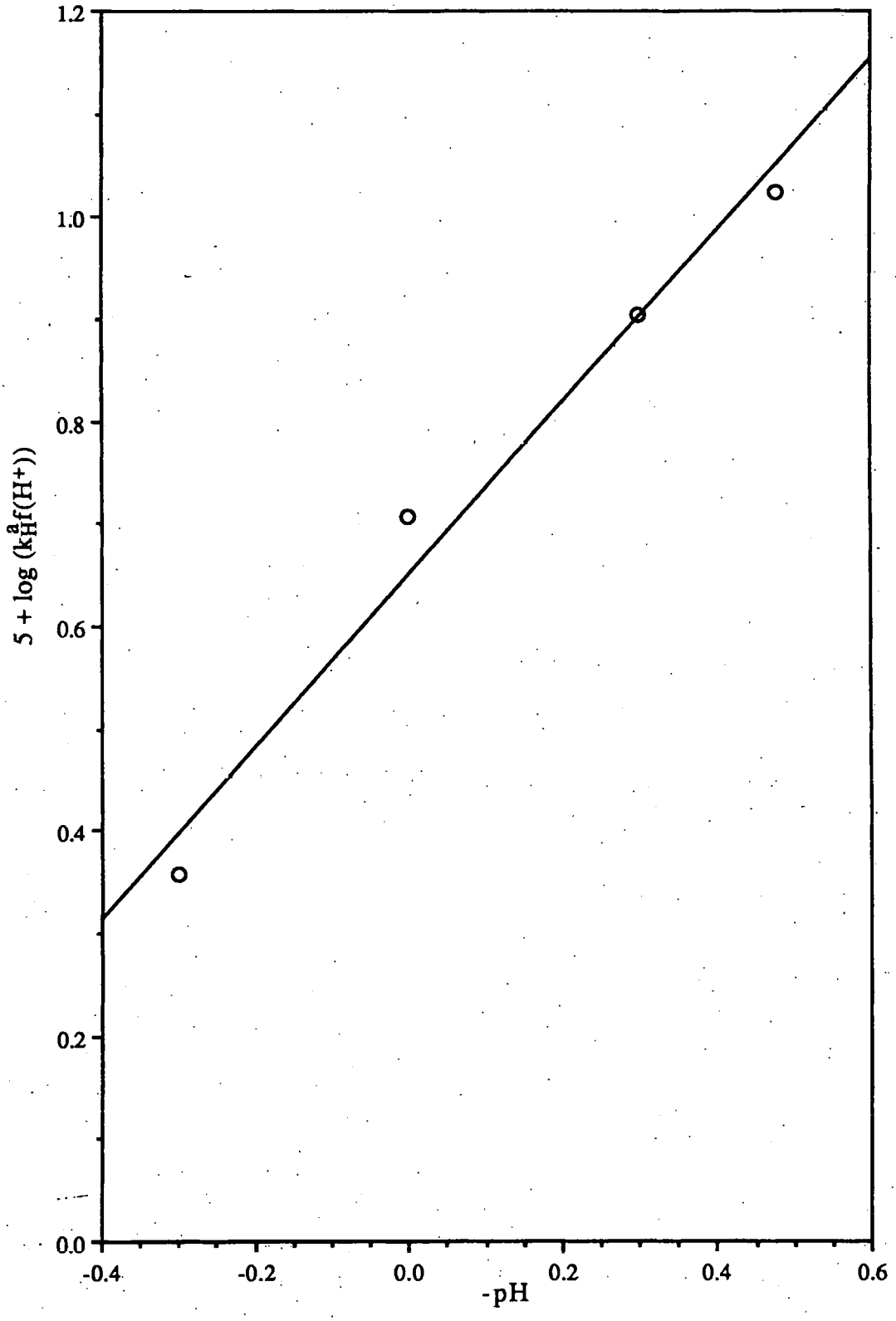

Figure 2.10 *A plot of Log ($k_H^a f(H^+)$) versus -pH for the hydrolysis of (1) in $HClO_4$ at 37°C*

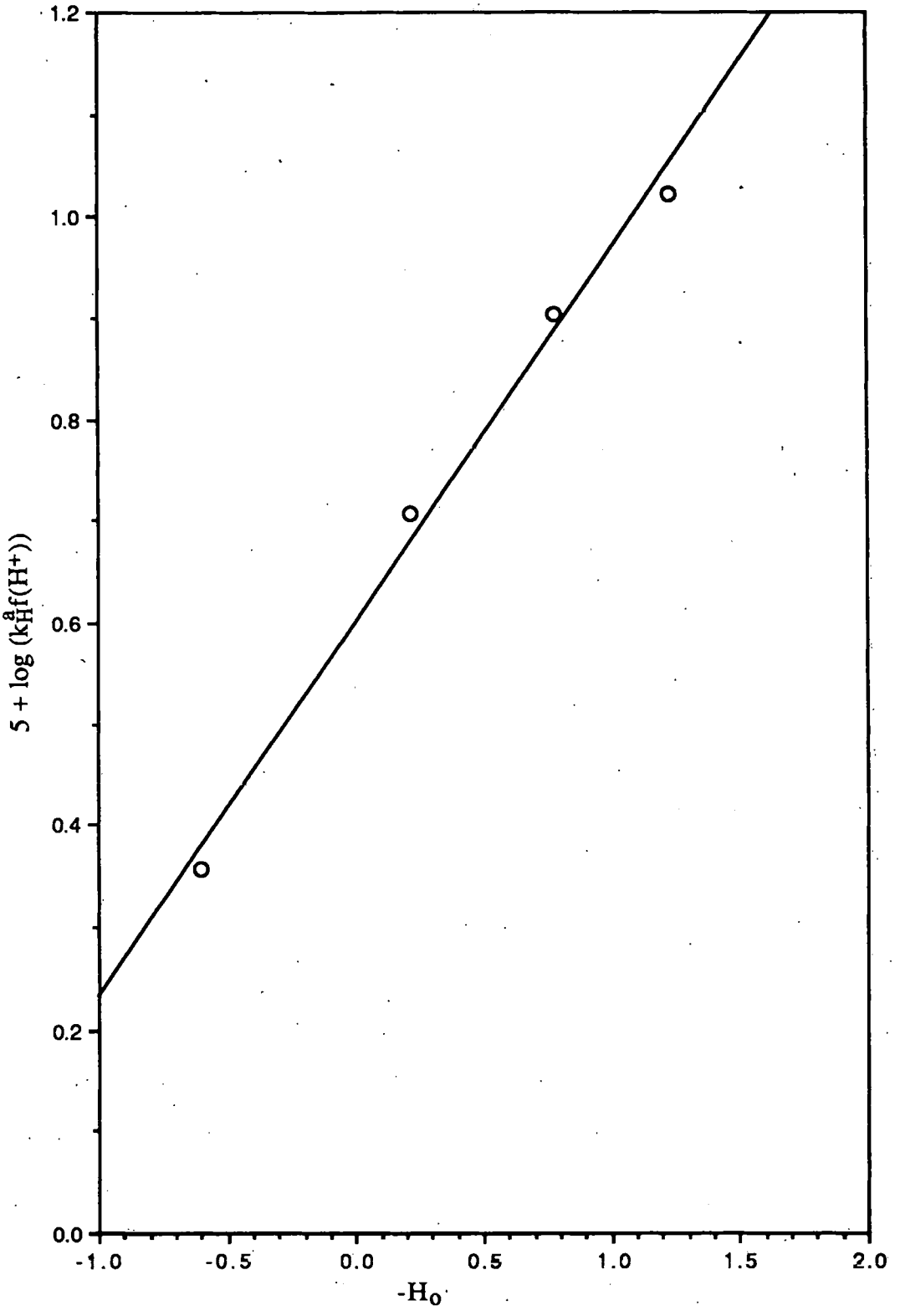

Figure 2.11 Log ($k_H^a f(H^+)$) versus $-H_o$ for the hydrolysis of (1) in acid at 37°C

indicates hydrolysis by an $A_{AC}2$ mechanism rather than the $A_{AC}1$ mechanism ($k \alpha H_o$) found previously for β-propiolactone and β-butyro-lactone.[104] A possible explanation for the different hydrolysis mechanisms is that electron withdrawal by the carboxamide function of (1) destabilises the acylium ion intermediate for the $A_{AC}1$ pathway and the $A_{AC}2$ pathway is therefore energetically favoured.

2.3.3 Hydrolysis of (1) in dilute NaOH

The hydrolysis of (1) above pH7 at 37°C became too fast to follow by the HPLC procedure. The reactions could be assessed, however, by monitoring the uptake of OH^- using a pH-stat procedure (see Chapter 7).

The hydrolysis of (1) in base (as in acid) is complicated by two possible pathways (Figure 2.12), both of which consume 2 moles of OH^- and give the same final product

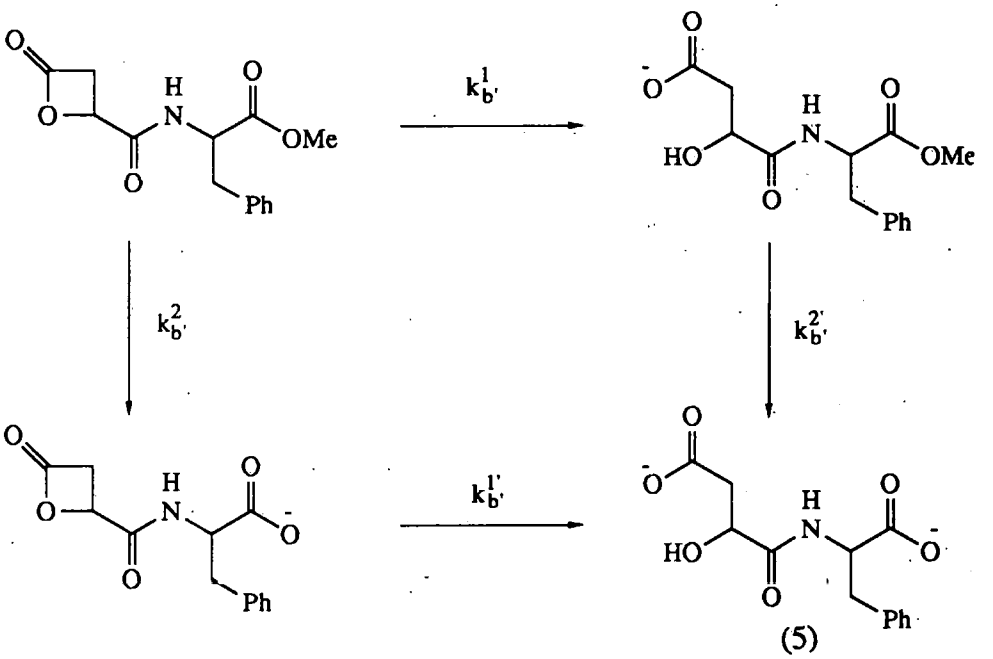

Figure 2.12 Hydrolysis of (1) in aqueous alkali

(5). Although the individual rate coefficients k_b^1, k_b^2, $k_b^{1'}$, $k_b^{2'}$ cannot be evaluated from the pH-stat data, an approximate solution can be obtained assuming $k_b^1 = k_b^{1'}$ and $k_b^2 = k_b^{2'}$ and treating the experimental data as two parallel reactions.

2.3.3.1 Hydrolysis of aspartame in dilute NaOH

The rate constant $k_b^{2'}$ ($\simeq k_b^{2'}$) was estimated independently by measuring the rate of hydrolysis of aspartame in dilute alkali. A typical profile for the addition of NaOH to aspartame under pH-stat conditions is shown schematically in Figure 2.13. Addition of aspartame to the pH-stat solution at pH 9 resulted in an initial rapid addition

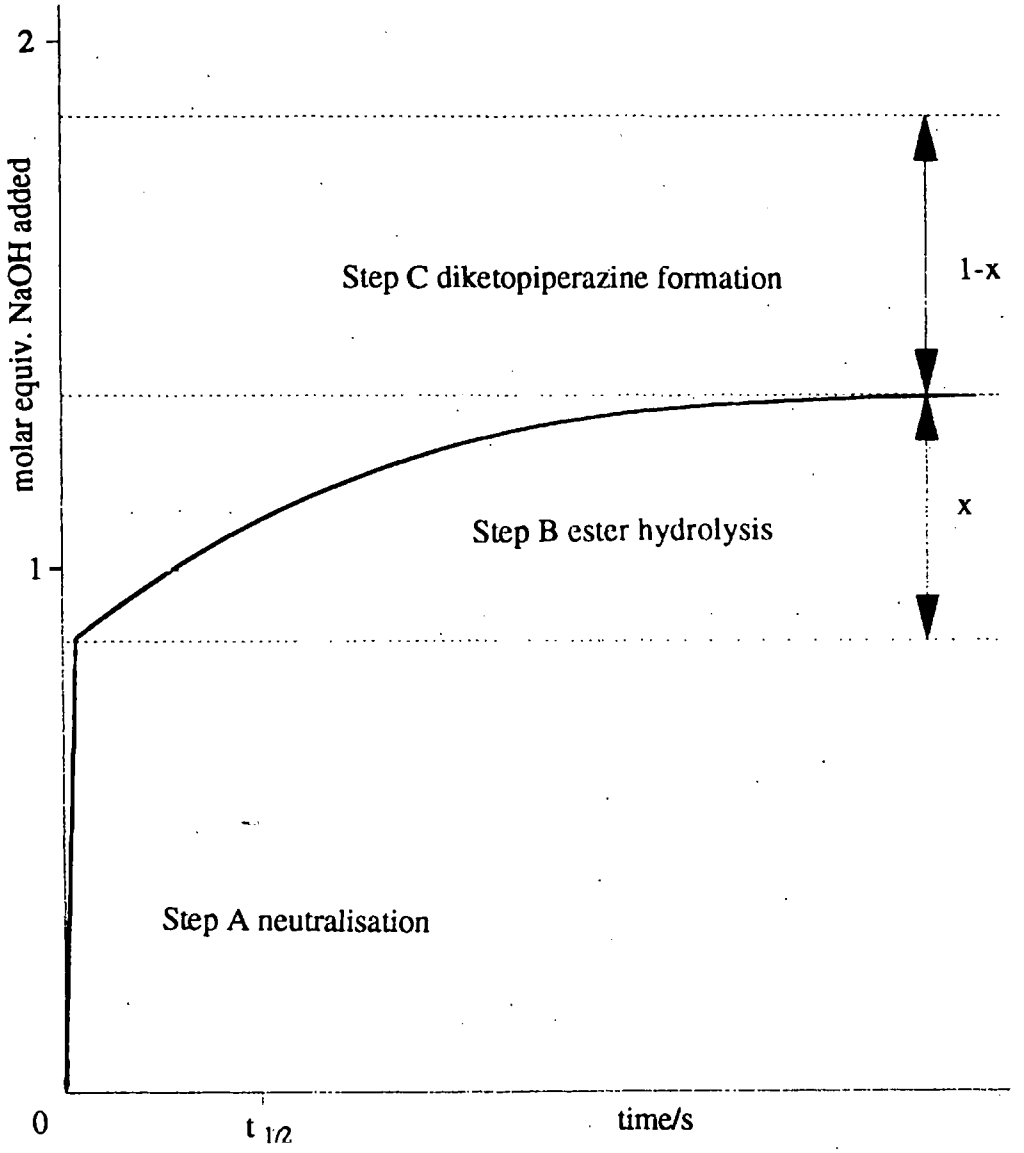

Figure 2.13 *Schematic representation of reaction profile of hydrolysis of aspartame by OH^- at 37°C.*

of 0.86 molar equivalents of base (step A) corresponding to neutralization of the carboxylic acid group. Only 0.86 molar equivalents were required presumably because of buffering by the terminal amino group (pK_a 7-8). Subsequent addition of further NaOH occurred in consort with hydrolysis of the terminal methyl ester (step B). The slow addition terminated with less than 1 molar equivalent of base added implying that only a fraction of the methyl ester is hydrolysed. The remainder probably reacts *via* an alternative pathway which does not either produce an acid or consume hydroxide ions. It is known that dipeptides readily form cyclic diketopiperazines in basic solution[124] and the diketopiperazine (6) is a known metabolite of aspartame.[125] Thus, formation of (6) is probably the second pathway by which aspartame reacts in aqueous base resulting in less than quantitative uptake of NaOH. (Figure 2.14).

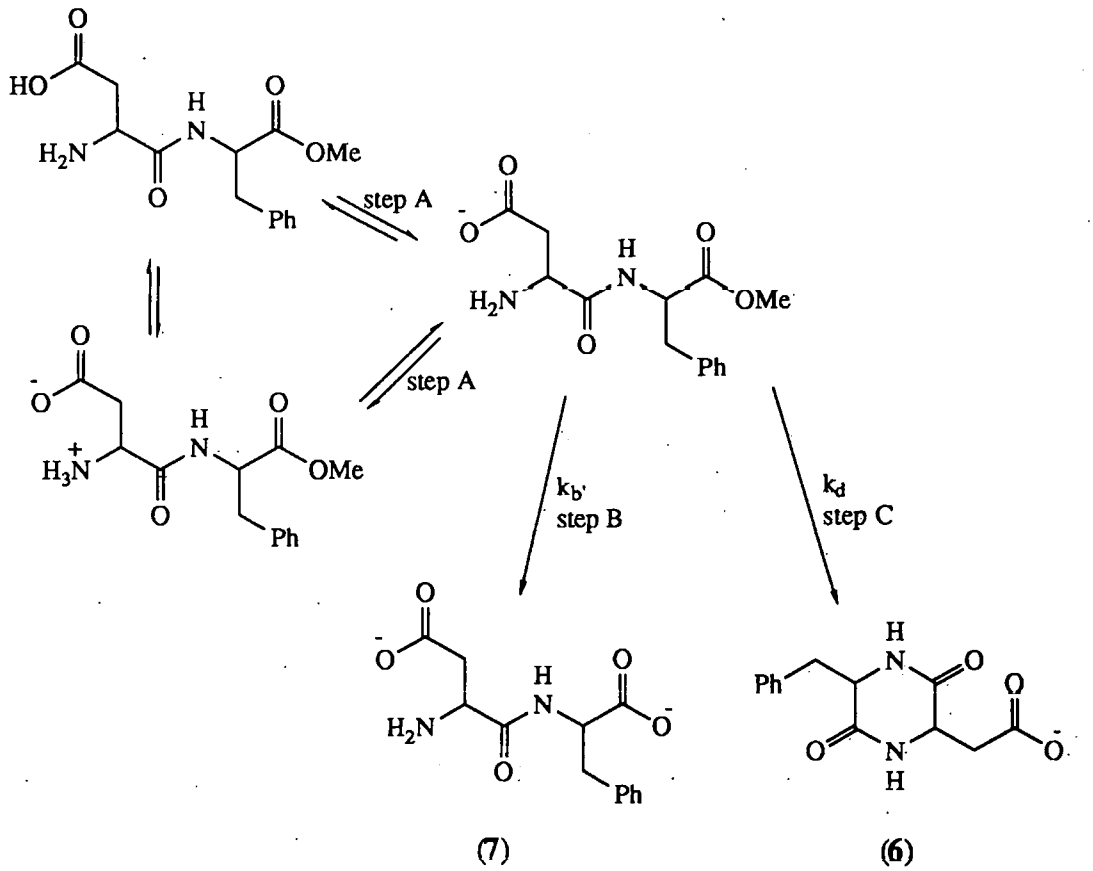

Figure 2.14 Possible reactions of aspartame in aqueous base at pH 9.

From a careful analysis of the NaOH addition by pH-stat, rate coefficients for both the hydrolysis of the methyl ester (k_b') and the formation of the diketopiperazine (k_d) can be estimated. For concurrent, first-order reactions (ie. steps B and C of (Figure 2.14), the overall rate of loss of aspartame equals the sum of the *pseudo* first-order rate coefficients (equation 2.8). Further, the ratio of the diketo-piperazine (6) to

$$\text{Rate} = (k_b' + k_d)\,[\text{aspartame}] \qquad \ldots(2.8)$$

dicarboxylic acid product (7) equals the ratio of the *pseudo* first-order rate coefficients (equation 2.9). The sum ($k_b' + k_d$) is given by the observed half-life, and the k_d/k_b'

$$\frac{k_d}{k_b'} = \frac{[6]}{[7]} \qquad \ldots(2.9)$$

ratio by (1-x)/x where x = the total molar equivalents of NaOH added to effect hydrolysis. The results obtained for the hydrolysis of aspartame at pH9 and 37°C, summarised in Table 2.7, give an average $k_{h'} = 4.4\times10^{-5}\ s^{-1}$. Thus, the second order rate coefficient for the base catalysed hydrolysis of aspartame methyl ester (Rate = k_b' [aspartame][OH^-]) has an approximate value $k_b' = 4.4\ M^{-1}s^{-1}$ at 37°C.

Table 2.7 Rate coefficients obtained from the hydrolysis of aspartame at pH9 using pH-stat method. Initial addition of aspartame ca. 10^{-6} mole.

$t_{1/2}$/s	$10^5\,(k_b'+k_d)/s^{-1}$	k_d/k_b'	$10^5 k_b'/s^{-1}$	$10^5\,k_d/s^{-1}$
8280	8.37	1.04	4.09	4.28
7080	9.79	1.09	4.68	5.11

2.3.3.2 Hydrolysis of (1) in dilute NaOH

A typical pH-stat plot for the hydrolysis of (1) at pH9 and 37°C is shown in Figure 2.15. Two molar equivalents of NaOH are ultimately added, so the product must be the dicarboxylic acid (5). The overall rate of loss of (1) is given by equation 2.10 where $k_o = k^1_{b'} + k^2_{b'}$ (Figure 2.12). It follows that the rate of β-lactone hydrolysis

$$\frac{-d[(1)]}{dt} = k_o[(1)] \qquad ...(2.10)$$

can be obtained from the overall rate by allowing for the concurrent rate of methyl ester hydrolysis. To obtain $k^2_{b'}$ a value of $k^2_{b'}$ = rate of methyl ester hydrolysis of aspartame (Section 2.3.3.1) was assumed. The values of k_o calculated from the initial rate measurements and approximate values of $k^1_{b'}$ and $k^2_{b'}$ are summarised in Table 2.8.

Table 2.8 Rate coefficients obtained from the hydrolysis of (1) in NaOH at 37°C.

pH	10^9 Initial Rate/mol^{-1}s^{-1}	10^5[(1)]/mol	10^4k_o/s^{-1}	$10^5k^2_{b'}$ /s^{-1}	$10^4k^1_{b'}$ /s^{-1}
8.0	1.80	1.07	1.68	0.44	1.64
8.0	1.65	1.07	1.54	0.44	1.50
9.0	14.8	1.07	13.8	4.4	13.4

The results suggest that the rate of β-lactone hydrolysis for (1) at pH8.9 and 37°C is ca. 35 fold faster than the rate of hydrolysis of the terminal methyl ester. Thus, to a good approximation, the rate coefficient for β-lactone hydrolysis ($k^1_{b'}$) can be obtained from the integrated kinetic data (ie. plots of $\ln\{(V_\infty - V_t)/V_\infty\}$ against time, where V_∞=the calculated volume of NaOH added (cm^3) to hydrolyse the β-lactone moiety and V_t = NaOH volume added at time t). These plots are reasonably linear for ca. 90% of the reaction of the first equivalent of NaOH, as shown in Figure 2.16 for the hydrolysis of

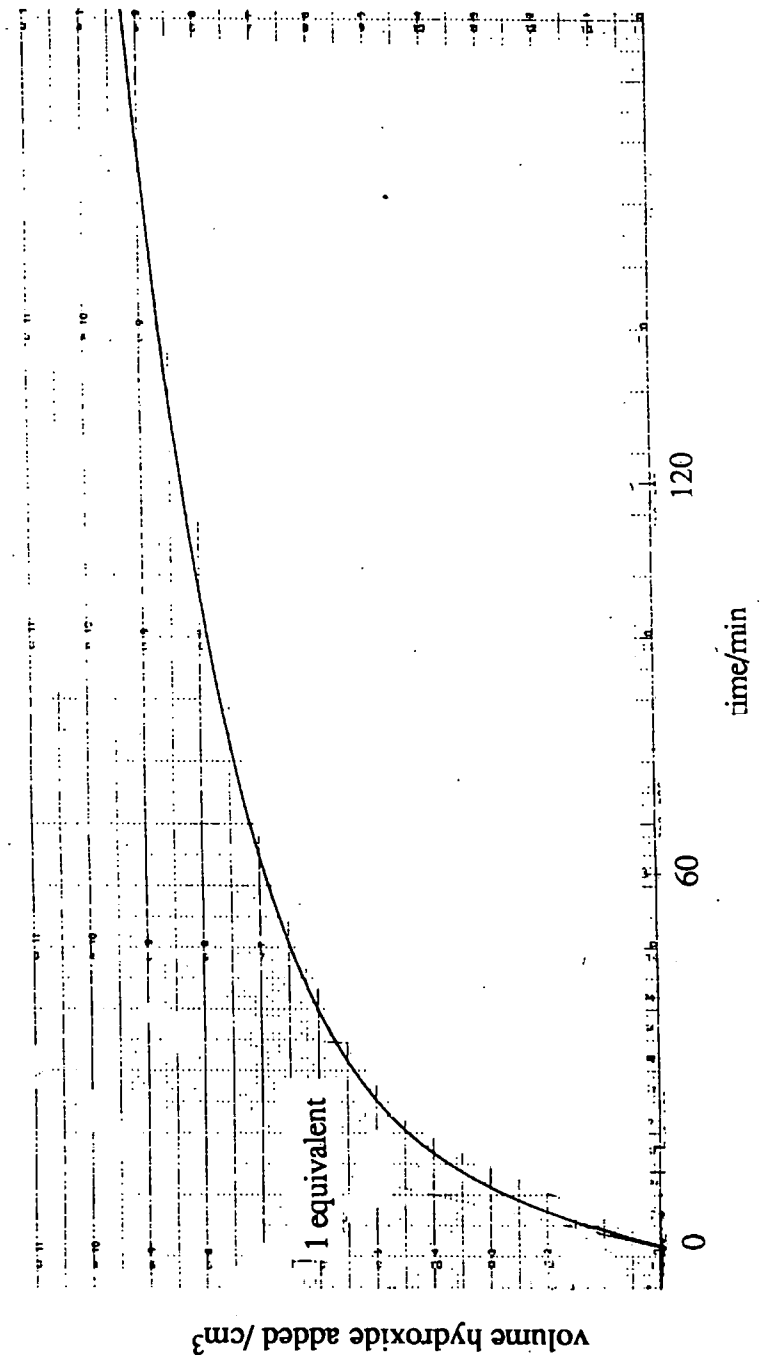

Figure 2.15 Typical pH- stat plot for the hydrolysis of (1) at pH 9 and 37°C.

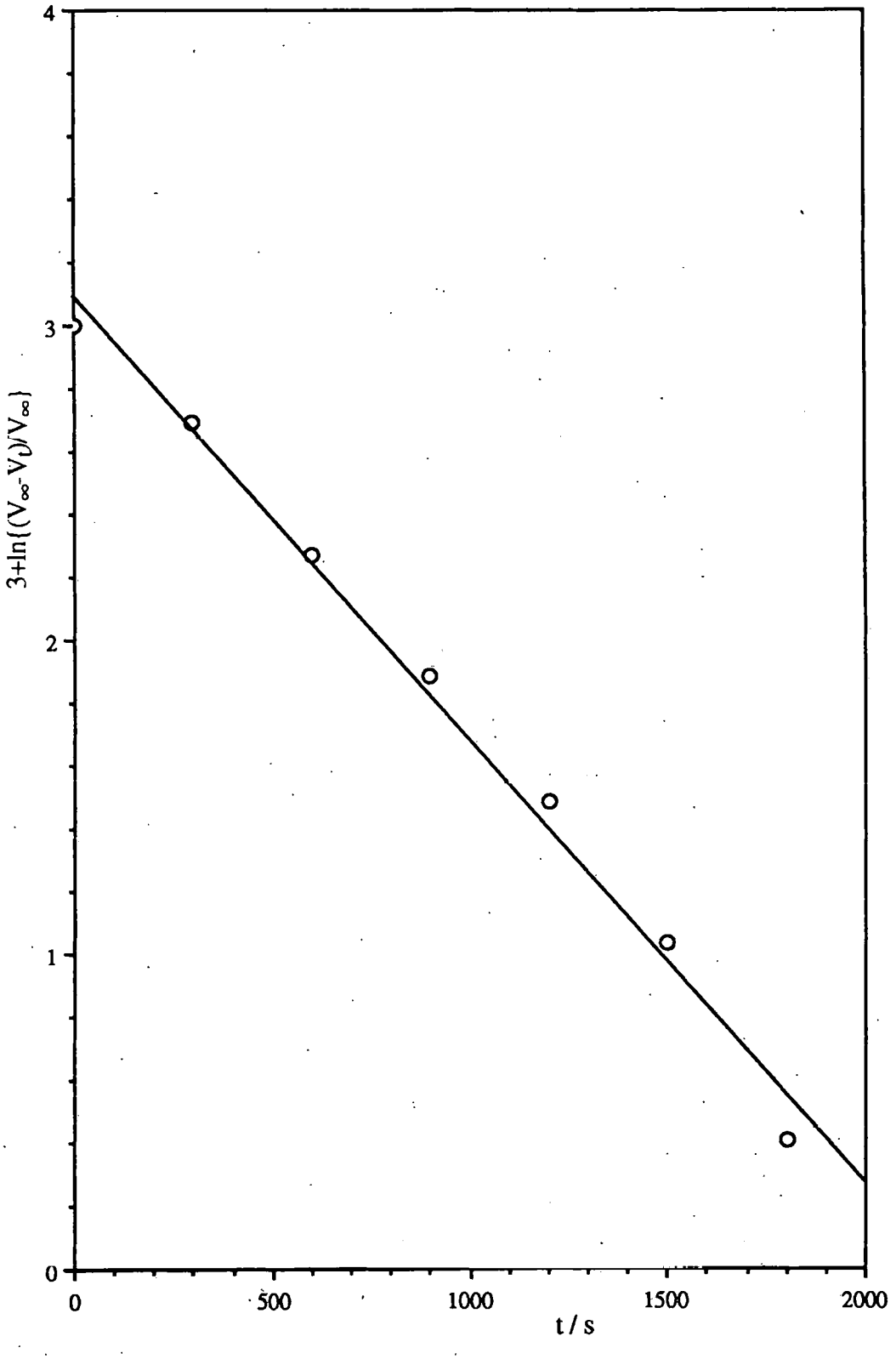

Figure 2.16 *First order plot of $\ln\{(V_\infty - V_t)/V_\infty\}$ against time for the hydrolysis of (1) at pH9 and 37°C.*

(1) at pH9 and 37°C. The values of k_b^1 obtained by this method are summarised in Table 2.9 and they agree satisfactorily with those in Table 2.8.

Table 2.9 Determination of k_b^1 at 37°C from integrated plots of NaOH addition under pH-stat conditions.

pH	$10^4 k_b^1/s^{-1}$
8.0	1.62
8.0	1.50
9.0	14.1

The results of the hydrolysis of β-lactone (1) were also examined by the time ratio method[126] to evaluate k_b^2 at pH9. The time ratio method depends on a best fit to a set of tabulated data and is therefore approximate. This corresponded to $k_b^2/k_b^1 = 0.05$, $k_b^1 = 13 \times 10^{-4} s^{-1}$ and $k_b^2 = 6.5 \times 10^{-5} s^{-1}$ at pH9 and 37°C. The k_b^2 value agrees well with that estimated from the hydrolysis of aspartame, which justifies the assumption of similar rates for the hydrolysis of the methyl ester in (1) and aspartame.

Optimum values of k_o, k_b^1 and k_b^2 for the hydrolysis of β-lactone (1) at 37°C are summarised in Table 2.10. These suggest that both hydrolyses have a first-order

Table 2.10 Summary of rate constants for reaction of (1) with NaOH at 37°C. (Initial [(1)] = ca. 10^{-5} mole).

pH	$10^4 k_o/s^{-1}$	$10^5 k_b^1[OH^-]/s^{-1}$	$10^5 k_b^2[OH^-]/s^{-1}$
8	1.61	15.6 ± 1.4	0.57
9	13.8	133 ± 26	5.65 ± 2.7

dependence on [NaOH] (equation 2.11) which is indicative of a base catalysed

$$\text{Rate} = (k_b^1 + k_b^2)\,[OH^-][(1)] \qquad \ldots(2.11)$$

acyl-oxygen fission ($B_{AC}2$) mechanism for both reactions. Further, above pH8 contributions from the spontaneous water reaction (k_w) are negligible. The results lead to values of $k_B = 143\ M^{-1}s^{-1}$ and $k_b^2 = 6\ M^{-1}s^{-1}$ for the second order rate coefficients for the hydrolysis of the β-lactone and methyl ester of (1) respectively, at 37°C. The estimated value of k_B for the hydrolysis of β-propiolactone at 37°C is $5.27\ M^{-1}s^{-1}$.[104] Hence, (1) is ca. 30 fold more reactive than β-propiolactone to OH^--catalysed hydrolysis probably because of electron withdrawal by the carboxamide moiety at the C_4 position.

2.4 The pH profile

In the absence of buffer components, the hydrolysis of the β-lactone of (1) is described by equation 2.12 where $k_H^a = 3.19 \times 10^{-5}\ M^{-1}s^{-1}$; $k_w = 1.43 \times 10^{-5}\ s^{-1}$ and $k_B = 143\ M^{-1}s^{-1}$ at 37°C. These lead to the calculated pH- log k_o profile shown in Figure 2.17.

$$\text{Rate} = k_o[(1)] = (k_H^a[H_3O^+] + k_w a_w + k_B[OH^-])\,[(1)] \qquad \ldots(2.12)$$

The points of inflection in the pH-log k_o profile indicate changes in the hydrolysis mechanisms from $A_{AC}2$ to $B_{A1}2$ and finally to $B_{AC}2$ pathway with increasing pH. In the physiological pH range (2-7), β-lactone (1) undergoes alkyl-oxygen bond fission, which generates an alkylating agent.

2.5 Reaction of (1) with nucleophiles other than H_2O

Evidence in the previous section showed that buffer components catalysed the decomposition of the β-lactone (1), but the catalytic mechanism was not established. This section reports the decomposition of (1) in the presence of various nucleophiles including the buffer components. The reactions were examined at several pH values, a constant ionic strength of 0.2 ($NaClO_4$) and 37°C. In some examples, the products

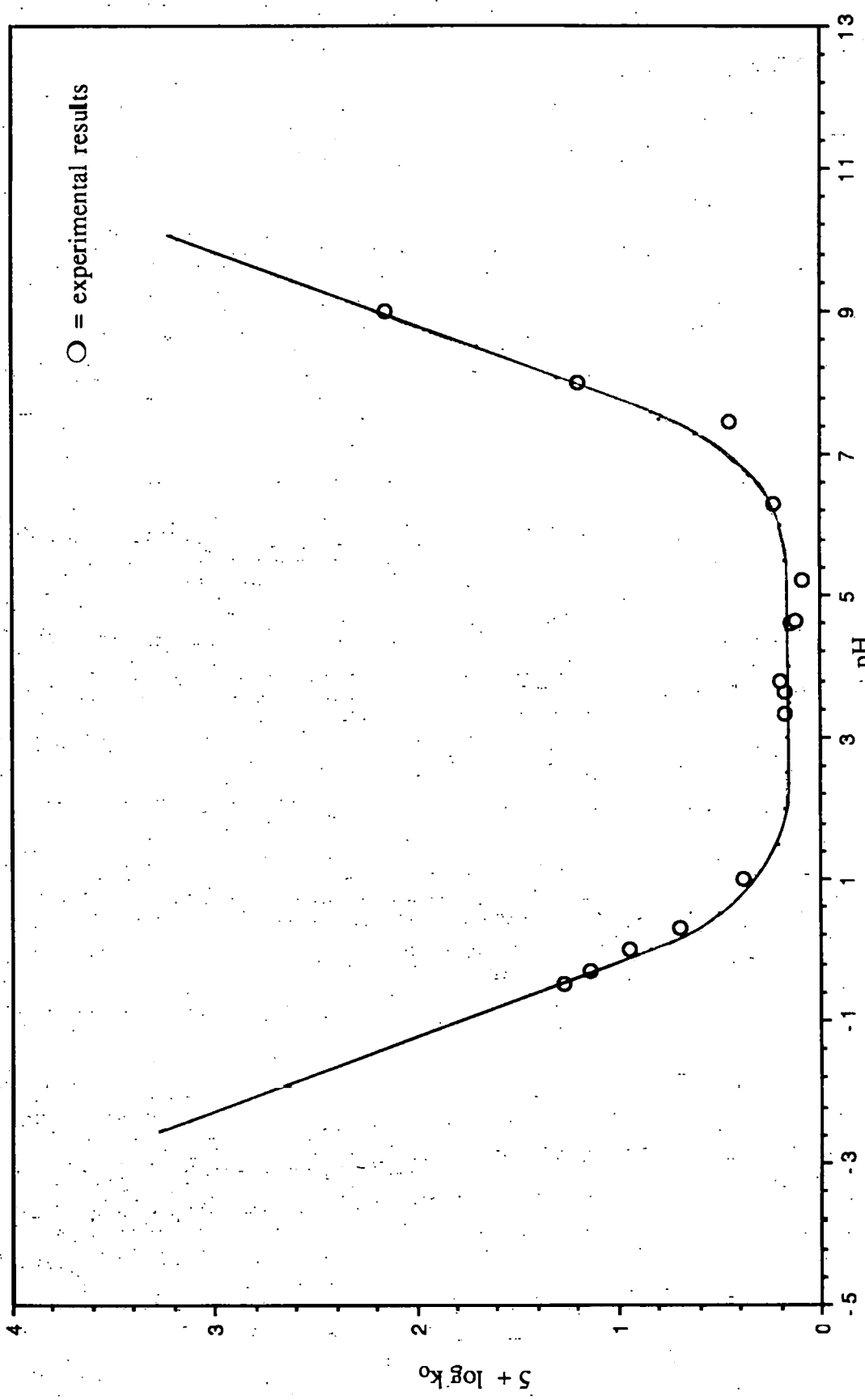

Figure 2.17 Calculated pH- log k_o profile for the hydrolysis of the β-lactone moiety of (1) at 37°C.

were either isolated and characterised or examined *in-situ* by ^{13}C-nmr spectroscopy. The results are compared with literature data for β-propiolactone and ^{13}C-nmr data for reaction of other β-lactones with nucleophilic reagents.

2.5.1 Reaction of β-lactone (1) with NaSCN

The reactions were followed by the disappearance of (1) using the HPLC procedure described in Chapter 7. Good *pseudo* first-order kinetics (Equation 2.13) were

$$\text{Rate} = k_o\,[(1)] \qquad \ldots(2.13)$$

observed and are exemplified by the typical linear plot of $\ln(A_t/A_o)$ against time for the reaction of (1) with 0.05M NaSCN in 0.1M $HClO_4$ at 37°C in Figure 2.18. At constant pH, k_o increased linearly with [NaSCN] as shown in Table 2.11 and by the plot of k_o against [NaSCN] at pH 4.62 in Figure 2.19.

It follows that the decomposition of (1) in the presence of thiocyanate ion conforms with (Eqn. 2.14), where k_o' refers to the uncatalysed decomposition and k_{SCN^-} refers

$$\text{Rate} = (k_o' + k_{SCN^-}\,[SCN^-])[(1)] \qquad (2.14)$$

to the NaSCN catalysed component. Values of k_{SCN^-} at 3 different pHs,summarised in Table 2.12, are virtually constant with an average value of $k_{SCN^-} = 9.43\ (\pm.26) \times 10^{-3}\ M^{-1}s^{-1}$.

Table 2.12 Variation of k_{SCN^-} as a function of pH

pH	$10^3 k_{SCN^-}$ /$M^{-1}s^{-1}$
(0.1 M $HClO_4$)	9.28
4.62	9.51
6.28	9.51

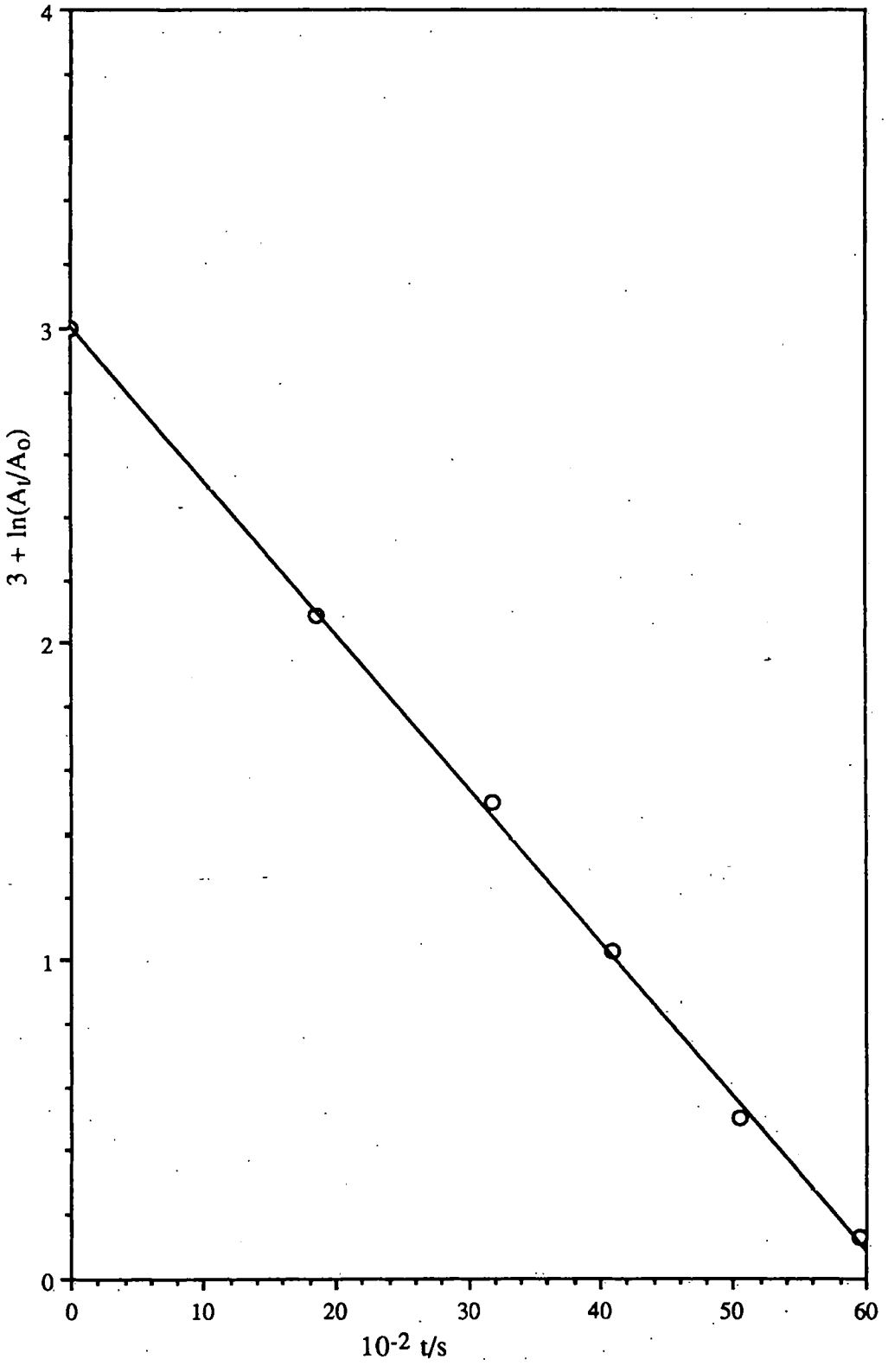

Figure 2.18 First-order plot of $ln(A_t-A_o)$ versus time for the reaction of (1) with 0.05 M NaSCN in 0.1M$HClO_4$ at 37°C.

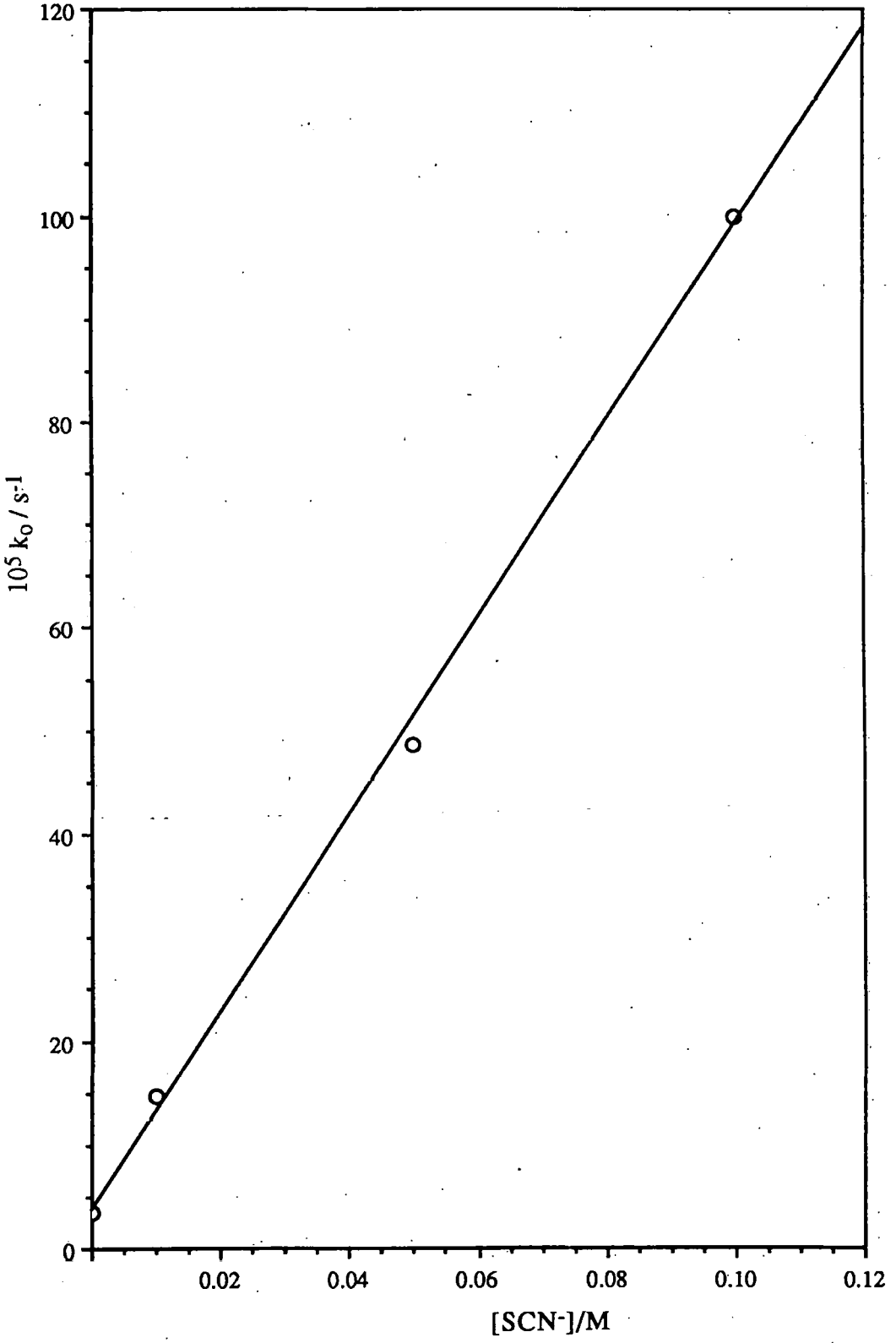

Figure 2.19 Variation of k_o with [SCN⁻] for decomposition of (1) at pH 4.62 and 37°C.

Table 2.11 Variation of k_o with [NaSCN] for decomposition of (1) at 37°C. Initial [(1)] = ca. 1mM.

pH	[SCN]/M	$10^5 k_o/s^{-1}$
(0.1M $HClO_4$)	0.05	48.7
(0.1M$HClO_4$)	0.01	11.2
(0.1M$HClO_4$)	0.00	2.5
4.63	0.10	100.0
4.62	0.05	48.7
4.61	0.01	14.8
4.63	0.00	3.5
6.28	0.10	96.1
6.25	0.05	51.3
6.22	0.01	10.3

Since reactions involving acyl-O fission are not prone to nucleophilic catalysis, it seems probable that reaction of (1) with NaSCN involves pH independent alkyl-oxygen bond cleavage ie. neutral (1) is involved. This points to attack by SCN^- on the C_4-atom of (1), which is confirmed by the product analysis reported below.

2.5.2 Reaction of β-lactone (1) with NaCl and NaBr

The effect of added Br^- and Cl^- on the decomposition of (1) in 0.1M $HClO_4$ at 37°C was briefly examined. The reactions were similar to those with added NaSCN,

showing good *pseudo* first-order behaviour and catalysis by added halide ions. Variation of k_o (Eqn. 2.1) with halide ion concentration are reported in Table 2.13.

Table 2.13 Effect of [X^-] on k_o for the reaction of (1) with X^- at 37°C in 0.1M $HClO_4$ initial [(1)] = ca 1mM.

X^-	[X^-]/M	$10^5 k_o/s^{-1}$
none	0.0	2.50
Br^-	0.1	11.7
Br^-	0.05	6.90
Br^-	0.01	3.37
Cl^-	0.1	4.37

As for NaSCN, k_o is linearly proportional to the concentration of added halide ion and values of $k_{Br} = 9.24 \times 10^{-4}$ $M^{-1}s^{-1}$ and $k_{Cl} = 4.4 \times 10^{-4}$ $M^{-1}s^{-1}$ are obtained for second order rate coefficients equivalent to equation 2.14.

2.5.3 Product analysis

The HPLC fractions for the decomposition of the β-lactone (1) in aqueous solution containing added nucleophiles show that different products form in the presence of nucleophilic anions such as SCN^- and Cl^- (Figure 2.20). In trace (A), a new product is evident at Rt = 5.65 min. for decomposition in the presence of SCN^- whereas in trace (B) for added Cl^-, the new product is evident at Rt = 2.78 min. Since both products are stable in the aqueous reaction solutions, they probably relate to nucleophilic displacement at the alkyl rather than acyl C-atom of the β-lactone (1).

For reactions with added NaSCN and morpholine, the products were isolated and further characterised by mass spectrometry. The product experiments were carried out in acetonitrile to minimise competing hydrolysis reactions. It was established,

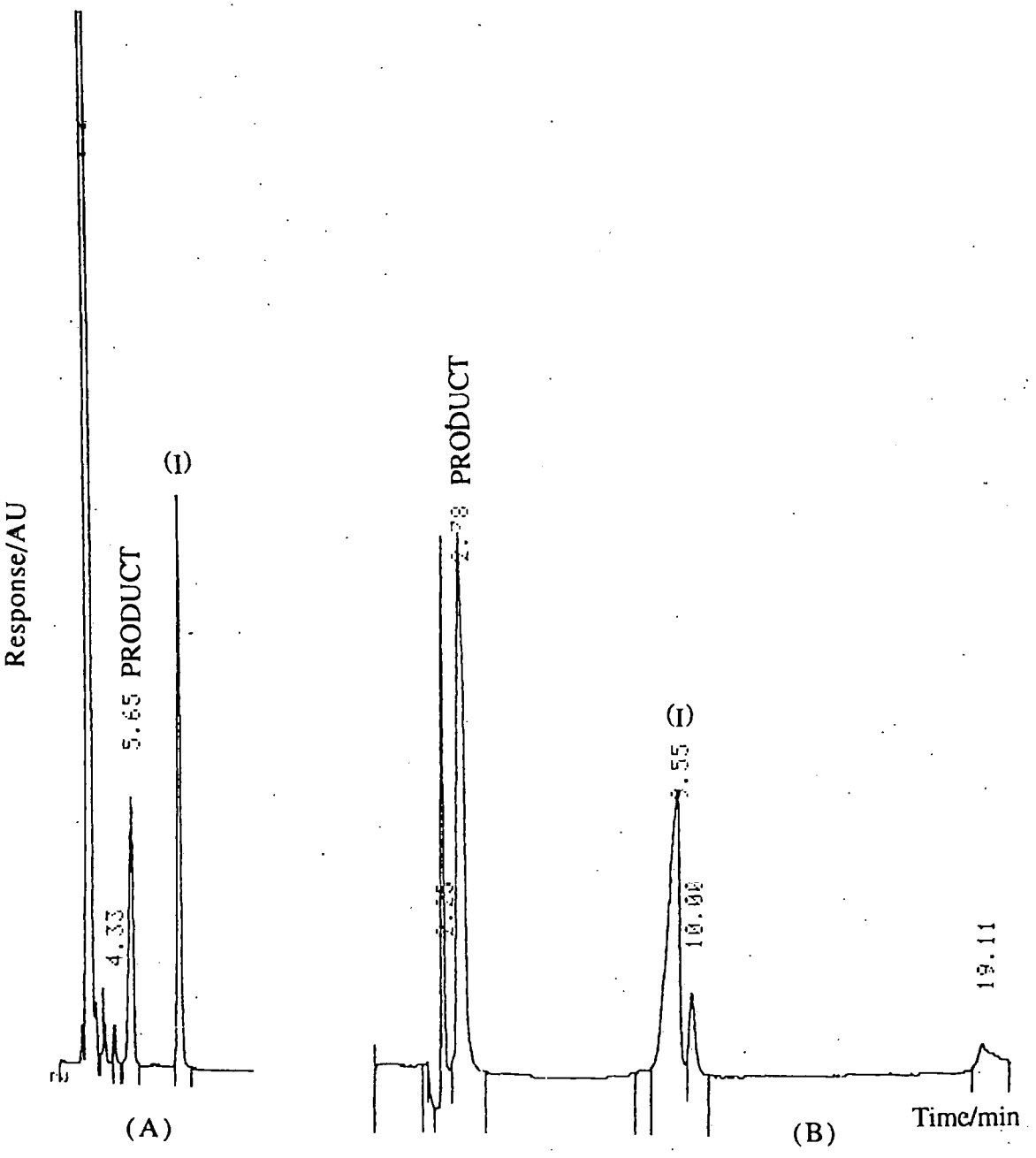

Figure 2.20 HPLC traces for the decomposition reactions of (1) in the presence of SCN^- (A) and Cl^- (B)

however, that in the case of SCN^- at least, that the isolated product had a similar HPLC retention time to that formed in aqueous media.

2.5.3.1 Reaction of (1) with NaSCN

The FAB mass spectral fragmentation of the product with Rt= 5.65 min. (Figure 2.20) is summarised in Table 2.14.

The base peak at m/z 130 and the molecular ion at m/z 337 ($M+H^+$) in the positive FAB mass spectrum indicates the incorporation of a thiocyanate moiety. Since acyl thiocyanates hydrolyse readily under the conditions used for product purification (ie.acidification with heptafluorobutyric acid) the product is likely to be the alkyl thiocyanate (8) rather than the acyl thiocyanate (9). The peak at m/z 319 related to the loss of water from the molecular ion is consistent with either (8) or (9), but ions at m/z 291 ($M+H^+-H_2O-CO$) are indicative of a carboxylic acid.

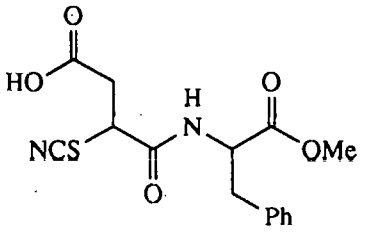

(8)

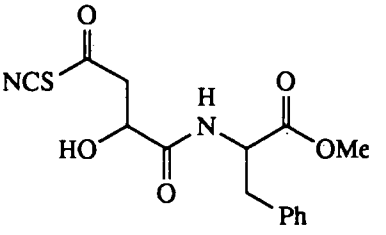

(9)

2.5.3.2 Reaction of (1) with morpholine

The spectroscopic evidence strongly suggests morpholine reacts at the acyl C-atom of the β-lactone (1) to give the hydroxysuccinamide derivative (10). Thus, the ir spectrum shows a broad OH band at 3489 cm^{-1}, characteristic of an alcohol rather than a

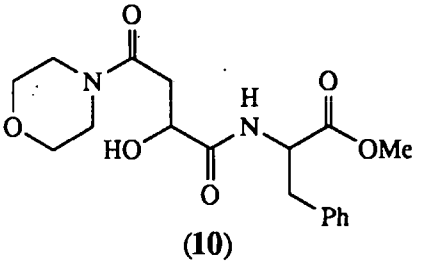

(10)

Table 2.14 FAB mass spectral fragmentation of product with Rt = 5.65 min. (Figure. 2.20).

m/z	R.A./%	Assignment
130	100	$M+H^+$-CO-PheOMe
337	96.9	$M+H^+$
41	80.0	-
115	77.8	-
74	58.2	-
91	54.2	$C_7H_7^+$
120	32.0	$H_2^+N=CHCH_2Ph$
319	3.1	$M+H^+ -H_2O$
291	1.8	$M+H^+-H_2O-CO$

hydrogen- bonded carboxylic acid. There is no evidence in the carbonyl stretching region for either a carboxylic acid or a carboxylate salt, but two amide bands are apparent at 1654 and 1620 cm^{-1}. The EI mass spectrum is summarised in Table 2.15. This shows an ion at m/z 346 corresponding to the loss of water from the molecular ion. There is no subsequent loss of CO (m/z=318) or any evidence for the loss of 45 amu from the molecular ion, a common fragmentation in the EI mass spectrum of carboxylic acids. The ion at m/z 114 is assigned to structure (11) and is consistent with an amide structure for the reaction product.

Table 2.15 Mass spectral fragmentation of the product from reaction of (1) with morpholine

m/z	R.A./%	ion	m/z	ra/%	ion
158	100	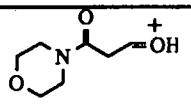	120	12.8	H_2NCHCH_2Ph
57	45.4	-	364	5.5	$M^{\bullet+}$
86	39.7	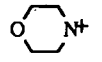	261	3.7	-
114	37.2	(11)	278	2.9	$M^{\bullet+}$ - 
29	30.9	$C_2H_5^+$	303	1.7	-
70	27.1	-	305	1.6	$M^{\bullet+}$-CO_2Me
43	26.6	-	346	0.5	$M^{\bullet+}$-H_2O
91	23.3	$C_7H_7^+$	333	0.3	$M^{\bullet+}$-MeO$\bullet$
186	22.6	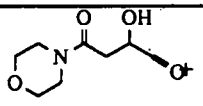			

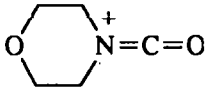

(11)

The product analyses show that nucleophiles react with β-lactone (1) at both the alkyl and acyl C-atoms, depending on their structure. For SCN^- however, the preferred reaction occurs at the alkyl C-atom.

2.5.4 Reactivity of β-lactone (1) towards nucleophiles

The pH independence of the SCN^-, Br^- and Cl^- catalysed decompositions and the isolated product for SCN^- catalysed decomposition show that some nucleophiles react at the alkyl C-atom of β-lactone (1). It is interesting to examine support for this conclusion from the magnitudes of the catalytic rate coefficients obtained for added anions and/or buffer components. Values of the catalytic rate coefficients for Cl^-, Br^-, SCN^-, AcO^-, HCO_2^-, OH^-, and H_2O are summarised in Table 2.16.

Table 2.16 Second order catalytic rate coefficients for the decomposition of (1) at 37°C. Initial [(1)] ca. 1mM.

Catalyst	pK_a[127]	$10^4 k_A^-/M^{-1}S^{-1}$
OH^-	15.75	149×10^4
SCN^-	-2	94.3
Br^-	-8.0	9.24
Cl^-	-7.0	4.3
OAc^-	4.76	3.54
$HCOO^-$	3.75	1.11
H_2O[a]	-1.75	2.6×10^{-3}

a. $k_{H_2O} = k_w/55.5$

All of the nucleophiles significantly enhance the rates of decomposition of (1). Thus OH^-, which reacts *via* the $B_{AC}2$ mechanism, is ca. 16000 fold more reactive towards (1) than SCN^- which reacts nucleophilically at the alkyl C_4-atom.

For several entries in Table 2.16, general base catalysis can be immediately discounted because k_A^- values correlate poorly with catalyst pK_a. In the case of SCN^- and Cl^-, this supports the conclusion drawn from the product analysis (see above). Further, with the exception of catalysis by formate ion (no n-data available) and OH^- ($B_{AC}2$

pathway), the results in Table 2.16 generate a satisfactory, linear Swain-Scott correlation. This is shown in Figure 2.21 as the plot of log $k_{nuc}/k_w^{'}$ (where $k_w^{'}$ = second order rate constant for the reaction of (1) with water) against the Swain Scott parameter (n).[128] This is reasonably linear with a slope (s=nucleophilic selectivity) ca. 0.88. This compares with s=0.77[128] for the nucleophilic selectivity of β-propiolactone. The higher s value indicates greater S_N2 character for the reactions of (1) with nucleophiles. This is not surprising in view of the electron withdrawal by the acyl group which will enhance the electron deficiency of the C_4 atom. Nonetheless, there is coherence between the results obtained for β-lactone (1) and β-propiolactone as shown by a good correlation between the second order catalytic rate constants for (1) at 37°C with those of β-propiolactone[129] at 25°C in Figure 2.22. The linear plot implies that similar mechanisms apply to both compounds for a particular nucleophile.

From Figure 2.22, it is possible to compare the transition states for (1) and β-propiolactone. Thus, the Eyring relationship (Equation 2.15) expresses the rate constant k in terms of the Gibbs free energy of the transition state ($\Delta G^{\ddagger}$) and temperature (T), where k_B=Boltzmann constant.

$$k = \frac{k_B T}{h} \exp(-\Delta G^{\ddagger}/RT) \qquad \ldots(2.15)$$

Equation 2.15 can be rearranged for comparison with a similar reaction in the following way:

$$\text{let} \quad k_i^{'} = \frac{k_i h}{k_B T_i}$$

$i = 1$, k_i = rate constant for nucleophilic reaction with (1)

$i = 2$, k_i = rate constant for nucleophilic reaction with β-propiolactone

$$k_1^{'} = \exp(-\Delta G_1^{\ddagger}/RT_1), \qquad k_2^{'} = \exp(-\Delta G_2^{\ddagger}/RT_2)$$

$$\log k_1^{'} = -\Delta G_1^{\ddagger}/RT_1 \qquad \ldots(2.16) \qquad \log k_2^{'} = -\Delta G_2^{\ddagger}/RT_2 \qquad \ldots(2.17)$$

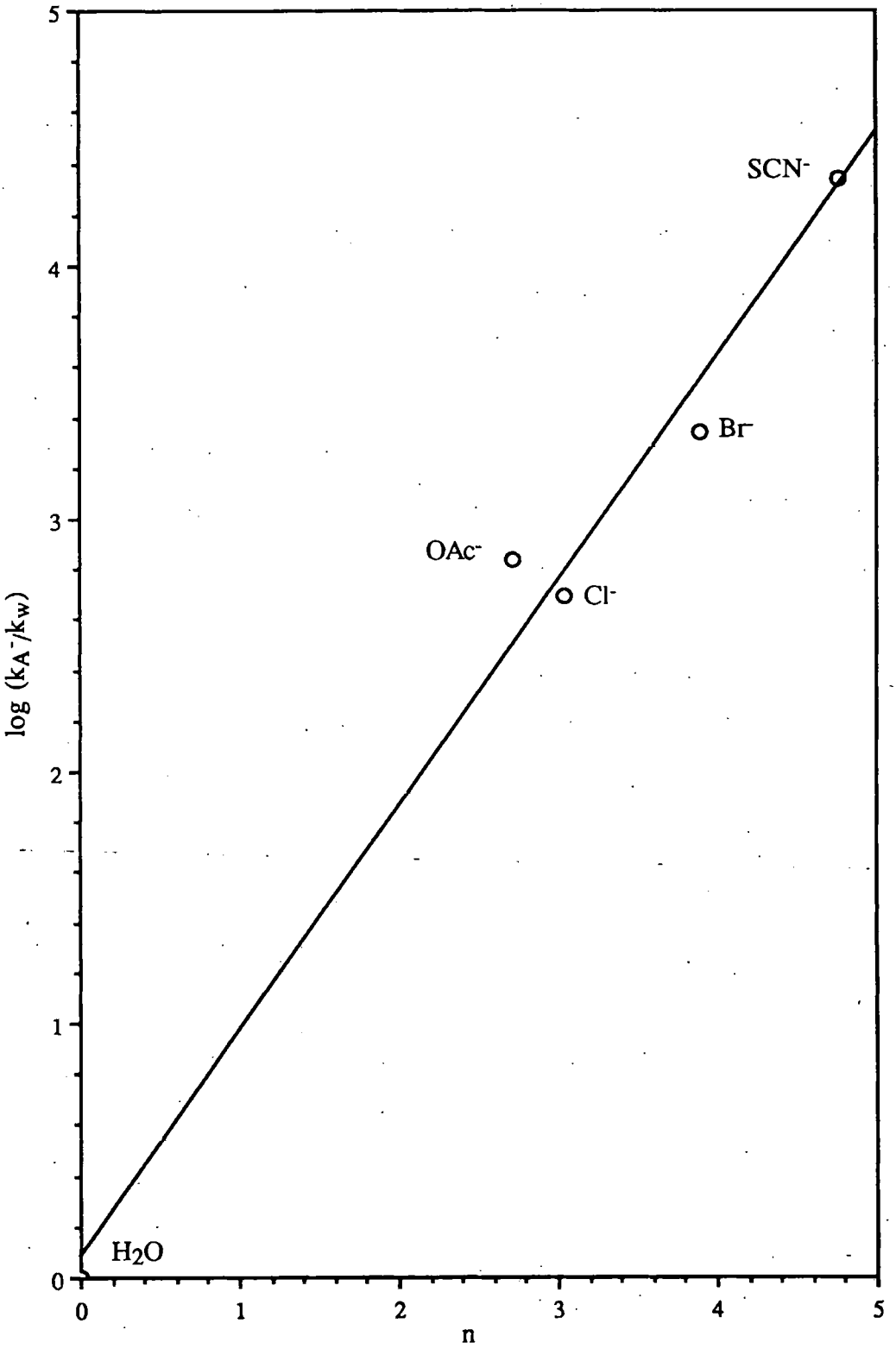

Figure 2.21 Swain-Scott plot of log (k_A^-/kw) against n for the decomposition of (1) in the presence of nucleophiles at 37°C.

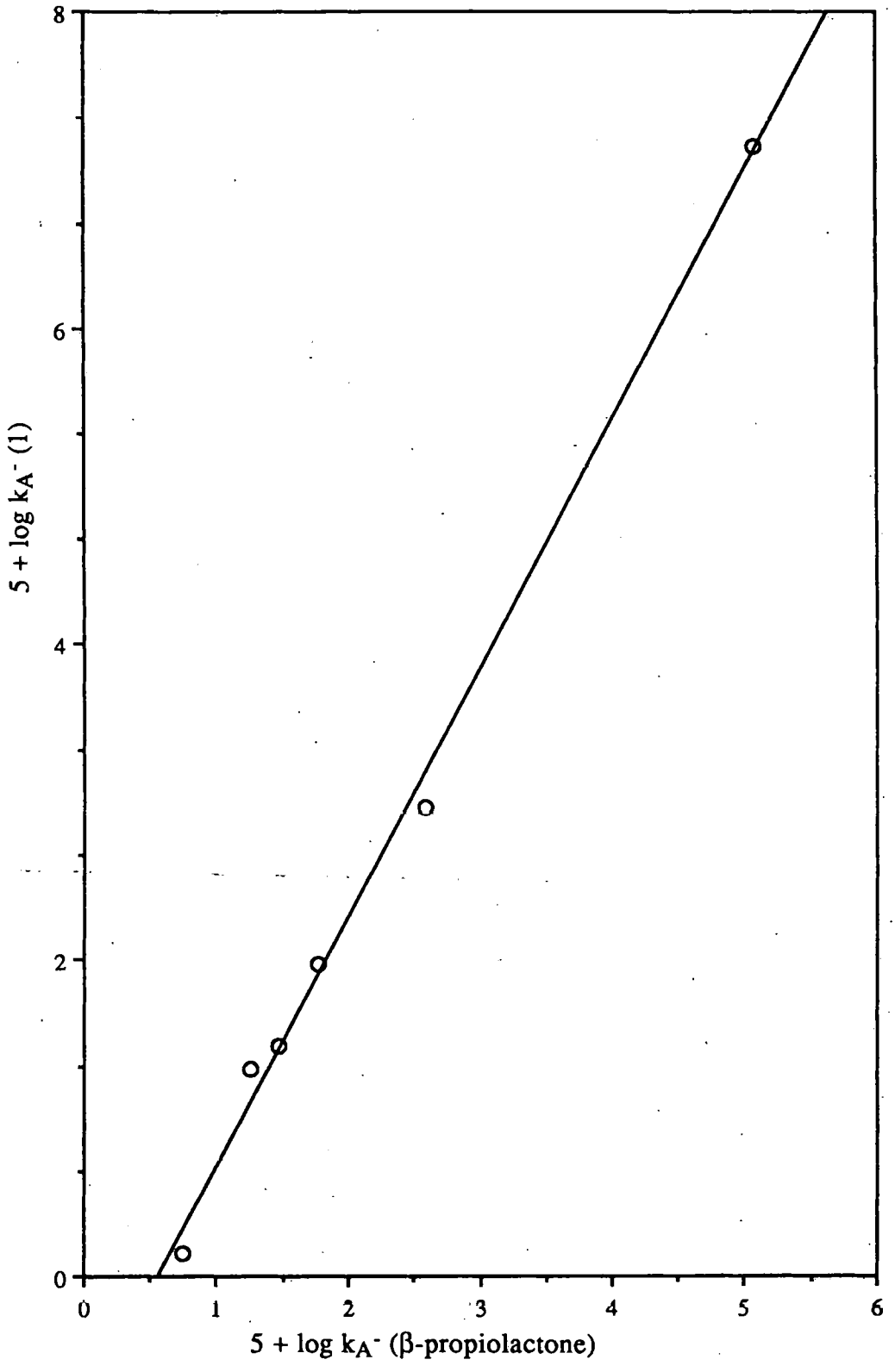

Figure 2.22 A comparative plot of k_A^- (1) against k_A^- (β-propiolactone)

Dividing (2.16) by (2.17)

$$\log k_1' = \frac{\Delta G_1^{\ddagger} T_2}{\Delta G_2^{\ddagger} T_1} \log k_2'$$

$$\log k_1 = \frac{\Delta G_1^{\ddagger} T_2}{\Delta G_2^{\ddagger} T_1} \log k_2 + \frac{h}{k_B T_2} \frac{\Delta G_1^{\ddagger} T_2}{\Delta G_1^{\ddagger} T_1} + \log (k_B T_1/h) \qquad ...(2.18)$$

Thus, from Equation (2.18) the linear free energy plot has a gradient of $\Delta G_1^{\ddagger} T_2 / \Delta G_2^{\ddagger} T_1$. Allowing for the difference in temperature between the two sets of data the ratio of the Gibbs free energies of the transition states is 1.6. The higher $\Delta G^{\ddagger}$ for (1) reflects increased steric hindrance at the reactive site and a more electron deficient C_4 atom because of the carbamoyl substitution.

2.6 Reaction of β-butyrolactone (12) with nucleophiles

The product analyses suggest that the interaction of β-lactone (1) proceeds mainly at the alkyl C_4 atom with the thiocyanate anion and at the acyl C_2 atom with morpholine. Because this difference was unexpected, its general validity was examined by additional ^{13}C-nmr experiments using β-butyrolactone (12) as a model compound. In these experiments the nucleophile (ca. 6mM) was added to a cooled solution of (12) (6mM) in CD_3CN (or CD_3CN/D_2O as necessary) (1ml) at 0°C and after 10 minutes, the ^{13}C nmr spectra were recorded. Further ^{13}C nmr spectra were recorded at later intervals as necessary until the reaction had gone to completion or significant reaction had occurred. The results were interpreted on the basis of the chemical shift of the carbonyl group of the product, assuming that the chemical shift of the carboxylic acid product resulting from alkylation occured at ca. δ 176.4 ppm. Lower ^{13}C chemical shifts imply acylation of the nucleophile.

The two possible products resulting from reaction of morpholine with (1) at the C_2 atom (acylation) (13) and the C_4 atom (alkylation) (14) are shown in Figure 2.23.

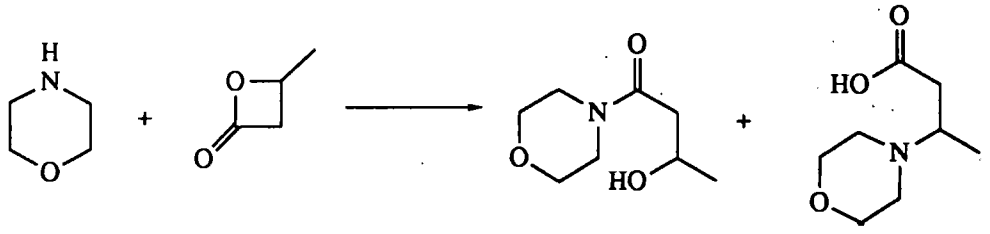

(12) **(13)** **(14)**

Figure 2.23 Two possible reaction products from the reaction of β-butyrolactone with morpholine

Both compounds are observed in the ^{13}C-nmr spectrum (Figure 2.24), but amide (13) (δCO 171.2ppm) is produced in larger amounts than the carboxylic acid (14) δCO 176.5 ppm). Some unreacted (12) is also present. From the ratio of the integrals of the carbonyl peaks, the approximate ratio of (13):(14) is 13:1.

β-Butyrolactone (12) was also reacted with the ambident nucleophile 2-hydroxy pyridine. Potential reaction products are described by Figure 2.25. This reaction was very slow and both starting materials were still apparent in the ^{13}C-nmr spectra (Figure 2.26) after 14 days, together with three products identified by new ^{13}C=O signals at δ172.9, 174.8 and 176.6ppm. The signal (k) at δ174.8ppm is consistent with the O-acyl product (15) and that (1) at 172.9ppm with the aryl-N-acyl product (16).

These assignments are confirmed by additional peaks, (n) and (o) at δ 65.1 and 23.2ppm, respectively, similar to those observed for the CHOH and CH_3 in other acylated products. The ^{13}C=O signal (p) at 176.6ppm is consistent with a carboxylic acid moiety as in (17) and (18). Compounds (17) and (18) however, should give distinct ^{13}CH-X chemical shifts. Only one, (g), is apparent at 69.2ppm, with a corresponding $^{13}CH_3$ signal (r) at 20.0ppm. This suggests that only one alkylated product is formed, although it is not clear whether this is (17) or (18).

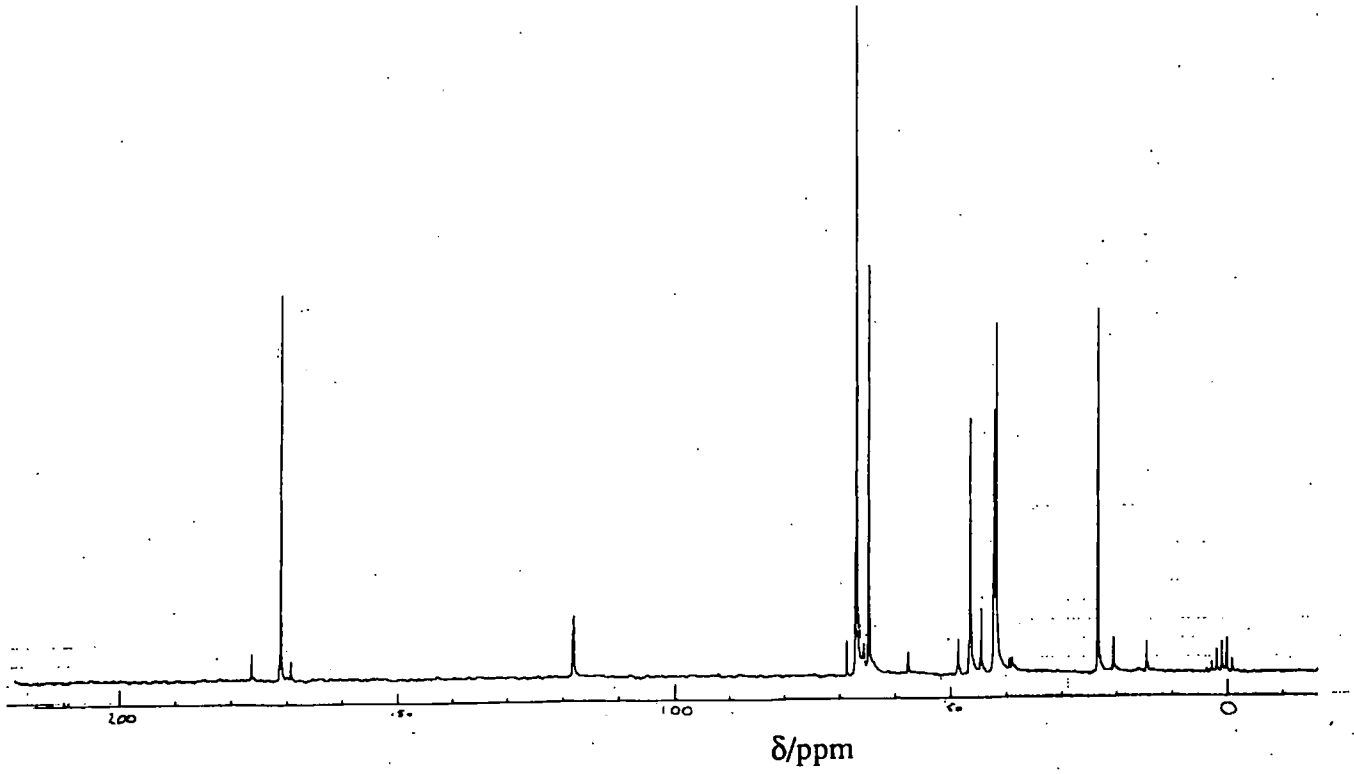

Figure 2.24 22.5 MHz ^{13}C-nmr spectrum of the reaction mixture of β–butyrolactone with morpholine

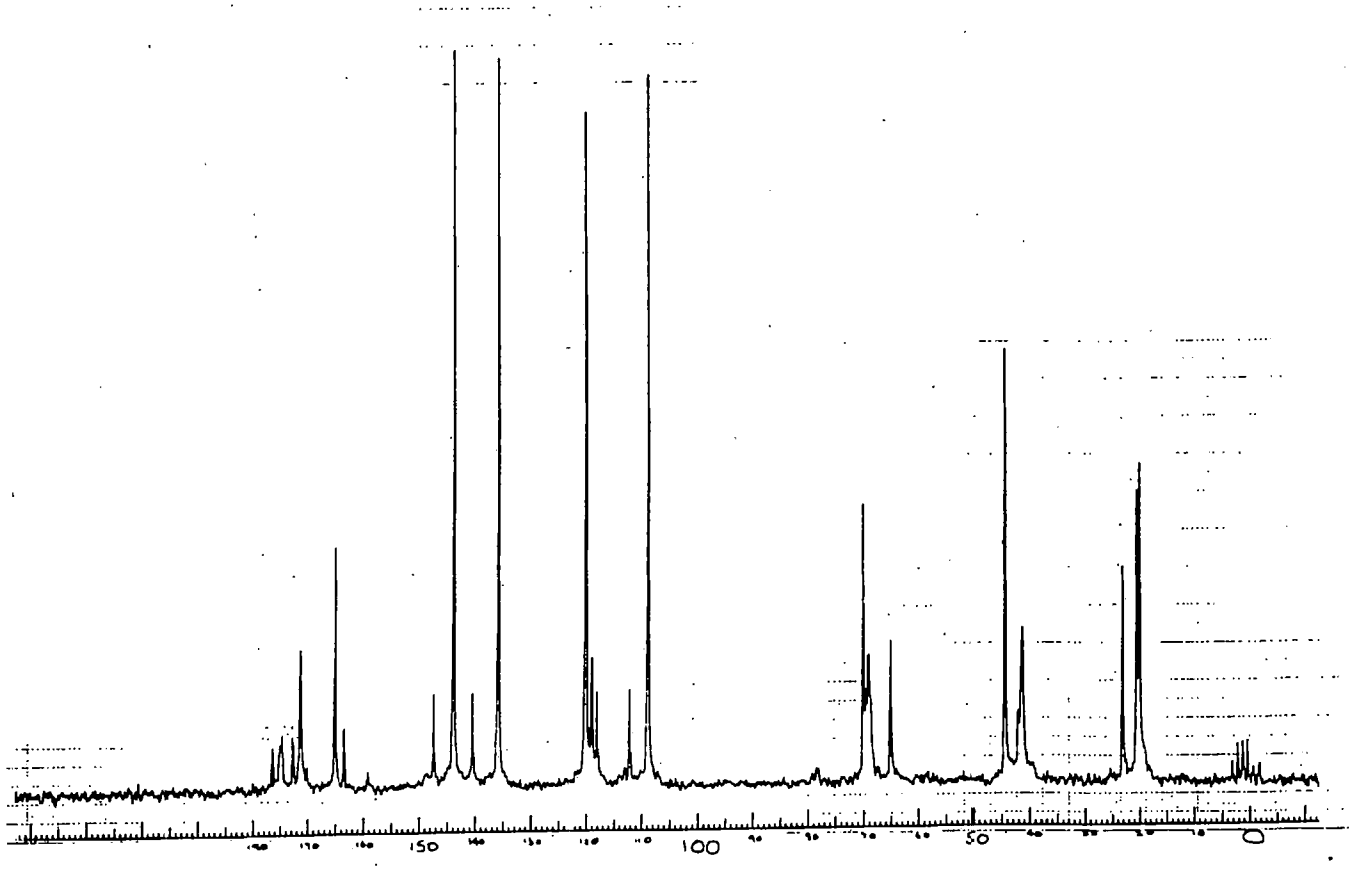

Figure 2.26 22.5 MHz ^{13}C-nmr spectrum of the reaction mixture of β-butyrolactone with 2-hydroxypyridine

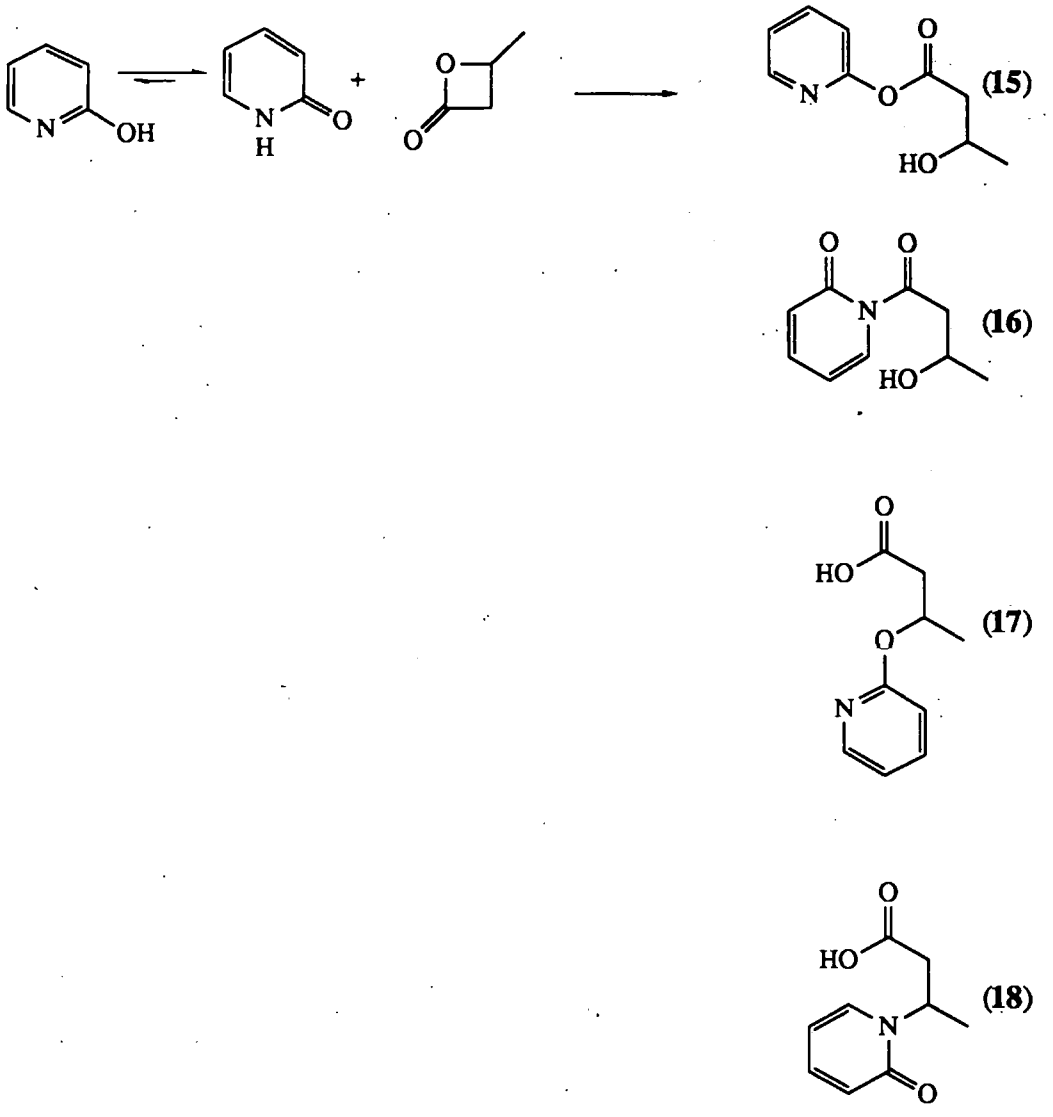

Figure 2.25 Potential reaction products for reaction of (12) with 2-hydroxy pyridine

The ^{13}C chemical shifts of the carbonyl, CH-X (X=OH or NU) and CH_3 groups in products for reactions of β-propiolactone with several nucleophiles are summarised in Table 2.17.

These results parallel the product analysis studies for β-lactone (1). Thus, reaction of β-butyrolactone with SCN^- proceeds at the alkyl C_4 atom and predominantly at the acyl C_2 atom with morpholine. The results for 2-hydroxy-pyridine are of special interest as this is an approximate model for the genetically sensitive 2-deoxyguanosine base (19)

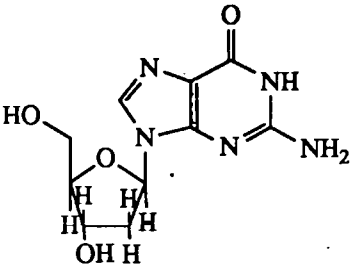

(19)

of DNA, where alkylation of the O^6 position is considered as the important pro-mutagenic event.[130] Although alkylation is observed, it is not clear whether this involves the O-atom of2-hydroxypyridine.

Table 2.17 ^{13}C **Chemical shifts of products from reaction of β-butyrolactone (12) with nucleophiles**

Nucleophile	$\delta^{13}CO$	$\delta^{13}CH$-X	$\delta^{13}CH_3$/ppm	Mechanism
SCN^-	176.4	42.9	22.1	Alkylation
	177.1	70.7	20.2	Reaction with H_2O[a]
Morpholine	171.2	64.8[b]	23.4	Acylation
	176.5	57.7	14.6	Alkylation
2-Ethoxyethylamine	172.8	64.9[b]	23.4	Acylation
2-Hydroxypyridine	176.6	69.2	20.0	Alkylation
	174.7	65.14[b]	23.2	O-Acylation
	172.9	65.14[b]	23.2	N-Acylation

a 3-Hydroxybutanoic acid v. minor component - unclear if product from reaction of (12) with H_2O or if from subsequent hydrolysis of alkyl thiocyanate.

b X=OH

2.7 Regiospecificity of reactions of β-lactones with nucleophiles

There is much evidence that β-propiolactone reacts with nucleophiles regiospecifically.[106] Thus, sulphur compounds, inorganic and carboxylic acid salts form the appropriate propanoic acid derivatives in good yields from reaction at the alkyl C_4 atom. Alcohols react similarly in neutral solution or in the presence of an acid to give 3-alkoxypropanoic acids but at the acyl C_2 atom in the presence of a base to give 3-hydroxyalkyl propanoates. The opposite regiospecificity applies to reactions of phenols with the formation of 3-phenoxypropanoic acid in neutral and basic solutions but phenyl 3-hydroxypropanoate in the presence of acids. Thiophenol reacts faster than phenol to yield 3-thiophenoxypropanoic acid. Reactions with Grignard reagents are complicated by concurrent attack of halide ion at the alkyl C_4 atom, but phenyl-magnesium bromide and methylmagnesium chloride give vinyl ketones *via* 3-hydroxypropylketones. In contrast, benzyl magnesium chloride gives phenyl butyric acid. These results are summarised in Table 2.18.

Table 2.18 Regiospecificity of reaction of nucleophiles with β-propiolactone

C_4-alkylation	C_2-acylation
sulphur nucleophiles	nitrogen nucleopohiles
halides	hydroxide
phenoxides	phenol
alcohols	alkoxides
stabilised carban ions	carban ions

There has been no attempt to rationalise the regiospecificity of these reactions, but there is little evidence that steric hindrance is a dominant factor. Most of the results can be

explained by hard soft acid base (HSAB) theory where hard nucleophiles react preferentially at the harder acyl C_2 atom and soft nucleophile at the softer alkyl C_4 atom.

The HSAB explanation can be further tested by the application of more rigorous perturbation molecular orbital theory (Equation 2.19) where three types of forces are involved in the early stages of bond formation between the nucleophile and the electrophile. In Equation 2.19, E_i is the total energy for the interaction, $E_{(core)}$ is the positive electron-electron repulsion energy, $E_{(electrostatic)}$ is dependent upon the charge (or dipolar) character of the reagents and $E_{(overlap)}$ reflects the interaction energy of the frontier (HOMO/LUMO) orbitals.

$$E_i = E_{(core)} + E_{(electrostatic)} + E_{(overlap)} \qquad ...(2.19)$$

The HSAB explanation was therefore examined for β-propiolactone and oxetan-2-one-4-carboxamide (20) using the AM1 molecular orbital package to calculate LUMO energies and charge distributions.

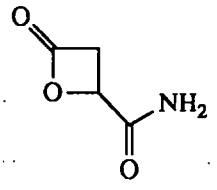

(20)

Compound (20) is a good model for (1), as further N-substitition is unlikely to significantly affect the electron distribution about the C framework.

The AM1 method calculates both the contribution (C_i) of each atomic orbital to the overall molecular orbital and the net charges on each atom. The C_i coefficients of the atomic orbitals contributing to the LUMOs in β-propiolactone and the β-lactone (1) are given in Table 2.19, the net charges on each atom in Table 2.20 and the numbering system in Figure 2.27.

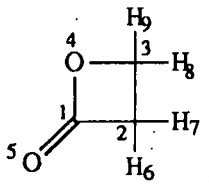

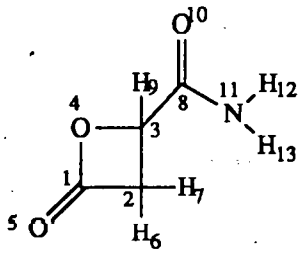

(20)

Figure 2.27 Numbering system for AMI calculations

For both β-propiolactone and (20), the LUMO is a π antibonding orbital centred on the ring carbonyl with energies of 0.91343 eV for β-propiolactone and 0.61412 eV for (20). Thus, the preferred site for reaction by soft nucleophiles (highest overlap) is the acyl C_2 atom. The net charges on each atom show the acyl C_2 atom of the ring is the most positively charged centre. Thus, reaction with hard nucleophiles should also preferentially proceed at the acyl C_2 atom (maximum electrostatic interaction). In view of the experimental findings, either the valididity of the AM1 calculations must be questioned, (they apply only to molecules in the gas phase and do not allow for solvation which may change the charge distribution quite considerably) or an alternative explanation applies.

Table 2.19 Contribution to LUMOS of β-propiolactone and β-lactone (20) from atomic orbitals

(β-propiolactone) ψ25			(20) ψ23		
Atom	Orbital	Ci	Atom	Orbital	C_i
C1	S	-0.00036	C1	S	-0.00060
	Px	-0.00412		Px	0.21633
	Py	-0.00522		Py	-0.10841
	Pz	-0.77048		Pz	-0.73534
C2	S	0.00010	C2	S	0.00367
	Px	0.00012		Px	0.02003
	Py	-0.00080		Py	-0.01037
	Pz	-0.08336		Pz	-0.06308
C3	S	-0.00014	C3	S	0.00664
	Px	0.00017		Px	-0.00232
	Py	0.00009		Py	0.01227
	Pz	0.01172		Pz	0.02052
O4	S	0.00010	O4	S	-0.00080
	Px	-0.00101		Px	-0.6379
	Py	0.00143		Py	0.03056
	Pz	0.23641		Pz	0.21441
O5	S	0.00002	O5	S	0.00008
	Px	-0.00282		Px	-0.14991
	Py	0.00365		Py	0.07542
	Pz	0.53296		Pz	0.51123
			C8	S	-0.01842
				Px	0.01166
				Py	0.02172
				Pz	0.00844
			O10	S	0.00009
				Px	-0.00867
				Py	-0.00772
				Pz	-0.00300
			NH	S	-0.00143
				Px	0.00377
				Py	-0.00797
				Pz	0.00645

Table 2.20 Net charges on atoms in β-propiolactone and β-lactone (20)

β-propiolactone		β-lactone (20)	
Atom	Net charge	Atom	Net charge
C1	0.3001	C1	0.3003
C2	-0.2235	C2	-1.1934
C3	-0.0409	C3	-0.0142
O4	-0.2653	O4	-0.2773
O5	-0.2596	O5	-0.2469
		C8	0.2964
		O10	-0.3675
		N11	-0.4127

An alternative is that products derived from acyl C_2 atom substitution reflect kinetic product control whereas those from alkyl C_4 atom substitution reflect thermodynamic product control (Figure 2.28).

Nucleophiles which are poor leaving groups, such as carbanions, amines and OH^-, give rise to the kinetic product since cleavage of the acyl carbon oxygen bond is preferred for the decomposition of the tetrahedral intermediate (21). However, if the nucleophile is also a good nucleofuge (eg. sulphur nucleophiles, alcohols, phenoxides and water), the tetrahedral intermediate (21) preferentially returns to starting materials. Only the slower reaction at the alkyl C_4 proton is therefore observed, giving the thermodynamically stable alkylated product. This hypothesis explains the experimental findings for the reaction of nucleophiles with β-lactones, but validation requires further critical tests.

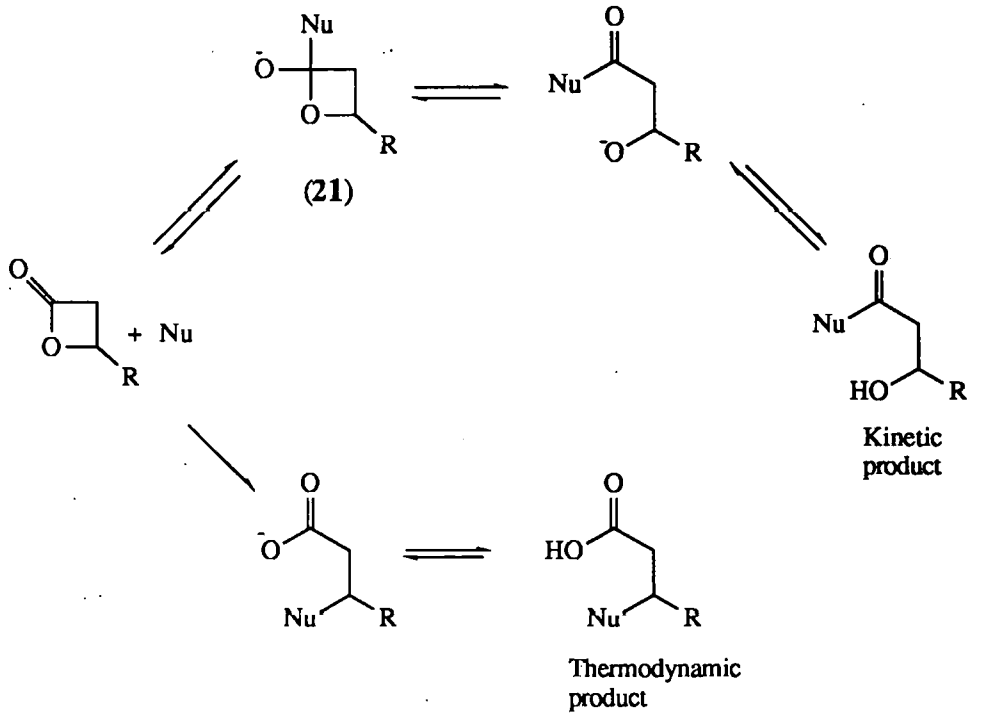

Figure 2.28 Possible reaction mechanism of β-lactones with nucleophiles

2.8 Biological implications of the reactions of β-lactone (1)

Aspartame is initially metabolised in the small intestine where intestinal esterases, predominanatly chymotrypsin, hydrolyse the terminal methyl ester to liberate the carboxylic acid.[131] It is only in the form of the carboxylic acid that aspartame can migrate through the intestinal wall into the bloodstream.[132] Therefore, hydrolysis of the terminal methyl ester may prove to be a critical step in the bioactivation of β-lactone (1).

The work of Shephard et. al.[119,120] indicates that treatment of aspartame with nitrous acid generates an alkylating agent with a mutagenic response. The alkylating agent has half-lives at 37°C and pH 2.5 and 7 of 200 and 15 min., respectively. These are not inconsistant with the stability of the β-lactone (1) with half-lives at 37°C of 800 and 400 min. at pH 2.5 and 7 respectively, in the absence of any added nucleophiles. The primary N-nitrosamine proposed by Shephard[120] is clearly wrong, because these compounds rapidly transform to diazo compounds which are unstable at low pH.

These results tentatively suggest that the β-lactone (1) may act as a biological alkylating agent. Alkyl-oxygen bond fission (and therefore alkylation) proceeds with some nucleophiles and its reactivity parallels β-propiolactone and β-butyro-lactone, both known carcinogens. In general however, alkyl-oxygen bond fission is slower for (1) than β-propiolactone and (1) has a higher nucleophilic selectivity (s) than β-propiolactone.

Potent carcinogens are usually nonselective, with a high degree of S_N1 character in reactions with nucleophiles and therefore a low s value. Further, the carcinogenicity of alkylating agents correlates with the ratio of N^7 to O^6 guanine alkylation of double stranded DNA *in vitro*, and the N^7 to O^6 alkylguanine can be predicted from the s value of the reagent.[133] It has also been demonstrated that the s value correlates with the TD_{50} of the carcinogenic agent.[134] From these relationships values of TD_{50}=7200 mg/kg and N^7/O^6 alkylguanine ratio = 302 can be estimated for β-lactone (1). These imply a similar carcinogenicity to glycidaldehyde and benzyl chloride and greater than either ethylene oxide or epichlorohydrin. A similar study,[135] relating carcinogenicity of a compound to its s value, predicts that the β-lactone (1) has a similar level of potency to dimethyl sulphate and methyl methanesulphonate. The experimental TD_{50} of β-propiolactone is ca. 104-1180 mg/kg depending on the route of administration,[134] in qualitative agreement with TD_{50} =1900 mg/kg based on its s value. Thus, β-lactone (1) appears to be ca. 4-70 fold less carcinogenic than β-propiolactone. In the absence of animal test data, these correlations suggest that the β-lactone (1) should be regarded as a potential carcinogen.

CHAPTER 3 SUMMARY OF CHAPTER 2

3 SUMMARY OF CHAPTER 2

Prompted by reports that treatment of aspartame with nitrous acid generates an unknown alkylating agent[119,120] and the findings of Sandhu that treatment of aspartame with nitrous acid generates the β-lactone N-(1'-methoxycarbonyl-2'-phenyl)ethyloxetan-2-one-4-carboxamide (1),[97] an investigation into the behaviour of β-lactone (1) was undertaken. β-Lactones can exhibit dual reactivity, behaving as either acylating or alkylating agents (Figure 3.1). Since the type of reactivity seems to be highly dependent on the structure of the nucleophile,[106] the present study was aimed at measuring the alkylating potential of the β-lactone (1) in order to assess the potential risk posed by aspartame.

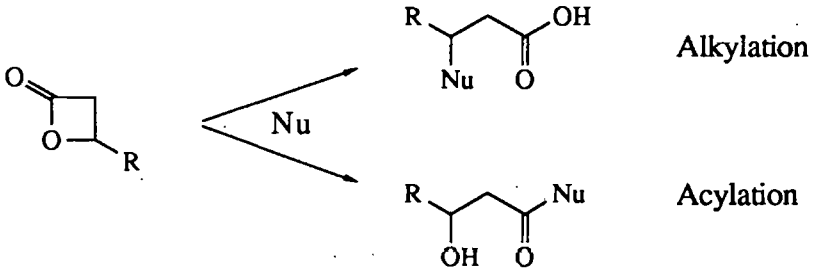

eg. Nu=DNA

Figure 3.1 Dual reactivity of β-lactones

Two fundamental requirements for carcinogenic activity of β-lactone (1) are sufficient stability for reaction with the cell nucleus and alkyl-oxygen bond fission to generate an alkylating agent. Using water as the nucleophile, both requirements could be assessed from the pH-hydrolysis rate profile. Due to the method chosen to follow the hydrolysis of the β-lactone moiety (ie. loss of (1) with time) the experimental data had to be adjusted for the loss of (1) by concurrent hydrolysis of the terminal methyl ester group. The rate of hydrolysis of the methyl ester of (1) was not measured directly but approximate values were obtained from hydrolysis of the methyl ester of aspartame and assuming that both esters have similar reactivity. The methyl ester of aspartame

hydrolysed *via* the $A_{AC}2$ pathway in concentrated acid and the $B_{AC}2$ pathway in dilute alkali. It was also assumed that only these two mechanisms applied over the pH range 1-10.[136]

With allowance for the concurrent hydrolysis of the terminal methyl ester, the pH-log k_o (rate=k_o[(1)]) profile was deduced for the hydrolysis of the β-lactone moiety of (1). The profile has three distinct areas and very closely resembles those of β-propiolactone and β-butyrolactone.[104] Thus, below pH 3 an acid catalysed pathway, dependent upon $[H_3O^+]$ is observed and the $A_{AC}2$ mechanism probably applies. Above pH7 the hydrolysis is strongly base-catalysed, characteristic of the $B_{AC}2$ pathway. At intermediate pH 3-7, the rate of hydrolysis is pH independent which by analogy to other β-lactones probably reflects hydrolysis *via* the $B_{AL}2$ mechanism and therefore alkyl-oxygen bond cleavage. At pH 3-7, the β-lactone (1) was relatively stable with $t_{1/2}$ ca. 13.5h at 37°C which is more than sufficient for passage intact through the stomach. The complete rate equation for the hydrolysis of the β-lactone moiety of (1) is given by Equation 3.1 where k_H= 3.17 x 10^{-5} $M^{-1}s^{-1}$; k_w= 1.43 x $10^{-5}s^{-1}$ and k_B= 143 $M^{-1}s^{-1}$ at 37°C.

$$\text{Rate} = (k_H[H_3O^+] + k_w a_w + k_B[OH^-])\,[(1)] \qquad \ldots(3.1)$$

The decomposition of (1) was also catalysed by SCN^-, Br^- and Cl^-, by a pH independent pathway for SCN^-. Since acyl-oxygen bond fission is not prone to nucleophilic catalysis, it was concluded that these nucleophiles act by alkyl-oxygen bond cleavage. This was confirmed by isolation of the alkyl thiocyanate product from the reaction of (1) and NaSCN.

With morpholine the acylated rather than alkylated product was obtained from the β-lactone (1). This observation prompted a comparative study using β-butyrolactone and identical results were obtained. Investigation of literature data for β-propiolactone showed clear evidence of ambident reactivity towards nucleophiles, although no simple rationale for this behaviour could be deduced. From both the

literature and current experimental data it was evident that hard/soft acid/base theory may explain the ambident reactivity, with hard nucleophiles preferentially attacking the C_2 (acyl) position and the soft C_4 (alkyl) position. Attempts to confirm this perturbation theory explanation by molecular modelling to determine the position of the HOMO and greatest positive charge proved disappointing. The semi-empirical AM1 package was used to perform the calculations for β-butyrolactone and a simple model of β-lactone (1). For both compounds the calculations showed that under charge-controlled and orbital-controlled conditions the C_2 (acyl) position was the preferred site of reaction. These results are inconclusive insofar as the calculations are semi-empirical without allowances for solvation. An alternative explanation consistent with the experimental results, is that reaction at the C_2 (acyl) position reflects kinetic product control, whilst reaction at the C_4 (alkyl) position reflects thermodynamic product control. Thus, alkylation by β-lactone (1) reflects conversion of the kinetic to the thermodynamic product.

For the decomposition of β-lactone (1) by nucleophiles reacting at the C_2 position, the Swain-Scott plot of k_A^* (the first order rate constant for nucleophilic catalysis) against the Swain-Scott parameter (n) is linear, giving a nucleophilic selectivity parameter of s=0.88. This is larger than the comparable s=0.77 found for β-propiolactone[128], which suggests that β-lactone (1) will be a weaker carcinogen, probably of comparable toxicity to glycidaldehyde, benzyl chloride, dimethyl sulphate and methyl methanesulphonate.[133-135] The evidence suggests that the cytotoxicity of β-lactone (1) should be examined experimentally.

In conclusion, the chemical behaviour and reactivity of β-lactone (1) is remarkably similar to those of β-propiolactone and β-butyrolactone, two known carcinogens. β-lactone (1) is probably the unidentified alkylating agent and mutagen observed by Shepherd[119,120] on treatment of aspartame with nitrous acid, rather than the primary nitrosamine postulated.[119] The present results further question the safety of aspartame as an artificial sweetener and indicate the need for further biological testing.

CHAPTER 4 DIAZOAMINO ACIDS

4 DIAZOAMINO ACIDS

4.1 Introduction

Aspartame,[97] an aspartic acid derivative, glutamic acid[94] and glutamine[94] are known to form lactones on treatment with nitrous acid, the reactions proceeding via a diazo intermediate. The work described in this chapter is concerned with the diazotisation and cyclisation of the amino acids L-glutamine and L-asparagine bearing carboxyl terminii protected as ester derivatives to minimise competing reactions and facilitate product analysis. The expected products were independently synthesised and characterised for comparison with the products from the reactions of the amino acid esters. The rates of nitrosation of the amino acids were determined. The amino acid esters were nitrosated in the presence of an organic solvent and deamination products, which migrated into the organic phase were analysed by GLC and GLC/MS. The intermediate diazocompounds were synthesised, isolated, purified and characterised and their physical properties are reported. The stabilities of these intermediates in aqueous buffers at 25°C were determined, along with solvent deuterium isotope effects, to elucidate the mechanism of hydrolysis. These data are compared with those for the hydrolysis of other aliphatic diazocompounds reported in the literature. The diazo-compounds were also decomposed thermally in aprotic media and the products were determined by GLC/MS using both electron impact and chemical ionization techniques. The mass spectral assignments are discussed in detail and possible reaction mechanisms for the formation of products are proposed.

4.2 Preparation of amino acid esters

To prevent reaction of the α-carboxylic acid with the diazo moiety in the course of nitrosation (e.g. formation of an α-lactone), the α-carboxylic acid moieties of the two amino acids were protected as methyl esters. The use of methyl esters had other beneficial effects. These include an increased solubility in organic solvents for the aprotic nitrosation experiments, increased stability of diazo esters relative to diazo

acids, easier purification of the diazo derivatives by column chromatography and more volatile products for GLC analysis. One other reason for the choice of methyl esters was their ease of synthesis by careful reaction of the parent amino acid with diazomethane without concurrent alkylation of the amide side chains. It was, however, necessary to protect the amino-terminus as the N-α-carbobenzyloxy derivative.

Thus, the methyl esters of L-glutamine (GlnOMe) (1) and L-asparagine (AsnOMe) (2) were prepared from the reaction of ethereal diazomethane with the N-α-carbobenzyloxy derivative of the amino acid at 0°C, using a similar method to that reported by Sondheimer and Holley.[137] A slight excess of diazomethane was used and there was no evidence by ^{1}H-n.m.r. and m.s. of methylation of the amide side chain. After isolation and purification, the N-α carbobenzyloxy protecting group was removed by catalytic hydrogenolysis in the presence of Pd/C and HCl. The acid was added to form the HCl salt of the amino acid ester and therefore prevent dimerisation to a dipeptide. As Sondheimer and Holley[138] reported, it is necessary to sparge continually with hydrogen during hydrogenolysis to remove CO_2 which slows the uptake of hydrogen. Although reaction times are shorter with palladium black catalyst, 10% Pd/C was found to be an acceptable, commercially available catalyst.

4.3 Rates of nitrosation of glutamine and asparagine in aqueous HCl

Both L-glutamine and L-asparagine were nitrosated using $NaNO_2$ in dilute HCl. Rates of nitrosation and reaction products were studied.

The rates of nitrosation of L-glutamine, L-asparagine, glutamine methyl ester, (1) and glycine ethyl ester were measured under *pseudo* first-order conditions (excess substrate) in 0.1M HCl at 37°C. The reactions were followed by monitoring the loss of nitrous acid with time using Shinn's method.[139] A coloured azo dye is formed in the test with an absorbance at 541nm proportional to the concentration of nitrite.[139] All of these reactions followed equation 4.1, and the first order plots are shown in Figure 4.1.

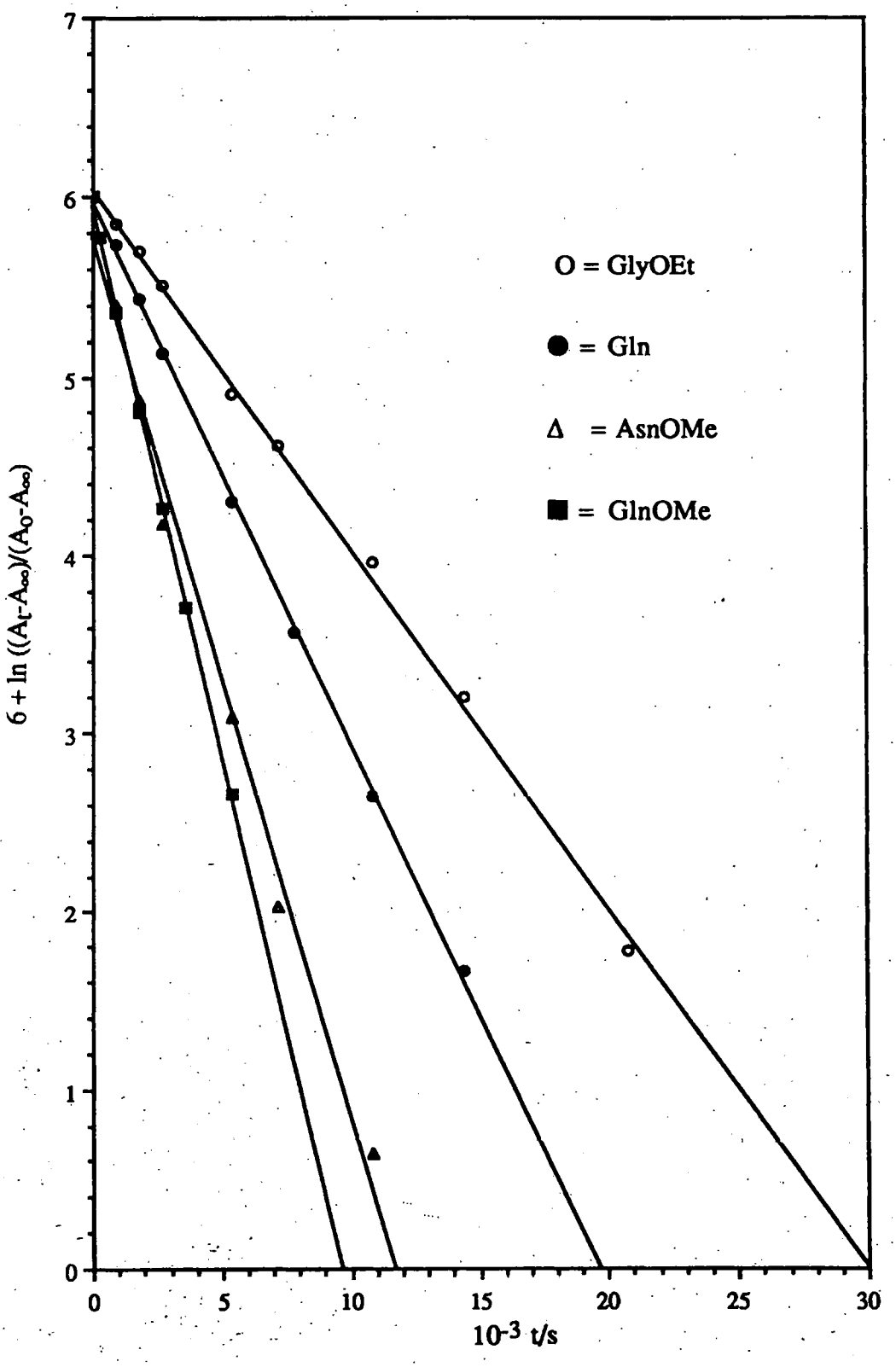

Figure 4.1 *ln $((A_t-A_\infty)/(A_0-A_\infty))$ versus time for the nitrosation of Asp, Gln, GlnOMe, GlyOEt in 0.1M HCl at 37° C. Initial [substrate] = 0.1M, [$NaNO_2$] = 0.1mM*

$$\text{rate} = k_o[NO_2^-] \qquad \ldots(4.1)$$

The values of k_o are summarised in Table 4.1 together with k_o for the thermal decomposition of nitrite in the absence of any substrate.

Table 4.1 Rates of nitrosation of amino acid derivatives in 0.1M HCl at 37°C. Initial [substrate] = 0.1M, [$NaNO_2$] = 0.1mM

Substrate	pKa	$10^4 k_o/s^{-1}$
None	-	0.069
Asparagine	8.8[140]	4.9
Glutamine	9.13[140]	3.0
GlnOMe	(<9.1)	6.2
Glycine ethyl ester	7.8[140]	2.0

Clearly, the thermal decomposition of nitrite is insignificantly slow compared with the rate of nitrosation of the amino acid derivatives and no correction in the values of k_o was made for it.

Although not proven here, the nitrosation of the amino acids in dilute HCl probably involves a rate-limiting reaction between NOCl and the neutral amino acid.[17] The rate of reaction is therefore dependent upon the concentration of substrate, nitrous acid and HCl[17], (equation 4.2), and Table 4.1 shows that all four substrates undergo nitrosation at similar rates in 0.1M HCl at 37°C and that L-asparagine and L-glutamine

$$\frac{-d[HNO_2]}{dt} = k_3[RNH_2][HCl][HNO_2] \qquad \ldots(4.2)$$

$$k_o = k_3[RNH_2][HCl]$$

behave similarly to glycine. There is no evidence for an additional nitrosation of L-glutamine and L-asparagine involving the amide side chains. Further, k_o values for L-asparagine, L-glutamine and L-glutamine methyl ester (1) but not glycine ethyl ester, correlate qualitatively with the pK_a of the amino group as expected for reaction *via* the neutral substrate.

4.4 Synthesis of methyl 2-diazo-4-carbamoylbutanoate (N_2GlnOMe) (3) and methyl 2-diazo-3-carbamoylpropanoate (N_2AsnOMe) (4)

The feasibility of synthesising the diazoderivatives of L-glutamine and L-asparagine methyl esters, (3) and (4), respectively, was investigated by preliminary *in-situ* nitrosation experiments. The aim was to obtain evidence for the formation of N_2GlnOMe and N_2AsnOMe by uv measurements and to assess their stabilities under conditions of synthesis.

Thus, the substrates (0.1M) in 0.1M aqueous borax buffer were treated with an aliquot ($0.5cm^3$) of gaseous NO_2 at 25°C. The NO_2 gas was injected into the dead volume above the solution of the substrate in a conical flask sealed with a Suba-seal stopper. The mixture was shaken vigorously and fumes of nitric and nitrous acids were seen to form and dissolve. The reaction solutions were analysed by HPLC using the conditions described in Section 7.3.2. Eluted peaks were assayed by a uv/visible diode array detector to aid identification of the diazocompounds (λ_{max} ca. 260nm). Both GlnOMe and AsnOMe gave the respective diazo esters (3) and (4) on treatment with NO_2. There was no significant decomposition of either ester in the borax buffer over 8h at ambient temperature indicating that both were relatively stable in basic media. On addition of concentrated acid to the reaction mixtures, the peaks, at λ_{max} 260nm due to the diazocompounds, disappeared and were not restored when NaOH was added to adjust the solution to ca. pH9.

Both diazocompounds were subsequently synthesised by aprotic nitrosation of the parent amino acid esters (1) and (2) using liquid N_2O_4 in dry CH_2Cl_2. The reactions

were carried out in the presence of both excess triethylamine and anhydrous sodium sulphate to remove both acid and water respectively. The best yields were obtained at low temperatures (ca -40°C) using a slight excess (1.2 equivalents) of liquid N_2O_4. Although the diazo products are relatively stable in clean organic solvents - no appreciable decomposition was observed over 24h at room temperature in ethanol - they decompose quite rapidly in the reaction mixtures. Temperatures below -40°C were impractical because of precipitation of the amine substrates. On warming the reaction solutions, the solids were quickly removed by filtration and the organic solvent by vacuum evaporation. The residue was then purified by column chromatography on neutral alumina using a $CHCl_3$/EtOH gradient. Both acidic alumina and silica were found to be inappropriate for purification due to extensive decomposition of the diazo esters on the column and both compounds were too strongly retained on basic alumina. It was beneficial to carry out both the syntheses and purifications in the absence of light. With these precautions, both diazo esters were obtained in acceptable yields of 40%.

Both N_2GlnOMe and N_2AsnOMe were obtained as yellow solids with well defined decomposition points. They were analytically pure by HPLC (see Section 7.3.2) monitoring at both λ=258nm and 215nm, but their analyses were unsatisfactory, with low (ca. 1%) values for nitrogen. This problem is often encountered with diazocompounds. They were characterised by both accurate mass measurement and spectroscopic analysis using uv, ir, ^{1}Hnmr, ^{13}C nmr and ms.

The spectroscopic data for the two compounds is summarised in Table 4.2.

UV-vis spectra.

Both compounds have a characteristic strong absorbance at λ_{max} 260nm in ethanol (log ε 4.1) corresponding to the $\pi \rightarrow \pi^*$ transition.

Table 4.2 Spectroscopic data for N_2GlnOMe (3) and N_2AsnOMe (4)

	N_2GlnOMe	N_2AsnOMe
λ_{max}/nm (log ε)	261 (4.11)	259 (4.10)
ν_{max}/cm^{-1}	3430, 2105, 1678	3394,2095,1703,1668
δ_C C=$\overset{+}{N}$=$\overset{-}{N}$/ppm	55.4	53.5
m/z (FAB+ve(glycerol))	144,112,172,84,100,127, 264,343	130,158,98,70,113,250, 315,287

IR spectra

A characteristic strong absorbance at ν_{max} 2100cm^{-1} is seen for both (3) and (4) corresponding to the C=$\overset{+}{N}$=$\overset{-}{N}$ stretching vibration. The amide NH stretches are observed at ca 3400cm^{-1} and the amide C=O stretches are apparent at ca 1673 cm^{-1}. It is also interesting to note that the ester C=O stretch is not observed in the spectrum of N_2GlnOMe and occurs at 1703cm^{-1} in the spectrum of N_2AsnOMe. This can be accounted for by a delocalisation of the π-electrons over the $\overset{-}{N}$=$\overset{+}{N}$=C – CO systems, giving some degree of enolate character to the carbonyl resulting in a lowering of its frequency (Figure 4.2).

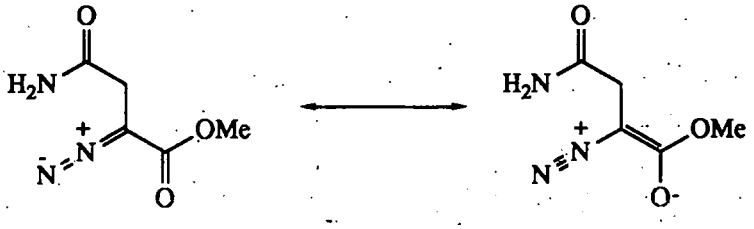

Figure 4.2 Resonance delocalisation of the diazo group

^{1}H nmr spectra

The changes in the ^{1}H nmr spectra of the amino acid ester HCl salts (1) and (2) upon diazotisation (Figures 4.3 and 4.4) are minimal. The protons of the carboxamide side chain of N_2GlnOMe(4) α to the diazo moiety were slightly deshielded (from 2.2 to 2.5ppm) but no change was observed in the position of the methylene group of N_2AsnOMe (3.2ppm). The CH_3 protons of N_2AsnOMe moved slightly upfield on diazotisation (from 4.0 to 3.8ppm) but no change was observed in the position of the methyl group of N_2GlnOMe (3.8ppm).

^{13}C nmr spectra

More significant changes in the position of the ^{13}C peaks were observed upon diazotisation of the amino acid ester hydrochlorides (Figures 4.5 and 4.6) In both cases, the carbon bearing the diazo moiety was deshielded,from 54.6 to 55.4 for N_2GlnOMe (3) and from 51.9 to 53.5 for N_2AsnOMe (4). The remaining carbons showed a significant upfield shift however, reflecting the delocalisation of the electrons shown in Figure 4.2 The changes are summarised in Table 4.3.

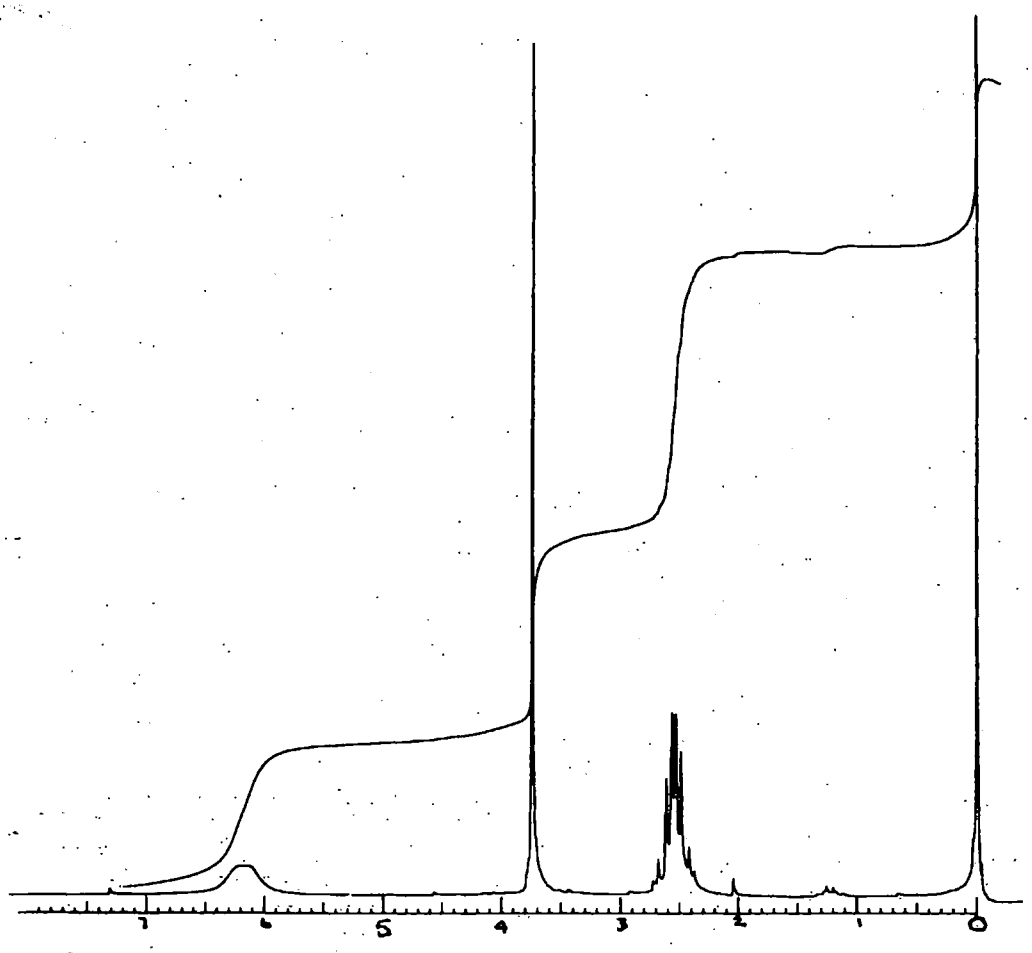

Figure 4.3 90MHz ^{1}Hnmr spectrum N_2GlnOMe ($CDCl_3$)

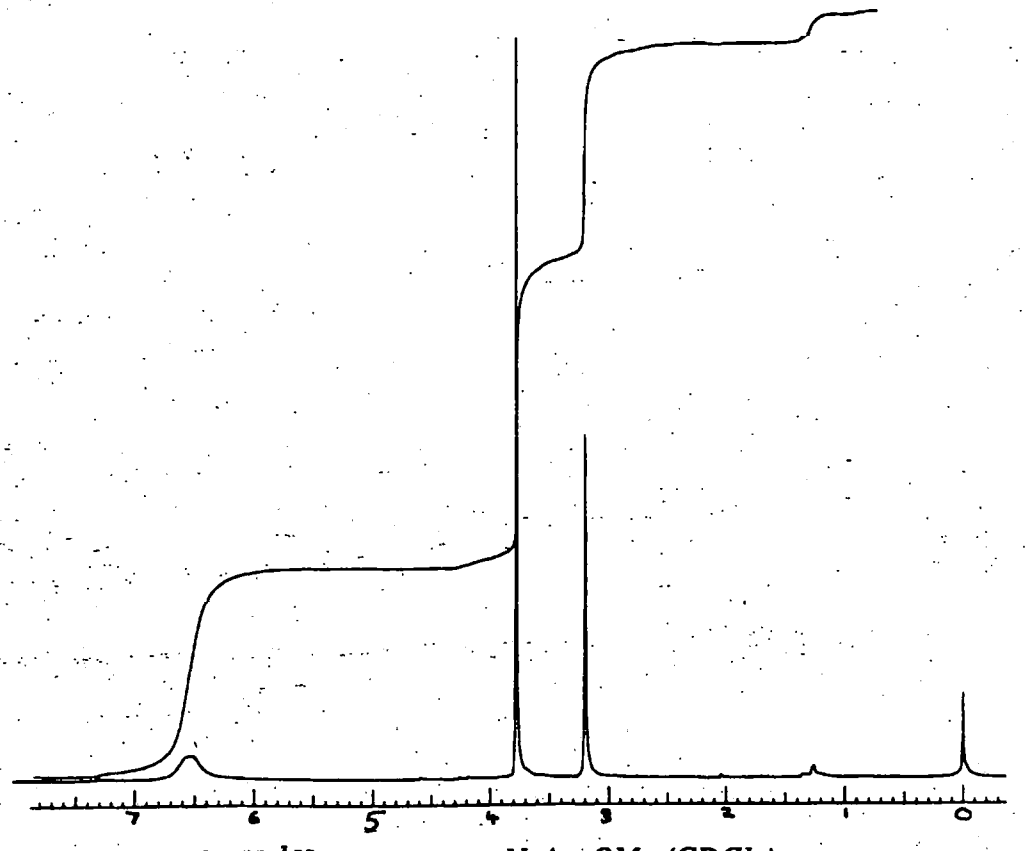

Figure 4.4 90MHz ^{1}Hnmr spectrum N_2AsnOMe ($CDCl_3$)

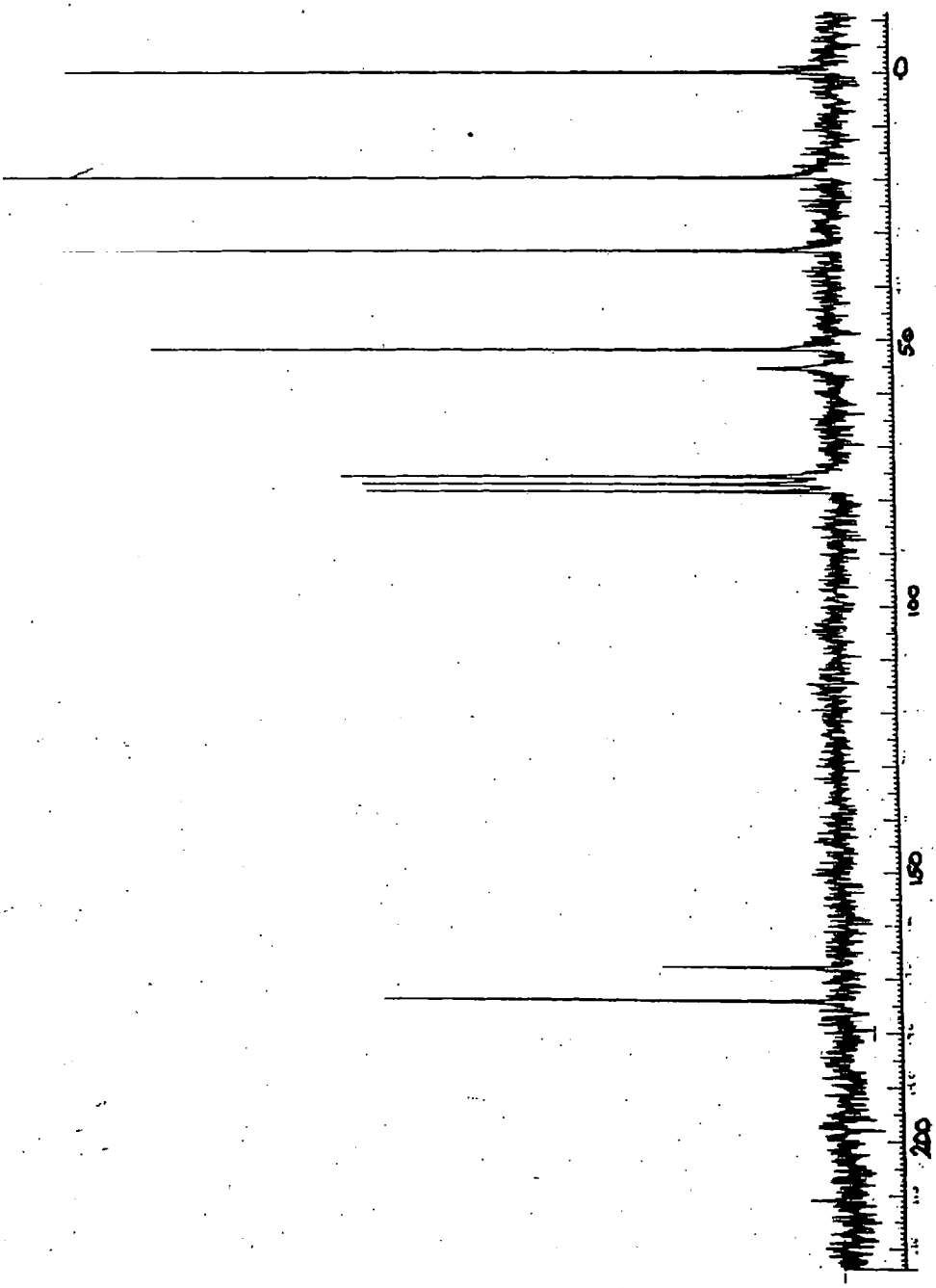

Figure 4.5 22.5MHz ^{13}Cnmr spectrum N_2GlnOMe ($CDCl_3$)

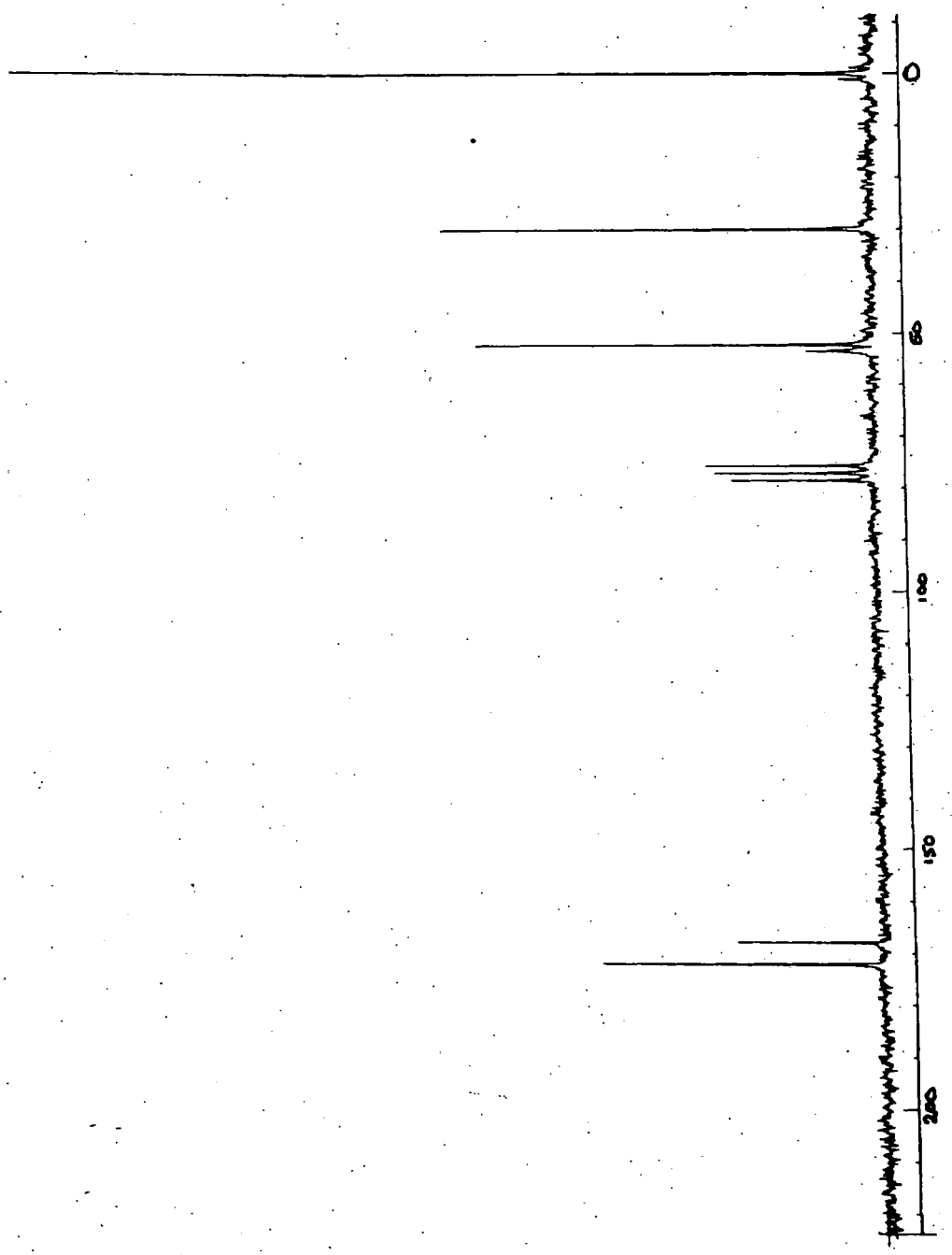

Figure 4.6 22.5MHz ^{13}Cnmr spectrum N_2AsnOMe ($CDCl_3$)

Table 4.3 ^{13}C **NMR chemical shifts (δ-ppm) for diazoamino acid esters (3), (4) and parent amino acid ester HCl salts (1) (2)**

Carbon	δN_2GlnOMe ppm	δGlnOMe ppm	Δδ/ ppm	δN_2AsnOMe/ ppm	δAsnOMe ppm	Δδ/ ppm
OCH_3	51.9	56.0	-4.1	52.3	56.3	-4.0
CO ester	174.2	178.9	-4.7	172.1	175.3	-3.2
$C=\overset{+}{N}=\overset{-}{N}$	55.4	54.6	0.8	53.5	37.9	1.51
α CH_2	19.7	27.6	-7.9	30.1	36.1	-6.0
β CH_2	33.4	32.7	0.7	-	-	-
CO amide	168.0	172.4	-4.4	167.8	172.0	-4.2

Mass spectra

In a glycerol matrix both diazocompounds show a reasonably intense (ca. 25%) protonated molecular ion ($M+H^+$), and also a strong ion (60-100%) due to the loss of N_2 from the protonated molecule. It was not possible to obtain accurate mass measurement using the glycerol matrix. Accurate mass analyses were carried out using a polyethylene glycol matrix. Unfortunately neither N_2GlnOMe (3) nor N_2AsnOMe (4) gave a molecular ion in this matrix and mass measurements were made on the ($M+H^+-N_2$) fragment ions. The data in Table 4.4 show that the deviations of the measured masses from the calculated masses are within acceptable limits.

Table 4.4 Accurate mass analyses of ($M+H^+N_2$) for (13) and (14)

Compound	Ion	Measured mass/mu	Calculated mass/mu	Δ/mmu
N_2GlnOMe	$C_6H_{10}NO_3$	144.05870	144.0661	-7.36
N_2AsnOMe	$C_5H_8NO_3$	130.03730	130.0502	-13.11

All these data are entirely consistent with the proposed structures of N_2GlnOMe and N_2AsnOMe.

4.5 Stabilities of N_2GlnOMe (3) and N_2AsnOMe (4) in aqueous media

The rates of decomposition of N_2GlnOMe and N_2AsnOMe were measured in both aqueous buffer solutions at a constant ionic strength of μ=0.5 ($NaClO_4$) and dilute $HClO_4$, all at 25°C. Reactions in dilute $HClO_4$, with half lives of less than 2min. were studied using a stopped-flow technique, whilst slower reactions, in buffer solutions, were carried out in the cuvettes of a uv visible spectrophotometer. In both cases the [diazoester] was monitored by the change in absorbance at λ=260nm with respect to time. The reactions were either followed to completion or quenched with a drop of conc. HCl to obtain an infinity valve.

All reactions were *pseudo* first-order in substrate (equation 4.3) and plots of

$$\text{Rate} = k_0\,[\text{diazocompound}] \qquad \ldots(4.3)$$

$\ln((A_t-A_\infty)/(A_0-A_\infty))$, where A_t=absorbance at 260nm at time t, against time were linear over at least 4 half lives. Typical plots for the reaction of N_2GlnOMe (3) with 0.01M $HClO_4$ and 0.1M acetic acid buffer (pH 4.48) at 25°C are shown in Figures 4.7 and 4.8 respectively.

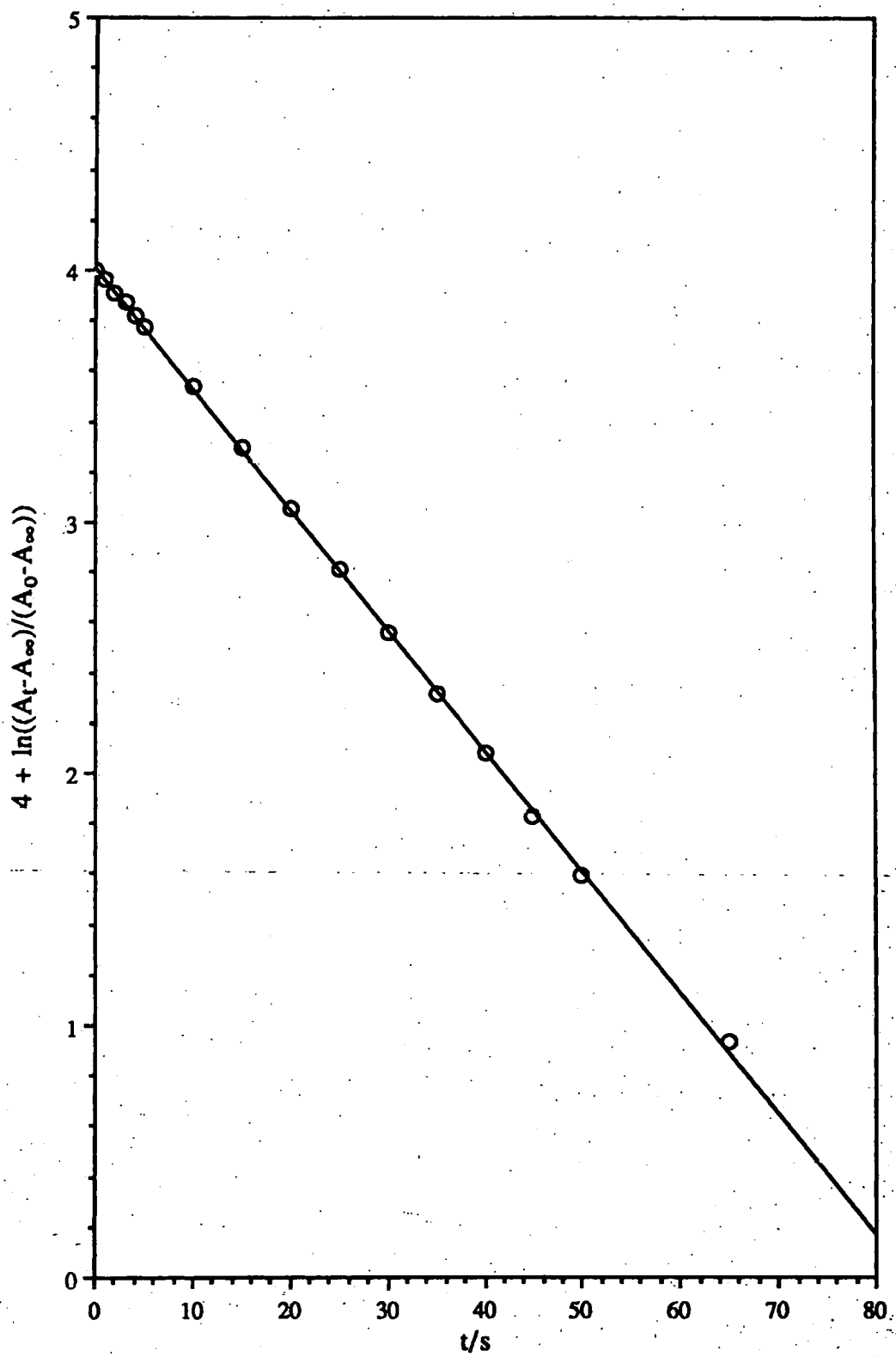

Figure 4.7 *ln $((A_t - A_\infty)/(A_0 - A_\infty))$ v time for the decomposition of N_2GlnOMe (3) in 0.01M $HClO_4$ at 25°C. Initial [N_2 GlnOMe] = ca 10^{-4}M.*

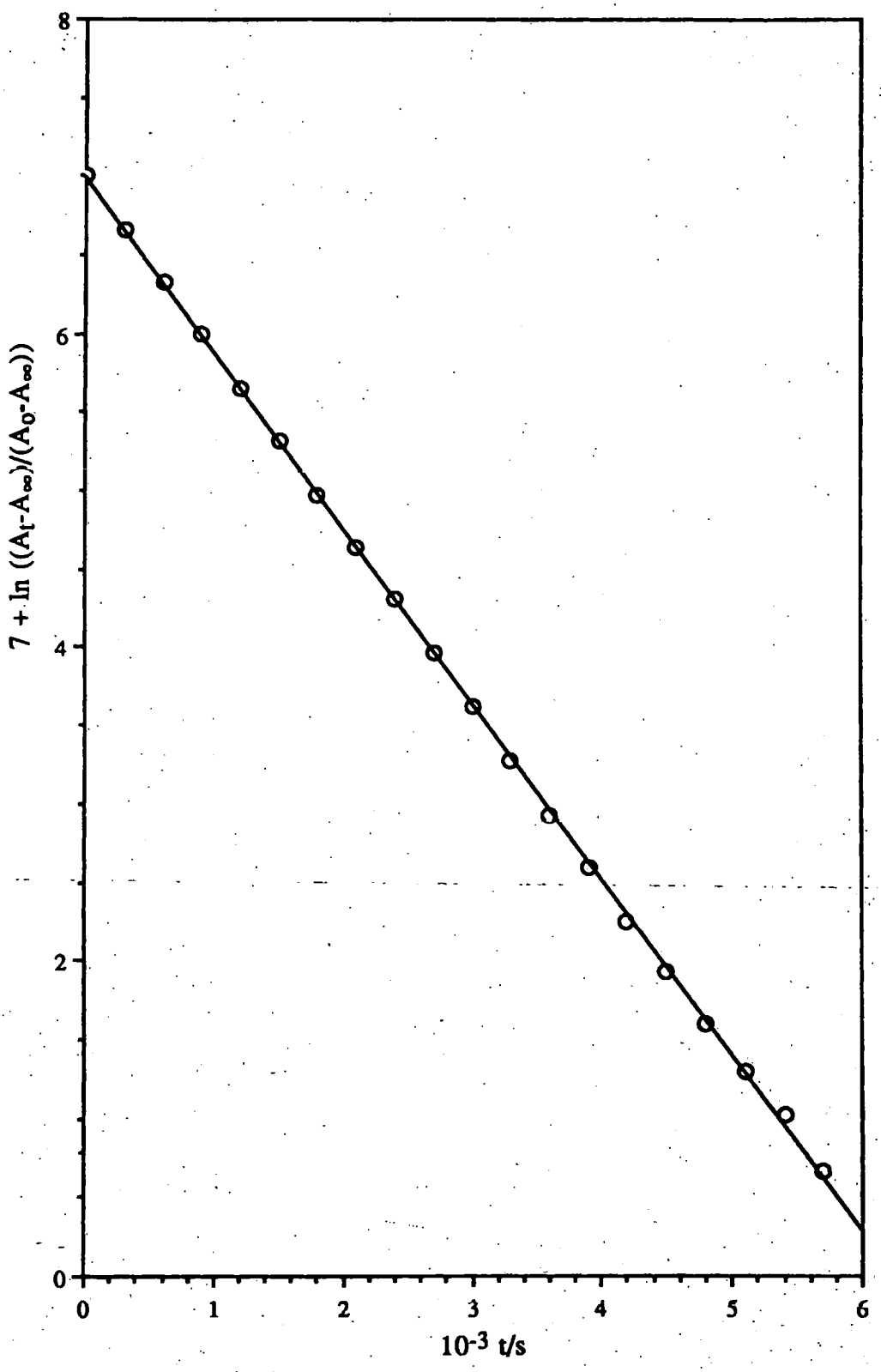

Figure 4.8 *ln ((A$_t$-A$_\infty$)/(A$_0$-A$_\infty$)) v time for the decomposition of N$_2$GlnOMe (3) in 0.1M AcOH buffer (pH 4.48) at 25°C. Initial [N$_2$GlnOMe] = ca 10^{-4}M*

4.5.1 Decomposition in $HClO_4$

The mean values (obtained from at least 5 duplicate experiments) of k_o for the decomposition of N_2 GlnOMe (3) and N_2AsnOMe (4) in aqueous $HClO_4$ at 25°C are summarised in Table 4.5. The variance of the k_o values were less than ± 2.4%.

Table 4.5 k_o Values for the decomposition N_2GlnOMe and N_2AsnOMe in dilute $HClO_4$ at 25°C. Initial [substrate] = ca. 10^{-4}m.

Substrate	$[HClO_4]$/M	$10^2k_o/s^{-1}$
N_2GlnOMe	0.0971	51
N_2GlnOMe	0.00971	4.76
N_2AsnOMe	0.0971	21.8
N_2AsnOMe	0.00971	2.13

The k_o values correspond to $t_{1/2}$ <32s, so the decomposition of both diazoesters is rapid at 25°C. The results show that decomposition is acid catalysed.

4.5.2 Decomposition in buffer solutions

Values of k_o for the decomposition of (3) and (4) in aqueous buffer solutions at 25°C are summarised in Table 4.6.The plots of k_o *versus* [HA] were usually linear with a positive intercept, as shown, for the decomposition of N_2GlnOMe (3) in aqueous acetic acid buffer (pH 4.47) at 25°C, in Figure 4.9. Further, for acetic acid, the slopes of these plots are independent of the buffer ratio which implies that the buffer acid (ie. AcOH) is the catalytic entity. It is clear from these data that the decomposition of the diazoamino acid esters is catalysed by both H_3O^+ and the buffer acid (HA). Thus the reactions are subject to general acid catalysis and the full rate equation is given by

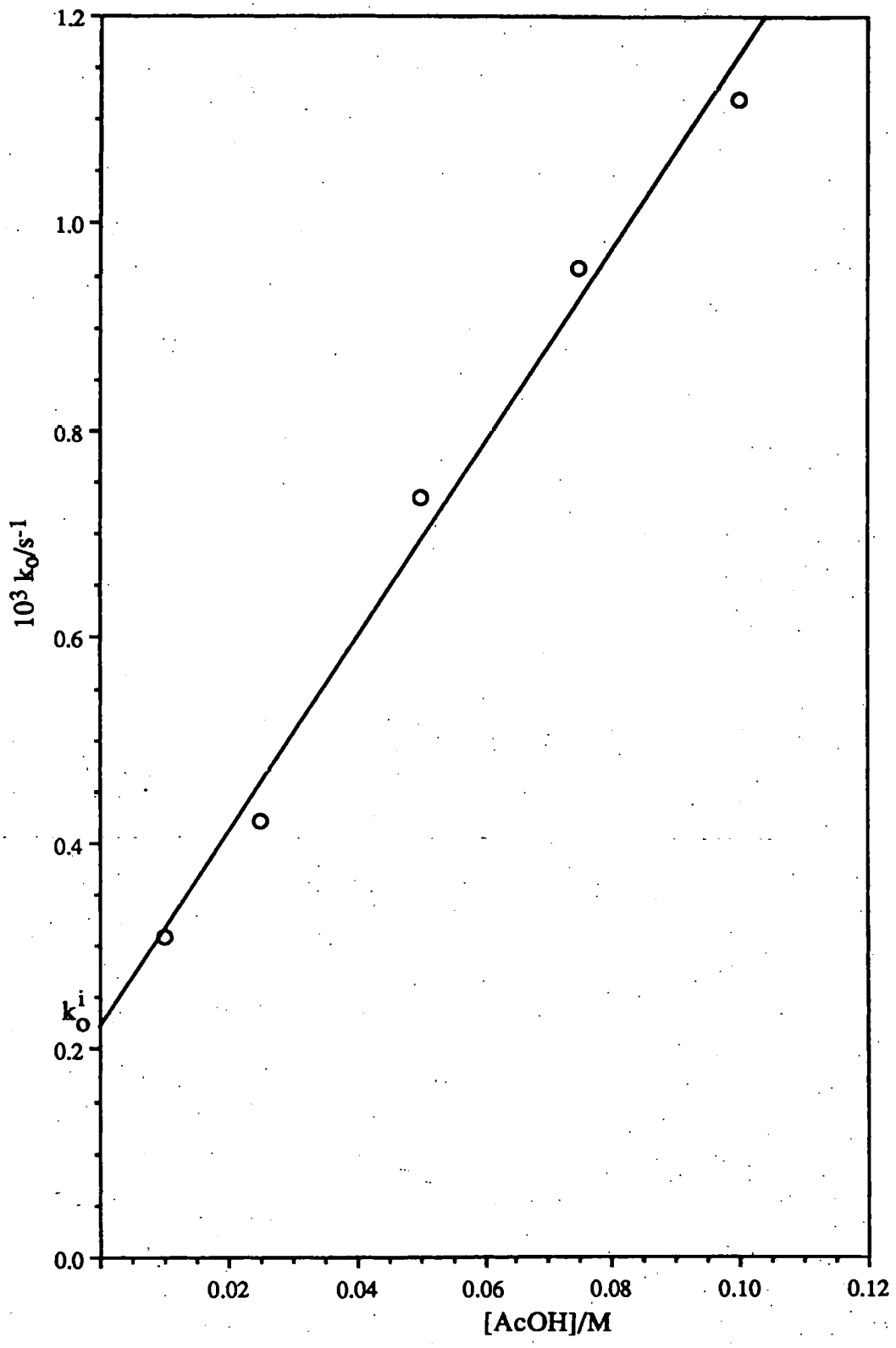

Figure 4.9 k_o *versus [AcOH] for the decomposition of* N_2*GlnOMe (3) in AcOH buffers (pH 4.47) 25°C,* μ*=0.5 (*$NaClO_4$*)*

Table 4.6 **Observed *pseudo* first-order rate coefficients for decomposition of (3) and (4) in aqueous buffer solutions at 25°C. Initial [substrate]= ca.10^{-4}M.**

Buffer	$[HA]/[A^-]$	[HA]/M	pH	$10^5k_o(3)/s^{-1}$	$10^5k_o(4)/s^{-1}$
Formate	1	0.1	3.44	727	185
		0.075	3.45	614	178
		0.050	3.46	449	157
		0.025	3.46	353	133
		0.01	3.47	259	105
Acetate	4	0.08	3.86	189	65.7
		0.06	3.87	163	60.7
		0.04	3.88	140	53.7
		0.02	3.89	112	47.5
Acetate	1	0.10	4.48	112	18.5
		0.075	4.47	95.8	17.5
		0.05	4.47	73.6	17.1
		0.025	4.48	42.1	14.4
		0.010	4.47	30.9	12.2
Acetate	0.25	0.02	5.14	25.3	5.40
		0.015	5.13	21.3	5.02
		0.010	5.13	15.4	4.92
		0.005	5.13	10.6	4.20
Phosphate	1	0.10	6.57	3.07	-
		0.075	6.49	2.68	-
		0.050	6.44	2.14	-
		0.025	6.39	1.35	-
		0.01	6.39	0.717	-

equation 4.4, where k_H and k_{HA} refer to catalysis by H_3O^+ and HA, respectively.

$$\text{Rate} = (k_H[H_3O^+] + k_{HA}[HA])\,[\text{substrate}] \qquad \ldots(4.4)$$

Values of k_H and k_{HA} were obtained from the intercept ($=k_o^i \approx k_H[H_3O^+]$) and the slopes ($= k_{HA}$) of the buffer catalysis plots respectively, and these are summarised in Table 4.7.

Table 4.7 Values of k_o^i and k_{HA} for the decomposition of N_2GlnOMe (3) and N_2AsnOMe (4) at 25°C.

pH	HA	$k_o^i(3)/s^{-1}$	$k_o^i(4)/s^{-1}$	$10^4k_{HA}(3)/m^{-1}s^{-1}$	$10^4k_{HA}(4)/m^{-1}s^{-1}$
1.01	$HClO_4$	0.51[a]	0.22	-	-
2.01	$HClO_4$	4.76×10^{-2}[a]	2.13×10^{-2}	-	-
3.46	HCOOH	2.10×10^{-3}	1.00×10^{-3}	520	126
3.88	AcOH	8.79×10^{-4}	4.16×10^{-4}	126	30.8
4.47	AcOH	2.22×10^{-4}	1.11×10^{-4}	93.5	12.1
5.13	AcOH	5.66×10^{-5}	3.80×10^{-5}	99.6	8.04
6.40	H_2PO_4	4.05×10^{-6}	-	3.52	-

a $k_o^i = k_o$ for reactions in $HClO_4$ where no k_{HA} term is present.

In some cases, especially for the decomposition of N_2AsnOMe (4), the plots of k_o *versus* buffer acid (HA) showed curvature at high acid concentrations. Such a plot for the decomposition of N_2AsnOMe (4) in formic acid buffers (pH 3.46) at 25°C is shown in Figure 4.10. In these cases, the intercepts ($k_o^i \approx k_{H_3O^+}[H_3O^+]$) were determined from the lower HA concentrations only. The decrease observed in the values of k_{HA}, for the decomposition of N_2AsnOMe in AcOH buffers on decreasing

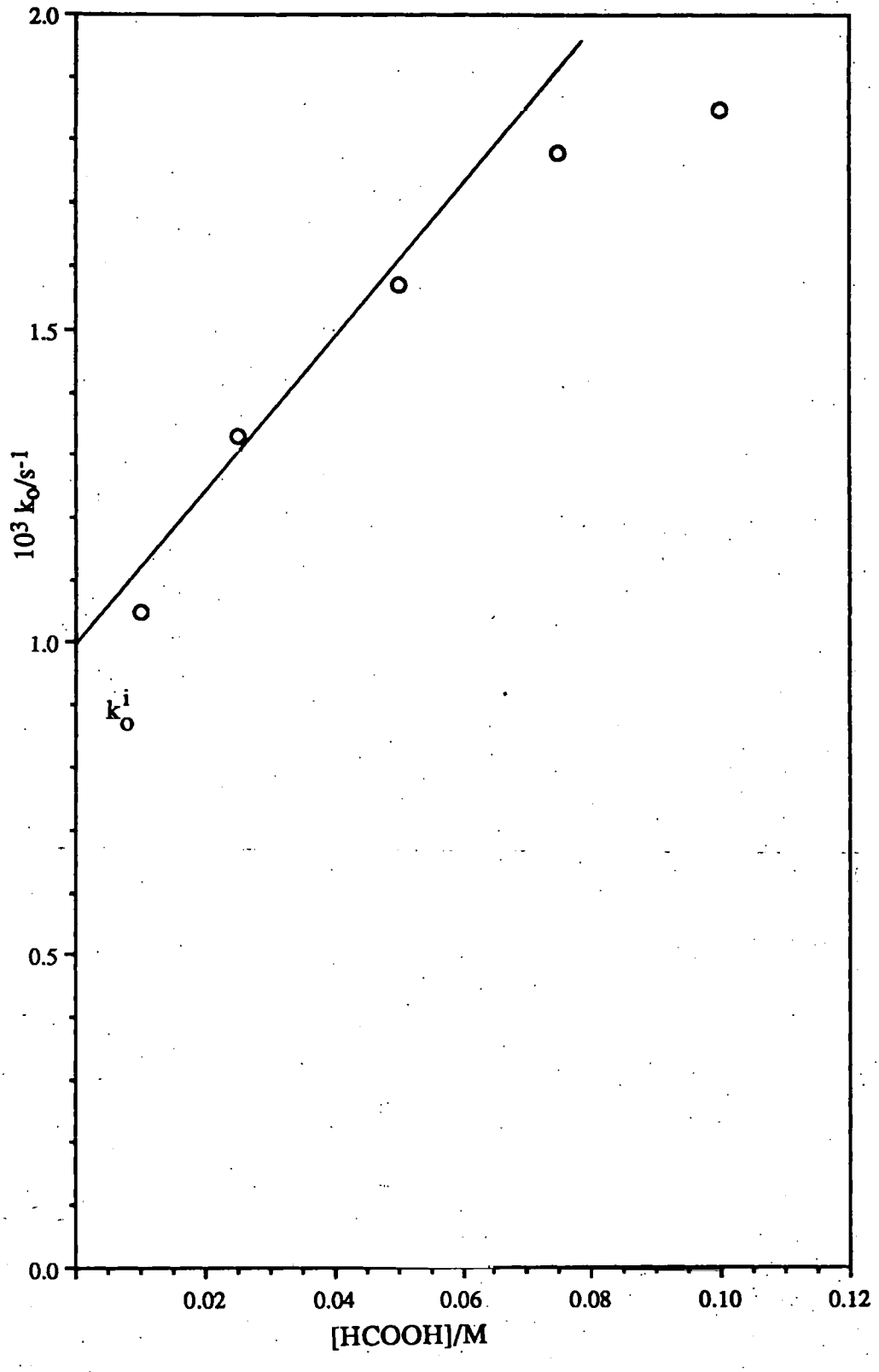

Figure 4.10 . k_o *versus [HCOOH] for the decomposition of* N_2*AsnOMe (4) in formic acid buffers (pH 3.46) 25°C,* μ*=0.5 (*$NaClO_4$*)*

the [HA]/[A$^-$] ratio, was unexpected and possible reasons for this behaviour are discussed later in this Section.

Values of log k_o^i are plotted against pH for the decomposition of N_2 GlnOMe (3) and N_2AsnOMe (4) at 25°C under various conditions in Figure 4.11. Both plots, with unit gradient, show that the decomposition of the diazoesters (3) and (4) has a first order dependence upon [H_3O^+]. The second order rate coefficients (k_H) obtained from the gradient of plots of k_o^i against [H_3O^+] are summarised in Table 4.8. The intercept values of these plots give a *pseudo* first order rate constant (k_w) for the spontaneous hydrolysis of the diazoester by water (equation 4.5) and these values are also summarised in Table 4.8.

$$k_o^i = kw + k_H [H_3O^+] \qquad ...(4.5)$$

Table 4.8 Rate constants k_H and k_w for the hydrolysis of N_2GlnOMe and N_2AsnOMe in aqueous solution at 25°C.

Compound	$k_H/M^{-1}s^{-1}$	$10^5k_w/s^{-1}$
N_2GlnOMe	6.06	1.83
N_2AsnOMe	2.81	3.01

4.5.3 Solvent deuterium isotope effects

The decomposition of N_2GlnOMe (3) and N_2AsnOMe (4) at 25°C was also examined in dilute $DClO_4$ to examine the magnitude of the solvent deuterium isotope effect. Average values of k_o (equation 4.3), obtained from at least five separate determinations, for the decomposition of (3) and (4) in $DClO_4$ at 25°C are summarised in Table 4.9. Plots of k_o against [$DClO_4$] are linear as shown in Figure 4.12.

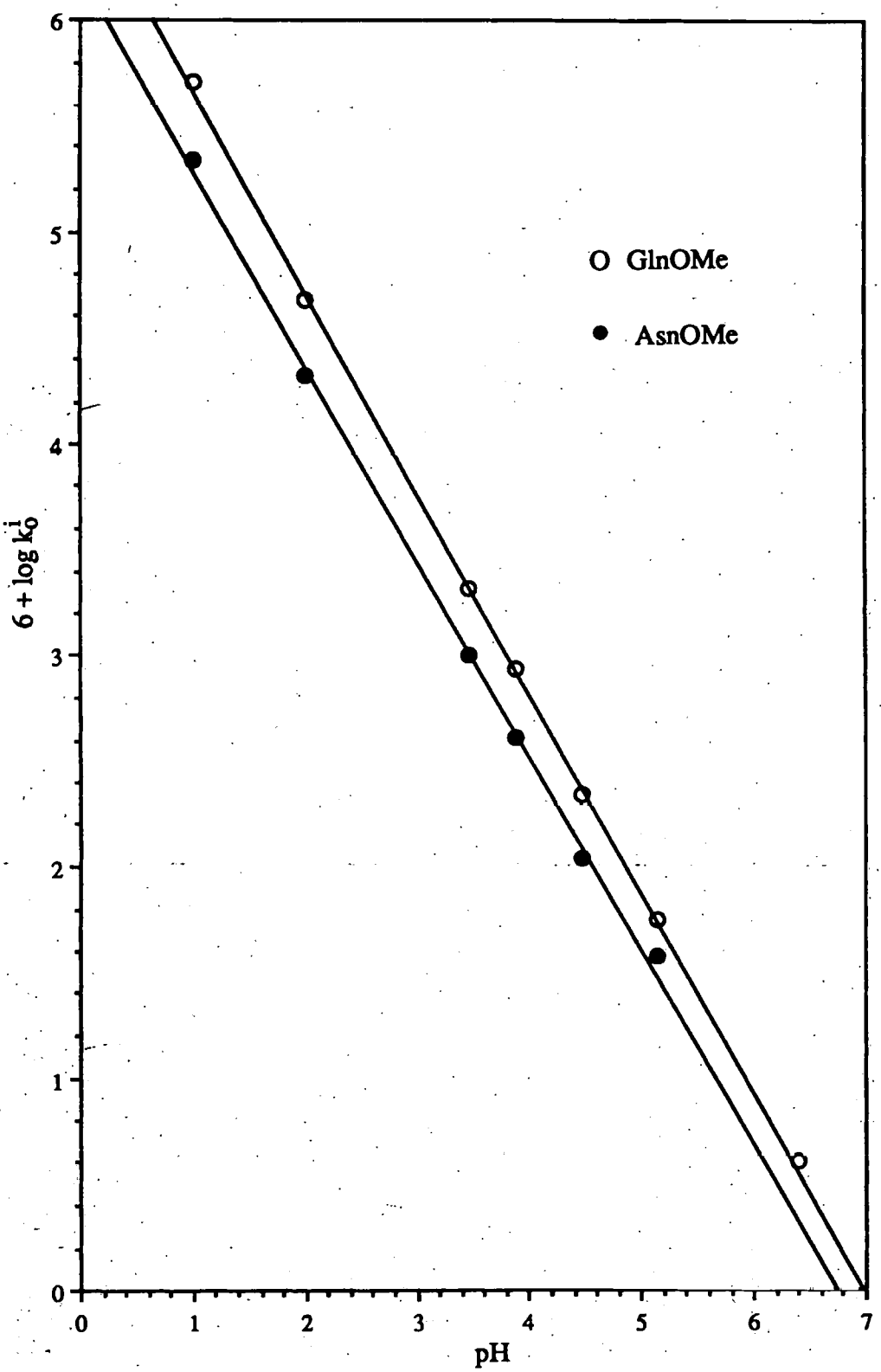

Figure 4.11 *log k_o^i v pH for the decomposition of N_2GlnOMe and N_2AsnOMe in aqueous $HClO_4$ and buffer solutions at 25°C.*

Table 4.9 **k_0 for the decomposition of (3) and (4) in $DClO_4$ at 25°C. Initial [substrate] = ca. 10^{-4}M.**

$[DClO_4]$/M	$10^2 k_0$ (3)/s^{-1}	$10^2 k_0$ (4)/s^{-1}
0.0985	25.2	13.4
0.0492	11.3	6.40
0.0099	2.10	1.27

The values of k_D, the second order rate coefficient for the deuterio acid catalysed decomposition of substrate and the kinetic solvent isotope effects, k_H/k_D, are given in Table 4.10.

Table 4.10 **Second order rate coefficients for the D_3O^+ catalysed decomposition of (3) and (4) at 25°C.**

Substrate	k_D /$M^{-1}s^{-1}$	k_H/k_D
N_2GlnOMe	2.62	2.31
N_2AsnOMe	1.37	2.05

It is clear from these data that the H_3O^+ catalysed decomposition of the diazoamino acid ester (3) and (4) shows a normal deuterium isotope effect, indicative of the rate determining step involving proton transfer.

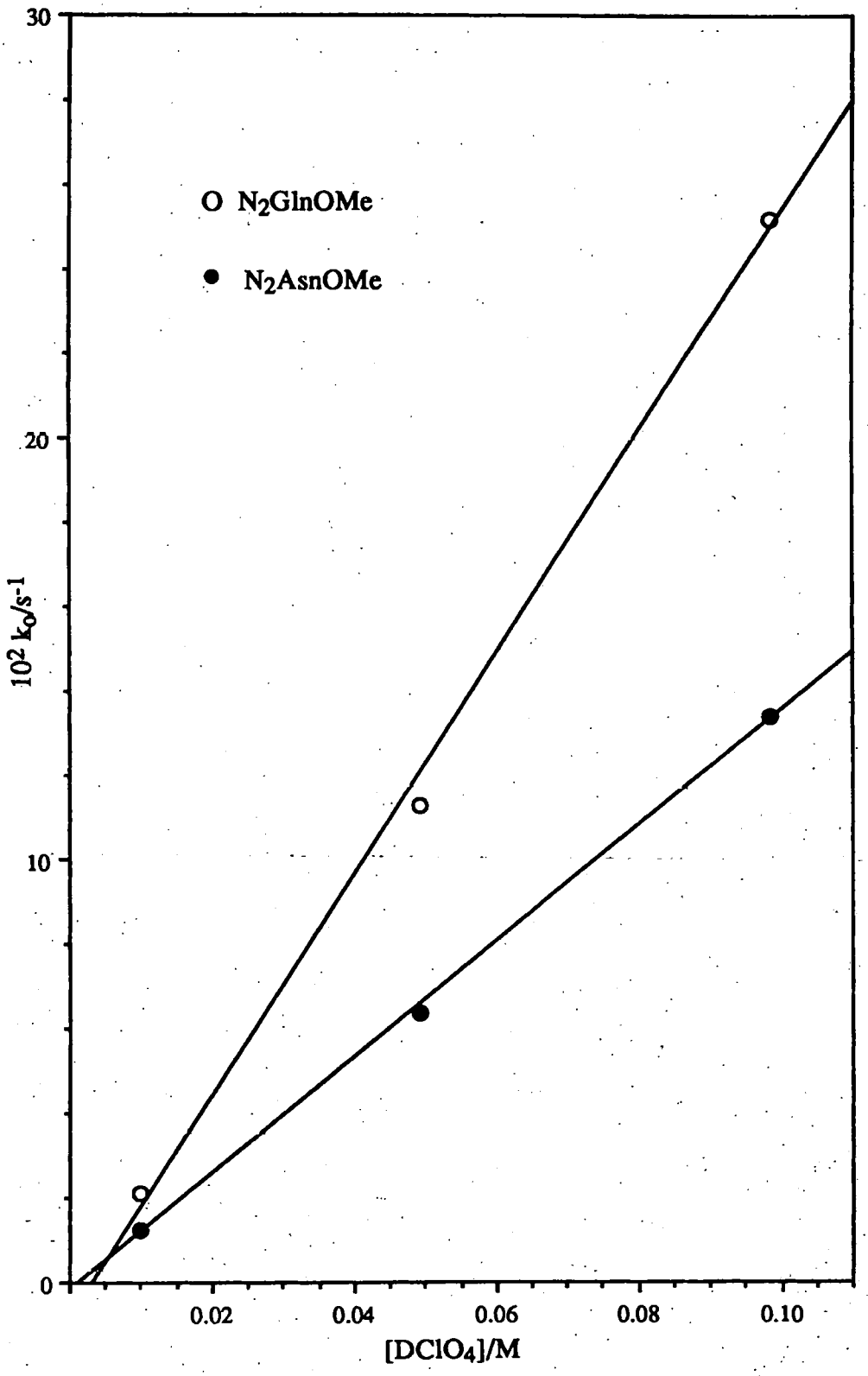

Figure 4.12 k_o *v* $[DClO_4]$ *for the decomposition of* N_2*GlnOMe and* N_2*AsnOMe in* $DClO_4$ *at 25°C. Initial [substrate] = ca* 10^{-4}*M.*

4.5.4 Brønsted relationships

For general acid catalysed reactions, the kinetic effect of catalysts is directly proportional to the acid strength (pK_a). This is known as the Brønsted relationship.

The Brønsted plot of log k_{HA} against -pK_a for the catalysed decomposition of N_2GlnOMe (3) is shown in Figure 4.13. The plot is linear with a slope (α) of 0.62. This is consistent with slow proton transfer being the rate determining step and indicates that the extent of protonation in the transition state is approximately 60%. The reaction is therefore relatively sensitive to the strength of the catalyst and the transition state lies just on the product side. Similar values of α (0.61, 0.59) were observed by Albery et. al. for the decomposition of 3-diazobutan-2-one and ethyl diazopropionate respectively.[141]

4.5.5 Discussion

The decompositions of the diazoamino acid ester (3) and (4) in aqueous media (pH 1 6.4) shows a dependence on [H_3O^+], are subject to general acid catalysis and exhibit normal solvent deuterium isotope effects. Further, the decomposition of N_2GlnOMe (3) shows a positive Brønsted correlation (α=0.62). These factors are all consistent with a bimolecular acid catalysed pathway in which the rate determining step is a slow proton transfer to the substrate (A-S_E2 mechanism Figure 4.14).

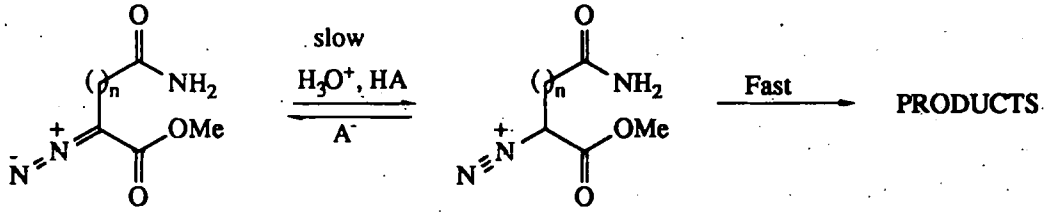

Figure 4.14 A-S_E2 mechanism of decomposition of N_2GlnOMe and N_2AsnOMe.

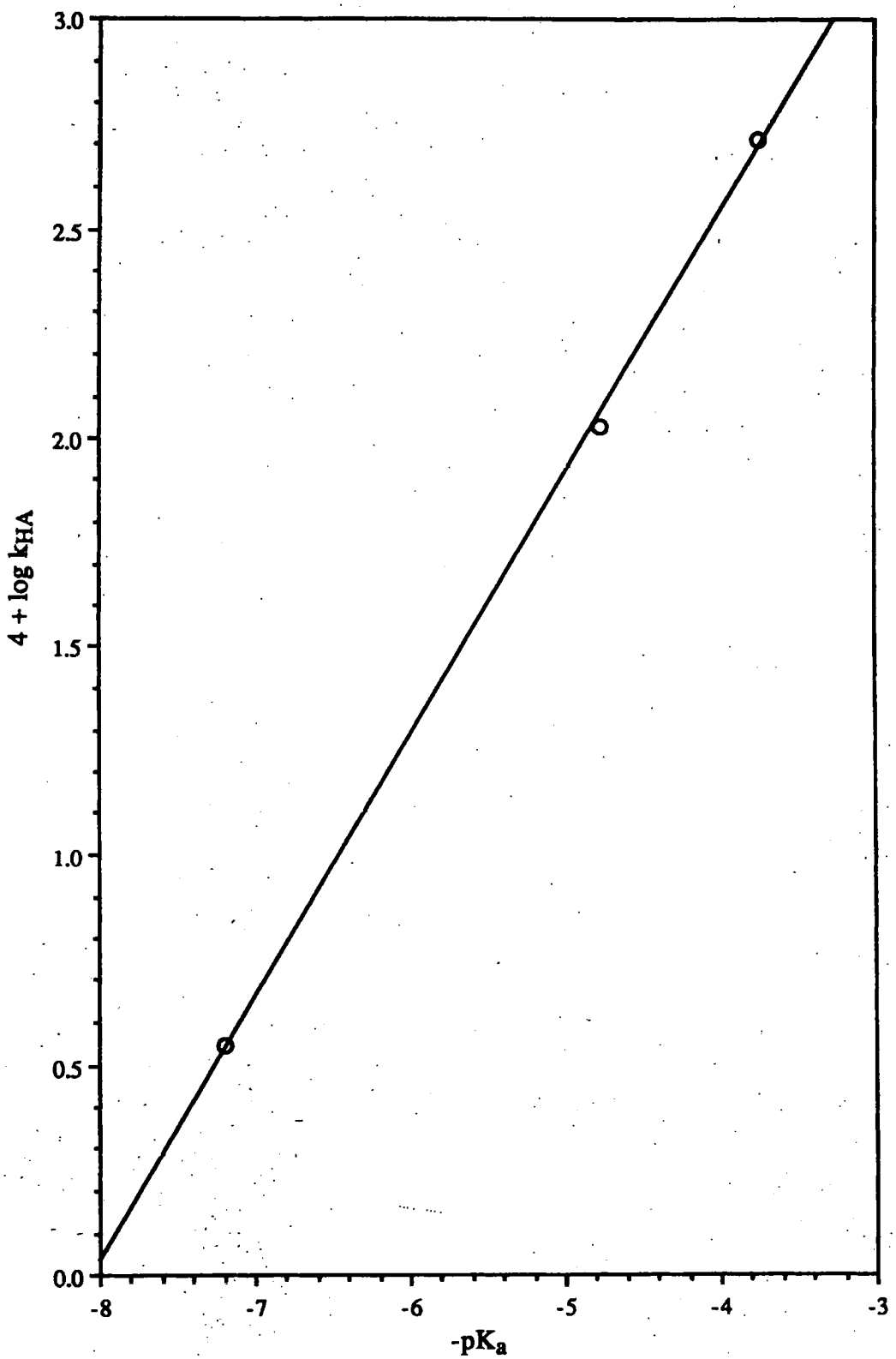

Figure 4.13 Bronsted plot, log k_{HA} v -pK_a for the HA catalysed decomposition of N_2GlnOMe (3) at 25°C.

Values of $k_H/k_D = 2.31$ (N_2GlnOMe) and 2.05 (N_2AsnOMe) are consistent with those reported for the A-S_E2 decomposition of secondary diazoketones CH_3COCN_2R, (R=Me, Et, i-Pr) in $HClO_4$.[142]

N_2GlnOMe is ca. twice as reactive as N_2AsnOMe. This is consistent with reduction in the basicity of the α- C atom due to electron withdrawal by the amide group and proton transfer being the slow step. Increasing the length of the side chain reduces the effect of the amide group, rendering the α-C atom more basic. Hence it is more easily protonated and N_2GlnOMe is more reactive than N_2AsnOMe.

Curvature in plots of k_o against [HA] may be tentative evidence for a change in the rate-limiting step at high [HA]. Application of steady-state kinetic theory to the reaction scheme for the HA catalysed decomposition of N_2AsnOMe (Figure 4.15) leads to

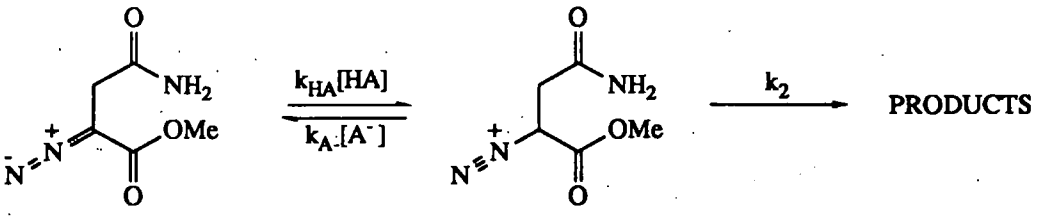

Figure 4.15 Reaction scheme for A-S_E2 catalysed decomposition of N_2AsnOMe

equation 4.6 as the full rate expression. At low [A^-], it is anticipated that $k_2 >> k_A^-[A^-]$

$$\frac{-d[N_2AsnOMe]}{dt} = \left\{\frac{k_2 k_{HA}[HA]}{k_A^-[A^-]+k_2}\right\} [N_2AsnOMe] \qquad ...(4.6)$$

and equation 4.6 approximates to the experimentally determined rate expression (equation 4.4). At high [A^-], however, the possibility that $k_2 << k_A^-[A^-]$ exists and equation 4.6 approximates to equation 4.7. Under these conditions, plots of log k_o against [HA] would be curved and tend to a constant value at high [HA].

$$\frac{-d[N_2AsnOMe]}{dt} = \left\{\frac{k_2 k_{HA}[HA]}{k_A^-[A^-]}\right\} [N_2AsnOMe] \qquad ...(4.7)$$

This implies a change in the rate determining step at high [HA] and loss of nitrogen becomes rate limiting.

Similar effects have been reported for the decomposition of 3-diazobutan-2-one at high concentrations.[143] A more detailed study of the HA catalysed pathway of this reaction by Albery *et.al.*,[148] (Figure 4.16) gave rise to equation 4.8, where k_w is the forwards

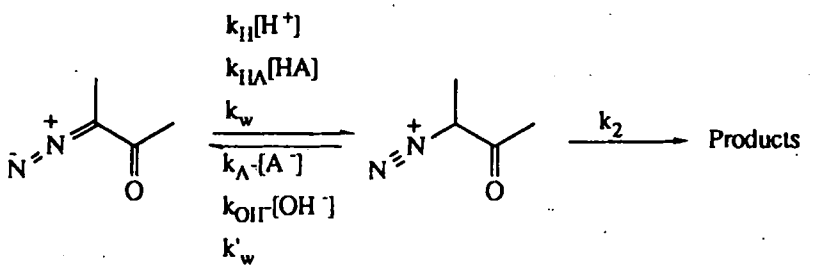

Figure 4.16 Decomposition of 3-diazobutan-2-one in acid buffers

$$\text{Rate} = k_o\,[\text{diazocompound}] \qquad \ldots(4.8)$$

$$k_o = \frac{(k_H[H^+] + k_{HA}[HA] + k_w)\,k_2}{k_2 + k'_w + k_A[A^-] + k_{OH^-}}$$

rate constant for catalysis of the protonation step and k'_w and k_{OH^-} are the backwards rate constants for this step. At low pH, the terms k_w and k_{OH^-} are small compared to k_o and can be discounted, giving equation 4.9.

$$k_o = \frac{(k_H[H^+] + k_{HA}[HA] \quad\quad)k_2}{k_2 + k'_w + k_A[A]} \qquad \ldots(4.9)$$

A second, thermodynamic relationship exists (equation 4.10) and combination of

$$\frac{k_{HA}k'_w}{k_H k_A} = \frac{[H^+][A^-]}{[HA]} \qquad \ldots(4.10)$$

equations 4.9 and 4.10, to eliminate $k_A[A^-]$, leads to equation 4.11. The term $k_2k_H[H^+]/(k_2 + k'_w)$ is equal to the rate of reaction in the absence of buffer catalysis and, at low pH, can be approximated to $k_H[H^+]$.

$$\frac{1}{k_o - k_2k_H[H^+]/(k_2+k'_w)} = \frac{1}{[HA]} \cdot \frac{(1 + k'_w/k_2)^2}{k_{HA}} + \frac{1}{[H^+]} \cdot \frac{k'_w(k_2+k'_w)}{k_2k_H} \qquad \ldots(4.11)$$

Using the value of k_H determined from the decomposition of N_2AsnOMe in $HClO_4$ at 25°C, a plot of $1/(k_o-k_H[H^+])$ against $1/[HA]$ for the decomposition of N_2AsnOMe in formic acid buffer (pH 3.46) was linear (Figure 4.17, cf. Figure 4.10) (at higher pH the relationship is no longer valid since the inequality $k_o >> k_w$ is no longer true). Thus at least at low pH, it would appear that at high buffer ion concentrations, loss of nitrogen becomes partially rate limiting.

4.6 Deamination reactions

The side chains of N_2GlnOMe (3) and N_2AsnOMe (4) may react intramolecularly, with expulsion of N_2, to form either the lactams (5) and (6), or the imidate esters (7) and(8), respectively.

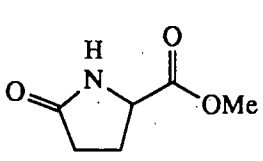

(5)

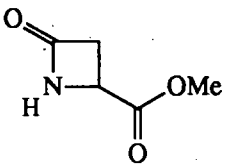

(6)

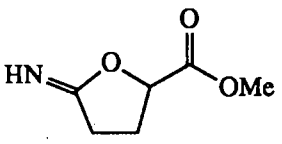

(7)

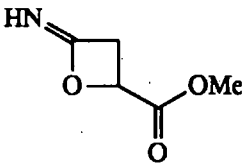

(8)

Most imidate esters, however, are labile and subsequent hydrolysis of (7) and (8) is expected to form the lactones (9) and (10). Compounds (9) and (10) were therefore considered to be likely isolable reaction products other than the lactams (5) and (6). Attempts to synthesise (5), (6), (9) and (10) are described below.

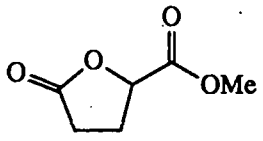

(9)

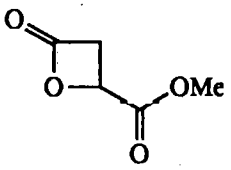

(10)

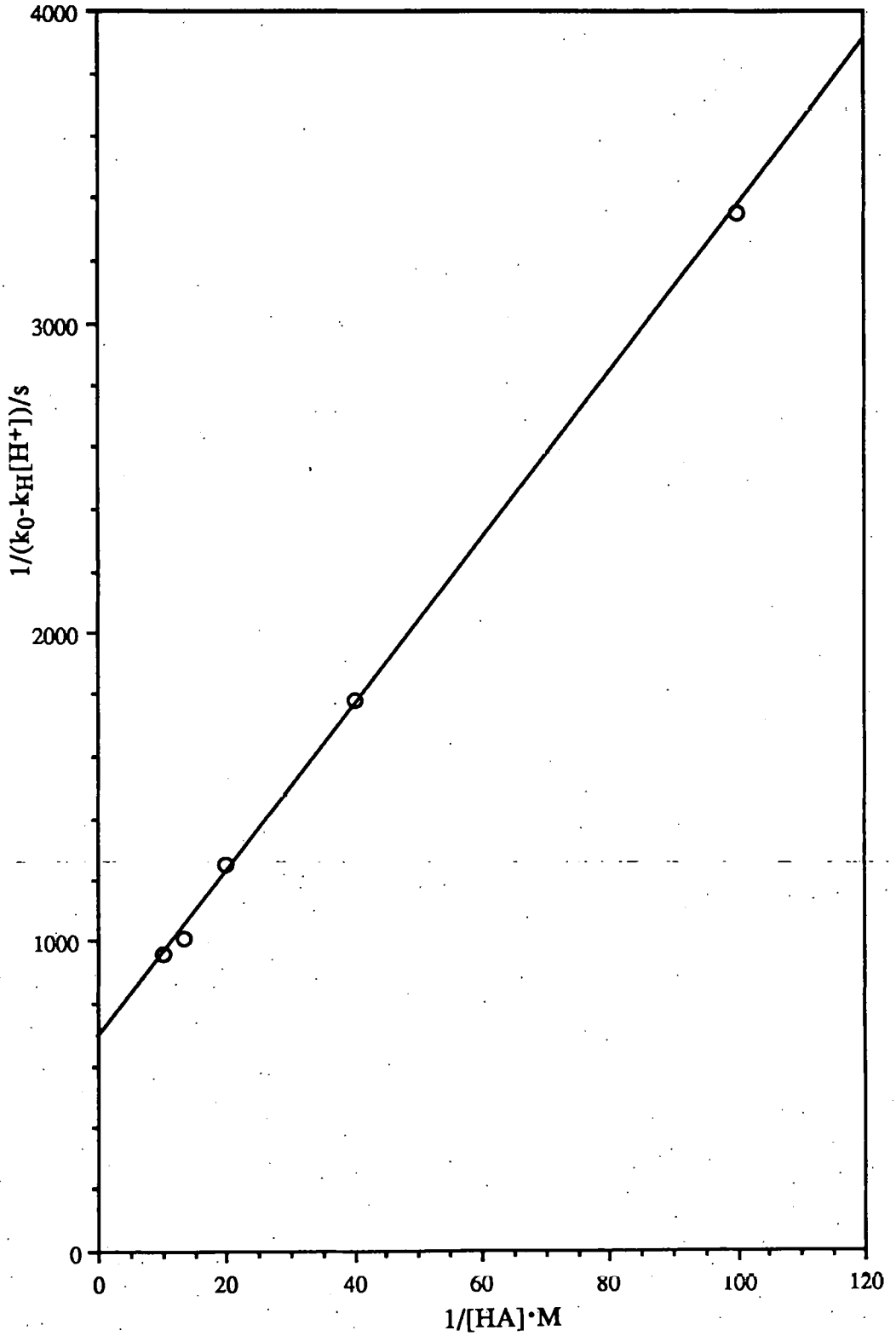

Figure 4.17 *$1/(k_o-k_H[H^+])$ v $1/[HA]$ for the decomposition of N_2AsnOMe (4) in formic acid buffers (pH 3.46) 25°C, μ=0.5 ($NaClO_4$)*

4.6.1 Synthesis of potential cyclic deamination products

4.6.1.1 Methyl 2-pyrrolidone-5-carboxylate (5)

Compound (5) was prepared by treatment of 2-pyrrolidone-5-carboxylic acid with ethereal diazomethane in methanol at 0°C. The product was isolated by removal of the solvent and purified by column chromatography as described in Section 7.5.

4.6.1.2 Methyl azetidin-2-one-4-carboxylate (6)

Compound (6) was synthesised from L-aspartic acid using the reaction sequence summarised in Figure 4.18. The yields obtained are given in parenthesis.

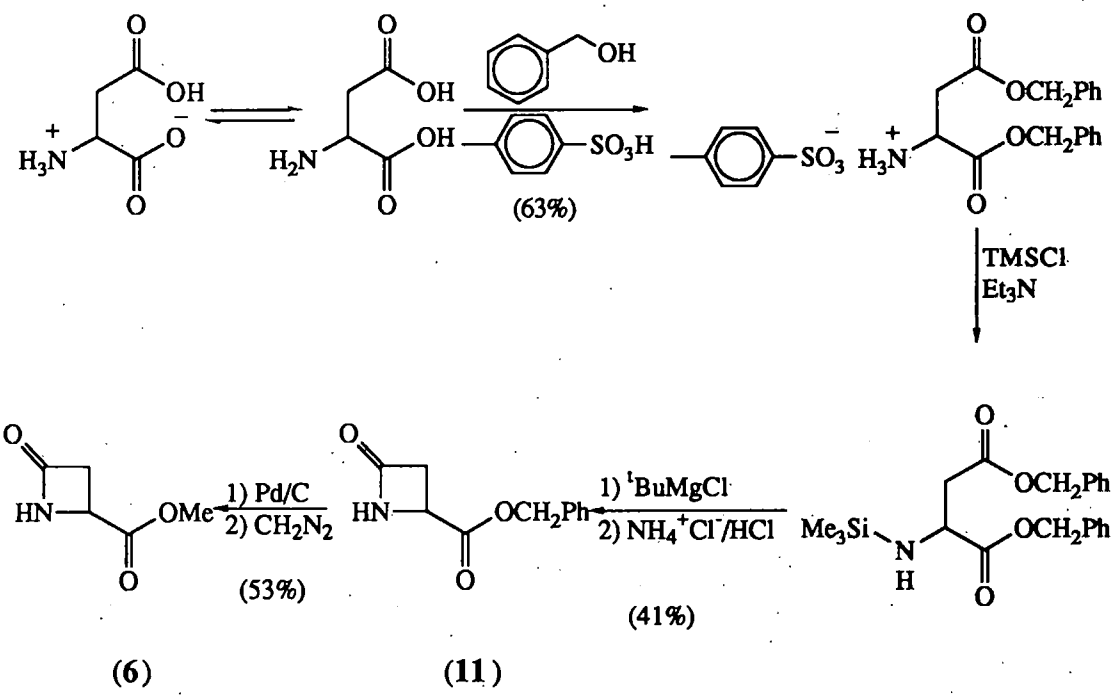

(6) (11)

Figure 4.18 Synthesis of compound (6) from L-aspartic acid.

The cyclisation of O,N bis(trimethylsilyl) β-amino acids has been reported by Birkofer and Schramm.[144] Later, Salzmann et.al.[145,146] reported the synthesis of (11) using a Grignard-mediated cyclisation of an N-silylated aspartate diester.

Thus, L-aspartic acid dibenzyl ester p-toluenesulphonic acid salt (12) was prepared from L-aspartic acid and benzyl alcohol in the presence of p-toluene sulphonic acid.[147] Treatment of the salt with triethylamine and trimethylsilyl chloride gives the N-trimethylsilylbenzyl aspartate. The TMS group makes the amino proton more acidic and stabilises the anion formed by subsequent treatment with t-butylmagnesium chloride. The amine anion undergoes an intramolecular cyclisation to give the lactam (11) in 43% yield after removal of the silyl protecting group. Attempts to effect a transesterification ((11)→(6)) were unsuccessful, so the benzyl ester was removed by catalytic hydrogenolysis in the presence of Pd/C, and the resulting acid was treated with diazomethane. Compound (6) was isolated and purified by column chromatography in 53% yield. The reaction with diazomethane was highly regiospecific and there was no evidence of concurrent N-methylation of the azetidinone nitrogen.

4.6.1.3 Methyl 5-oxo-2-tetrahydrofuran carboxylate (9)

Compound (9) was prepared in a similar manner to lactam (5), from 5-oxo-2-tetrahydrofuran carboxylic acid and diazomethane, as an oil which on recrystallisation gave (9) as a white solid in 74% yield.

4.6.1.4 Methyl 4-oxetan-2-one carboxylate (10)

Several attempts were made to synthesise (10) but none were successful. The method explored most thoroughly involved treating malic acid dimethyl ester with a hindered base. Neither LDA after 5 days at RT nor DBU under reflux effected the expected cyclisation to give the β-lactone (10) (Figure 4.19), despite its analogy to the formation of the azetidinone (6). There was no evidence of β-lactone (10) in reaction mixture, which after work-up, consisted mainly of starting material.

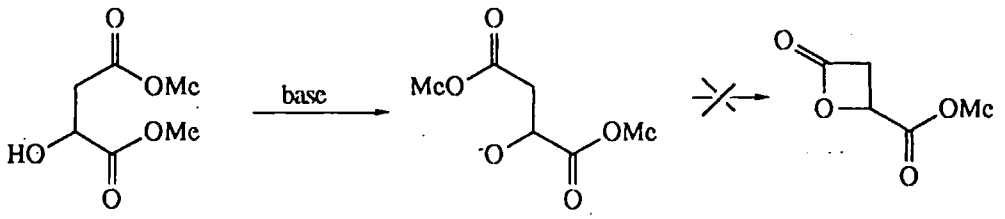

Figure 4.19 Synthesis of (10) from aspartic acid dimethyl ester

An alternative synthesis, briefly investigated, involved the treatment of N-α-carbobenzyloxy-L-aspartic acid-α-methyl ester (13) with N_2O_4 to form the N-nitroso compound (14), which was heated to affect a rearrangement and elimination of benzyl alcohol, nitrogen and CO_2 (Figure 4.20).

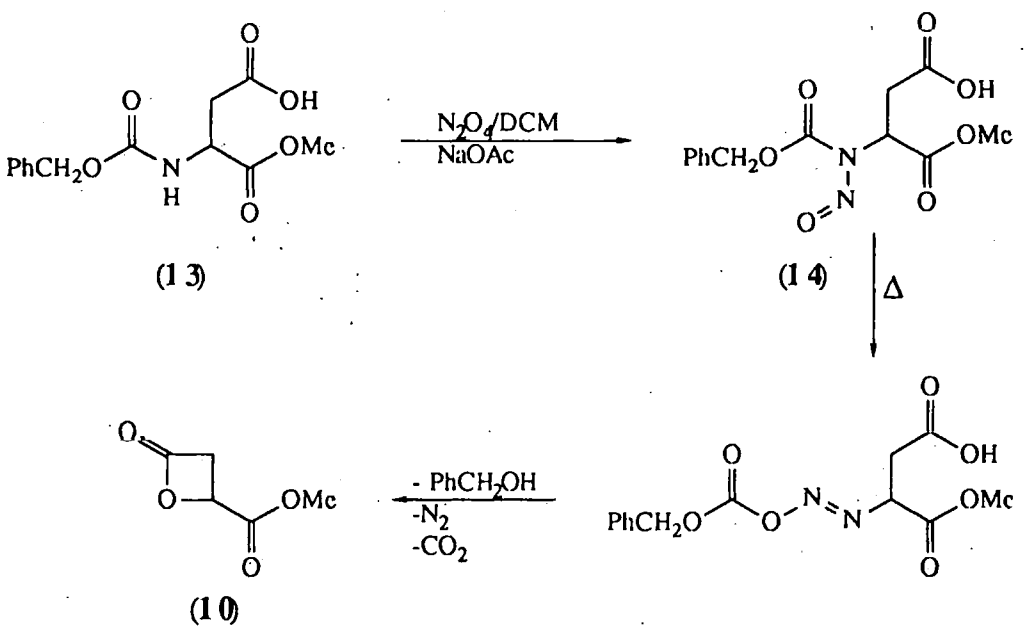

Figure 4.20 Route attempted for the synthesis of β-lactone (10)

However, after heating, the reaction mixture was found to consist of (13) indicating that nitrosation had not occurred. This synthetic route was pursued no further.

Compound (13) was deprotected by catalytic hydrogenolysis to give L-aspartic acid-α-methyl ester (15). Attempts to deaminate and cyclise (15) with aqueous nitrous acid were also unsuccessful. No further attempts to prepare the authentic β-lactone (10) were made.

4.6.2 Cyclic products from the deamination of GlnOMe and AsnOMe

4.6.2.1 Cyclic products from nitrosations in dilute HCl

L-Glutamine methyl ester (1) and L-asparagine methyl ester (2) were treated with nitrous acid in the presence of 0.1M HCl and CH_2Cl_2 or EtOAc. Products which migrated into the organic phase were analysed after drying and removal of the solvent, by capillary GLC and GLC/MS.

4.6.2.1.1 L-Glutamine methyl ester (1)

Treatment of L-glutamine methyl ester with nitrous acid in 0.1M HCl at 0°C gave only the γ-lactone (9) in the organic phase. The γ-lactone (9) was characterised by GLC/MS and comparison with authentic material. It is proposed that formation of (9) proceeds *via* the diazo intermediate which is trapped initially by an intramolecular substitution of the O-atom of the carboxamide sidechain to give the imidate ester (7). This ester is then hydrolysed in the aqueous reaction mixture to form the γ-lactone (9). (Figure 4.21).

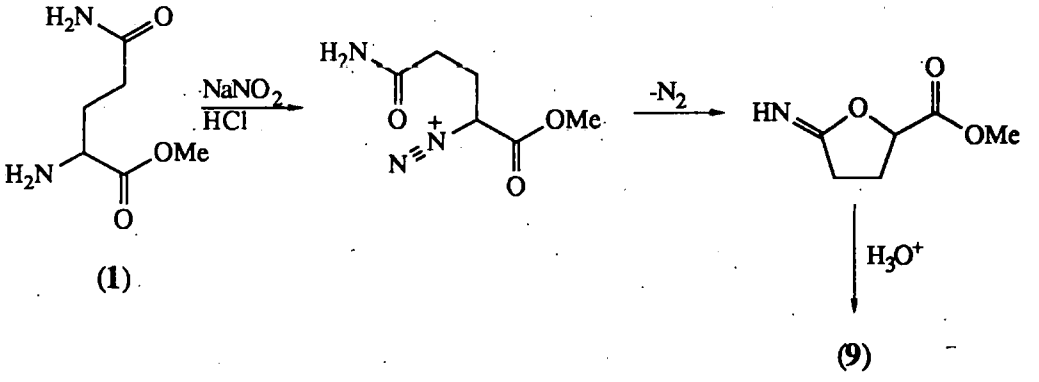

Figure 4.21 Deamination of GlnOMe (1) in aqueous nitrous acid

No evidence was obtained for concurrent formation of the γ-lactam (5) by an analagous reaction of the carboxamide N-atom even though in independent control experiments the γ-lactam (5) was extracted from aqueous 0.1M HCl containing HNO_2 into CH_2Cl_2 in excess of 70%. This suggests that intramolecular alkylation of the carboxamide side chain proceeds exclusively at the O-atom and therefore that (9) is the kinetic product.

4.6.2.1.2 Quantitation of (9)

The quantitation of the γ-lactone (9) was determined by capillary GLC following extraction into EtOAc as described in Section 7.2.5. Quantitation of the γ-lactone (9) is complicated by concurrent hydrolysis in the reaction solution. This is evident from the variation of γ-lactone concentration with time for the nitrosation of 3mM glutamine methyl ester (1) with 30mM $NaNO_2$ in 0.1M HCl at 37°C, shown in Figure 4.22. The concentration of (9) passes through a maximum value at about 4.7h.

It was shown in Section 4.3 that the formation of (9) follows equation 4.1, where $k_0 = k_3[HNO_2][HCl]$. It seems probable that the decomposition of (9) follows equation 4.12, where k_1 is dependent on the $[H_3O^+]$. It follows that the complete expression for the rate of formation of the γ-lactone (9) is therefore given by equation 4.13 and that the variation in the concentration of (9) with time can be solved by regarding the reactions as sequential *pseudo* first-order reactions (Figure 4.23) and applying literature procedures.[148]

$$\frac{-d[(9)]}{dt} = k_1[(9)] \qquad ...(4.12)$$

$$\frac{-d[(9)]}{dt} = k_0[\text{GlnOMe}] - k_1[(9)] \qquad ...(4.13)$$

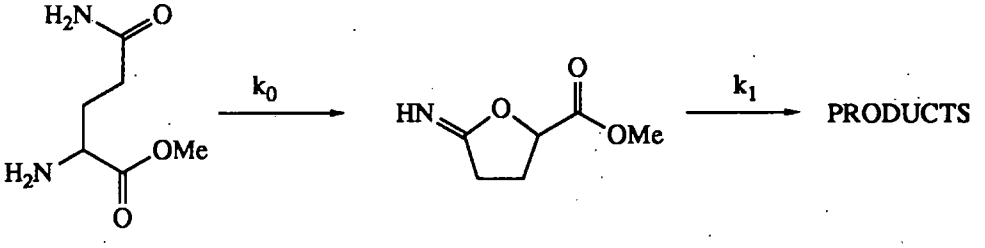

Figure 4.23 Series reactions for formation and decomposition of (9) from (1)

These show that the maximum yield (β_{max}) of γ-lactone (9) is given by equation 4.14 and at a time (τ_{max}) given by equation 4.15, where $\kappa = {}^{k_1}/_{k_0}$.

$$\beta_{max} = \kappa^{\kappa/(1-\kappa)} \qquad ...(4.14)$$

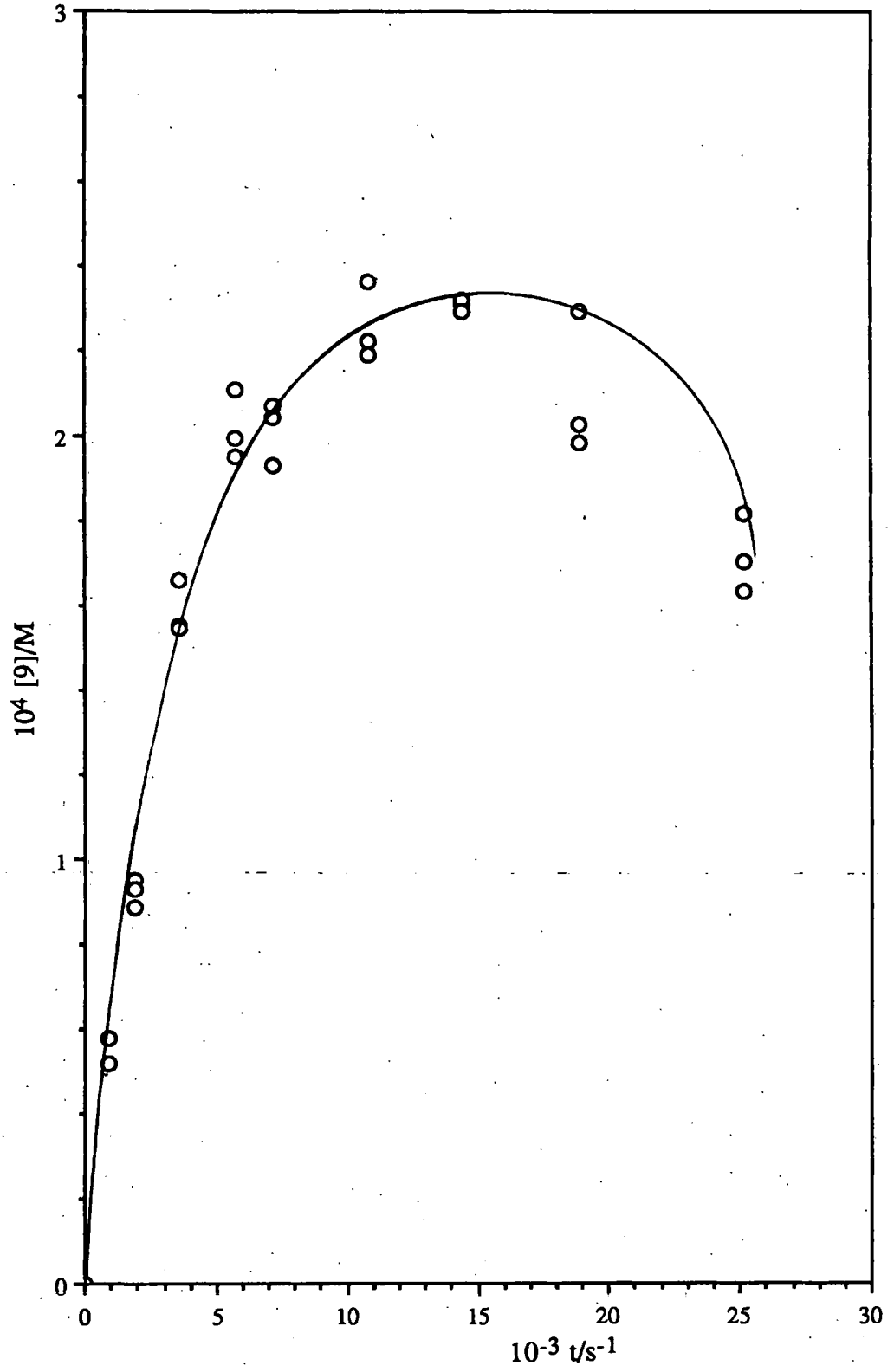

Figure 4.22 *Variation of γ-lactone (9) concentration with respect to time for the nitrosation of GlnOMe in 0.1M HCl with 30mM $NaNO_2$ at 37°C. Initial [GlnOMe] = 3mM*

$$t_{max} = \frac{1}{k_0} \frac{1}{\kappa - 1} \ln\kappa \qquad \ldots(4.15)$$

This explanation was tested by comparison of the experimental concentration of γ-lactone (9) with those calculated from the k_0 and k_1 rate coefficients. Values of k_0 were obtained from the initial slope of the plot of [γ-lactone (9)] against time (Figure 4.22), by the method of initial rates. Values of k_1 were determined independently by following the loss of authentic γ-lactone (9) using an HPLC analytical method (see Section 7.2.6). Results for the decomposition of 5mM (9) in 0.1M HCl containing 30mM HNO_2 are shown in Figure 4.24, where the plot of ln $\{A_t - A_\infty / A_0 - A_\infty\}$ is linear over 4 half lives. The *pseudo* first order rate coefficients k_0 and k_1 for reaction in 0.1M HCl at 37°C are summarised in Table 4.11 together with observed and calculated values of β_{max} and τ_{max}.

Table 4.11 Values of k_0 and k_1 for the formation and decomposition of (9) in 0.1M HCl containing 30mM NO_2^- at 37°C. Initial [GlnOMe] = 3mM, [(9)] = 5mM

Term	Value
k_0	$2.25 \times 10^{-5} s^{-1}$
k_1	$5.04 \times 10^{-5} s^{-1}$
β_{max} (obs)	8%
β_{max} (calc)	23%
t_{max} (obs)	17 000
t_{max} (calc)	28 900

Agreement between observed and calculated data is poor. This is probably due to the reaction of N_2GlnOMe (3) to give products other than the γ-lactone (9) (e.g. it may react intermolecularly with other nucleophiles (H_2O, NO_2^-, Cl^-) in the aqueous reaction

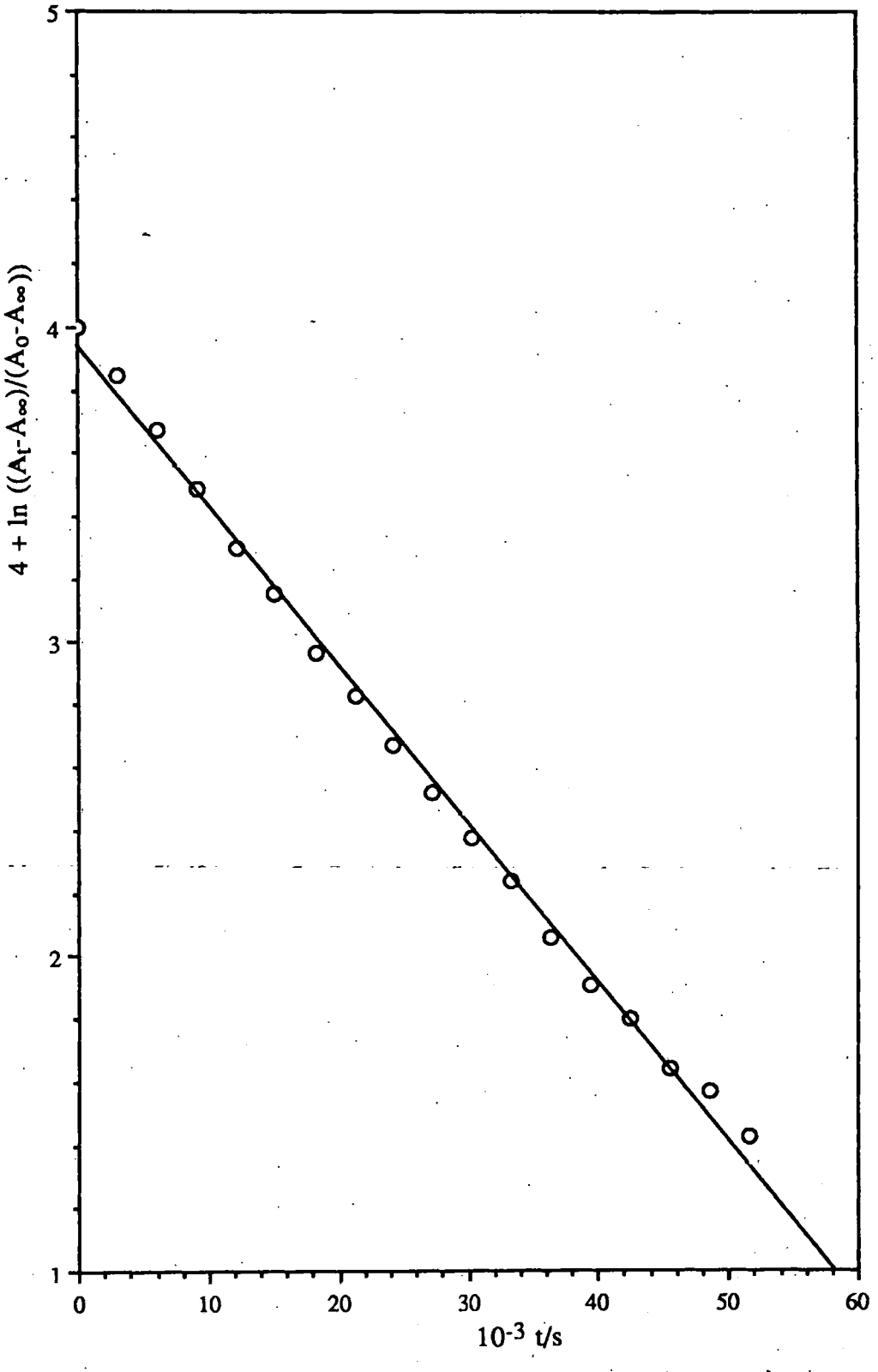

Figure 4.24 ln ((A$_t$-A$_\infty$)/(A$_0$-A$_\infty$)) v time for the decomposition of γ-lactone (9) in 0.1M HCl containing 30mM NaNO$_2$ at 37°C. Initial [(9)] = 5mM.

mixture) since at 37°C thermal nitrite ion decomposition has been shown to be slow compared with diazotisation (Section 4.4.1). By taking the ratio of the observed and calculated values of β_{max}, an indication of the percentage of glutamine methyl ester (1) converted to the γ-lactone can be obtained. This gives an approximate value of 30% for the total yield of (9).

4.6.2.1.3 Asparagine methyl ester (2)

Treatment of (2) with HNO_2 in 0.1M HCl at 0°C gave two products which partitioned into the organic phase. These were analysed by GLC/MS and are identified as peaks (B) and (C) on the GLC mass chromatogram of the reaction mixture (Figure 4.25).

Compound (B) was identified as maleimide by comparison of retention times and mass spectra (Figures 4.26 and 4.27) with an authentic sample. It is proposed that maleimide is formed from the diazonium ion (16) by β-elimination to give *cis* methyl-3-carbamoylacrylate (17), which then cyclises to form maleimide, with elimination of methanol (Figure 4.28). A suitable *trans*, anti-periplanar configuration of H and N_2 moieties in (16) to form the *cis* rather than *trans* isomer of (17) arises from a hydrogen bonding interaction between the amide proton and the ester CO moiety.

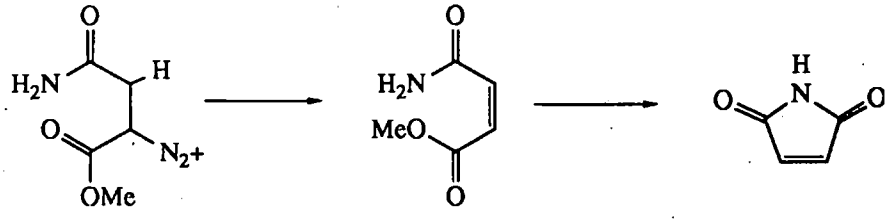

(16) **(17)**

Figure 4.28 Cyclisation of N_2AsnOMe to form maleimide

An alternative explanation for the formation of maleimide *via* a Wolff rearrangement of the carbene intermediate (18) to generate ketene (19) (Figure 4.29) is considered less likely because of the mild reaction conditions: the generation of carbenes usually requires either high temperatures or photolysis.

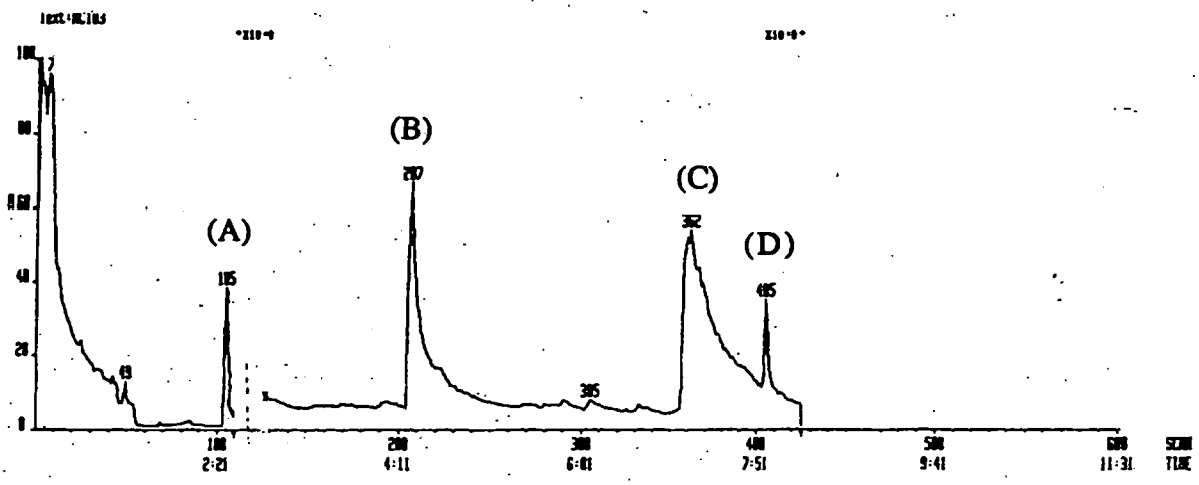

Peaks (A) (3-methylbutylacetate) and D (nicotine product) are adventitous contaminants from either the solvent or GLC injection port.

Figure 4.25 GLC mass chromatogram of organic extract of reaction mixture of AsnOMe with nitrous acid in 0.1M HCl at 0°C..

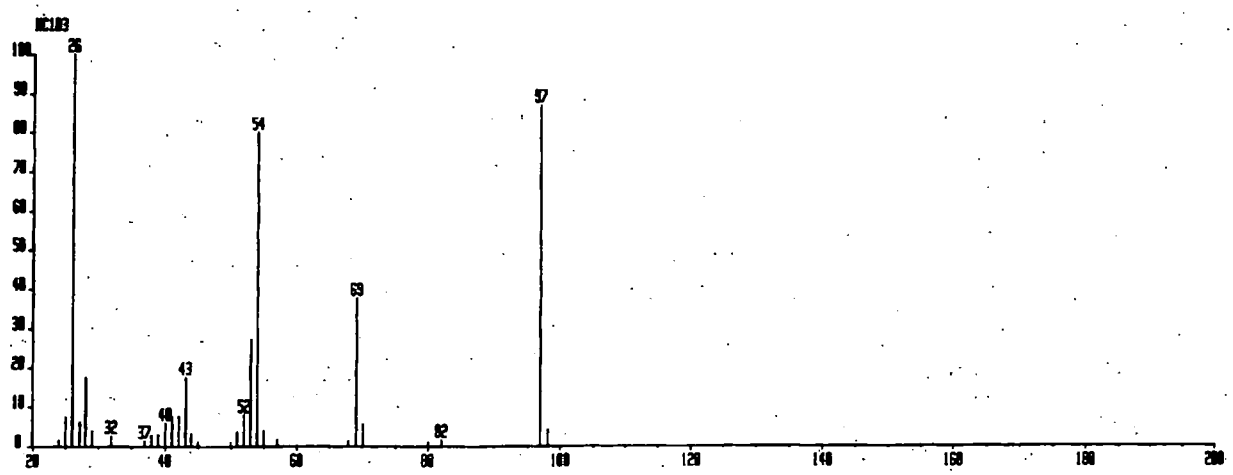

Figure 4.26 EI Mass spectrum of compound (B). (Scan 287).

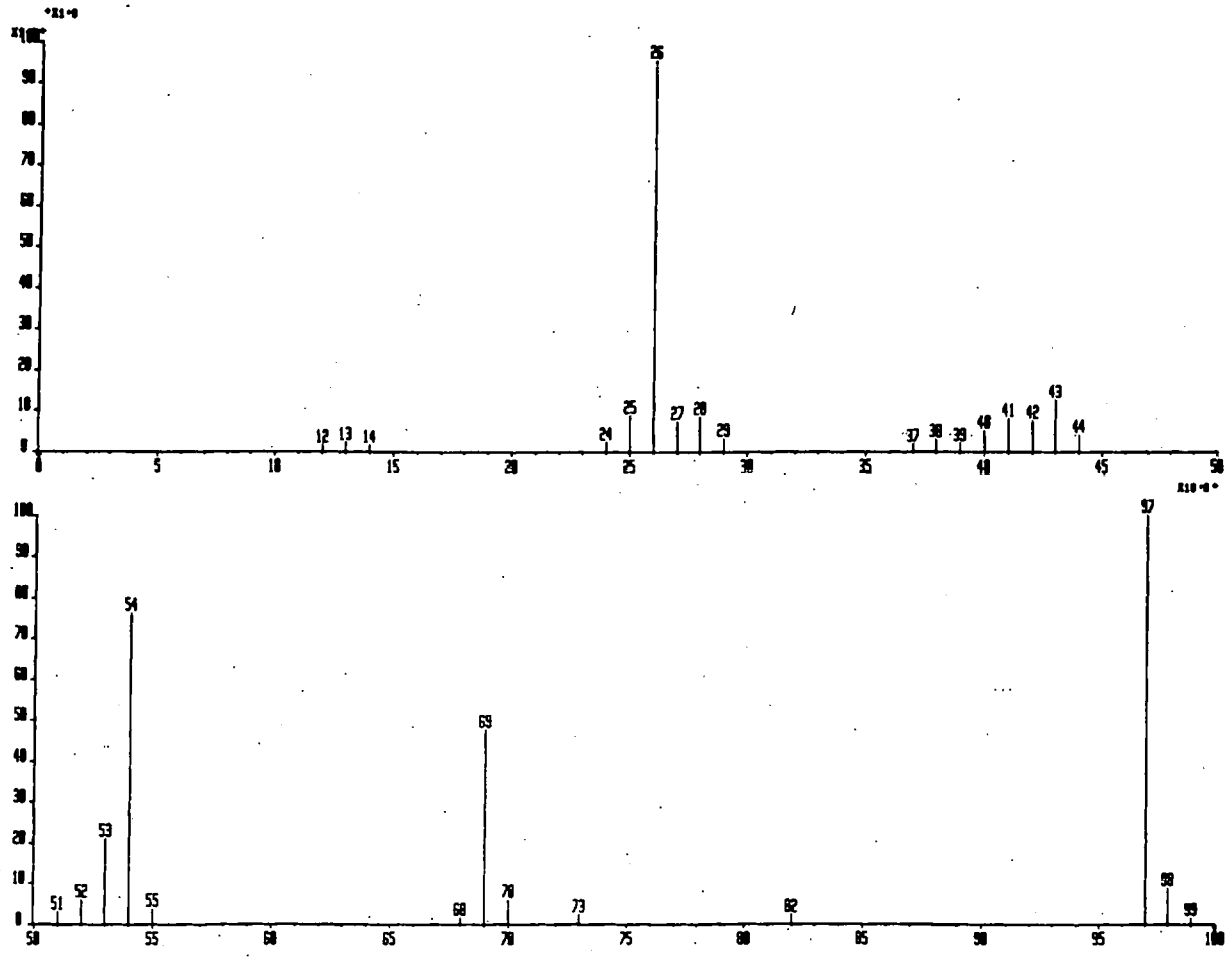

Figure 4.27 EI Mass spectrum of authentic sample of maleimide

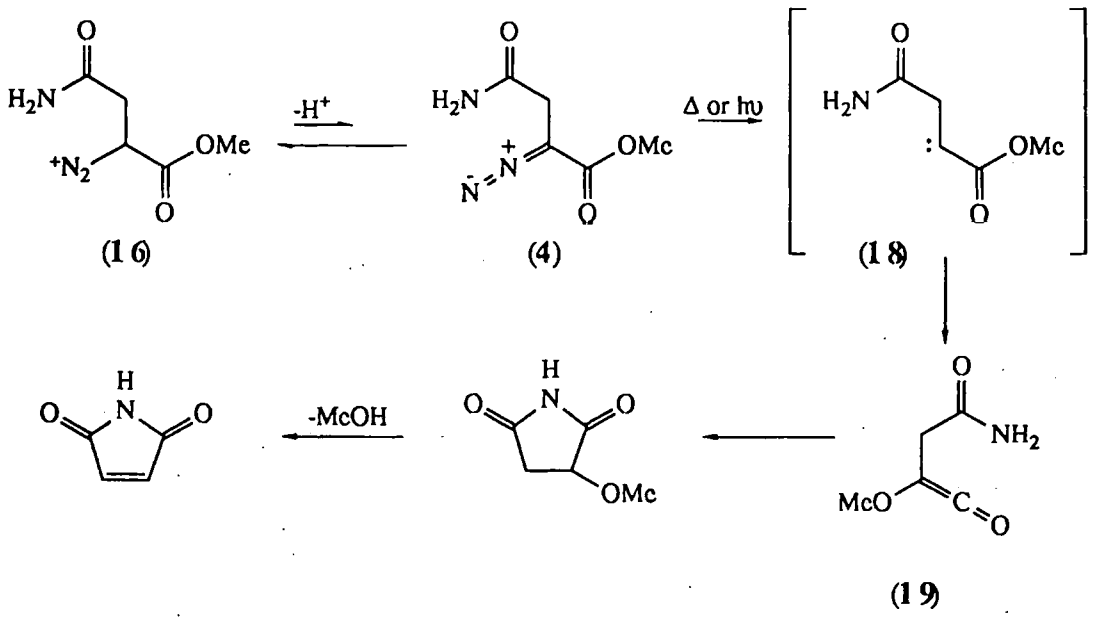

Figure 4.29 *Wolff rearrangement of N_2AsnOMe and subsequent formation of maleimide*

The mass spectrum (Figure 4.30) of component (C) shows a molecular ion at m/z 129 and some fragmentation (eg. m/z = 98; ($M^{\bullet+}$-$^{\bullet}OMe$) and 70 ($M^{\bullet+}$-$^{\bullet}CO_2Me$)) consistent with the β-lactam product (6). The ions at m/z 26, 54, 69, and 97 are due to maleimide which tails on the column and is thus observed in later spectra. However, neither the GLC retention time nor the entire mass spectral fragmentation correspond to an authentic sample of (6), shown in Figure 4.31. Three alternative structures were therefore considered for product (C). These are the tautomers (8) and (20) and the double bond isomer (21). The mass spectral fragmentation of compound (C) probably corresponds best to the imidate structure (8). Fragment ions at m/z = 98 ($M^{\bullet+}$-$^{\bullet}OMe$), 59 ($M^{\bullet+}$-$^{\bullet}CO_2Me$) and 44 (H_2NCO^+) are consistent with this structure as rationalised in Figure 4.49.

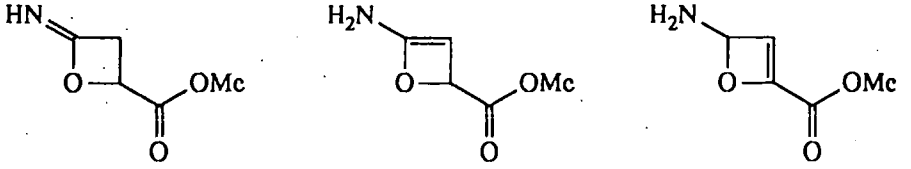

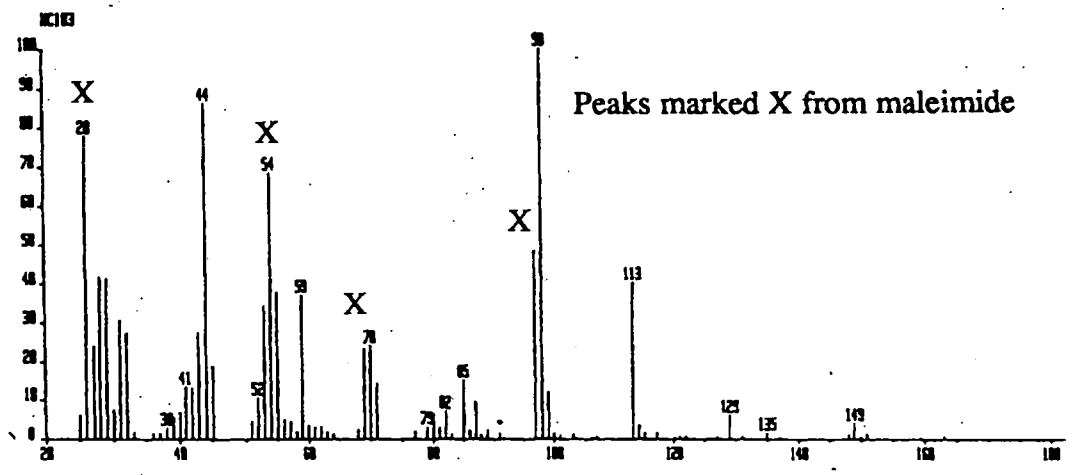

Figure 4.30 EI Mass spectrum compound (C) (Scan 362)

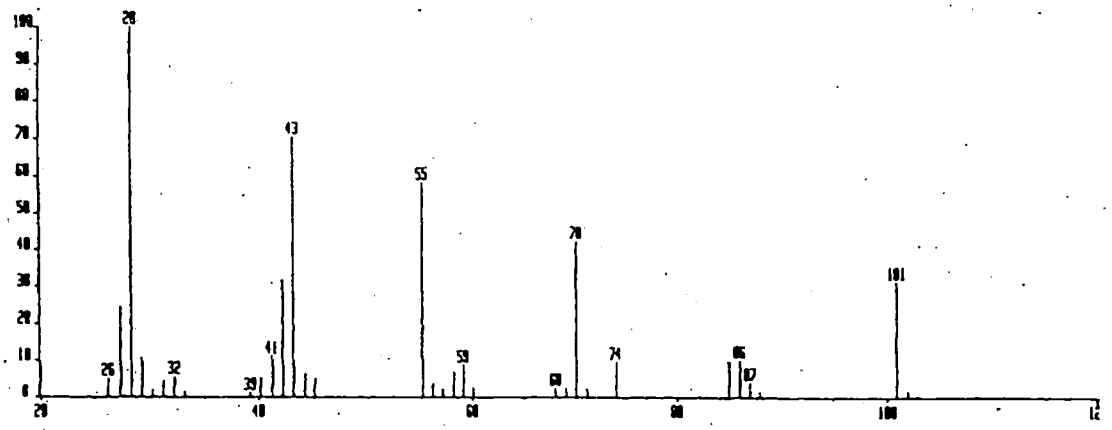

Figure 4.31 EI Mass spectrum of authentic sample of β-lactam (6)

Formation of the imidate (8) can be rationalised as proceeding *via* the diazonium ion (16) which reacts *via* a S_Ni reaction with the O-atom of the carboxamide side chain (Figure 4.32).

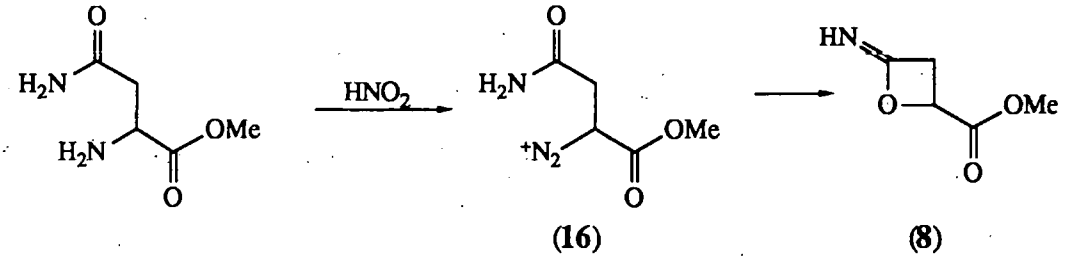

(16) (8)

Figure 4.32 Formation of imidate ester

From comparisons with an authentic sample of (6), there was no evidence in the organic extracts of concurrent cyclisation on the amide N-atom to form the lactam (6). The possibility that the β-lactam was not observed due to further reaction with HNO_2 was discounted. Results for the extraction of the γ-lactam (5) from nitrous acid indicate that the lactam does not react significantly. It was assumed that the β-lactam (6) would behave in a similar manner.

There is clear evidence that the nitrosation of both AsnOMe and GlnOMe in protic solvents results in the formation of an imidate ester *via* an intramolecular cyclisation of the diazonium ion intermediate with the O-atom of the carboxamide moiety. The imidate ester may undergo subsequent hydrolysis to the corresponding lactone. In the case of AsnOMe a second product maleimide probably arising from a β-elimination reaction of the diazonium intermediate was also identified. No evidence was found, for either AsnOMe or GlnOMe, of a comparable intramolecular cyclisation of the diazonium ion intermediate with the carboxamide N-atom to give lactam products.

4.6.3 Cyclic products from the thermal decomposition of N_2GlnOMe and N_2AsnOMe

It was considered that decomposition of the diazo amino acid esters in aprotic media may assist cyclisation on the N-atom of the amide moiety to give a lactam (Figure 4.33)

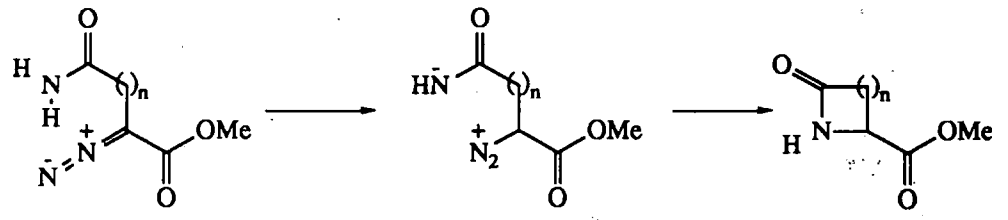

n = 1,2

Figure 4.33 Proposed mechanism of cyclisation of (3) and (4) to give lactam products

In the absence of solvent protons, the amino acid esters might abstract a proton from the amide N-atom to form the diazonium ion. The increased nucleophilicity of the nitrogen anion may facilitate formation of a lactam. Further, decomposition in aprotic solvents minimises competing reactions such as hydrolysis and intermolecular nucleophilic trapping of the diazonium ion intermediates.

4.6.3.1 N_2GlnOMe (3)

A 0.01M solution of (3) in ethyl acetate was decomposed by heating at 120°C until no diazocompound remained by HPLC. The reaction mixture was then examined by capillary GLC (Figure 4.34) to reveal 3 major components, (A), (B) and (C). These compounds were characterised by their mass spectra.

Compound (A) was identified as the γ-lactone (9) and confirmed *via* comparison of both retention time and fragmentation with an independently prepared authentic sample (Figures 4.35 and 4.36). The mass spectrum of (A) shows little fragmentation, a weak molecular ion is observed at m/z 144 and the base peak at m/z 85, corresponding to ion (23), is highly characteristic of γ-lactones.

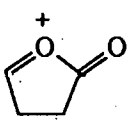

(**23**) m/z 85

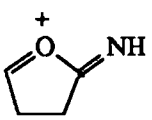

(**24**) m/z 84

Compound (B) did not generate a clean GLC/MS chromatogram. It was enhanced, however, by monitoring only peaks with an ion at m/z 143 (Figure 4.37) and the mass spectrum obtained for scan 454 is shown in Figure 4.38. Although the molecular ion at m/z 143 corresponds to the γ-lactam (5) comparison with an authentic sample of (5) (Figure 4.39) shows that Figure 4.38 refers to a different structure. The base peak at m/z 84 corresponds to either the ring structure (24) or an isomer. The structure which best fits Figure 4.38 is either the imidate (7) or its tautomer (25) and the observed fragmentation pattern can be rationalised as shown in Figure 4.40. Presumably the γ-lactone (9) also is observed in the reaction mixture (m/z=144) due to adventitious hydrolysis of the imidate ester product imidate (7). Further, when the reaction mixture was treated with 0.01M NaOH and reanalysed by GLC (Figure 4.41), both compounds (A) and (B) disappeared, consistent with the imidate ester structure proposed for compound (B).

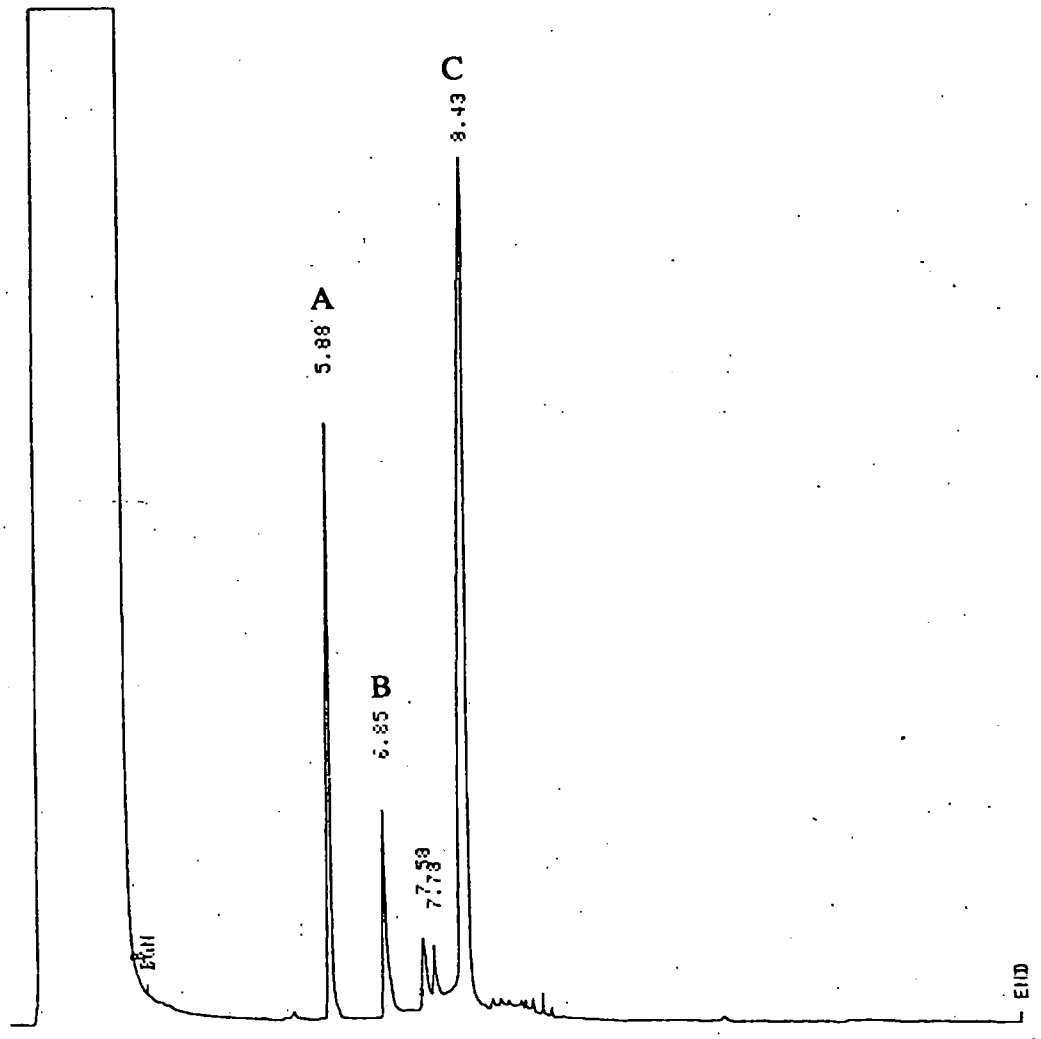

Figure 4.34 Capillary GLC chromatogram of reaction mixture from thermolysis of N_2GlnOMe at 120°C. Initial [GlnOMe] = 0.01M.

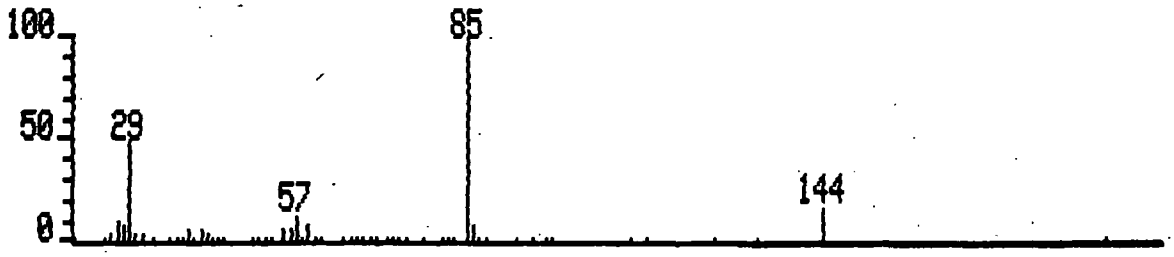

Figure 4.35 EI Mass spectrum of compound (A)

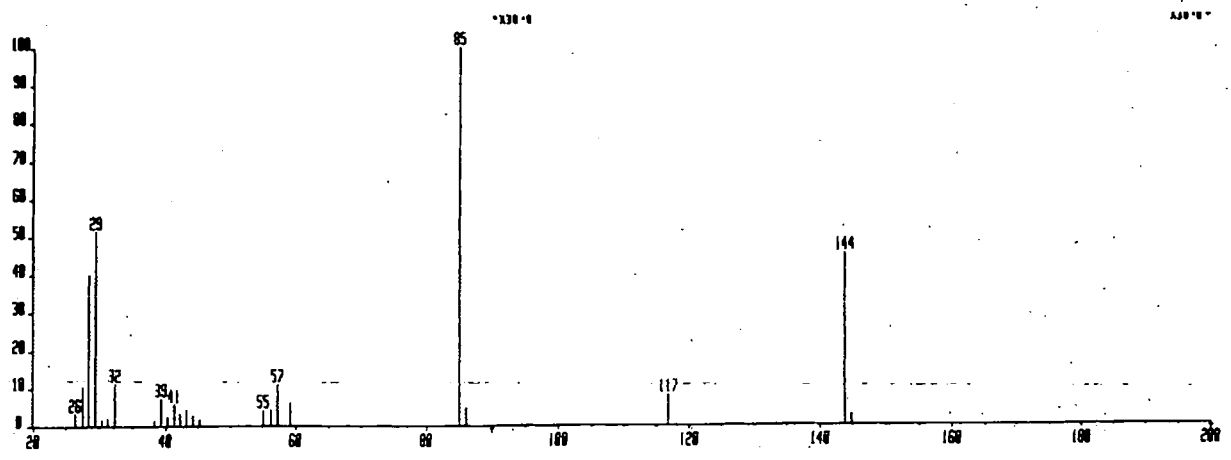

Figure 4.36 EI Mass spectrum of authentic γ-lactone (9)

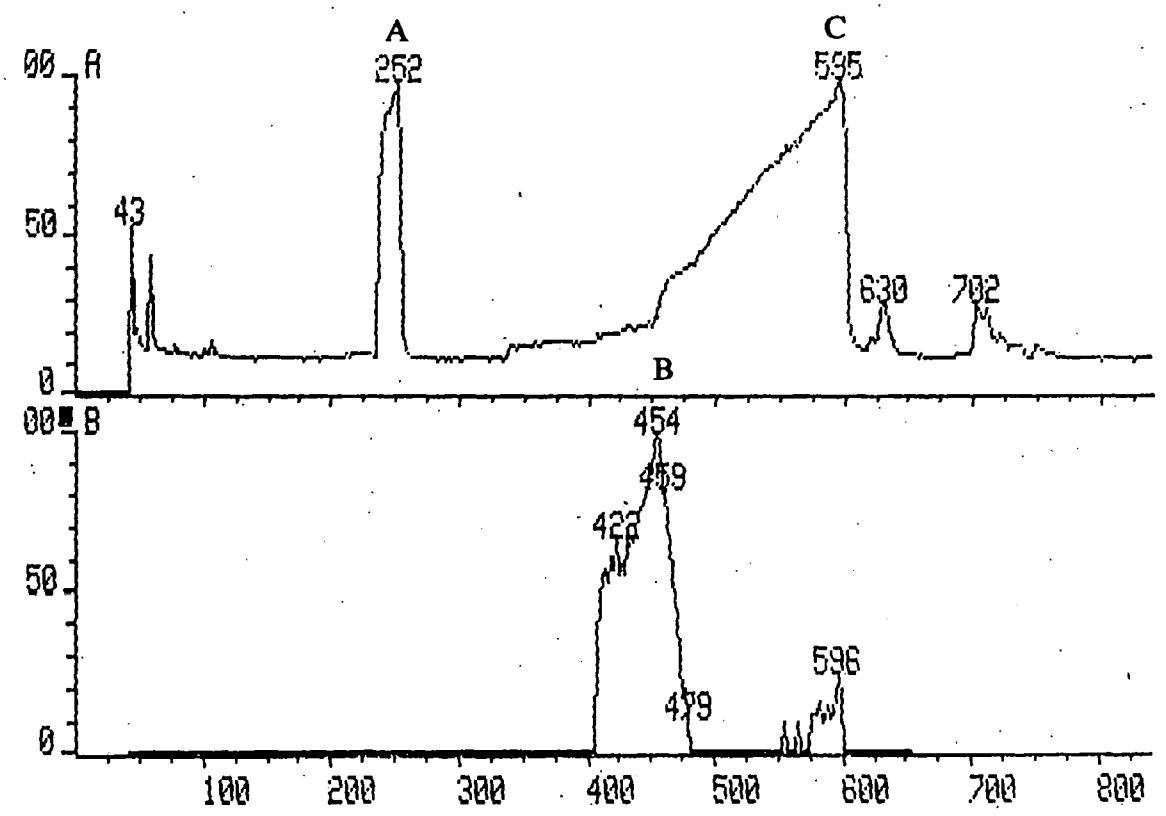

Figure 4.37 *GLC mass chromatogram and ion chromatogram (m/z 143) for analysis of reaction mixture from the thermolysis of N_2GlnOMc in EtOAc at 120°C.*

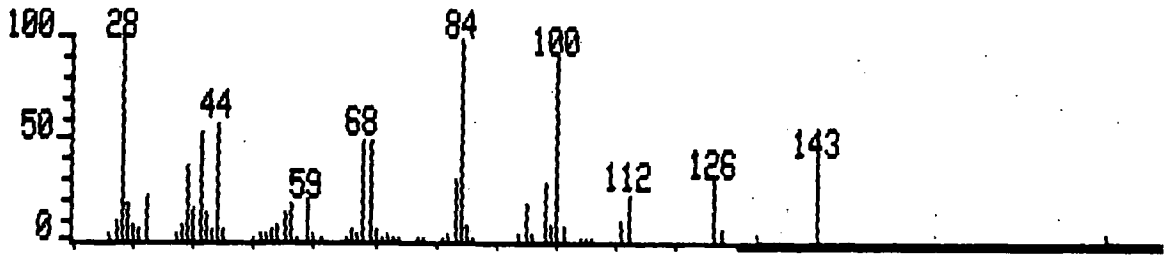

Figure 4.38 EI Mass spectrum of compound (B) scan 454.

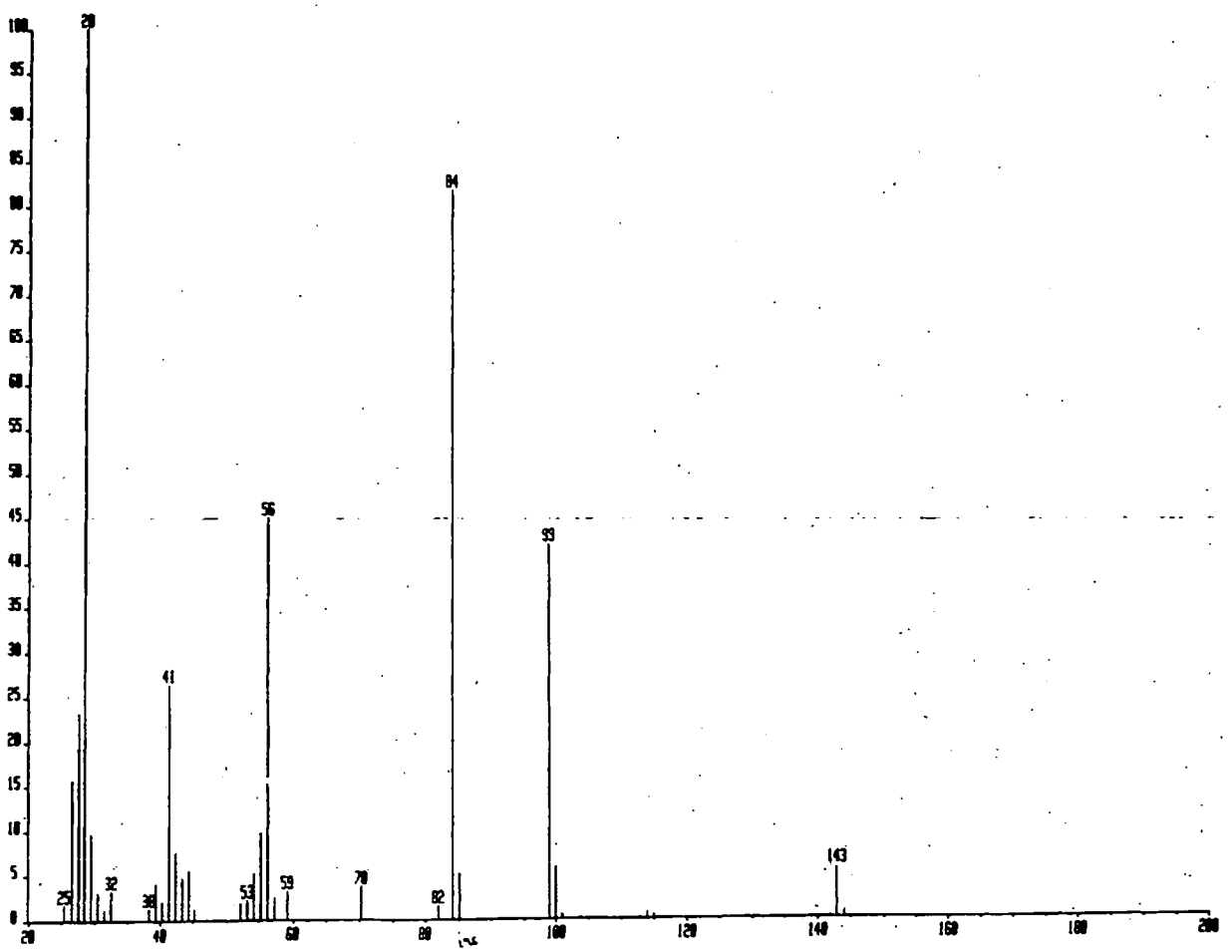

Figure 4.39 EI Mass spectrum of authentic γ-lactam (5)

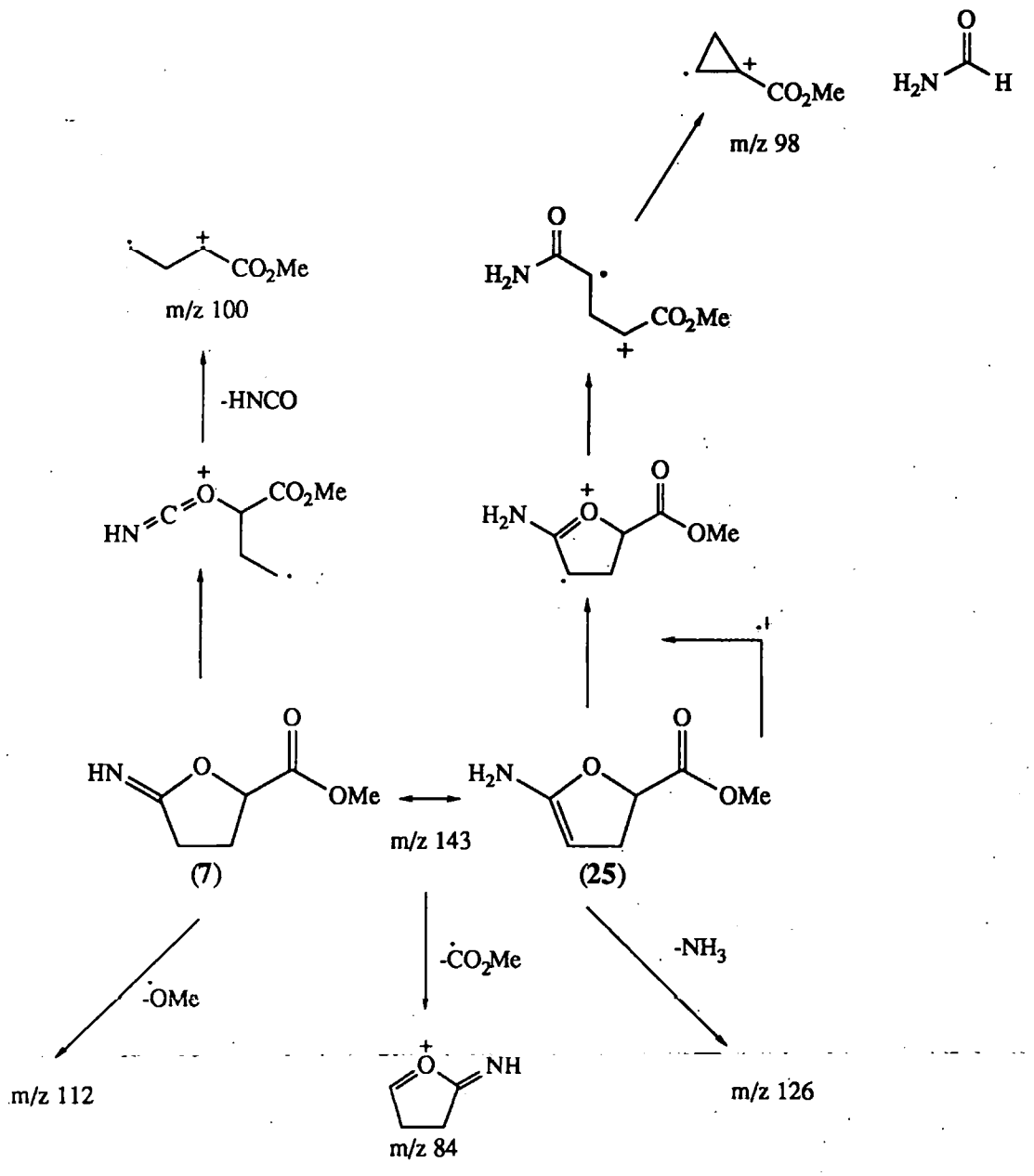

Figure 4.40 Rationalisation of major fragment ions in mass spectrum of compound (B)

The major component of the reaction mixture, (C), has a very similar mass spectrum (Figure 4.42) to that of (7). However, there is no observable molecular ion at m/z 143 under EI conditions, although a molecular ion ($M+H^+$) at m/z=144 is apparent in the CI-mass spectrum. Otherwise the major difference between the EI mass spectra of compounds (B) and (C) is the relative abundance of the peaks at m/z=100 and m/z=84. Thus, m/z=100 is the base peak for compound (C) whereas m/z=84 is the base peak for

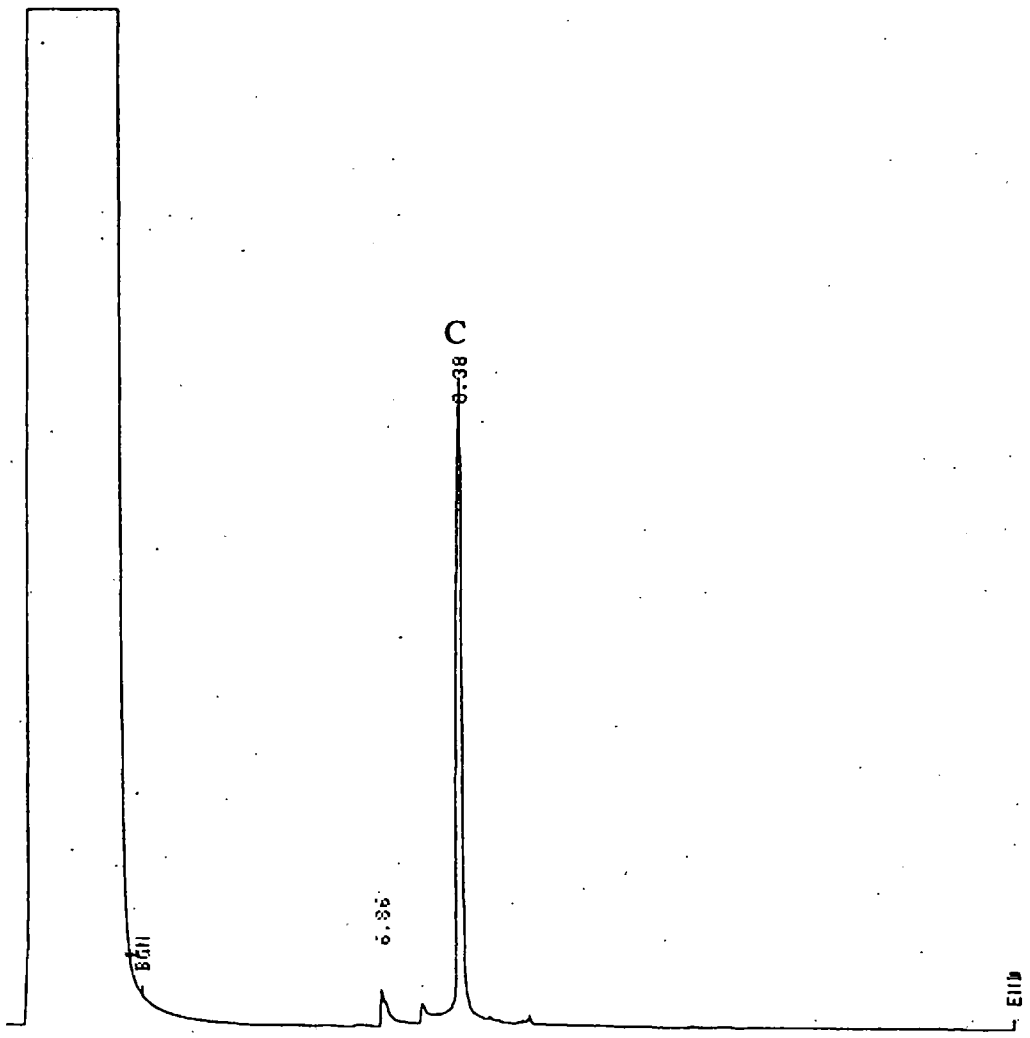

Figure 4.41 Capillary GLC chromatogram of reaction mixture from thermolysis of N_2GlnOMe at 120°C after hydrolysis with 0.01M NaOH.

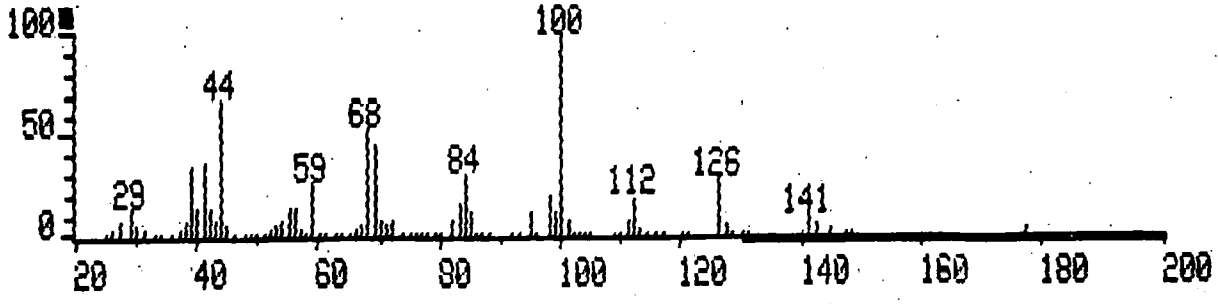

Figure 4.42 EI mass spectrum compound (C) scan 596.

compound (B). The similarity of the mass spectra indicates that compounds (B) and (C) are isomers. The subtle differences suggest that component (C) is the thermodynamic stable isomer (26), where the double bond has moved into conjugation with the ester and not the alternative double bond isomer (27).

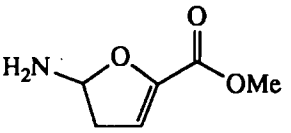

(26)

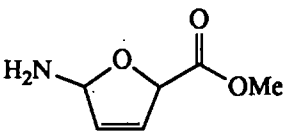

(27)

The m.s. fragmentation pattern can be rationalized as shown in Figure 4.43. The ion at m/z 84 has a low relative abundance since it cannot achieve a stable cyclic structure if ionisation occurs on oxygen. It requires ionisation of the double bond in order to be able to do this.

Additional experiments established that compound (C) is not hydrolysed in dilute NaOH (Figure 4.41), consistent with the structure proposed.

4.6.3.2 N_2AsnOMe (4)

N_2AsnOMe was thermally decomposed and the products analysed in an identical manner to N_2GlnOMe, to reveal 3 components by GLC (Figure 4.44). Fraction (F) is a minor component of high molecular mass, probably resulting from polymerisation. Both other components (D) and (E) gave molecular ions at m/z=129 in the EI mass spectra (Figures 4.45 and 4.46 respectively) and at m/z=130 in the CI mass spectra ($M+H^+$), but neither corresponded to an authentic sample of the β-lactam (6) (Figure 4.31). The mass spectra of (D) and (E) are identical except for a weak ion at m/z=99 for (D) but a much stronger ion at m/z=99 for (E). The two components differ chemically insofaras treatment with 0.01M NaOH decomposes (D) but leaves (E) unaffected. (Figure 4.47).

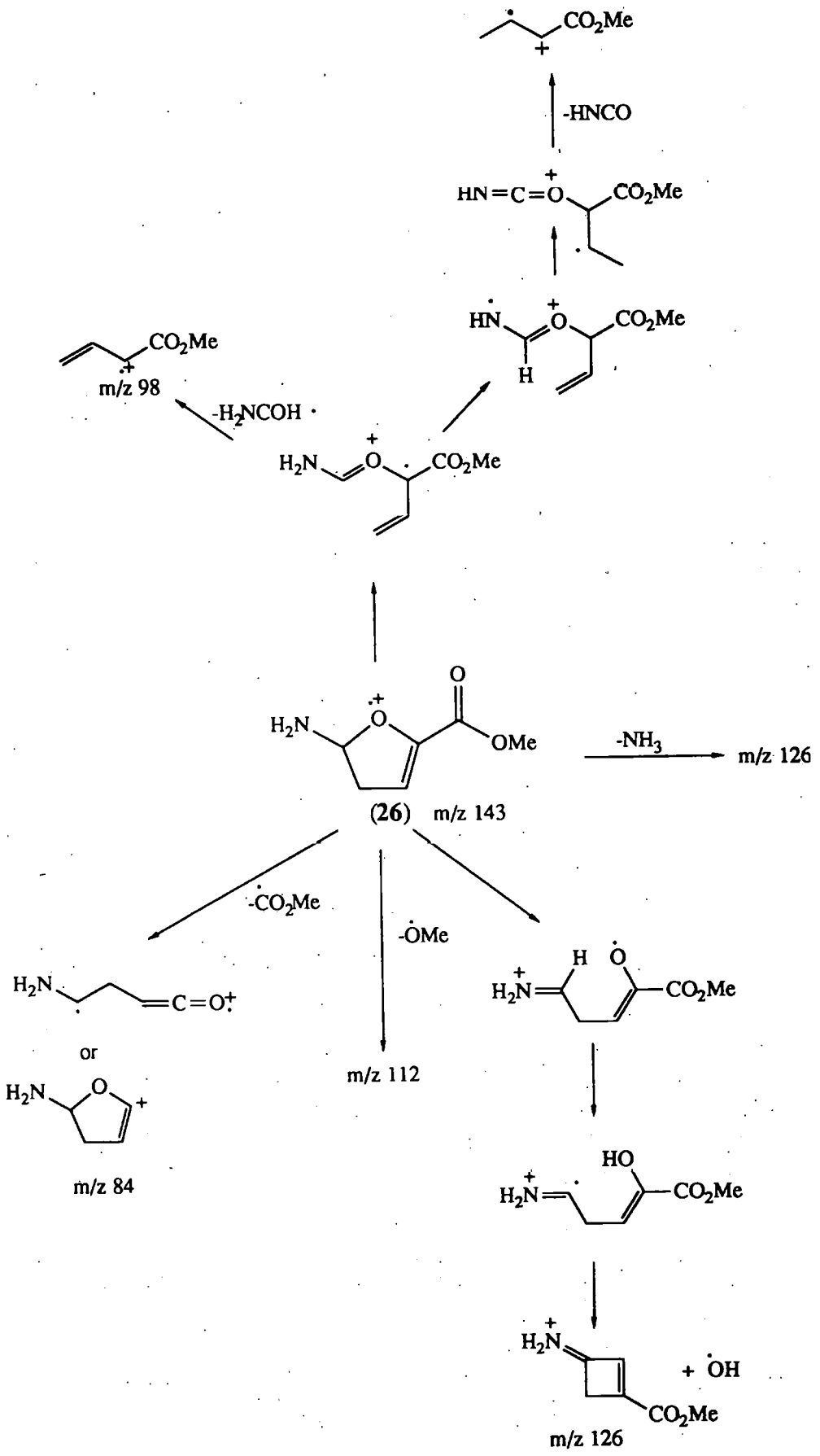

Figure 4.43 Rationalisation of fragmentation in EI mass spectrum of (26)

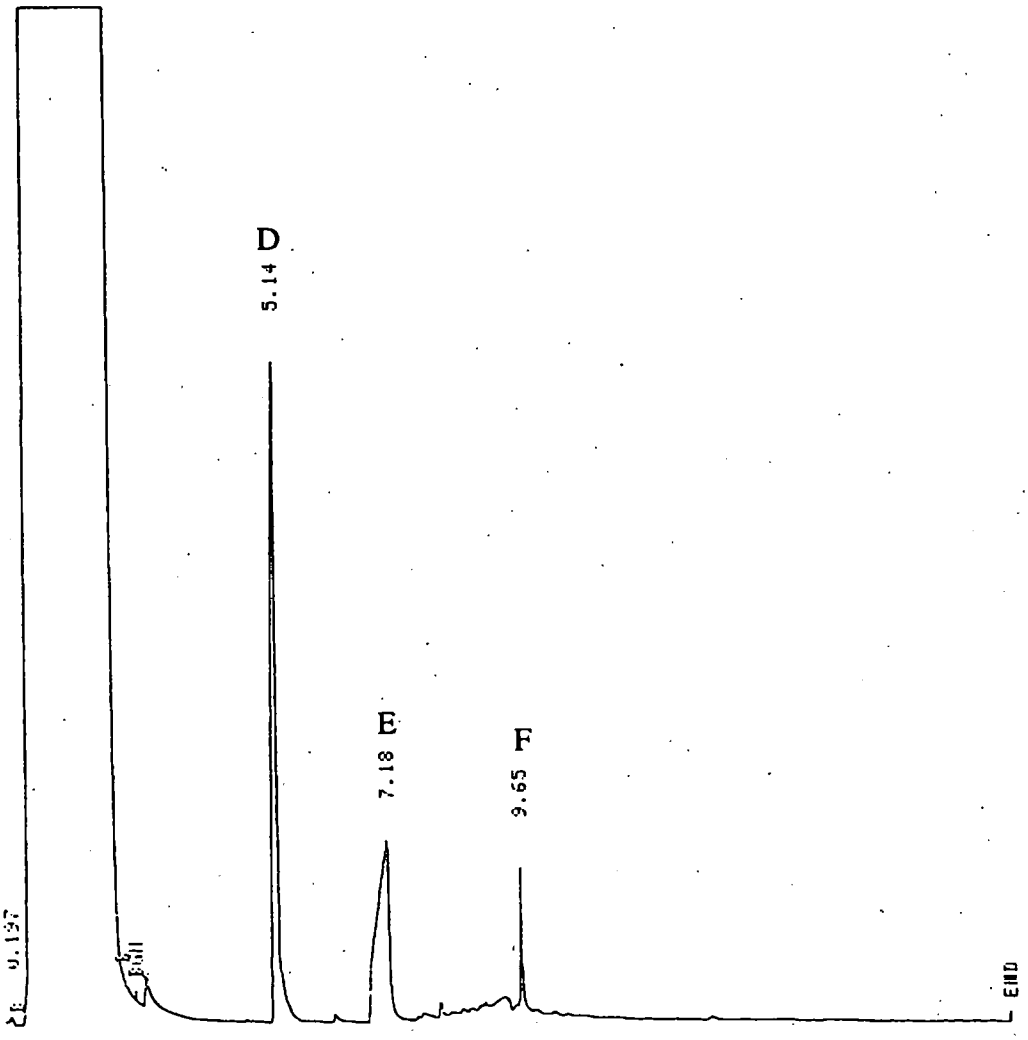

Figure 4.44 *Capillary GLC chromatogram of reaction mixture from thermolysis of N_2AsnOMe at 120°C.*

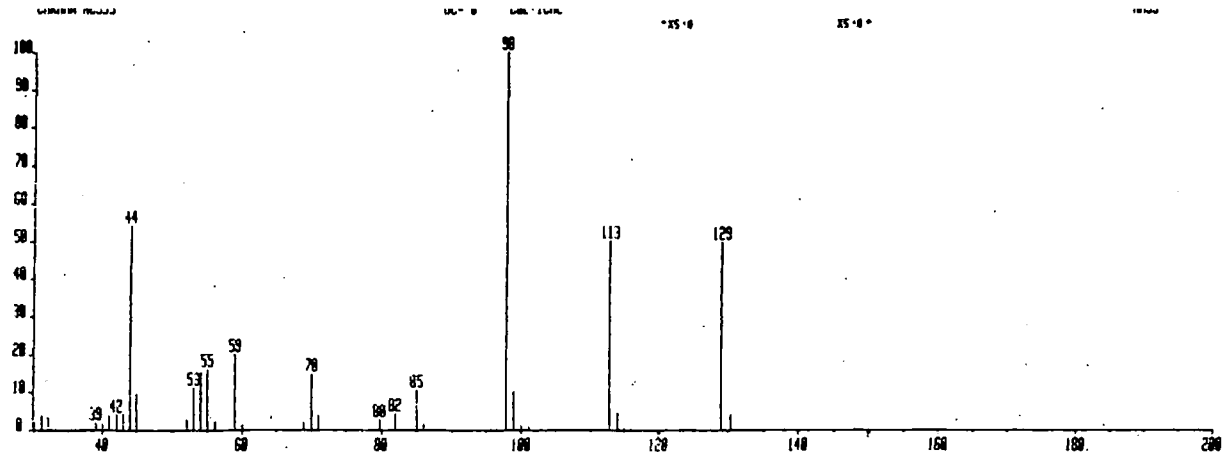

Figure 4.45 EI Mass spectrum compound (D) scan 253

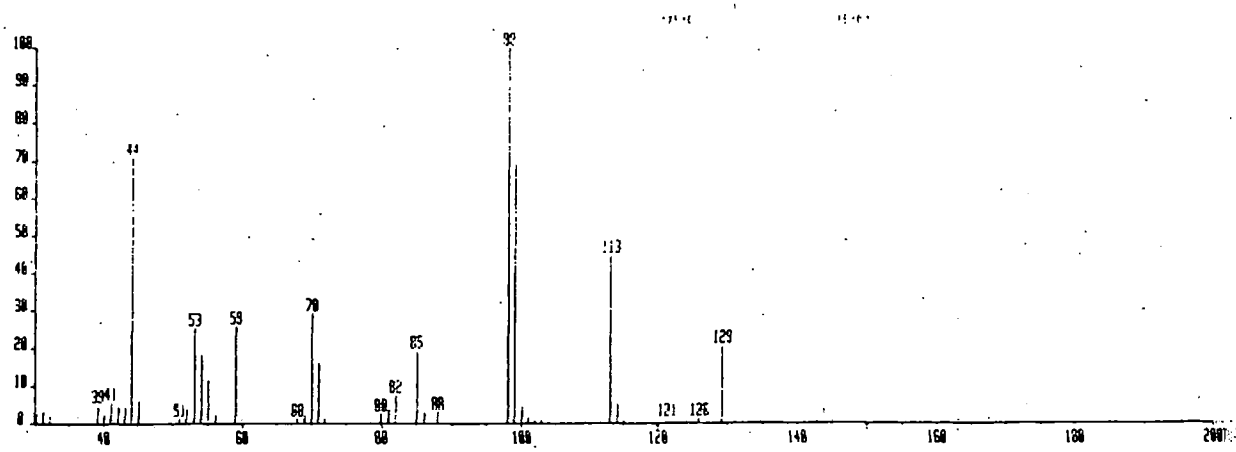

Figure 4.46 EI Mass spectrum compound (E) scan 506

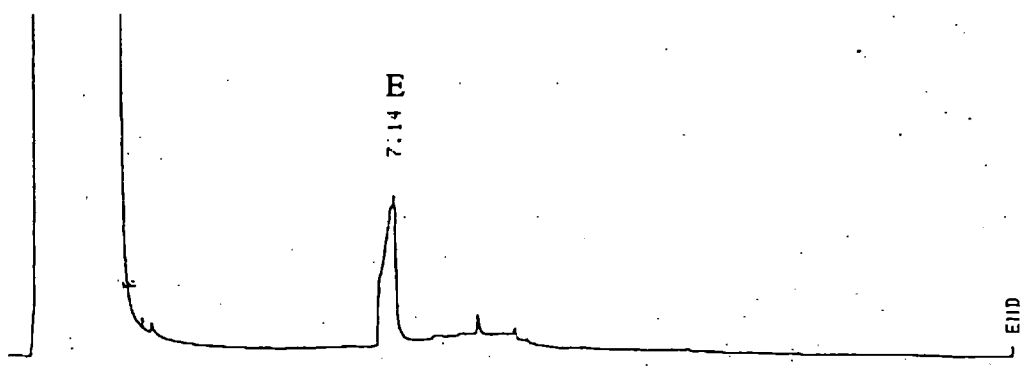

Figure 4.47 Capillary GLC chromatogram of reaction mixture from thermolysis of N_2AsnOMe at 120°C after hydrolysis with 0.01M NaOH.

On the basis of this information, (D) is assigned to the imidate structure (8) which was also formed by protic decomposition and (E) is deduced as the double bond isomer (21).

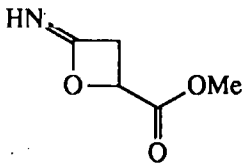

(8)

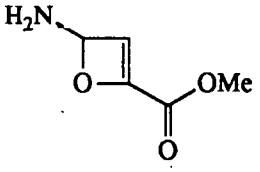

(21)

The strong peak at m/z=99 from (21) is best attributed to loss of formaldehyde by the mechanism shown in Figure 4.48.

Figure 4.48 Rationalisation of ion at m/z=99 in MS of (17)

The remaining fragmentation for both (8) and (21) can be rationalised as shown in Figures 4.49 and 4.50 respectively.

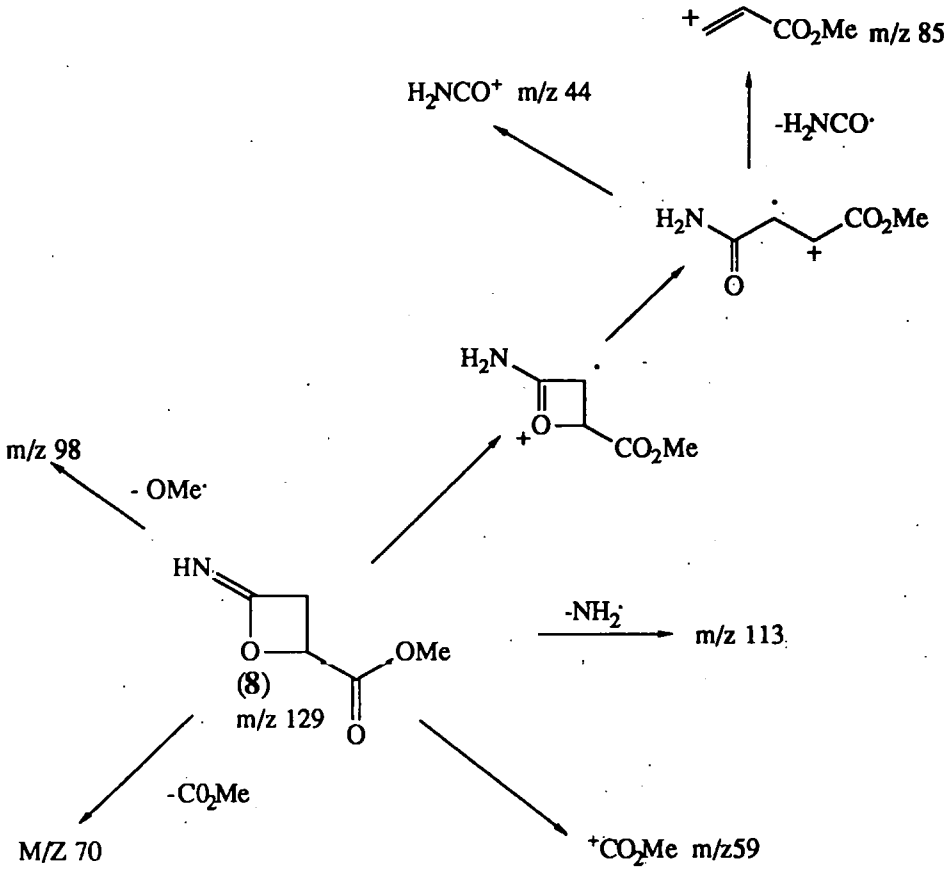

Figure 4.49 Rationalisation of fragmentation in EI mass spectrum of (8)

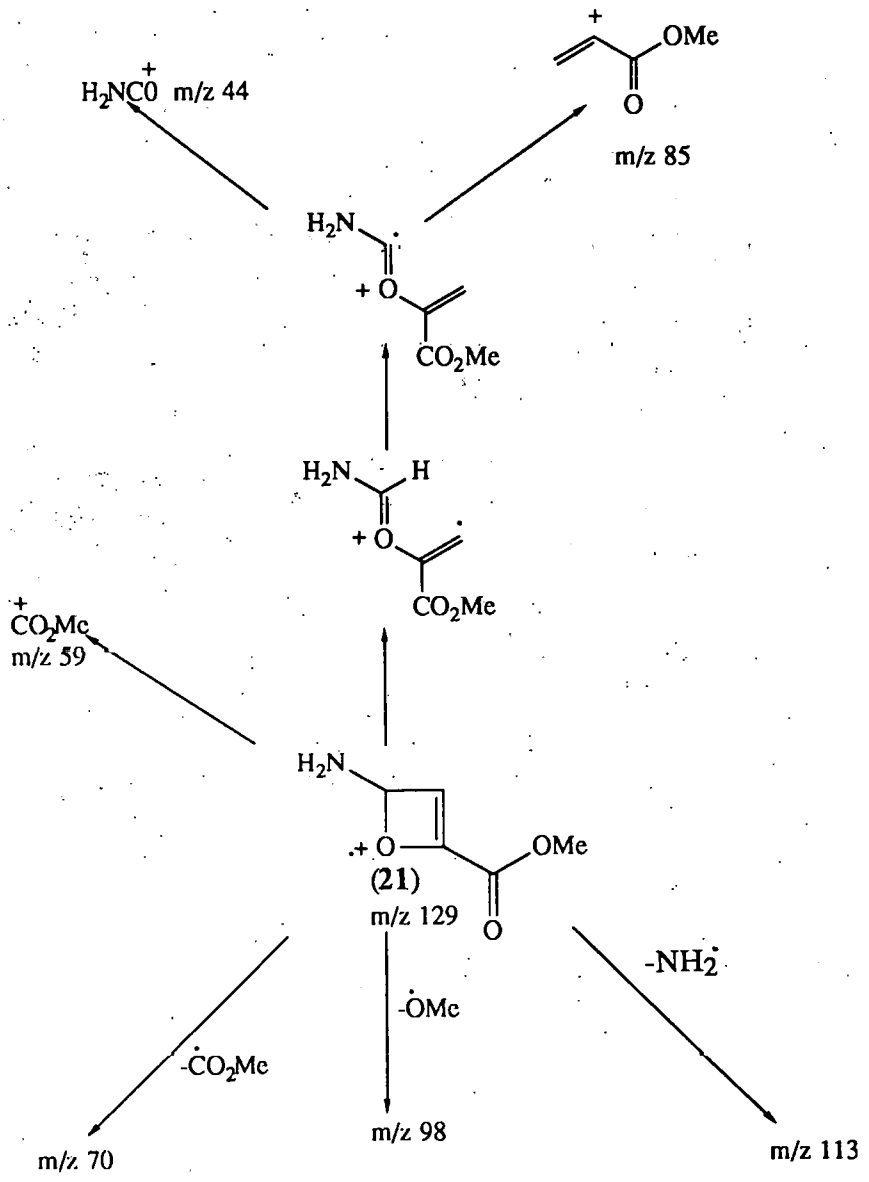

Figure 4.50 Rationalisation of fragmentation in EI mass spectrum of (21)

4.6.4 Discussion

In both protic and aprotic media, N_2GlnOMe and N_2AsnOMe decompose *via* an intramolecular pathway to give an imidate ester as the initial product (Figure 4.51).

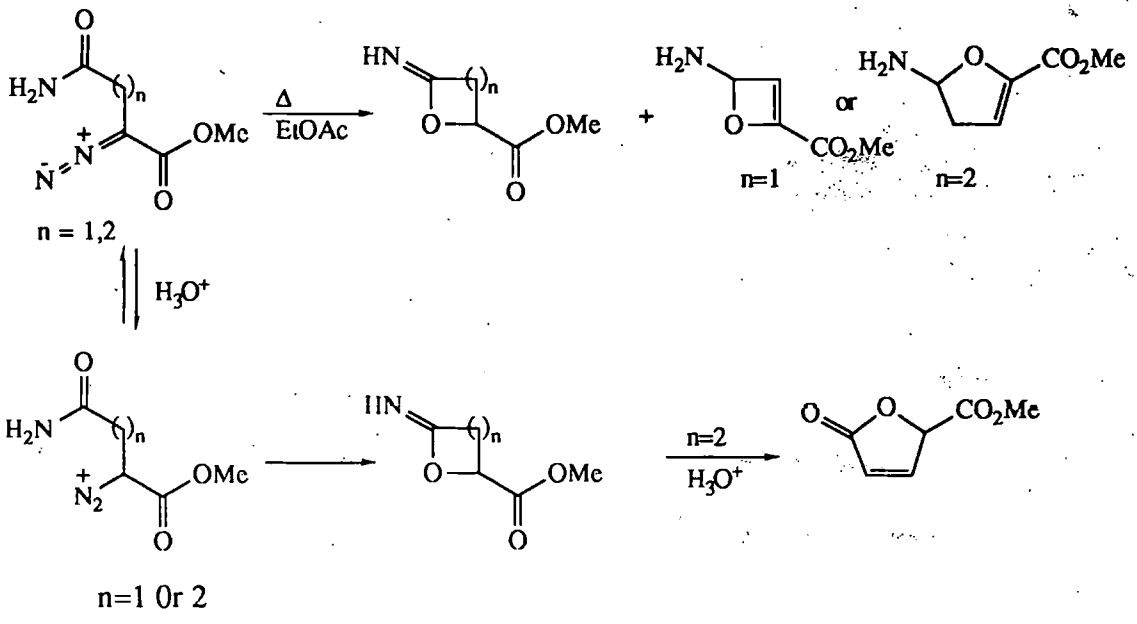

Figure 4.51 Cyclisation of N_2GlnOMe and N_2AsnOMe in aprotic and protic media

In protic media, the imidate ester formed from GlnOMe hydrolyses, forming the γ-lactone (9) in ca. 30% yield. This is consistent with the results of Austin[94] who reported a reduction in the yield of γ-butyrolactone, from the nitrosation of glutamic acid, of 93% to 33% and 25% when the α-carboxylate moiety was replaced by H and CH_3 respectively. Hydrolysis of the carboxamide moiety prior to cyclisation can be discounted. Extrapolation of the data of Leach and Hindley[149] for the hydrolysis of L-asparagine in dilute HCl at 70-100°C (Rate=k_o[L-asparagine]) gives $k_o=3.4\times10^{-9}s^{-1}$ in 0.1M HCl at 0°C which corresponds to a half life of 6.5 years. Further there is little evidence of a significantly increased rate of nitrous acid catalysed hydrolysis of the caboxamide side chain. From Kezdy's data for the nitrosation (hydrolysis) of acetamide,[150] a value of $k_o=7.1\times10^{-9}s^{-1}$ is estimated for the *pseudo* first order rate of nitrosation (Rate=k_o[acetamide]) in 0.1M HCl at 0°C. This corresponds to a half life of 3.1 years.

It has been reported previously that asparagine does not form cyclic products on treatment with nitrous acid.[85] However, it is clear from there results that AsnOMe does undergo cyclisation on treatment with HNO_2. The resulting imidate ester (8) does not hydrolyse to the β-lactone (10) in 0.1M HCl at 0°C. Presumably relief of ring strain strongly favours ring C-O bond cleavage to acyclic products which were not identified by the limited procedures employed. Because of the high ring strain involved in the formation of a 4-membered ring, other processes are observed to occur in the deamination of AsnOMe in a protic solvent including β-elimination which ultimately results in the formation of maleimide.

There was no evidence of β-elimination occurring in the deamination of GlnOMe. In aprotic media, the imidates isomerised at 120°C forming the double bond isomers (25) and (26). There was also some adventitious hydrolysis of (7) to the γ-lactone due to absorbed water. No evidence of β-elimination occuring in the decomposition of N_2GlnOMe and N_2AsnOMe was observed in aprotic media. Neither the reactions in water, nor the reactions in EtOAc showed any evidence of intramolecular cyclisation having occurred on the amide N-atom. Undoubtedly O-alkylation of the neutral amide moiety is favoured due to resonance stabilisation of the transition state[151] (Figure 4.52). No such stabilisation is possible in the case of the N-alkylated transition state (28).

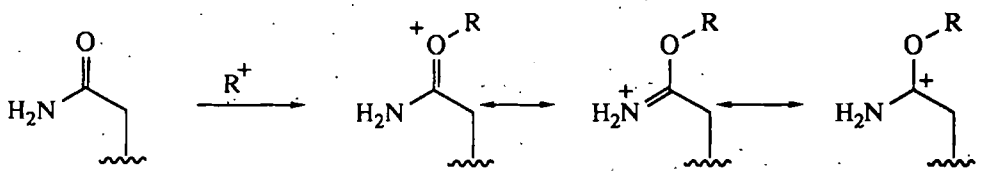

Figure 4.52 Resonance stabilisation of O-alkylated product

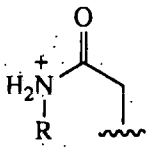

(28)

However, Kornblum demonstrated that diazomethane was sufficiently basic to abstract a proton from α-pyridone in an aprotic solvent at 0°C.[152] Thus it is reasonable to expect the amide anions to be generated in the decomposition of N_2GlnOMe and N_2AsnOMe in ethyl acetate at 120°C. If the regiospecificity of alkylation is determined by the relative stabilities of the transition states[151] then N-alkylation of the amide anion would be preferred. The results for the alkylation of the amide anion are best rationalised in terms of charge control. MO calculations show the negative charge of the amide anion resides predominantly on the oxygen atom,[151] whilst there will be considerable carbanion ion character to the carbon atom bearing the diazonium ion. Thus, in terms of charge control, O-alkylation is favoured.

In the absence of material balances it is not possible to say whether O-alkylation represents the major product forming reaction in aprotic solvents. However, there was no evidence of other reactions occuring, particularly those involving generation of reactive carbene intermediates (eg. Wolff rearrangement). Thus, an alternative mechanism considered for the formation of the imidate ester products involving the formation of a carbene, followed by isomerisation to the 1,3-dipole (29) and cyclisation on oxygen (Figure 4.53), was discounted.

In view of the possible biological implications of the β-lactone derived from protic nitrosation of aspartame, cyclic products derived from asparagine and its derivatives may also pose a potential cytotoxic risk.

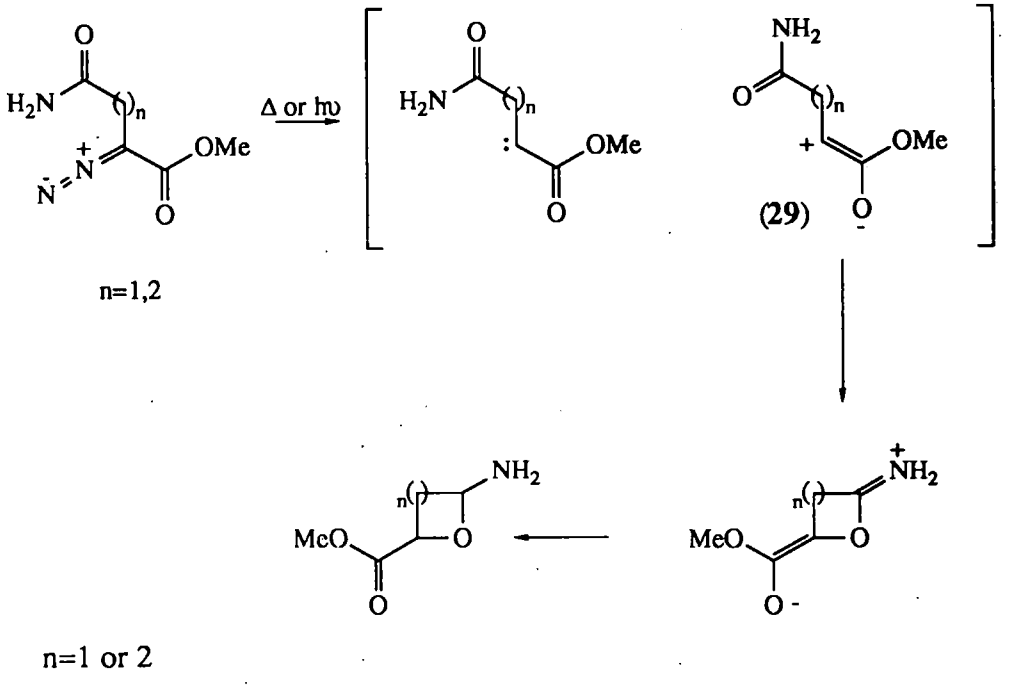

Figure 4.53 Generation of imidate esters via carbene intermediates

CHAPTER 5 DIAZOPEPTIDES

5 DIAZOPEPTIDES

5.1 Introduction

The diazotisation, deamination and intramolecular cyclisations of the simple diazoamino acid methyl esters described in Chapter 4 were examined as models for the more complex dipeptide derivatives of glutamine and asparagine reported in this chapter. Before examining these reactions, however, it was necessary to devise procedures for the synthesis of simple glutaminyl and asparaginyl dipeptides coupled to a phenylalanine methyl ester residue. The synthesis of the two dipeptides and their diazo derivatives is reported, together with their spectral and physical properties, and the rates of decomposition of the two diazopeptides in aqueous buffers, dilute acid and in the presence of added nucleophiles.

5.2 Synthesis of glutaminyl and asparaginyl dipeptides

Several classical methods[153] of forming peptide bonds were examined for the synthesis of L-glutamine and L-asparagine dipeptides. These included the carbodiimide, the active ester and the azide methods, all of which gave unacceptably low yields of dipeptide due to side reactions of the carboxamide groups. Dehydration of the carboxamide group precluded application of the mixed anhydride method. Ultimately a modified azide method[154] was found to give excellent yields of both dipeptides and this was used extensively. In all the reactions, the α-amino groups of the glutamine and asparagine residues were protected as carbobenzyloxy derivatives to prevent self condensation. To prevent possible side reactions of the diazodipeptides (eg. intramolecular cyclisation to diketomorpholines (Figure 5.1)[155]), the terminal carboxyl group was also protected as the methyl ester. This also improved the solubility of the dipeptides and their derivatives in organic solvents. The synthetic procedures used for the dipeptides are discussed below.

Figure 5.1 Formation of diketomorpholines from diazodipeptides

5.2.1 Carbodiimide method

Hydroxybenzotriazole (HOBt) was used in conjunction with dicyclohexyl-carbodiimide (DCC) to couple N-carbobenzyloxy-L-asparagine to glycine ethyl ester in 35% yield. HOBt is reported to reduce the amount of dehydration of the amide moiety of asparagine.[156] It reacts with the O-acylisourea (1) to form the activated ester (2) which affects rapid acylation of the second amino component (Figure 5.2).

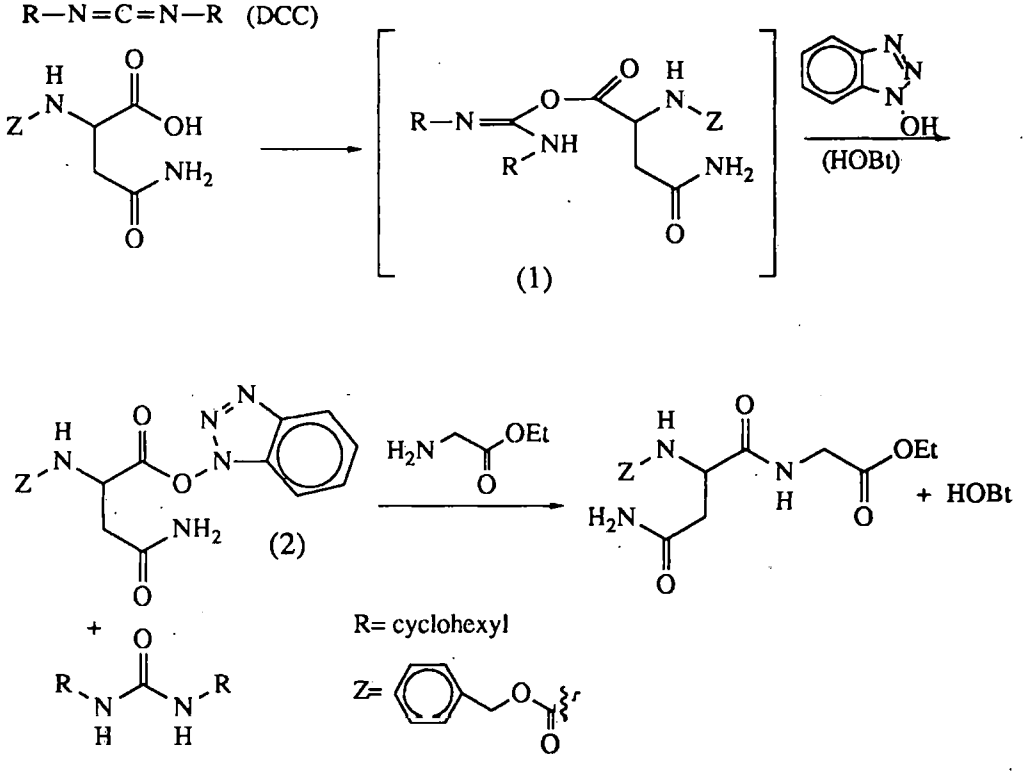

Figure 5.2 Mechanism of HOBt mediated DCC coupling of asparagine to glycine ethyl ester

In our hands the reaction had several drawbacks, such as low yield for a one step coupling process and long reaction times. Also, in order to maximise the yield it was

necessary to heat the HOBt with DCC under reflux and an atmosphere of argon to remove any water from the catalyst before commencing the reaction. Simply drying the HOBt over P_2O_5 was ineffectual. As mentioned above, reaction times were long being ca. 60h for 0.05g scale synthesis and invariably delivering an impure product. These factors make the DCC method unsuitable for the synthesis of asparaginyl and glutaminyl dipeptides.

5.2.2 Active ester method

The method of Bodanszky[157] was used to prepare the 4-nitrophenyl ester of N-α-carbobenzyloxy-L-glutamine. This method is very similar to that described above for the hydroxybenzotriazole ester of asparagine. Thus, N-α-carbobenzyl-oxyglutamine and a 20% excess of 4-nitrophenol were treated with a 1 molar equivalent of DCC in DMF. The work-up involved removal of the urea by filtration, addition of water to precipitate the product, followed by repeated recrystallisations from DMF and water to remove excess 4-nitrophenol from the product. An additional complication was the formation of the symmetrical urea from unreacted DCC on the addition of water. This impurity proved difficult to remove because of its limited solubility in DMF. A second impurity arose from dehydration of the carboxamide group by DCC. Bodanszky reported that DCC does not react directly with the amides and no reaction was evident when glutamine and asparagine were either part of the peptide chain, or protected as esters.[157] The conclusion drawn from these observations is that dehydration must be occurring intramolecularly in the O-acylisourea intermediate (3) to give the nitrile (4) which can then form an activated ester (5) with DCC and 4-nitrophenol (Figure 5.3).The problem of urea removal was overcome by using ethyl 3-(3-dimethyl aminopropyl) carbodiimide hydrochloride[158] as the coupling agent. This carbodiimide forms a water soluble urea which simplifies purification and this procedure gave the L-glutaminyl-4-nitrophenyl ester in 50% yield.

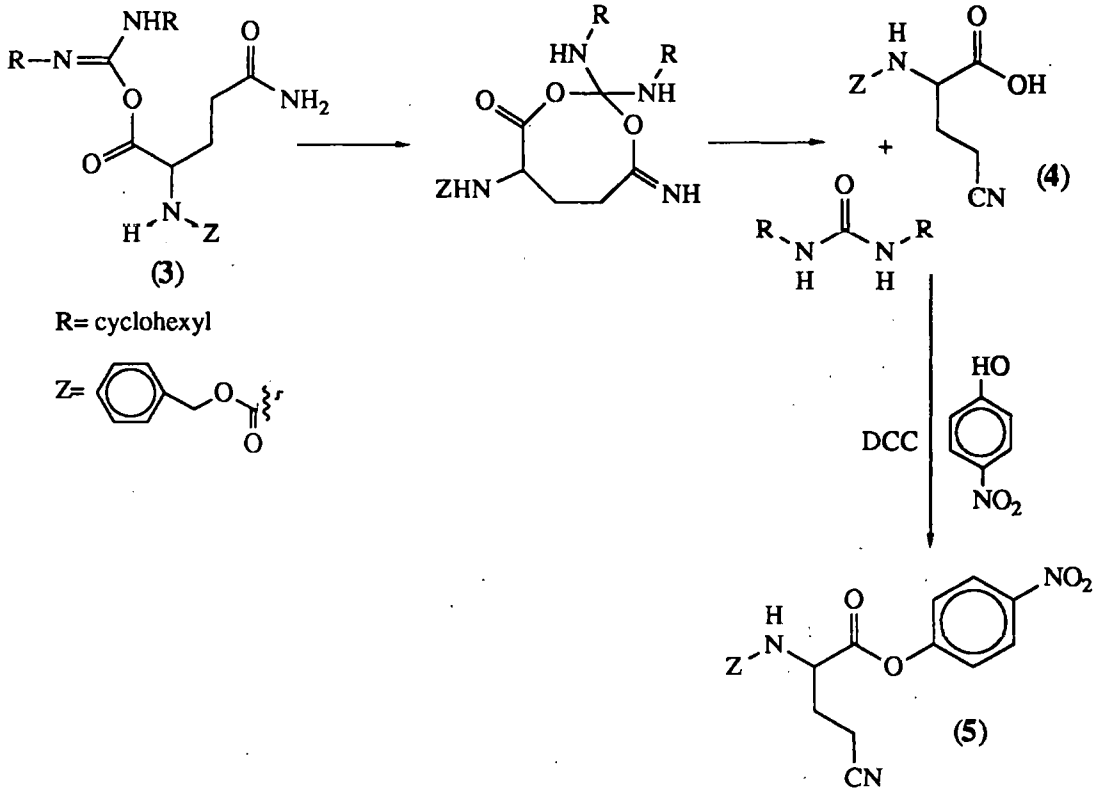

Figure 5.3 Formation of a nitrile in DCC active-ester formation

The mass spectrum of this ester showed no evidence of the dehydrated product (5) but 4-nitrophenol, present as an impurity, gave a depressed melting point. Nonetheless, it was used, slightly impure in the next stage of the synthesis.

Thus, the N-α-carbobenzyloxy-L-glutamine-4-nitrophenyl ester was coupled to phenylalanine methyl ester in the presence of triethylamine in DMF. The product was isolated, after treating the reaction mixture with water, in ca. 75% yield, giving an overall yield of ca. 37% for the complete synthesis. Although reasonable, a better method was sought for a larger scale synthesis of the dipeptides.

5.2.3 Azide method

The classical azide method involves the conversion of an activated ester to the hydrazide, followed by reaction with nitrous acid to give the azide which is then coupled to the second amino acid residue (Figure 5.4). The method of Sondheimer[137,138] was used to prepare both the N-α-carbobenzyloxy-L-glutaminyl

and N-α-carbobenzyloxy-L-asparaginyl leucine methyl esters in ca. 40% overall yield from the protected amino acid.

The methyl esters, prepared as described in Section 4, were converted to the hydrazides by the addition of hydrazine hydrate at 0°C and then to the azides by treatment with $NaNO_2$ in dilute HCl at 0°C. After filtration, washing and vacuum drying over P_2O_5, the solid azide was taken up in DMF and then treated with a freshly prepared ethereal solution of L-leucine methyl ester. The ether was removed under vacuum at 0°C and the dipeptide product precipitated by the addition of water. Although the yields of each individual step are acceptable (see Figure 5.4) the overall yield of dipeptide is only ca. 40%.

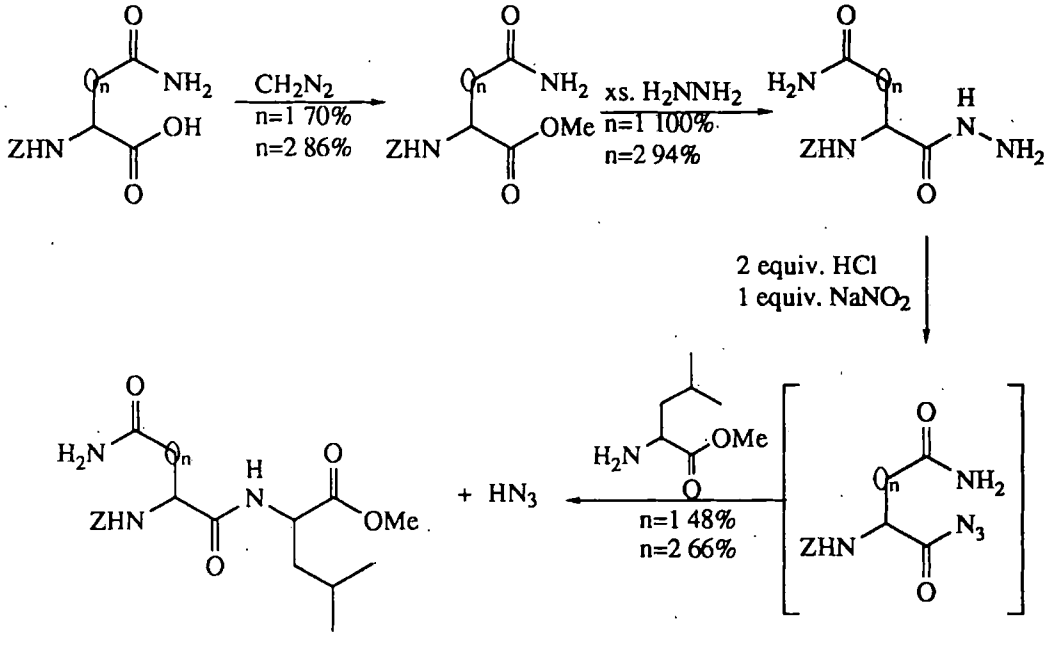

Figure 5.4 The azide coupling method

There was no evidence of substantial side reactions for the azide method such as the Curtius rearrangement of the azide to isocyanate which is sometimes encountered. It seems to offer several advantages over the other classical coupling methods. Thus, the products formed are relatively free from impurities and all by-products are water soluble and easy to remove. There is no evidence of secondary reactions involving the

carboxamide group, a major drawback of other procedures, and the chiral integrity of the amino acid residues is fully retained. The overall yields of both dipeptides were better than with the other methods but the syntheses were time-consuming because of the 4 steps required to produce the protected dipeptides.

5.2.4 Modified azide method

A relatively modern, and much underused modification of the azide method was reported by Yamada et. al.,[154] where the azide intermediate is generated directly in one step from the carboxylic acid by treatment with diphenylphosphoryl azide (6). The azide intermediate is not isolated, but treated with the second amino acid residue to give the protected dipeptide. Further, diphenylphosphorylazide (6) can be added to a mixture of the appropriately protected carboxyl and amino components in DMF. Whether the reaction proceeds *via* either the azide intermediate (7) or the phosphoryl ester (8), which reacts directly with the amino component (Figure 5.5), is not known.

Once the addition of (6) to a mixture of the 2 amino acids was complete, the L-phenylalanine methyl ester HCl salt was neutralised *in situ* by the addition of triethylamine. The protected dipeptide product was then isolated in an identical manner to that described for the classical azide method.[138] Both N-α-carbobenzyl-oxy-L-glutaminyl-L-phenylalanine methyl ester (9) and N-α-carbobenzyloxy-L-asparaginyl-L-phenylalanine methyl ester (10) were successfully synthesised in isolated yields of ca. 90%. Since all the by-products are water soluble, purification was effected by thorough water washing. The method gave a quick and convenient high yielding one pot synthesis of both the glutaminyl and asparaginyl dipeptides with all the advantages of the classical azide method. Further, there was no evidence of significant secondary reactions of the carboxamide side chains.

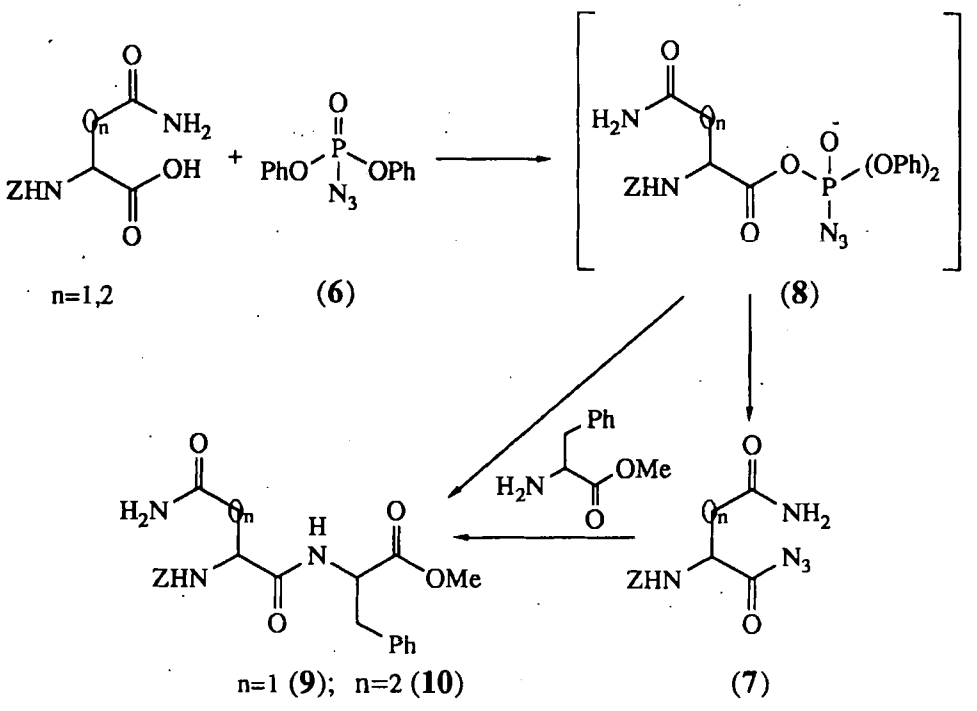

Figure 5.5 Modified azide coupling reaction

5.2.5 Deprotection of the dipeptides (9) and (10)

The N-α-carbobenzyloxy protecting groups of dipeptides (9) and (10) were removed by catalytic hydrogenolysis with 10% Pd/C. The dipeptides were isolated as the HCl salts to prevent intramolecular cyclisation to form diketopiperazines. Thus, L-glutaminyl-L-phenylalanine methyl ester hydrochloride salt (GlnPheOMe, 11) and L-asparaginyl-L-phenylalanine methyl ester hydrochloride salt (AsnPheOMe, 12) were prepared quantitatively and obtained as white hygroscopic solids.

Characterisation of GlnPheOMe (11) and AsnPheOMe (12)

Both dipeptides were characterised by their ^{1}Hnmr, ir and ms spectral properties.

^{1}H-NMR

The presence of two chiral centres in each dipeptide makes their ^{1}Hnmr spectra interesting. There is no evidence in the spectra of diastereoisomers so the peptide coupling must have been without racemisation as expected. Since both dipeptides were prepared from S-amino acids, they must have an S,S configuration.

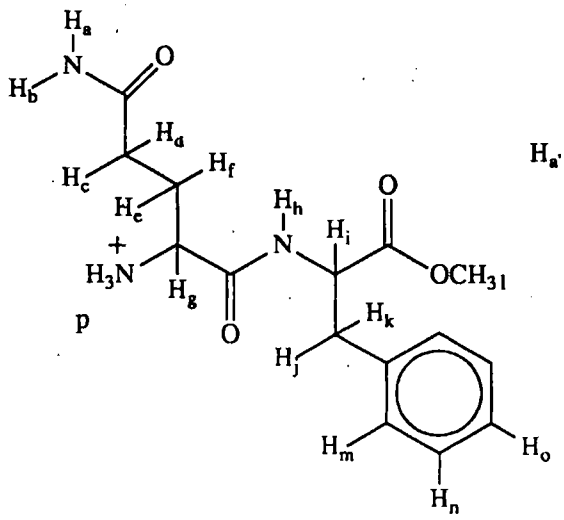

GlnPheOMe (**11**)

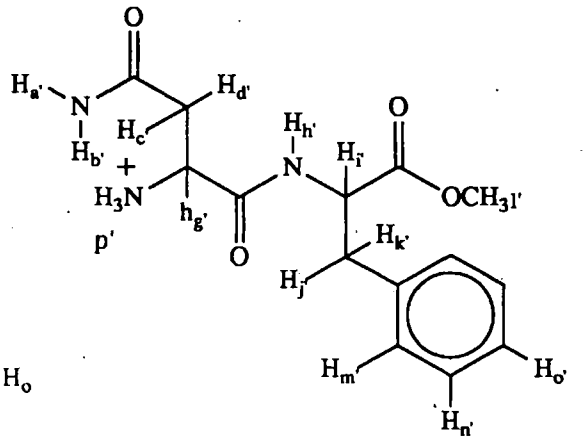

AsnPheOMe (**12**)

The 90MHz ^{1}H-nmr spectra in d^{6}DMSO using tetramethyl silane as an internal standard, shown in Figures 5.6 and 5.7, are summarised and assigned in Table 5.1. These are entirely consistent with the proposed structures.

Several interesting points emerge from the assignments, of which the most striking is probably the chemical shift differences of 0.6ppm for the amide NH_2 protons. Thus rotation about the C-N bond is restricted at ambient temperature presumably by intramolecular hydrogen bonding by the downfield N-H, with the peptide N-atom. The effect of temperature on the ^{1}H-nmr spectra was not examined. In the 90MHz spectra non-equivalence of the two prochiral protons of the amide side chains and their coupling constants cannot be discerned. The equivalence of the aromatic protons indicate that rotation of the benzyl groups is unhindered at ambient temperature.In the 90MHz spectrum the benzylic protons appear to be equivalent, but the 400MHz 2D COSY spectrum of GlnPheOMe (11) in D_2O (Figure 5.8) reveals otherwise and coupling between the chiral C-H (i) and the benzylic CH_2 (j and k) is evident.

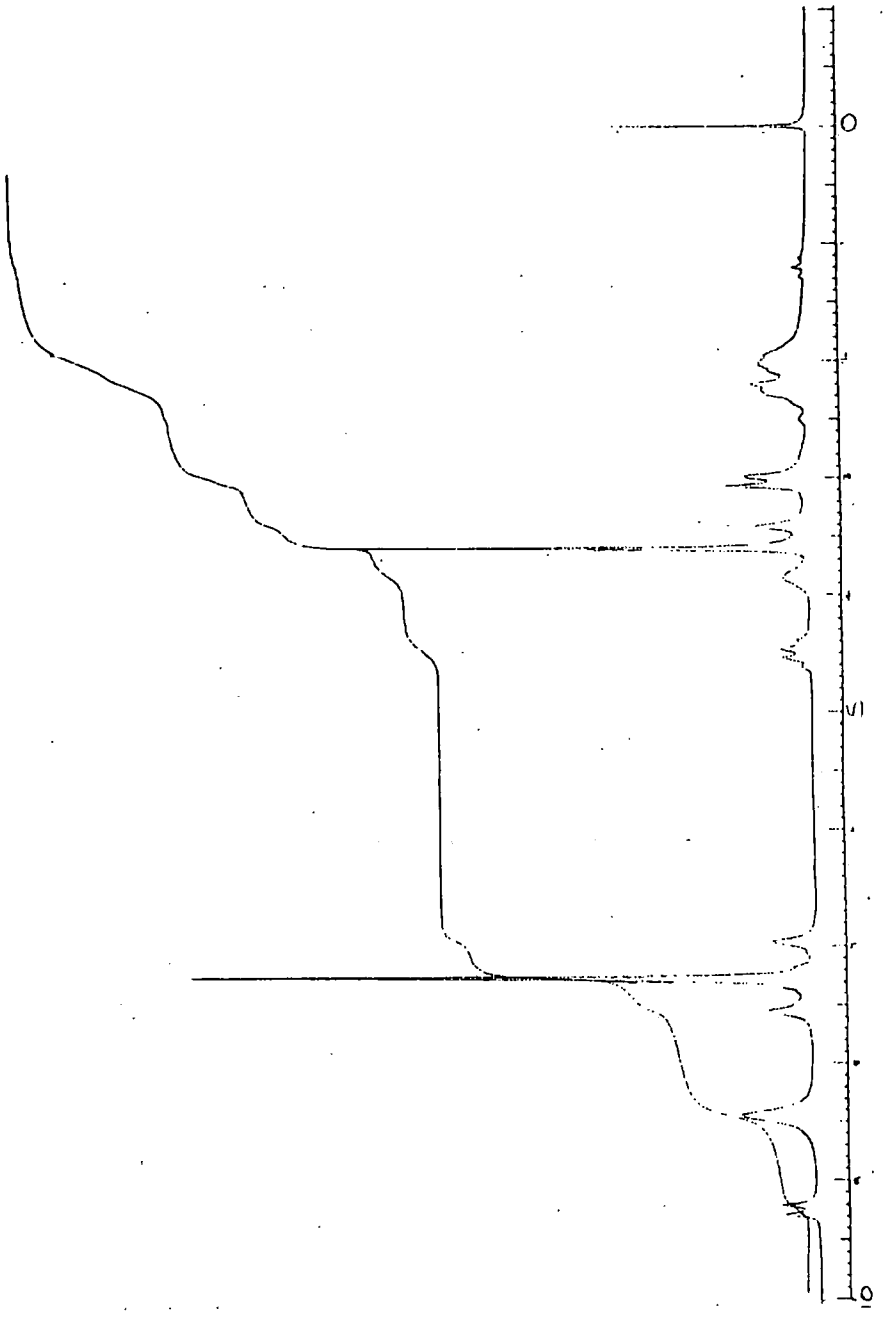

Figure 5.6 90MHz ^1H-nmr spectrm of GlnPheOMe(11) in d^6DMSO

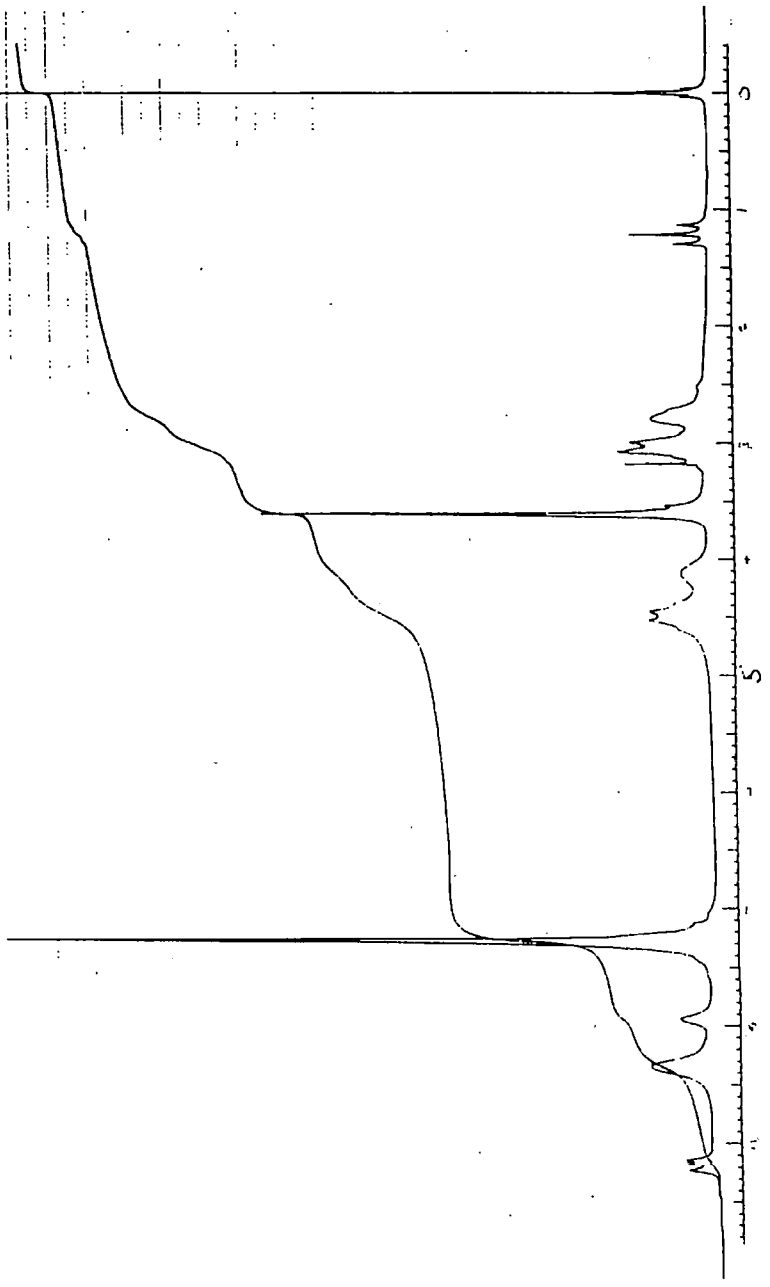

Figure 5.7 90MHz ^1H-nmr spectrum of AsnPheOMe (12) in d^6DMSO

Table 5.1 ^{1}H-nmr spectral assignments for GlnPheOMe (11) and AsnPheOMe (12)

GlnPheOMe			AsnPheOMe		
δ/ppm	Proton (s)	J/Hz	δ/ppm	Protons (s)	J/Hz
9.2	h	(h,i) 7.08	9.2	h'	(h',i') 7.08
8.4	p		8.4	p'	
7.6	a		7.9	a'	
7.3	m,n,o		7.3	m',n',o',b'	
7.0	b		4.5	i'	
4.5	i	(i,h) 7.08	4.1	g'	
3.9	g		3.6	l'	
3.6	l		3.0	j',k'	
3.0	j,k		2.8	c',d'	
2.2	c,d				
2.0	e,f				

The coupling constants for these interactions and also between the chiral C-H (g) and the prochiral CH_2 (e and f) can be determined from the 400MHz ^{1}H-J-resolved spectrum (Figure 5.9) and are reported in Table 5.2

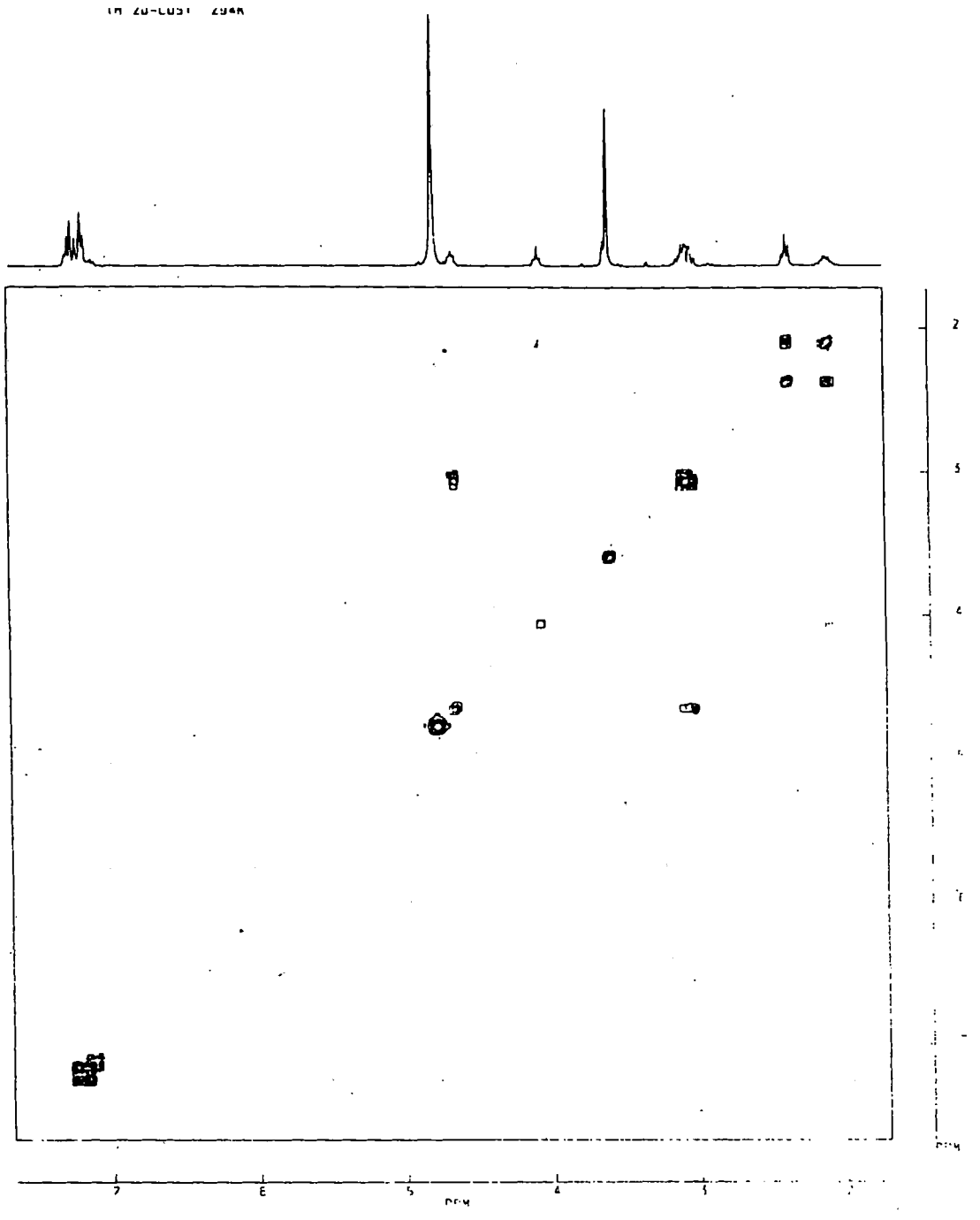

Figure 5.8 *2D COSY spectrum of GlnPheOMe (11) in D_2O*

Table 5.2 Coupling constants between chiral C-H and prochiral CH_2 for GlnPheOMe (11)

Protons	J/Hz
h,j (syn)	6.2
h,k (anti)	9.4
g,e (syn)	4.6
g,f (anti)	9.2

The 400MHz heteronuclear shift correlated 2-D spectrum of GlnPheOMe (11) allows the assignment of the ^{13}C-spectrum reported in Table 5.3.

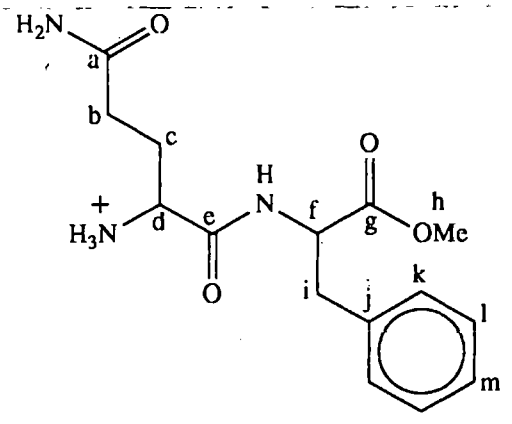

GlnPheOMe

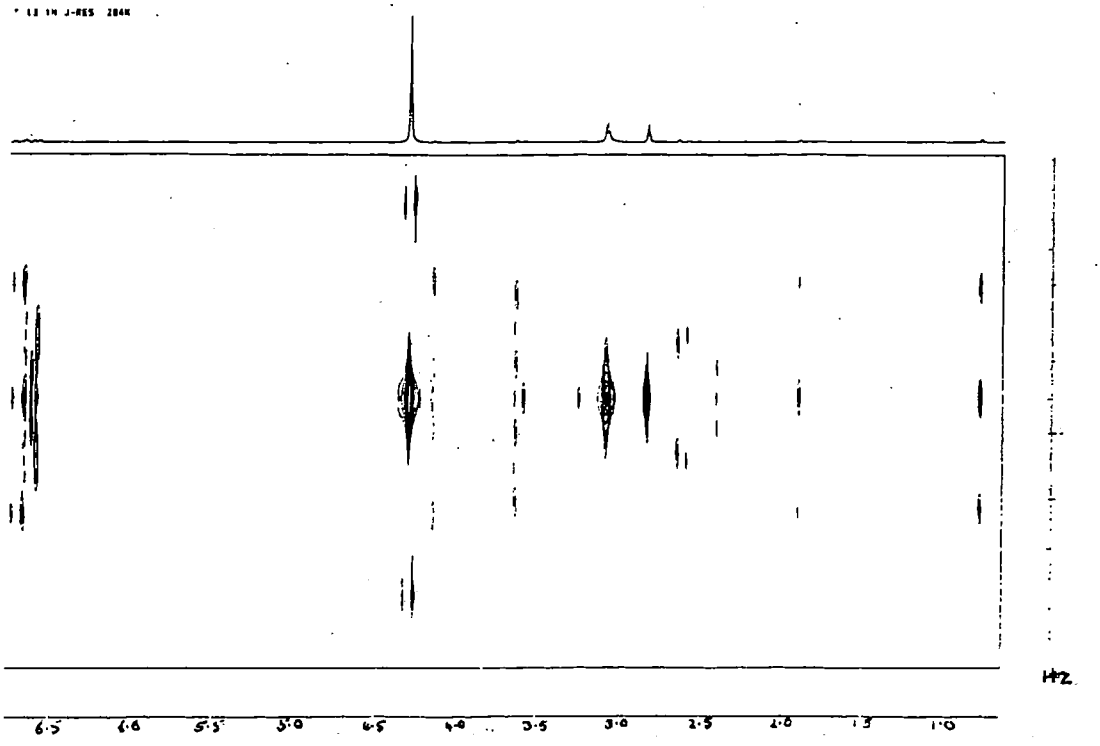

Figure 5.9 400MHz ^{1}H-J- resolved spectrum of GlnPheOMe (11) in D_2O.

Table 5.3 ^{13}C-nmr spectrum of GlnPheOMe

δ/ppm	Assignment	δ/ppm	Assignment
177.44	g	55.27	f
173.56	e	53.71	h
169.77	a	53.14	d
136.98	j	37.11	i
129.92	k	30.83	b
129.56	l	27.35	c
128.04	m		

Mass spectrum

The fast atom bombardment (FAB) +ve ion spectral data obtained using a glycerol matrix is summarised and assigned for both GlnPheOMe (11) and AsnPheOMe (12) in Table 5.4 and 5.5 respectively. The fragmentation is also consistent with the proposed structures (11) and (12). The ions at m/z 180, 120 and 91 are common to both molecules and relate to the phenylalanine methyl ester residue. It is interesting to note that the strongest ions in the spectrum of AsnPheOMe predominantly come from cleavage of the phenylalanine methyl ester moiety whilst those in the spectrum of GlnPheOMe are the molecular ion and the ion at m/z 84 which is consistent with a dehydropyrolidin-2-one structure. The equivalent ion in the spectrum of AsnPheOMe at m/z 70 has a much lower relative abundance (33.7%), reflecting the increased ring strain of the 4-membered ring.

Table 5.4 Assignment of FAB (+ve ion) mass spectral data for GlnPheOMe (11)

m/z	Relative Abundance/%	Ion
308	100	$M+H^+$
84	78.9	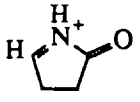
120	72.3	$(H_2N{=}CHCH_2Ph)^+$
180	56.6	$(H_3NCH(CH_2Ph)CO_2Me)^+$
101	51.9	$(H_2N{=}CH_2CH_2CONH_2)^+$
291	51.3	$M+H^+-NH_3$
91	20.0	$(C_7H_7)^+$
231	17.1	$(H_2NCOCH_2CH_2CHCONCHCH_2Ph)^+$

Table 5.5 Assignment of FAB (+ve ion) mass spectral data for AsnPheOMe (12)

m/z	Relative Abundance/%	Ion
120	100	$(H_2N{=}CHCH_2Ph)^+$
87	66.1	$(H_2N{=}CHCH_2CONH_2)^+$
91	59.2	$(C_7H_7)^+$
180	55.1	$(H_3NCH(CH_2Ph)CO_2Me)^+$
44	51.6	$(H_2NCO)^+$
294	43.8	$M+H^+$
70	33.7	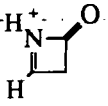
277	23.7	$M+H^+-NH_3$
235	23.4	$(H_2N{=}CHCONHCH(CH_2Ph)CO_2Me)^+$
260	22.0	$(OC{=}CHCHCONHCH(CH_2Ph)CO_2Me)^+$

Infra red

The infrared spectra of GlnPheOMe (11) and AsnPheOMe (12) are similar, as expected and both show strong bands at ca. 3400cm^{-1} (amide NH), ca. 3200cm^{-1} (NH_3^+), 1740cm^{-1} (ester CO), 1675/1667cm^{-1} (amide CO) and ca. 1555cm^{-1} (amide II). The amide CO of AsnPheOMe is slightly higher (1675cm^{-1}) than that of GlnPheOMe (1667cm^{-1}) and only single bands are apparent, presumably because the two amide CO absorbances overlap. Otherwise the ir spectra are also consistent with the structures proposed for (11) and (12).

5.3 Synthesis of potential cyclic deamination products

From the results for N_2GlnOMe and N_2AsnOMe (Chapter 4), the lactones (13) and (14) are the most likely products for deamination of 2-diazo-4-carbamoyl-butanoyl-L-phenylalanine methyl ester (N_2GlnPheOMe) (15) and 2-diazo-3-carbamoylpropanoyl-L-phenylalanine methyl ester (N_2AsnPheOMe) (16) respectively.

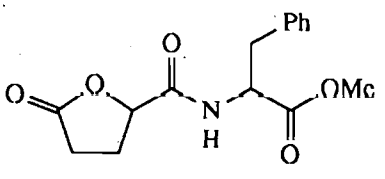

(13)

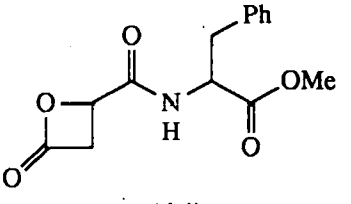

(14)

The synthesis of β-lactone (14) was reported in Chapter 2, but attempts to independently synthesise (13) were unsuccessful. The most appropriate synthetic route to (13) is to couple the γ-lactone carboxylic acid (17) with phenylalanine methyl ester (Figure 5.10) but this could not be effected using either the mixed carbonic anydride, activated ester or the modified azide methods. The lack of success probably relates to the inherent high reactivity of the γ-lactone itself, which may preferentially react with either the phenylalanine reagent, azide ion or chloride ion. These reactions may proceed either before or after coupling to the phenylalanine residue.

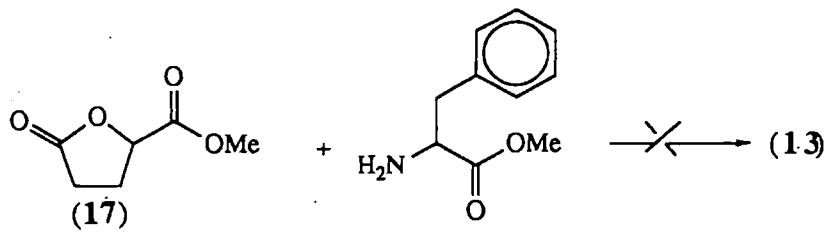

Figure 5.10

5.4 Synthesis of diazodipeptides

5.4.1 In-situ reactions

The formation of N_2GlnPheOMe and N_2AsnPheOMe was assessed in preliminary experiments of *in-situ* nitrosation of the parent dipeptide in aqueous buffers with nitrogen dioxide. The formation of diazo products was assessed by HPLC using an aqueous borax buffer/acetonitrile eluent. For both dipeptides (11) and (12) the diazo derivatives were obtained in borax but not in phosphate buffers. Further, decomposition of the diazo derivatives was observed in the borax buffers. Clearly, the diazodipeptides are less stable than their amino acid analogues.

5.4.2 Aprotic nitrosation reactions

Both N_2GlnPheOMe (15) and N_2AsnPheOMe (16) were synthesised by aprotic nitrosation of the neutral substrate in an organic solvent with a solution of dinitrogen tetroxide. These reactions were carried out under an inert atmosphere of argon and at a lower temperature (-78°C) than before. In practice 1.5 equivalents of dinitrogen tetroxide in DCM were added dropwise to the dipeptide in the cooled reaction solution which also contained 3 equivalents of triethylamine and anhydrous sodium sulphate to sequester the liberated water. Once addition was complete, the reaction solution was warmed to room temperature, filtered and the organic solvent removed under vacuum. The residue was taken up in dry acetone or ethyl acetate and the solid triethylammonium salts were removed by filtration. N_2GlnPheOMe was purified by column chromatography on silica using an eluent gradient of ether and acetone; N_2AsnPheOMe

was purified similarly on silica using ethyl acetate as the eluent. In contrast to the diazoamino acids, both diazopeptides chromatographed better on silica than alumina. After removal of the solvents, N_2GlnPheOMe and N_2AsnPheOMe were obtained as highly hygroscopic yellow solids in yields of 26% and 14% respectively, which probably reflects their low stabilities.

Characterisation of N_2GlnPheOMe (15) and N_2AsnPheOMe (16).

Both diazopeptides were characterised by their uv, ^{1}H and ^{13}C-nmr, ir and ms spectral properties.

UV

Both N_2GlnPheOMe and N_2AsnPheOMe had strong characteristic absorbances in the ultraviolet spectrum at λ_{max} (EtOH) 259 (log ε_{max} 4.02) and λ_{max} (EtOH) 260nm (log ε_{max} 3.76) respectively, corresponding to the $\pi\rightarrow\pi^*$ transition. The $n\rightarrow\pi^*$ transition at λ_{max} ca. 380nm accounting for the yellow colour of the compounds, was also observed in more concentrated solutions. The extinction coefficients are on the low side (Challis and Latif report values of $\log_\varepsilon$ ca. 260nm =4.00-4.35[59] for diazodipeptides), possibly because of the hygroscopic character of the compounds. Certainly, the ready uptake of water vapour was noted in weighing the compounds.

NMR

The 90MHz ^{1}Hnmr-spectra, recorded in $CDCl_3$ using tetramethylsilane as an internal standard, are summarised and assigned in Table 5.6 together with the differences in chemical shift between the parent dipeptide and diazo derivative. With the exception of the chemical shifts of the amide NH protons (which are solvent and concentration dependent) and the aromatic CH and OCH_3 (which show a small upfield shift), all the protons of the two diazo derivatives show a small to moderate (0.1-0.5ppm) downfield reduction in their chemical shifts. This deshielding effect by the diazo moiety has greatest influence on the α-H ($\Delta\delta$ = 0.5ppm (15) and 0.3ppm (16)), but its effects are

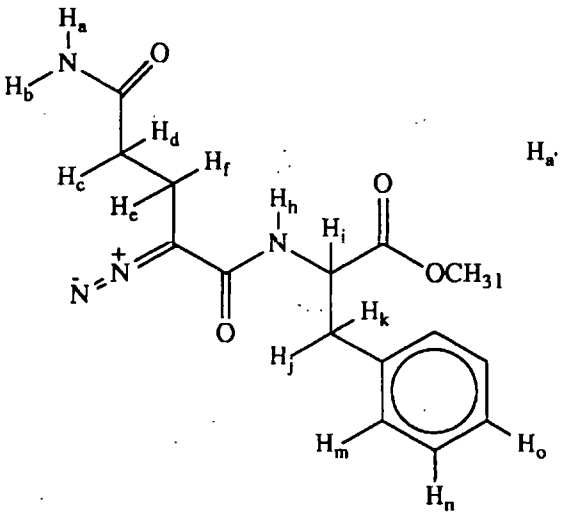

N_2GlnPheOMe (**15**)

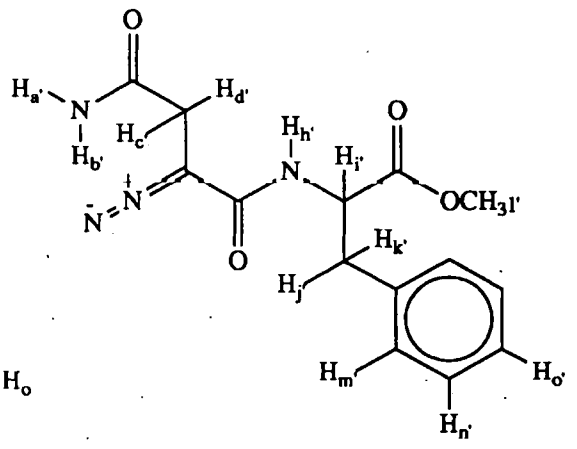

N_2AsnPheOMe (**16**)

Table 5.6 ^{1}Hnmr spectral assignments for N_2GlnPheOMe (15) and N_2AsnPheOMe (16)

N_2GlnPheOMe				N_2AsnPheOMe			
δ/ppm	Proton(s)	J/Hz	Δδ/ppm[1]	δ/ppm	Proton(s)	J/Hz	Δδ/ppm
7.2	m,n,o		-0.1	7.2	m',n',o'		-0.1
6.9	h	7.8	-2.3	7.0	h	8.05	-2.2
6.3	a		-1.3	6.8	a'		-1.1
6.1	b		-0.9	6.2	b'		-1.1
4.8	i		0.3	4.8	i'		0.3
3.7	l		0.1	3.7	l'		0.1
3.1	j,k		0.1	3.1	c',d'		0.3
2.5	c,d		0.3	3.1	j',k'		0.1
2.5	e,f		0.5				

1) Δδ = δ diazodipeptide - δ dipeptide

long range and the chiral CH of the phenylalanine moiety is affected significantly ($\Delta\delta$=0.3ppm). These data are consistent with the structures (15) and (16).

There is relatively little change in the ^{13}Cnmr spectra on diazotisation of the parent dipeptides. As expected, the $\overset{+}{C}=\overset{-}{N}=N$ is considerably deshielded occurring at δ=57.6ppm ($\Delta\delta$= +4.5ppm) for (15) and δ=54.6ppm ($\Delta\delta$= +5.7ppm) for (16) and the band for the 3-C-atom moves considerably upfield, from 27.35 to 19.4ppm for (15) and from 35.3 to 30.4ppm for (16).

Infra red

Both N_2GlnPheOMe and N_2AsnPheOMe gave strong absorbances of ca. 2090 cm^{-1}, highly characteristic of the $C=\overset{+}{N}=\overset{-}{N}$ moiety, as well as at ca. 3410 (NH amide) 1741 (CO ester) ca.1670 (CO amide) and ca.1620 cm^{-1} (amide II). Only one band is apparent for the amide CO absorbances, presumably due to overlapping bands as is the case with the parent dipeptides and there is no evidence of delocalisation of the α-carbonyl moiety electrons with those of the diazo group, as observed in the case of the diazoamino acid esters. This is presumably due to more favourable electron delocalisation of the amide moiety. Otherwise the ir-spectra are also consistent with the structures proposed for (15) and (16).

Mass spectra

The fragmentation of N_2GlnPheOMe (15) and N_2AsnPheOMe (16) was examined by FAB procedures in a variety of matrices. Glycerol was found to be unsatisfactory, particularly for N_2AsnPheOMe where the spectrum was observed to change with time, indicative of decomposition on the probe. Similar problems were encountered with N_2GlnPheOMe but a molecular ion was evident at m/z 319 and a reasonably strong fragment ion at m/z 291 due to ($M+H^+-N_2$).

Better mass-spectra were obtained using tetraethyleneglycol diethyl ether (TEGDE), an aprotic non-nucleophilic material as the FAB matrix. In the absence of matrix protons,

the FAB (+ve ion) spectra were poor (few, very weak ions only) but the FAB (-ve ion) spectra revealed $(M-H^+)^-$ as the base peak but unfortunately little other fragmentation. Also it was not possible to obtain accurate mass measurements in the negative ion mode using TEGDE.

FAB accurate mass measurements were made, however, using a polyethylene glycol (200) matrix and the positive ion mode. As noted above, no molecular ion was observable for N_2AsnPheOMe and the mass measurements were made on the $(M+H^+)$-28 ion corresponding to the loss of N_2 from the molecular ion. Mass measurements were possible on both the molecular ion $(M+H^+)$ and $(M+H^+-28)$ ion for N_2GlnPheOMe. The results, shown in Table 5.7, confirm the structures assigned to compounds (15) and (16) within acceptable limits.

Table 5.7 Accurate mass measurements of N_2GlnPheOMe (15) and N_2AsnPheOMe (16)

Compound	Ion	Measured mass/amu	Calculated mass/amu	Δ/mamu
N_2AsnPheOMe (11)	$C_{14}H_{17}N_2O_4$	277.1198	277.1188	0.98
N_2GlnPheOMe (15)	$C_{15}H_{19}N_4O_4$	319.1500	319.1406	9.38
N_2GlnPheOMe (15)	$C_{15}H_{19}N_2O_4$	291.1420	291.1344	7.53

5.5. Stabilities of N_2GlnPheOMe and N_2AsnPheOMe in aqueous media

The rates of decomposition of N_2GlnPheOMe and N_2AsnPheOMe were measured in both aqueous buffer solutions at a constant ionic strength of μ=0.5 ($NaClO_4$) and dilute $HClO_4$, all at 25°C. The reactions were followed by the decrease in uv absorbance at λ_{max}=260nm with time, using a stopped flow technique for dilute $HClO_4$, and

conventional uv spectrophotometry for buffer solutions. Usually the reactions were followed to completion and all gave good *pseudo* first order behaviour in substrate (Equation 5.1) over at least 4 half lives. Values of k_o were obtained from the integrated rate

$$\text{Rate} = k_o[\text{diazodipeptide}] \qquad \ldots(5.1)$$

equation and Figure 5.11 shows a typical plot of $\ln((A_t-A_\infty)/(A_o-A_\infty))$ against time for the decomposition of N_2GlnPheOMe (15) in 0.01M $HClO_4$ at 25°C. A similar plot for the decomposition of N_2AsnPheOMe in 0.025M phosphate buffer (pH6.53) at 25°C is shown in Figure 5.12.

5.5.1 Decomposition in $HClO_4$

The mean k_o values (obtained from at least 5 duplicate experiments) for the decomposition of (15) and (16) in dilute $HClO_4$ at 25°C are given in Table 5.8. These show the decompositions are strongly acid-catalysed.

Table 5.8 Mean observed rate coefficients for decomposition of N_2GlnPheOMe (15) and N_2AsnPheOMe (16) in $HClO_4$ at 25°C. Initial [substrate] = ca.10^{-4}M.

$[HClO_4]$/M	$10^2k_o/s^{-1}$ (15)	$10^2k_o/s^{-1}$ (16)
0.0098	16.5	17.7
0.0049	8.46	8.26
0.00098	1.54	1.59

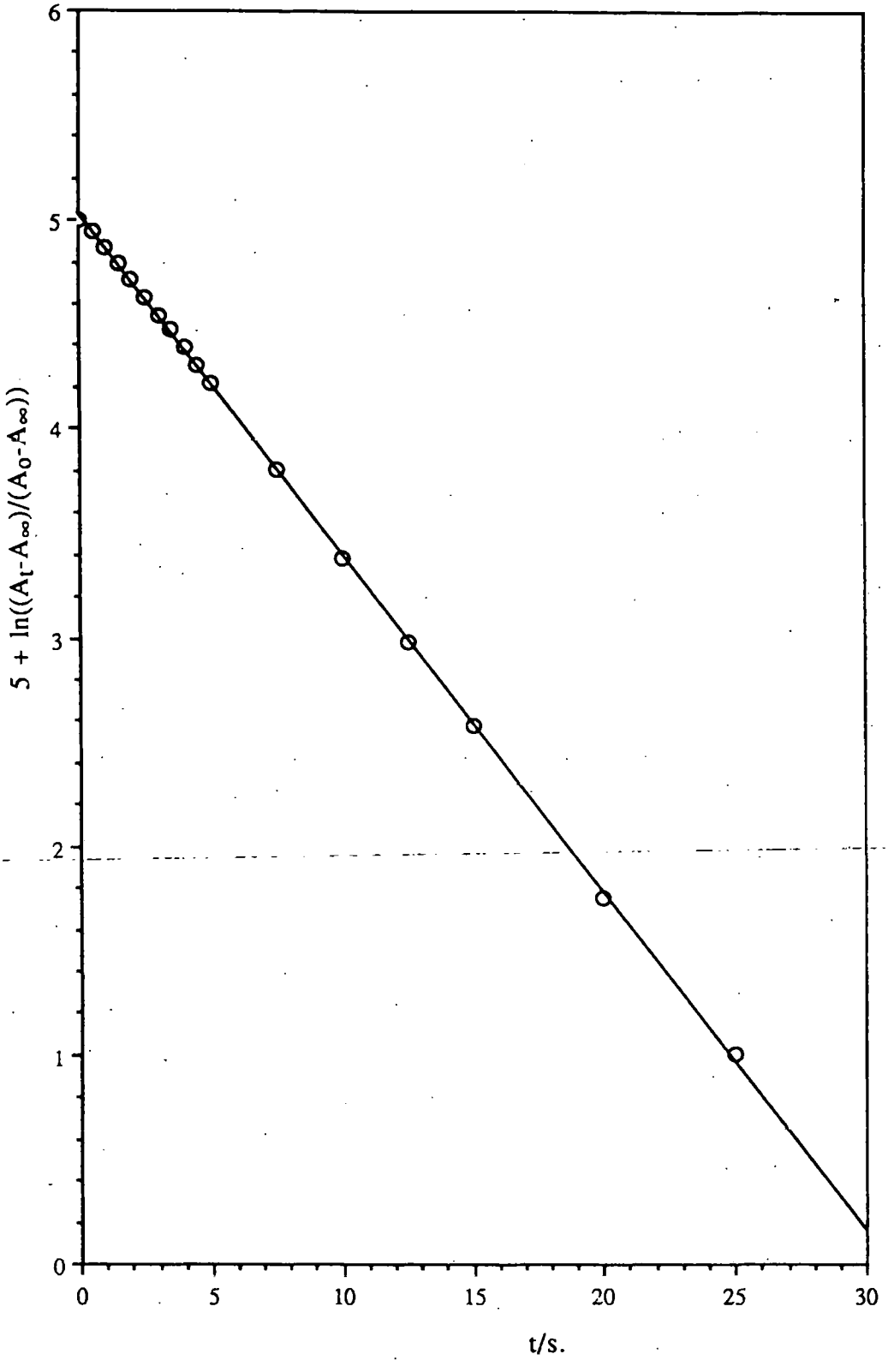

Figure 5.11 Plot of $ln((A_t-A_\infty)/(A_0-A_\infty))$ against time for the decomposition of N_2GlnPheOMe (15) in 0.01M $HClO_4$ at 25°C.

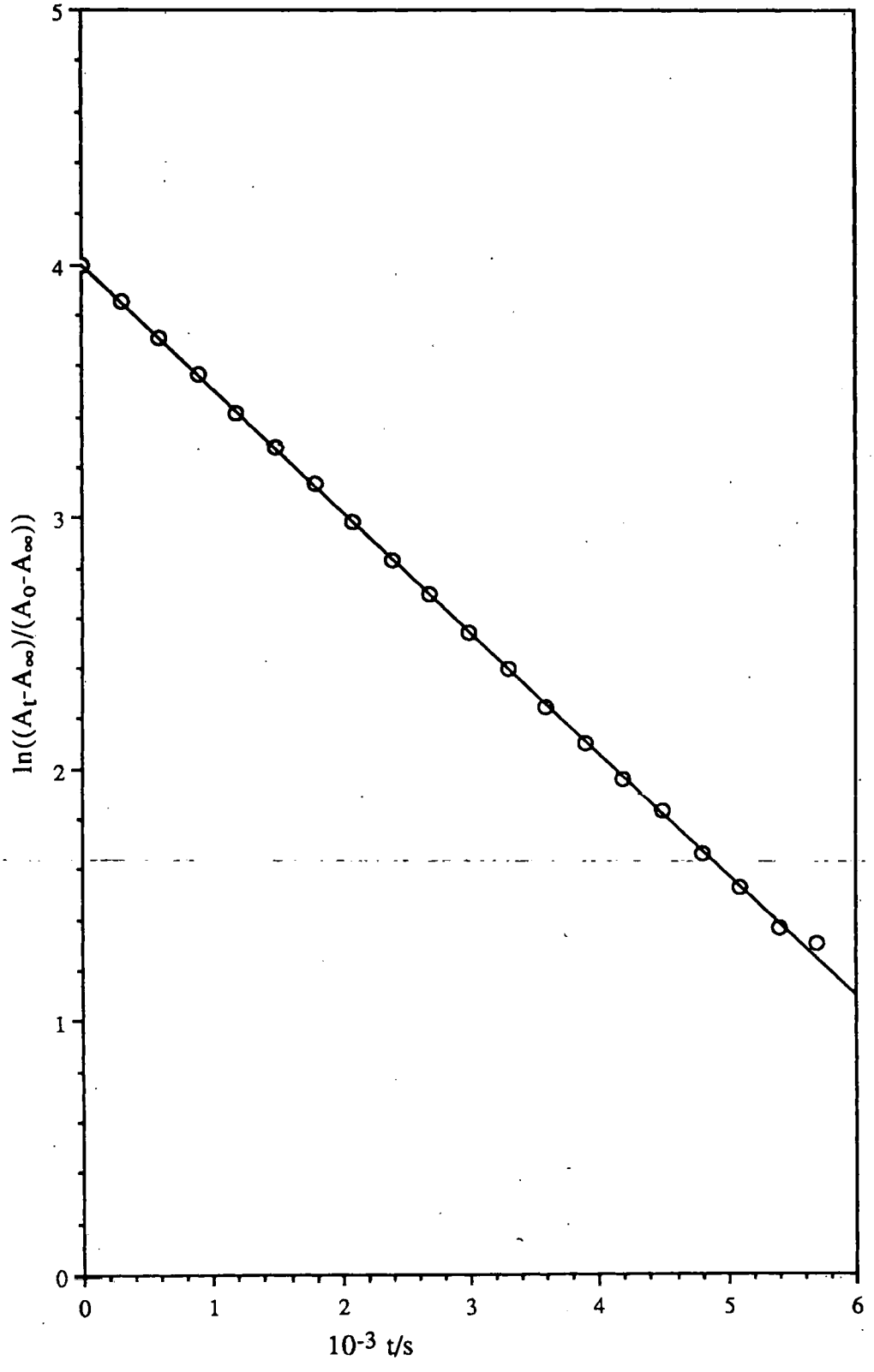

Figure 5.12 Plot of ln((A$_t$-A$_\infty$)/(A$_0$-A$_\infty$)) against time for the decomposition of N_2AsnPheOMe in 0.025M phosphate buffer (pH 6.53) at 25°C.

5.5.2 Decomposition in buffer solutions

Values of k_o for the decomposition of (15) and (16) in various buffer solution at 25°C are given in Table 5.9.

These results show that the decompositions are general-acid catalysed. Some of the plots of k_o against [HA] are linear as shown in Figure 5.13 for the decomposition of N_2GlnPheOMe in acetic acid buffers. Others however, show pronounced curvature for reasons which are not clearly understood, but may be related to a change in rate-limiting step. In these cases, the slopes and the intercept values were determined from the linear portion of the graph at lower [HA]. It therefore seems that decomposition of the diazodipeptides in buffer solutions follows equation 5.2, where k_H refers to H_3O^+ catalysis and k_{HA} to general acid catalysis. Values of the various rate coefficients obtained in both dilute $HClO_4$ and aqueous buffers are summarised in Table 5.10.

$$\text{Rate} = (k_H[H_3O^+] + k_{HA}[HA])\,[\text{substrate}] \qquad \ldots(5.2)$$

It is apparent that both N_2GlnPheOMe (15) and N_2AsnPheOMe (16) have similar reactivities.

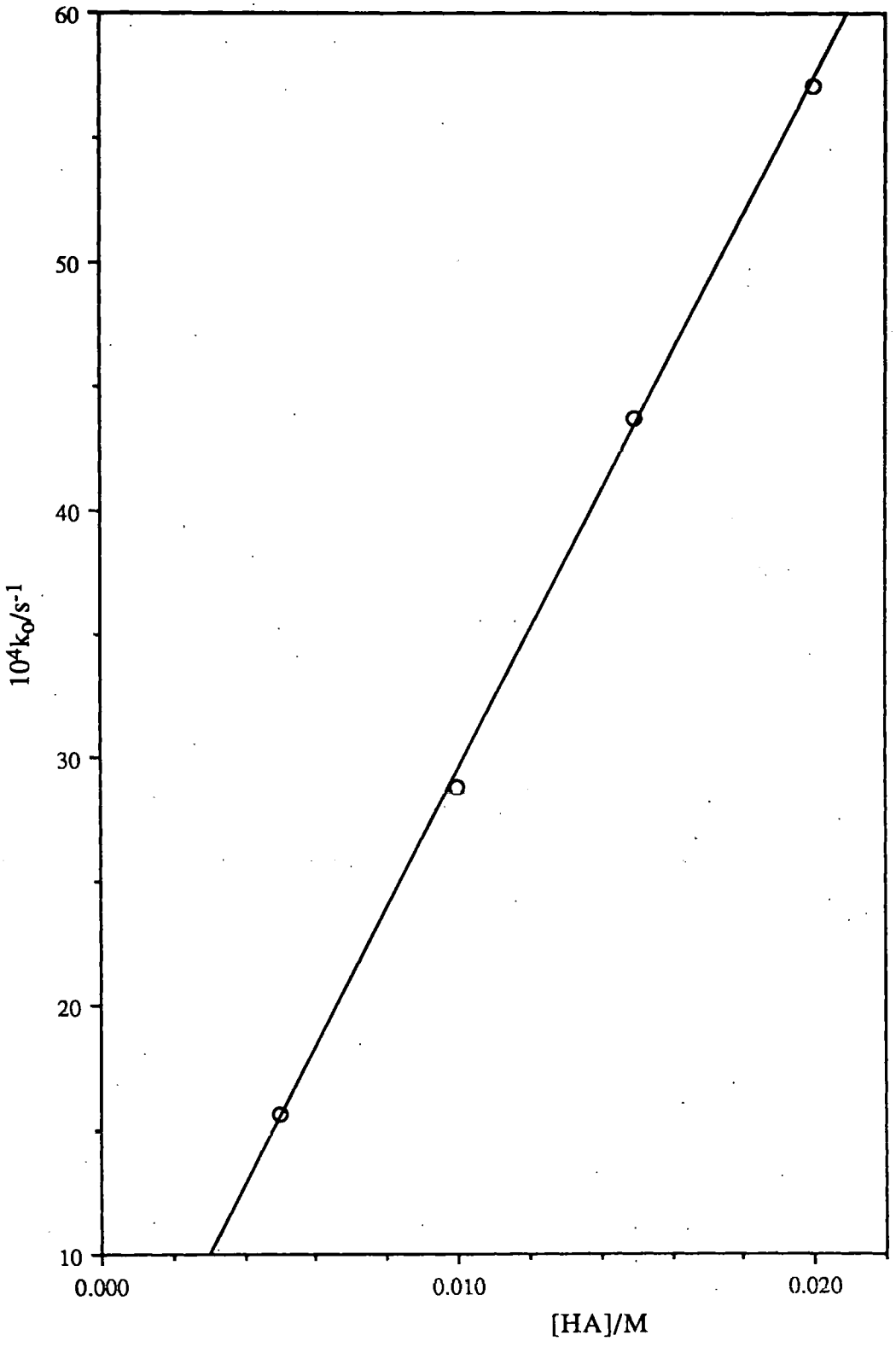

Figure 5.13 Plot of k_o against [HA] for the decomposition of N_2GlnPheOMe in acetic acid buffers at pH 5.13 and 25°C.

Table 5.9 Observed rate coefficients for decomposition of N_2GlnPheOMe (15) and N_2AsnPheOMe (16) in aqueous buffer solutions. Initial [substrate] = ca. 10^{-4}M.

Buffer	[HA]/[A⁻]	[HA]/M	pH	$10^4k_o/s^{-1}$(15)	$10^4k_o/s^{-1}$(16)
Acetate	0.25	0.02	5.14	57.1	35.0
		0.015	5.13	43.7	30.7
		0.010	5.13	28.8	22.2
		0.005	5.13	15.6	12.6
Phosphate	9	0.090	5.51	27.4	-
		0.0675	5.51	20.6	-
		0.045	5.51	13.6	-
		0.0225	5.51	6.27	-
Phosphate	1	0.075	6.50(6.60)	12.0	16.7
		0.050	6.45(6.55)	9.46	13.1
		0.025	6.38(6.52)	4.82	9.57
		0.010	6.35(6.48)	2.22	5.15
Phosphate	0.11	0.01	7.54	1.79	-
		0.0075	7.50	1.39	-
		0.005	7.46	1.02	-
		0.0025	7.40	0.586	-

pH values in parenthesis refer to compound (16) when pH different to that for compound (15).

Table 5.10 $k_H[H_3O^+]$ and k_{HA} values for N_2GlnPheOMe (15) and N_2AsnPheOMe (16).

pH	Catalyst	$10^4 k_H[H_3O^+]/s^{-1}$(15)	$10^4 k_H[H_3O^+]/s^{-1}$(16)	$10^2 k_{HA}/M^{-1}s^{-1}$(15)	$10^2 k_{HA}/M^{-1}s^{-1}$(16)
2.01	$HClO_4$	1650	1766	-	-
2.31	$HClO_4$	846	826	-	-
3.01	$HClO_4$	154	159	-	-
5.13	AcOH	1.42	6.14	27.9	18.1
5.51	H_3PO_4	0.64	-	3.12	-
6.39	H_3PO_4	0.36	-	1.81	-
6.54	H_3PO_4	-	1.57	-	1.53
7.47	H_3PO_4	0.20	-	1.59	-

5.5.3 pH Dependence

The log rate versus pH profiles for the decomposition of N_2GlnPheOMe (15) and N_2AsnPheOMe (16) by H_3O^+ are shown in Figure 5.14. For both diazo compounds, decomposition above pH5 is dominated by spontaneous reaction with water and is less strongly acid-catalysed. Below pH5, the plot is linear with unit slope implying a first order dependence upon $[H_3O^+]$. The second order rate coefficients for this catalysis (k_H) obtained from the linear portion of the plots in Figure 5.14 are given in Table 5.11 for both diazodipeptides. Insufficient data was available to reliably calculate a rate coefficient for the spontaneous water decomposition reaction (k_w).

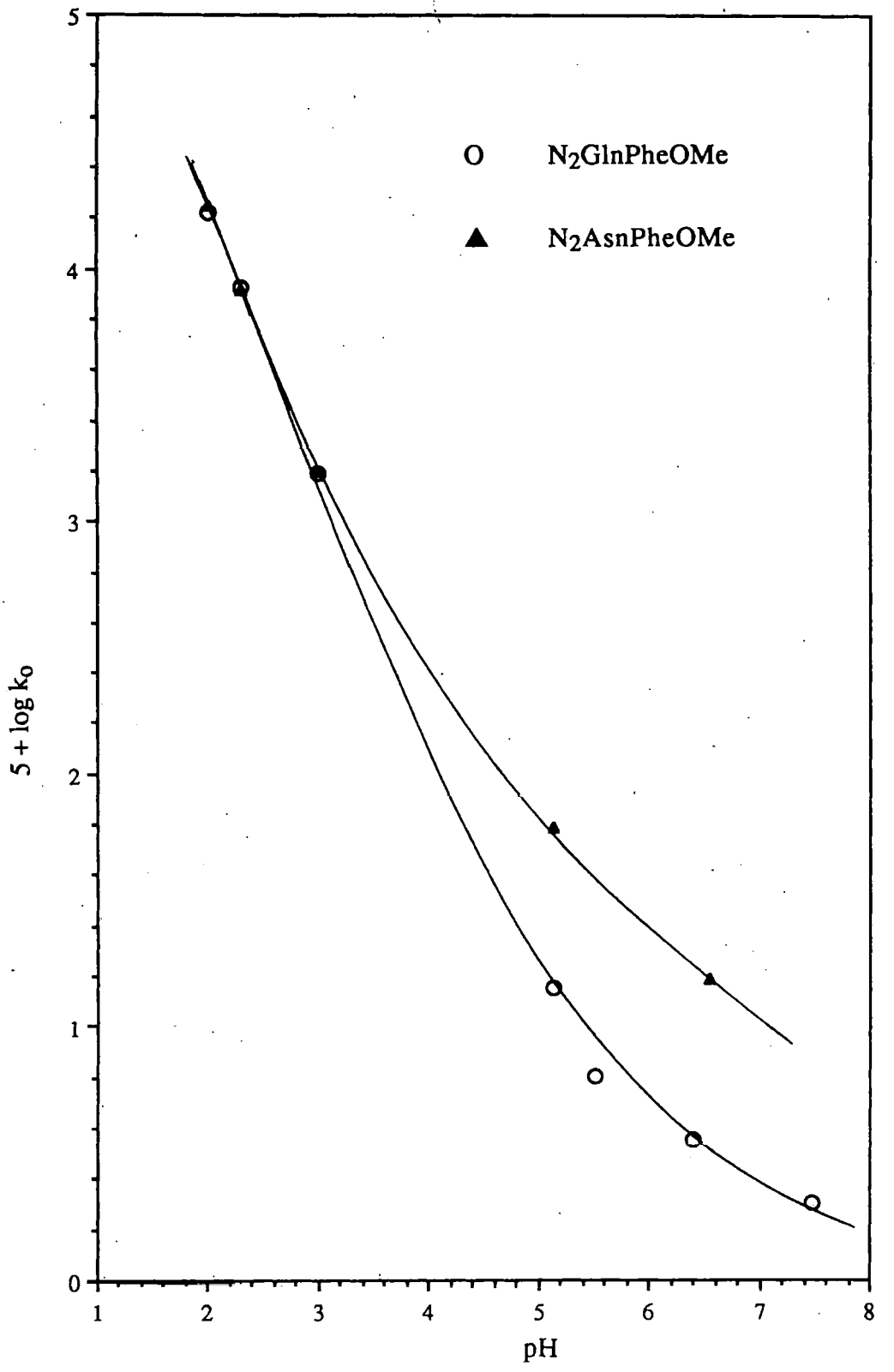

Figure 5.14 Log k_o versus pH profile for the acid catalysed decomposition of N_2GlnPheOMe (15) and N_2AsnPheOMe (16) at 25°C.

Table 5.11 Second order rate coefficients for acid catalysed decomposition of (15) and (16) at 25°C.

Substrate	$k_H/M^{-1}s^{-1}$
N_2GlnPheOMe	17.6
N_2AsnPheOMe	18.4

5.5.4 Solvent deuterium isotope effects

The rate of decomposition of N_2GlnPheOMe (15) was also examined in $DClO_4$ at 25°C, to determine the magnitude of the solvent kinetic isotope effect. Average values of the *pseudo* first-order rate coefficient (equation 5.1) from at least 5 duplicate runs are given in Table 5.12 and plotted against $[D_3O^+]$ in Figure 5.15. These lead to an average value of $k_{D^+} = 7.7\ m^{-1}s^{-1}$ for $DClO_4$ and the ratio $k_{H^+}/k_{D^+} = 2.3$. Thus, the H_3O^+- catalysed decomposition of (15) shows a normal deuterium isotope effect, which implies that H^+-transfer from the solvent to the substrate is slow.

Table 5.12 Values of observed rates of decomposition of N_2GlnPheOMe (15) in $DClO_4$ solutions at 25°C. Initial [(15)] = ca 10^{-4}M.

$[DClO_4]/M^{-1}$	$10^3k_o/s^{-1}$
0.0098	75.0
0.0049	38.0
0.0010	6.75

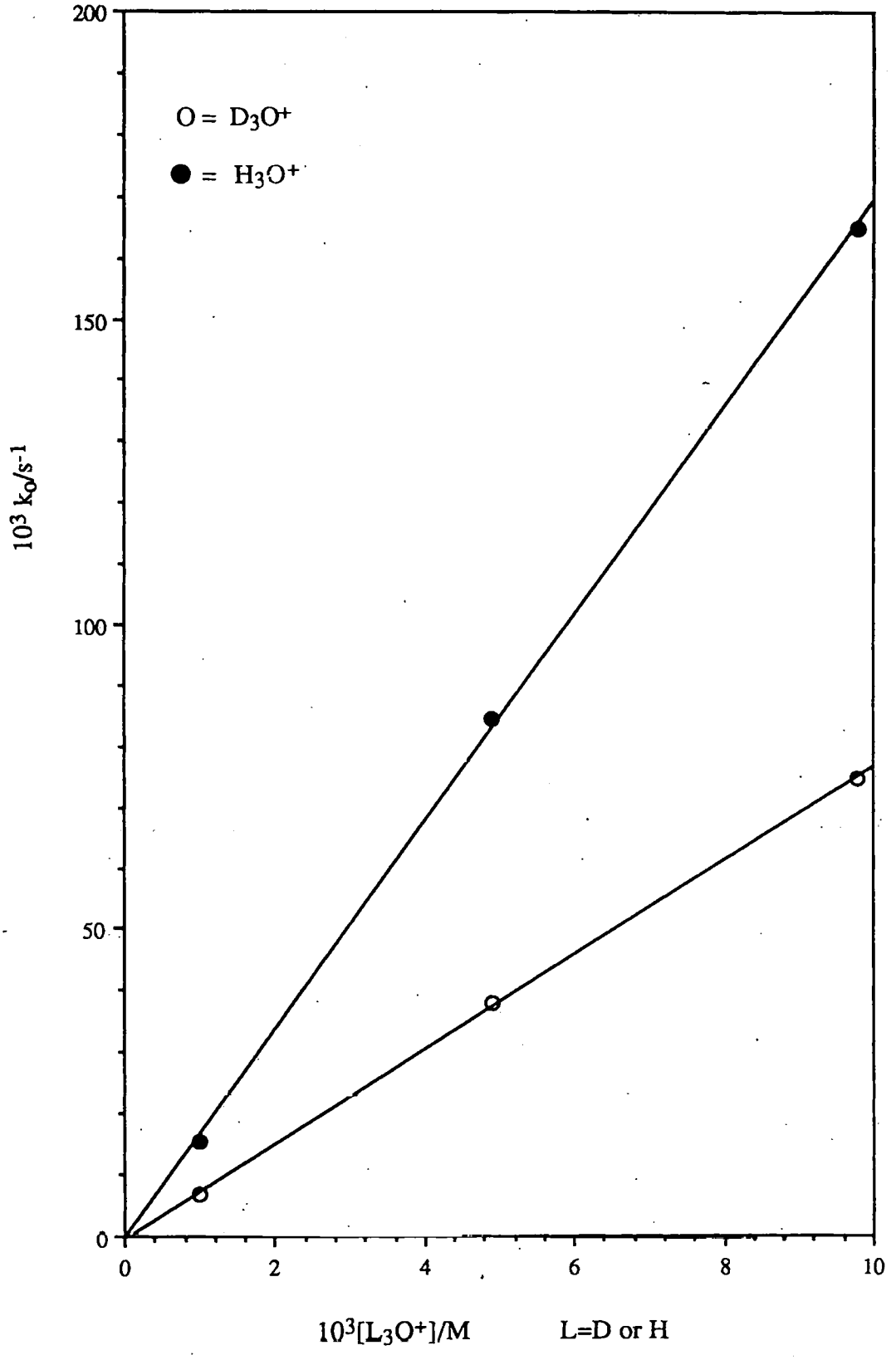

Figure 5.15 Plot of k_o against $[L_3O^+]$ for the decomposition of N_2GlnPheOMe (15) in dilute $DClO_4$ and $HClO_4$ at 25°C.

5.5.5 Effect of added nucleophiles

The effect of added nucleophiles was also briefly studied for the decomposition of N_2GlnPheOMe (15) at 25°C. Thiocyanate and iodide were chosen because they are powerful nucleophiles but generate poor general acid catalysts. Thus sodium thiocyanate and potassium iodide were added to buffer solutions with the ionic strength maintained at μ=0.5 by the addition of $NaClO_4$ and the rates of decomposition compared with those in the absence of NaSCN and KI. The results, summarised in Table 5.13, show no evidence for an additional nucleophilic catalysed decomposition pathway.

Table 5.13 Effects of added nucleophiles on the rate of decomposition of (15). Initial [(15)] = ca 10^{-4}M.

Buffer	[HA]/M	pH	[Nu]M	$10^4 k_o$ no Nu/s^{-1}	10^4 k_o with Nu/s^{-1}
phosphate	0.100	6.59(6.50)	0.01(KI)	-	14.4
	0.075	6.55(6.55)	0.01(KI)	12.0	11.6
	0.05	6.52(6.52)	0.01(KI)	9.46	8.66
	0.025	6.50(6.48)	0.01(KI)	4.82	4.61
	0.00[b]	6.54(6.54)	0.01(KI)	1.57	1.74
phosphate	0.100	6.57(6.50)	0.05(NaSCN)	-	13.8
	0.075	6.55(6.55)	0.05(NaSCN)	12.0	11.4
	0.05	6.52(6.52)	0.05(NaSCN)	9.46	8.07
	0.25	6.50(6.48)	0.05(NaSCN)	4.82	4.46
	0.00[b]	6.54(6.54)	0.05(NaSCN)	1.57	1.25
acetate	0.02	5.14	0.05(NaSCN)	57.1	44.2
	0.015	5.14(5.13)	0.05(NaSCN)	43.7	35.9
	0.01	5.13	0.05(NaSCN)	28.8	25.1
	0.005	5.12(5.13)	0.05(NaSCN)	15.6	13.5
	0.000[b]	5.13	0.05(NaSCN)	1.42	2.44
$HClO_4$	4.9×10^{-3}	2.31	0.05(NaSCN)	850	887

a) pH values in parenthesis refer to pH of solution in absence of nucleophile if different to pH in presence of nucleophilic.

b) Values at [HA]=0 are intercept values from plot of k_o v [HA].

5.5.6 Discussion

The decomposition of the diazodipeptides (15) and (16) in aqueous media at 25°C are characterised by a strong pH dependence, general acid-catalysis, a normal solvent deuterium isotope effect (k_H/k_O = 2.3 at 25°C for N_2GlnPheOMe (15) and the absence of appreciable catalysis by added nucleophiles. All of these factors are consistent with decomposition by an acid-catalysed pathway in which H^+ transfer from the solvent to substrate is rate limiting. This is described by Figure 5.16 and commonly referred to as an $A_{SE}2$ mechanism. It applies to decomposition over the range pH5-1 and is similar to the decomposition mechanism deduced previously for the diazoamino acid esters in aqueous media (Section 4). Because H^+ transfer is rate limiting the kinetic studies reveal nothing about the product forming stage of the reaction. Also, no product studies were carried out.

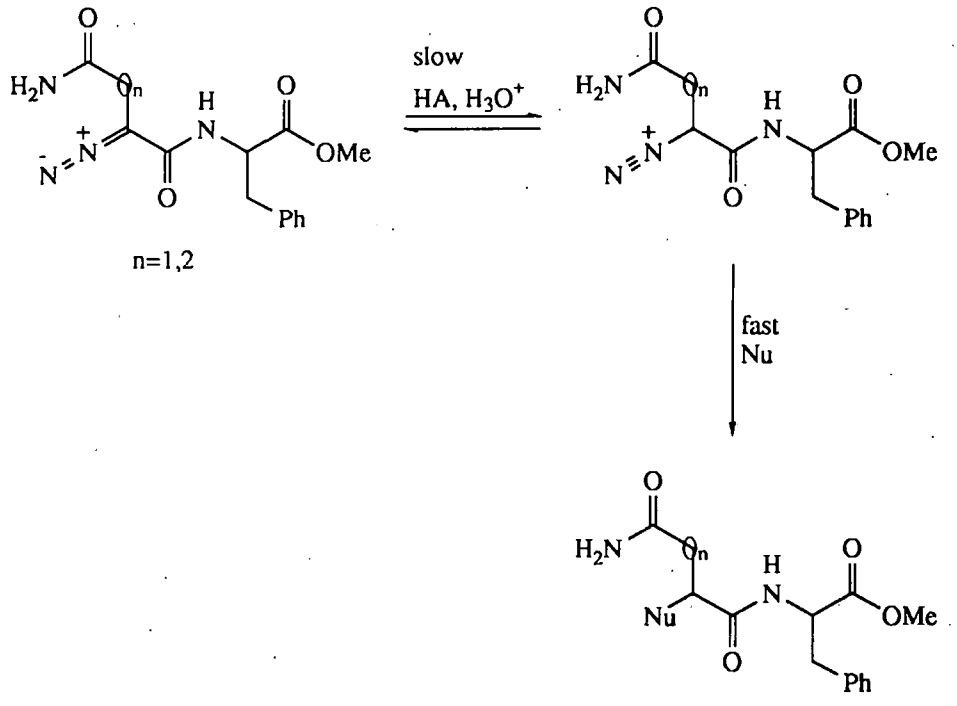

Figure 5.16 A-S_E2 mechanism of decomposition of diazodipeptides in pH range 1-5.

Thus, it is not known, for example, if interactions of neighbouring groups are a factor in the decomposition of the protonated diazodipeptide (15) to products. The

diazopeptides are less stable than the corresponding diazoamino acid esters. Thus, N_2GlnPheOMe decomposes ca 2.6 fold faster than N_2GlnOMe and N_2AsnPheOMe 6.5 fold faster than N_2AsnOMe. These differences relate entirely to the higher basicity of the α-carbon atom because H^+-transfer is rate-limiting. This is consistent with reduced electron withdrawal by the amide moiety relative to an ester moiety.

5.6 Cyclic products from the thermal decomposition of N_2GlnPheOMe (15) and N_2AsnPheOMe (16).

To find evidence for intramolecular interactions, the decomposition of the diazopeptides (15) and (16) were carried out in ethyl acetate at 120°C as described earlier for the diazoamino acid esters. The reactions were followed by HPLC to validate complete decomposition of the substrate and the reaction solutions were then analysed directly by a capillary GLC/MS procedure using both chemical (NH_3) and electron impact ionization techniques.

5.6.1 N_2GlnPheOMe (15)

N_2GlnPheOMe (15) decomposed to give only two products which eluted by GLC although no mass balance was attempted. The two products are identified as peaks (A) and (B) in the GLC mass chromatogram (Figure 5.17). Independent checks established that neither (A) nor (B) decomposed with either water or dilute base.

Examination of the CI and EI mass spectra of (A) and (B) (Figures 5.18, 5.19) suggest these compounds are the two diastereoisomers of the γ-lactone (13). The CI spectra show strong molecular ions at m/z 292 ($M+H^+$) and at m/z 309 $(M+NH_4^+)^+$ but little fragmentation is observed. In both of the EI spectra the second most abundant ion, at m/z 85, is highly characteristic of γ-lactones and is consistent with the proposed structures of (A) and (B). A molecular ion is just discernible in the EI spectra of peak (B) at m/z 291. Stronger ions at m/z 280 and m/z 232 (attributed to the loss of $(MeO)^\bullet$ and $(CO_2Me)^\bullet$ respectively from the molecular ion) are apparent in both the spectra of

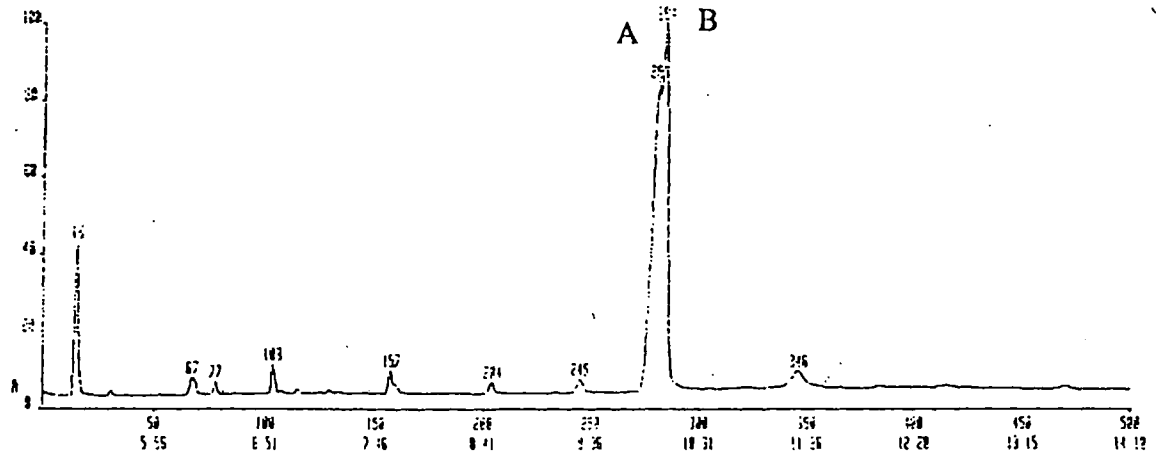

Figure 5.17 *GLC mass chromatogram of reaction mixture from thermolysis of N_2GlnPheOMe (15) in EtOAc.*

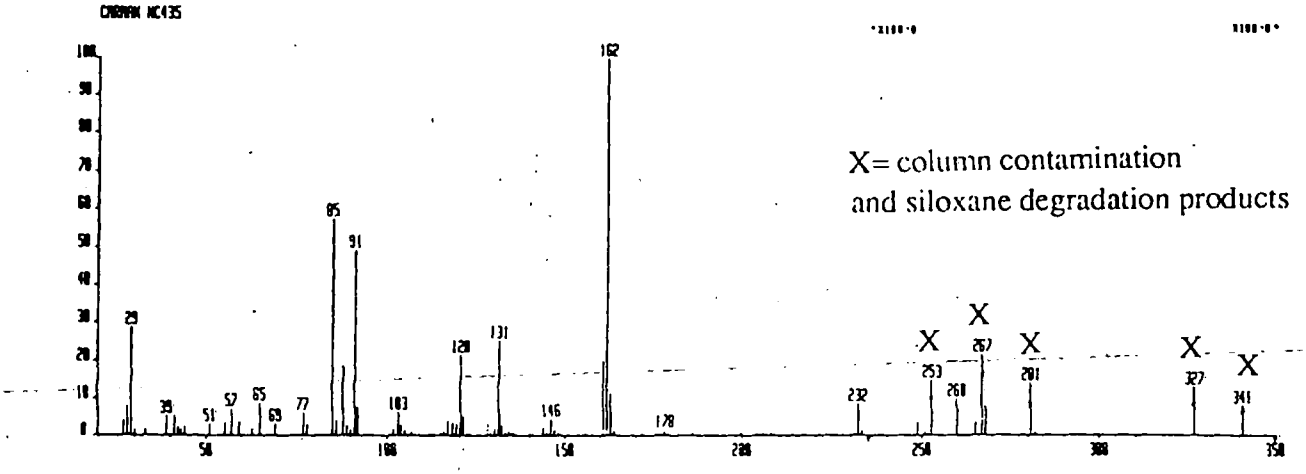

Figure 5.18 *EI mass spectrum of product A from the thermolysis of N_2GlnPheOMe (15) in EtOAc*

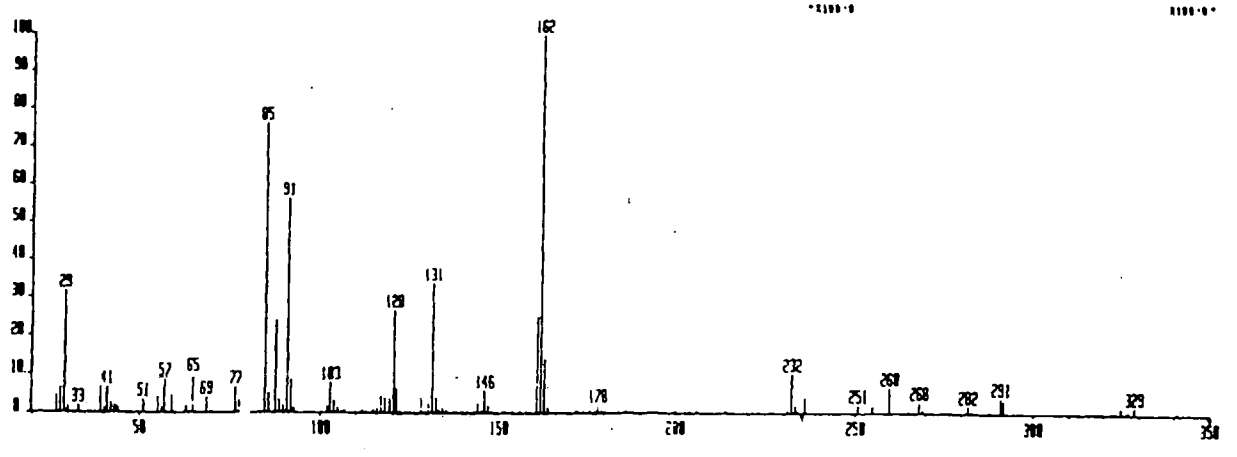

Figure 5.19 *EI mass spectrum of product B from the thermolysis of N_2GlnPheOme (15) in EtOAc*

(A) and (B). These suggest the methyl ester is present in both products. The base peak, in both spectra, at m/z 162 is a fragment ion of the phenylalanine methyl ester group, probably arising from a McLafferty rearrangement in which the charge is retained on the alkene fragment. Ions at m/z 131 and m/z 103 relate to the loss of $(MeO)^{\bullet}$ and $(CO_2Me)^{\bullet}$, respectively from the m/z 162 fragment and both are apparent for (A) and (B). The ion at m/z 120 is also characteristic of phenylalanine methyl ester residue, formed in two stages by elimination of a ketone and the carboxymethyl radical. Further fragmentation of the ion at m/z 85 leads to peaks at m/z 57 (loss of CO), m/z 41 (loss of CO_2), m/z 39 ($C_3H_3^+$) and m/z 29 (CHO^+). These fragmentations are all summarised in Figure 5.20. It is most unlikely that the γ-lactone (13) results from transformations in the source of the mass spectrometer because its open chain hydroxy acid precursor would not readily migrate on the GLC column. Therefore, the two products (A) and (B), which correspond to the γ-lactone (13) can only arise by an intramolecular cyclisation involving the amide O-atom to give an intermediate imidate (18) followed by hydrolysis to the γ-lactone (13) (Figure 5.21). Due to the hygroscopic nature of N_2GlnPheOMe (15), there was probably sufficient water in solution to bring about this hydrolysis.

It is interesting to note that both diastereoisomers are formed in the reaction in approximately equal ratios. This is entirely consistent with a planar structure of the diazodipeptide substrate (15).

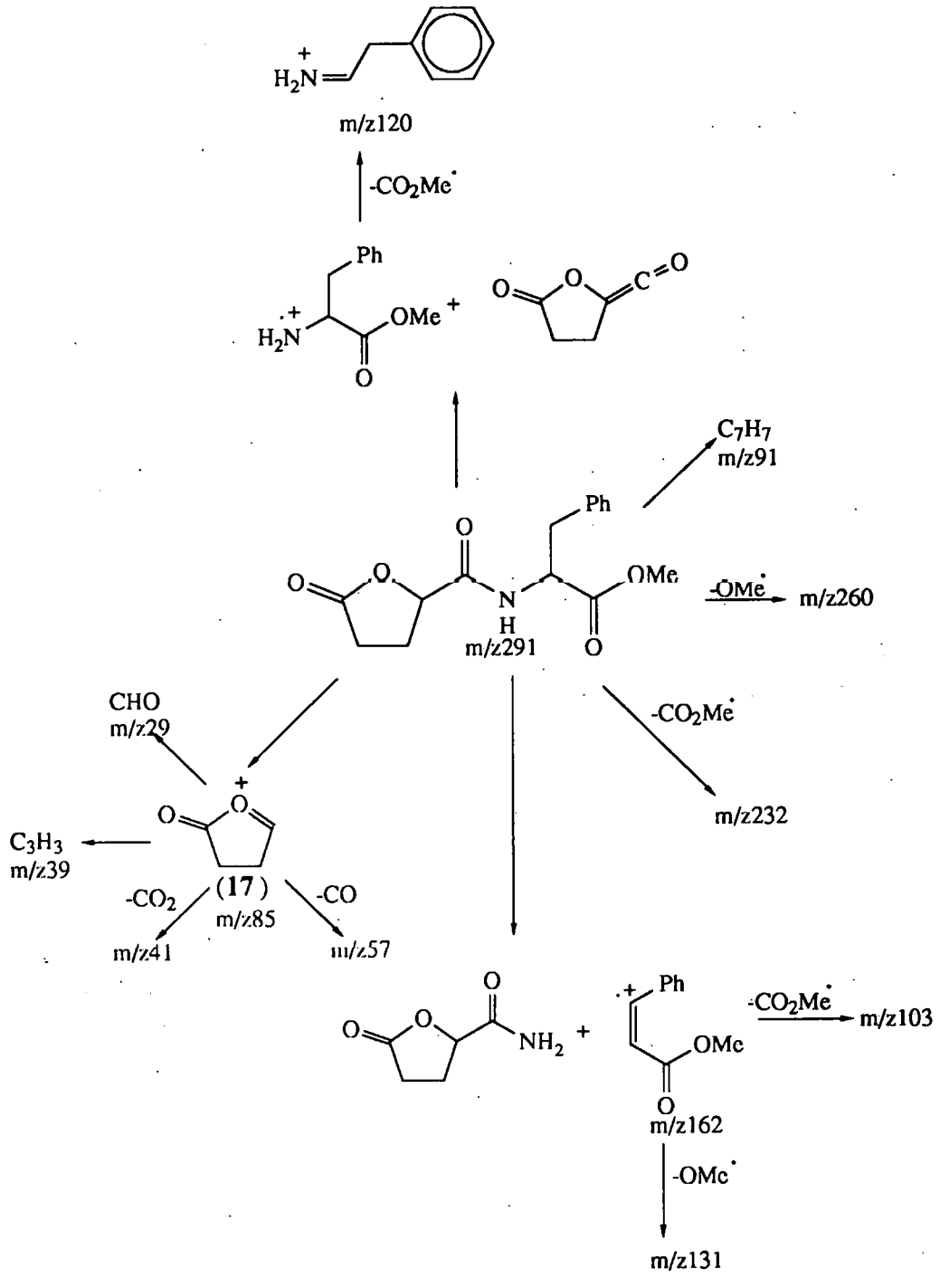

Figure 5.20 Rationalisation of the fragmention observed in the EI mass spectra of products A and B from the thermolysis of N_2GlnPheOme (15) in EtOAc

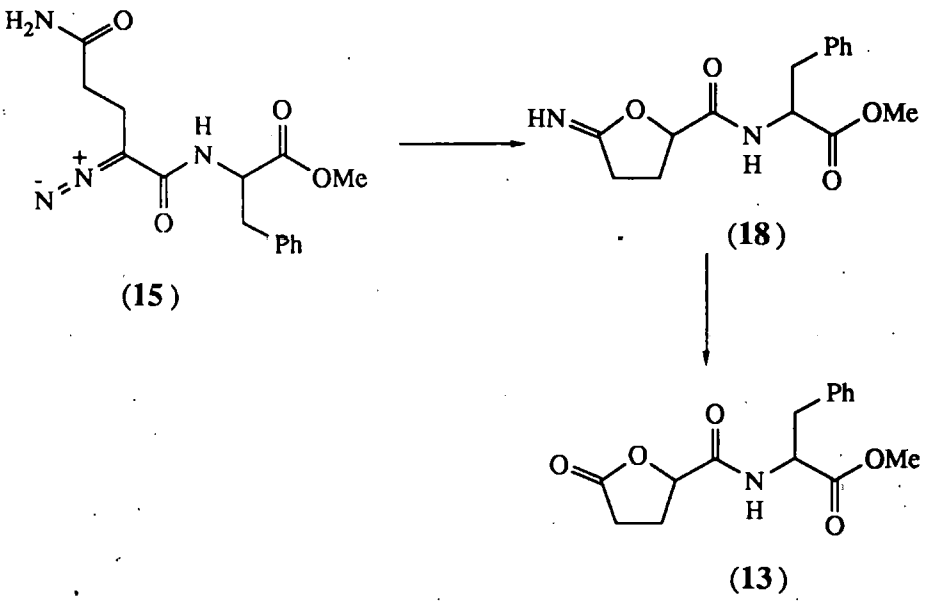

Figure 5.21 Formation of γ-lactone (13) from N_2GlnPheOMe (15)

There was no evidence in the mass chromatogram of the γ-lactam (19), which is expected to migrate along the GLC column. There was also no evidence of the β-elimination product (20) but this cannot be ruled out as a possible decomposition product since it is not known if this compound would migrate on a GLC column.

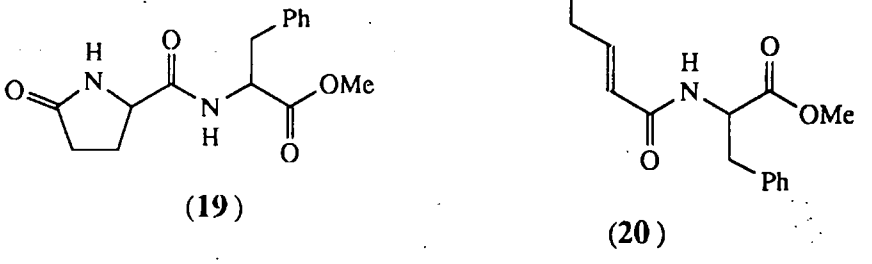

5.6.2 N_2AsnPheOMe

The products formed by the thermal decomposition of N_2AsnPheOMe (16) were more complicated than for N_2GlnPheOMe (15) partly because transformations occurred on storage of the sample prior to GLC/MS analysis. The GLC mass chromatogram (Figure 5.22) shows three major products as peaks (C), (D) and (E) and a fourth peak (F) which appears on standing. Again no mass balance was attempted.

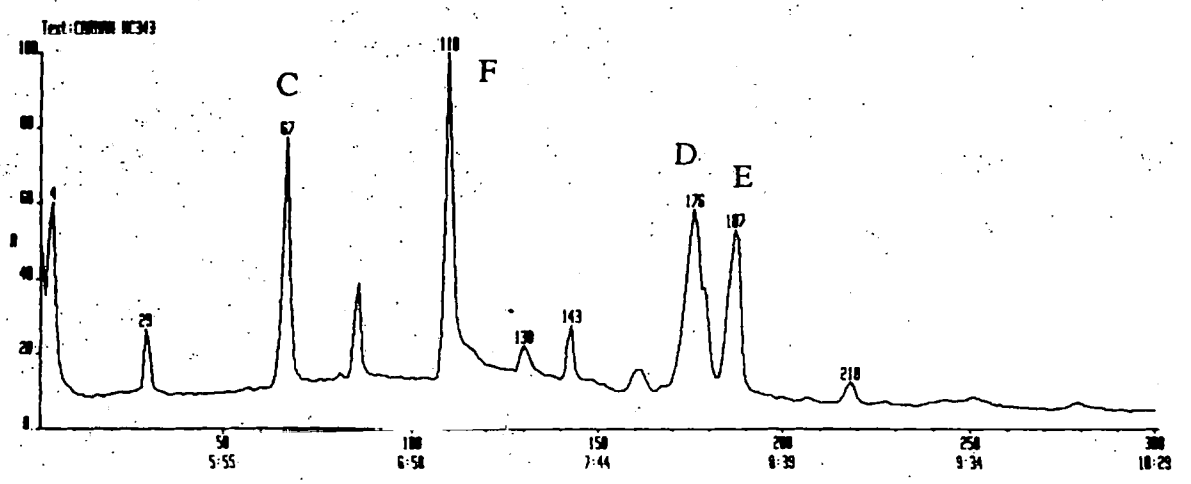

Figure 5.22 *GLC mass chromatogram of reaction mixture from the thermolysis of N_2AsnPheOMe (16) in EtOAc*

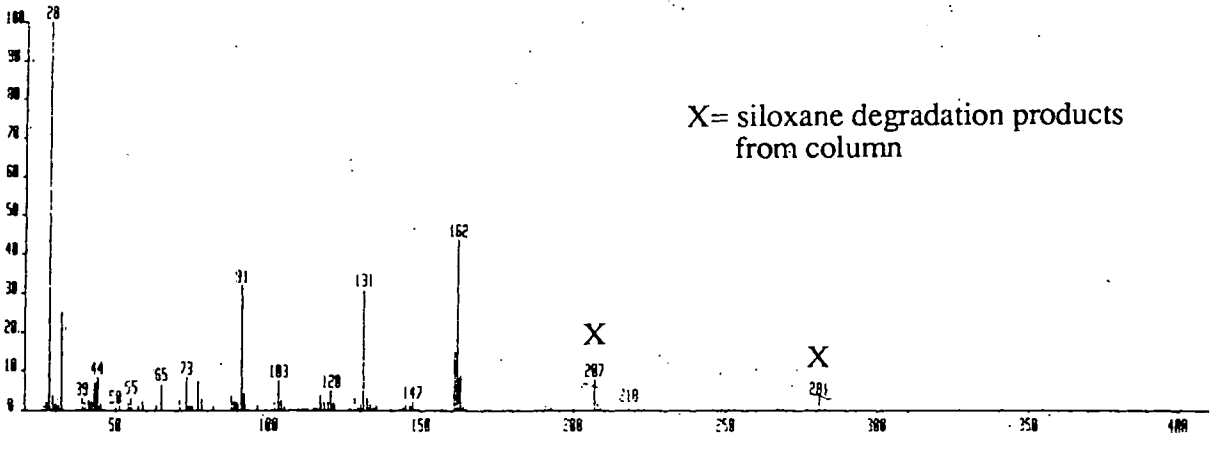

Figure 5.23 *EI mass spectrum of product D from the thermolysis of N_2AsnPheOMe (16) in EtOAc*

Peak (D) relates to the β-lactone (14) and this was confirmed by comparison of both retention times and fragmentation of an authentic sample of (14). The CI (NH_3) mass spectrum shows strong molecular ions at m/z (278) ($M+H^+$) and m/z 295 ($M+NH_4^+$). The major fragmentation in the EI mass spectrum (Figure 5.23) relates to the phenylalanine residue but there is a very weak ion at m/z 71 corresponding to the ion (21), consistent with the structure (14).

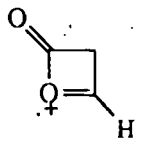

(21)

Product (C) has been identified as N-acetylphenylalanine methyl ester by comparison of both the retention times and mass spectrum with those of an independently prepared authentic sample. The CI (NH_3) mass spectrum shows a strong molecular ion at m/z 222 ($M+H^+$). Ions at m/z 162, 91, 120, 131 and 103 in the EI spectrum, are consistent with the phenylalanine methyl ester moiety (see Figure 5.20) whilst a strong ion at m/z 88 (22) is consistent with the elimination of ketene and a benzyl radical from the molecular ion. The ion at m/z 43 (CH_3CO^+) is also characteristic of an acetyl group.

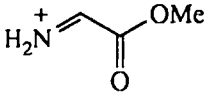

(22)

The formation of N-acetylphenylalanine methyl ester can be rationalised from the Wolff type rearrangement of the α-lactam intermediate (23) (Figure 5.24). The formation of the α-lactam (23) has already been proposed as an intermediate step in the formation of the β-lactone (14) from L-aspartylphenylalanine methyl ester (*cf* 2.2) and is also believed to be an intermediate in the formation of imino dialkanoic acids from diazodipeptides.[82] Subsequent ring opening of the α-lactam forms the succinimide derivative (24) which then eliminates maleimide to form phenylalanine methyl ester. The phenylalanine methyl ester reacts with the solvent to form the N-acetyl derivative.

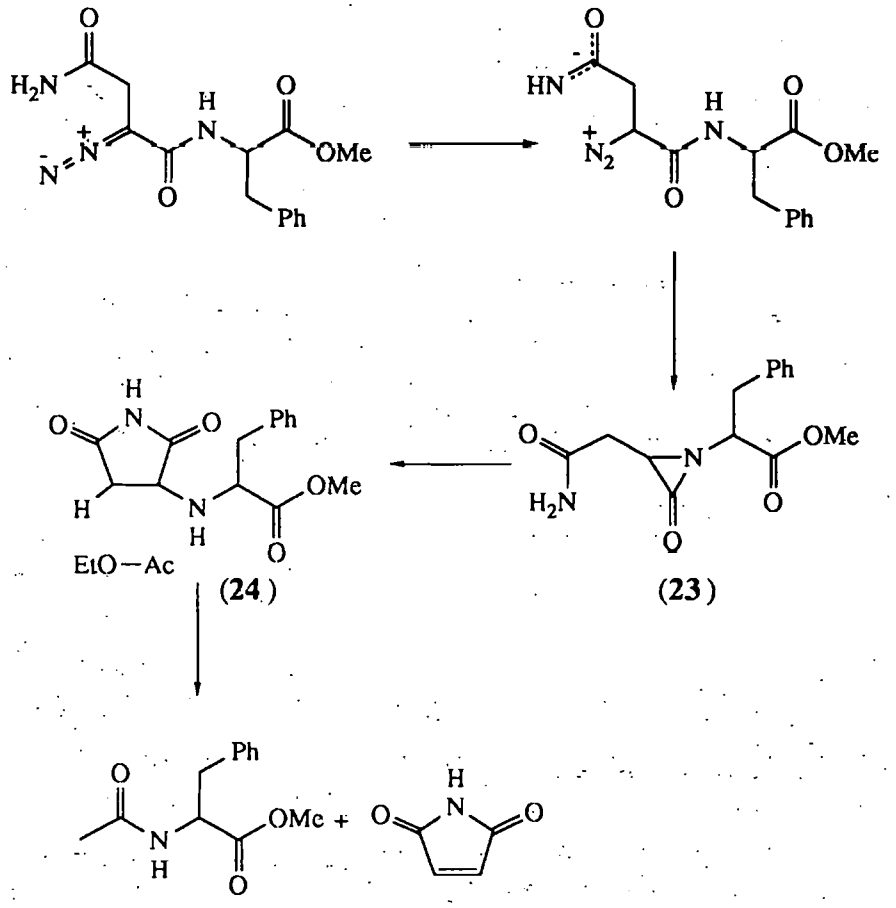

Figure 5.24 Formation of N-acetylphenylalanine methyl ester from thermolysis of N_2GlnPheOMe (16).

Maleimide was not, however, observed in the reaction solution, but it may have eluted during the solvent void and no further attempts were made to analyse for it.

The structure of product (E) has not been deduced. It has a ($M+H^+$) ion 44 mass units higher than the β-lactone (14) at m/z 322 in the CI mass spectrum and Figure 5.25 shows the EI mass spectrum of (E). The fragment at m/z 279 is consistent with the elimination of ketene from the molecular ion and the ion at m/z 43 corresponds to (CH_3CO^+). Both fragmentations suggest the addition of an acetyl moiety to the β-lactone product (14). There is good evidence that the phenylalanine methyl ester residue of the diazodipeptide is retained and the enhanced fragment ion at m/z 120 suggests that the proton α to the CO group of the peptide amide of the product (E) is more acidic.

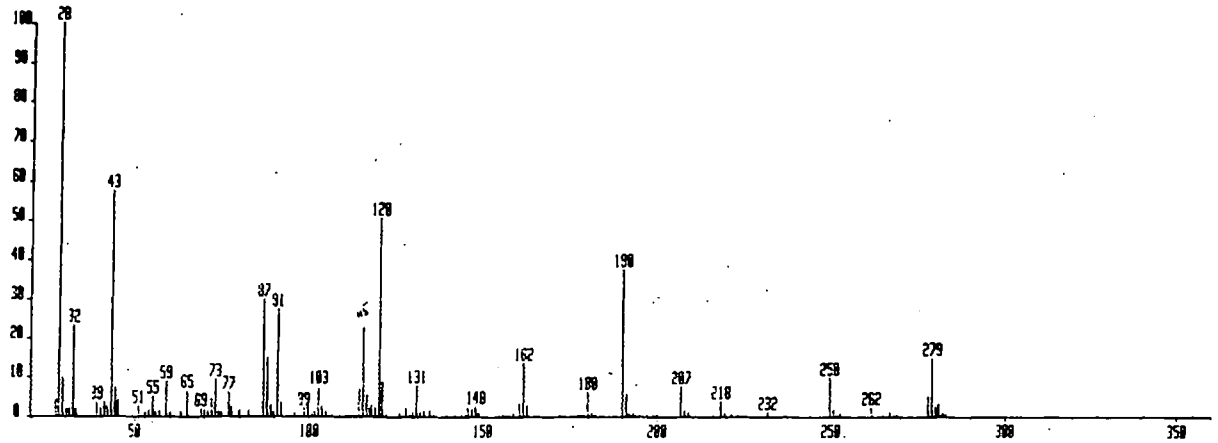

Figure 5.25 EI mass spectrum of product E from the thermolysis of N_2AsnPheOMe (16) in EtOAc.

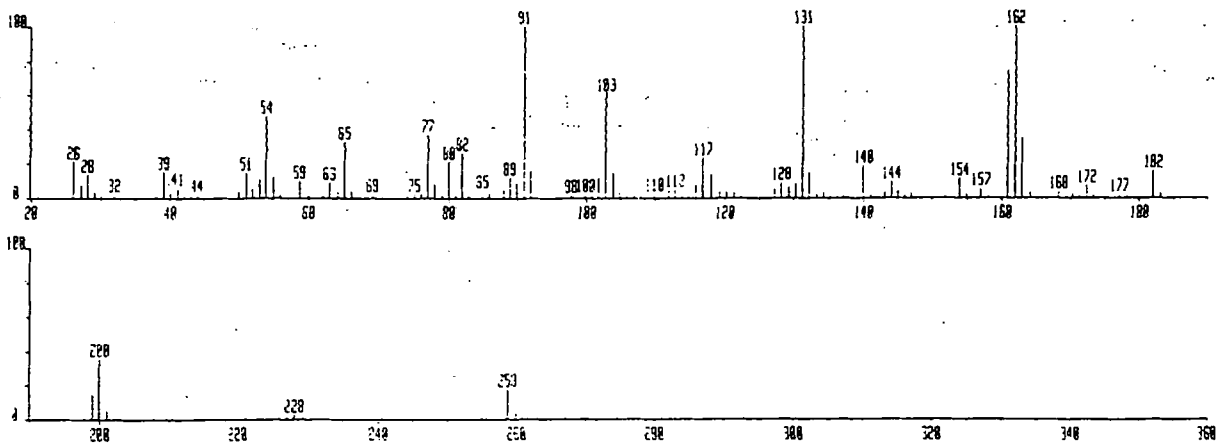

Figure 5.26 EI mass spectrum of compound F observed in the thermolysis reaction mixture of N_2AsnPheOMe (16) in EtOAc

The $(M+H^+)^+$ of 322 suggests that (E) contains a single N-atom which implies loss of both the diazo and the side chain amide N-atoms. This points to a transformation of the β-lactone product (14) involving acylation by ethyl acetate solvent. Unfortunately, neither the concentration relationships between (D) and (E) nor thermal decomposition in another solvent were investigated. The product (E), however, was not present in an authentic sample of (14) either when freshly prepared or after several weeks at ambient temperature.

Peak (F) was not present in the chromatogram immediately after thermal decomposition of N_2AsnPheOMe (12), but appeared on storage at -30°C. Further, it was also not present in a freshly prepared sample of the authentic β-lactone (14) but did appear on standing, both as the pure solid and in solution. This implies that compound (F) is a decomposition product of the lactone (14). The CI mass spectrum suggests that the molecular ion $(M+H^{+^+})$ for (F) is m/z 266 ie. 18 mass units less than that of (14). Compound (F) also shows fragment ions in the EI spectrum at m/z 162, 131 and 103 (Figure 5.26) which is consistent with the presence of the intact methyl ester and benzyl moieties and the presence of a carbonyl group able to engage in the McLafferty rearrangement. Thus, the loss of an 18 amu fragment must relate to the β-lactone containing portion of product (F). A possible explanation for this transformation is outlined in Figure 5.27. This requires interaction of the peptide N-atom with either the β-lactone carbonyl moiety, to give (25), or the alkyl C_4 atom to give the α-lactone (26). Dehydration of both (25) and (26) would give the maleimide derivative (27), tentatively identified as the peak (F). A rationale for this reaction would be a considerable reduction in ring strain. Structure (27) is consistent with other aspects of the mass spectrum found for peak (F). Thus, the absence of fragment ion at m/z 120 ($N{=}CHCH_2Ph$) is consistent with the presence of a tertiary N-atom and the higher abundance of the fragment at m/z 162 reflects the formation of a stable maleimide fragment in addition to the charged cinnamic acid methyl ester. Further, ions at m/z 69, 54 and 26 are consistent with the maleimide moiety.

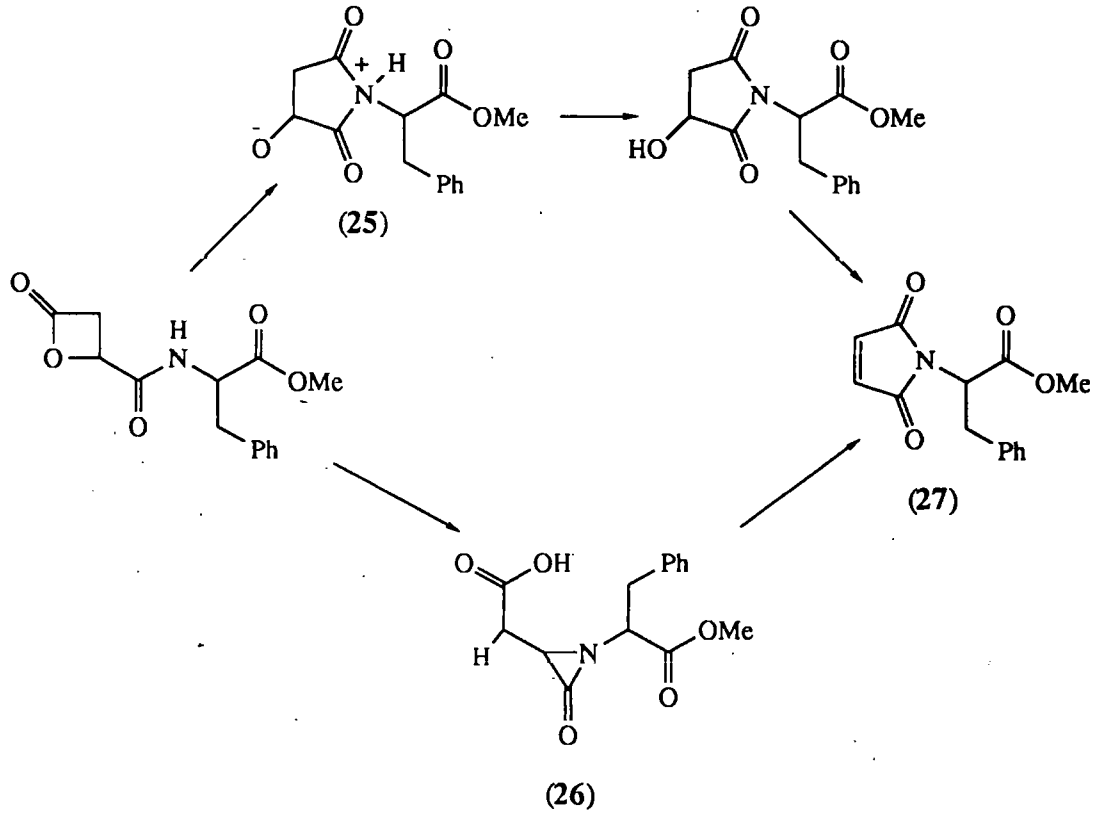

Figure 5.27 Formation of maleimide (25) from β-lactone (14)

5.6.3 Discussion

The thermal reactions of the diazodipeptides parallel closely those of the diazoamino acids. There is clear evidence from the product analyses that the carboxamide side chains of N_2GlnPheOMe (15) and N_2AsnPheOMe (16) are involved in intramolecular cyclisation reactions. Further, cyclisation occurs on the O-atom of the amide moiety forming an imidate which hydrolyses to the observed lactone products. In the case of N_2GlnPheOMe, the only products observed are the two diastereoisomers of the γ-lactone (13). Four products are formed in the thermal reaction of N_2AsnPheOMe. The major product is the β-lactone (14). One of the products (F) has been demonstrated to be a decomposition product of the β-lactone (14) and the third compound (E) is also believed to result from a decomposition of the β-lactone since the side chain amide group must have been hydrolysed as the molecular ion indicates that only one N-atom is present in the molecule. The fourth product has been identified as N-acetyl

phenylalanine methyl ester and can be rationalised as resulting from a secondary reaction of an intermediate in the formation of (14).

Unfortunately, in the absence of a material balance it is not possible to ascertain whether O-alkylation represents the major product forming pathway. There is no evidence of any lactam products resulting from N-alkylation. In view of the fact that 5-methyl-2-pyrrolidone-5-carboxylate and 4-methyl-azetidin-2-one-4-carboxylate have similar chromatographic properties to the analogous lactones (Section 7.3.7.1) the dipeptide lactams would, reasonably be expected to have similar properties to the lactones and therefore to migrate on the GLC column under the experimental conditions used. There was also no evidence of products resulting from the β-elimination of nitrogen (Figure 5.28).

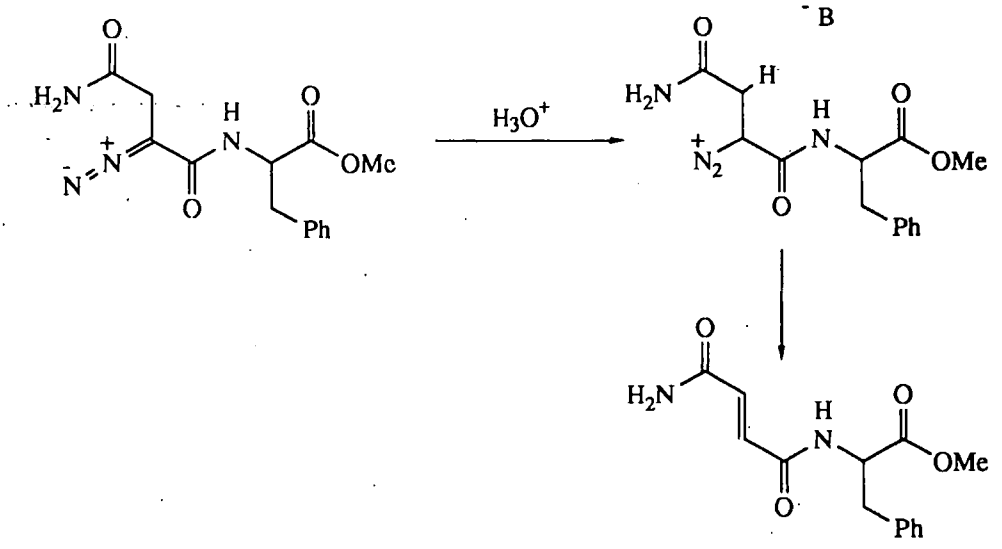

Figure 5.28- β-elimination from N_2AsnPheOMe

Although it can be argued that these reactions will not proceed thermally in an aprotic solvent as a separate proton source is required to generate the diazonium ion and a suitable base is required to initiate the elimination reaction, they also cannot be eliminated as potential reaction products since their chromatographic properties are not known.

CHAPTER 6 SUMMARY OF CHAPTERS 4 AND 5

6 SUMMARY OF CHAPTERS 4 AND 5

6.1 Introduction

Results reported in Chapters 4 and 5 concern the synthesis, properties, stabilities and reactivities of 4 new diazo derivatives of glutamine and asparagine. Particular regard is given to intramolecular cyclisation reactions which are of relevance to a wider study of the causal role of gastric nitrosations in human cancers.

Several methods of preparing L-glutaminyl and L-asparaginyl dipeptides were assessed. The results show that the diphenyl phosphoryl azide reagent offers a convenient, high yielding (>90% as the N-α-carbobenzyloxy derivatives), one-pot synthesis of the simple dipeptides L-glutaminyl-L-phenylalanine methyl ester and L-asparaginyl-L-phenylalanine methyl ester without racemisation.

A brief kinetic study of the nitrosation of glutamine and asparagine in 0.1M HCl at 37°C showed similar rates to glycine ethyl ester indicative of no significant nitrosation of the carboxamide moiety. The relative rates correlated qualitatively with the concentration of free base in solution (pKa).

The diazoamino acid esters and diazodipeptides were synthesised by aprotic nitrosation using N_2O_4. The diazoamino acids methyl 2-diazo-4-carbamoyl-butanoate (N_2GlnOMe) and methyl 2-diazo-3-carbamoylpropanoate (N_2AsnOMe) were obtained as yellow crystalline solids in 40% yield. The diazodipeptides N-(2-diazo-4-carbamoylbutanoyl)-L-phenylalanine methyl ester (N_2GlnPheOMe) and N-(2-diazo-3-carbamoylpropanoyl)-L-phenylalanine methyl ester (N_2AsnPheOMe) were obtained as yellow hygroscopic solids in yields of 23 and 16% respectively.

6.2 Stability in protic media

The stabilities of the 4-diazocompounds in aqueous buffers (μ=0.5, $NaClO_4$) and dilute $HClO_4$ were investigated at 25°C. All decomposition reactions were first-order

in [substrate] (Equation 6.1), with a strong dependence on both the pH and the presence of general acid catalysts and showed normal deuterium solvent isotope effects (k_H/k_D). The values of k_H and k_H/k_D at 25°C are summarised in Table 6.1.

$$\text{Rate} = \{k_H[H_3O^+] + k_{HA}[HA]\}\,[\text{Diazocompound}] \qquad \ldots.(6.1)$$

Table 6.1 Values of k_H and k_H/k_D for the diazocompounds at 25°C

Diazocompound	$k_H/M^{-1}s$	k_H/k_D
N_2GlnOMe	6.06	2.31
N_2AsnOMe	2.81	2.05
N_2GlnPheOMe	17.6	2.30
N_2AsnPheOMe	18.4	-

A Brønsted plot of log k_{HA} against -pKa for the decomposition of N_2GlnOMe was linear with a gradient α=0.62 and the decomposition of N_2GlnPheOMe was not subject to nucleophilic catalysis by either I^- or SCN^-. All of these results are consistent with an acid catalysed A-S_E2 decomposition pathway in which the rate-limiting step is proton transfer to the diazocompound (Figure 6.1). The greater reactivity of N_2GlnOMe over N_2AsnOMe,

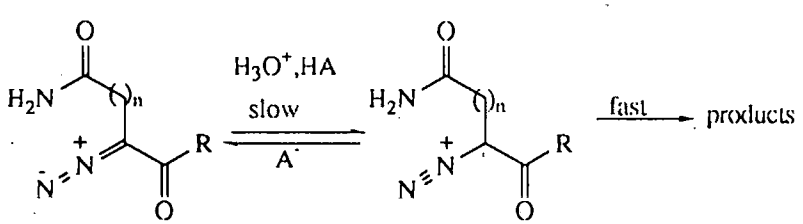

n=1,2
R=OMe, PheOMe

Figure 6.1 A-S_E2 decomposition of diazocompounds

and the diazodipeptides over the diazoamino acid esters may be attributed to the increased basicity of the α-carbon atom.

As proton transfer is rate determining, no kinetic information is available for the subsequent product forming reactions of the diazonium ions and therefore the role of the neighbouring group interactions. These questions were therefore addressed by product studies. In HCl at 0°C, the major decomposition pathway for the diazoamino acid esters (ca. 30% in the case of N_2GlnOMe) involved intramolecular trapping of the diazonium ion by the O-atom of the carboxamide moiety to give a cyclic imidate ester product. In the case of N_2GlnOMe, this imidate ester hydrolysed to methyl pyrolidin-2-one-5-carboxylate (1), whilst for N_2AsnOMe, the imidate ester was observable. There was no evidence, for either substrate, of cyclisation at the amide N-atom to give the thermodynamically favoured lactam products. Thus, cyclisation in protic solvents is subject to kinetic control, reflecting the enhanced stability of the O-alkyl transition state due to resonance delocalisation of the N-lone pair electrons. Products, probably resulting from a β-elimination pathway, were observed for N_2AsnOMe but not for N_2GlnOMe. Although not investigated in this study, it is assumed that the remaining products can be accounted for by intermolecular nucleophilic trapping of the diazonium ion (eg. with H_2O and Cl^-). These results are summarised in Figure 6.2.

The reactions of the diazodipeptides in protic solvents were not investigated, but studies in aprotic solvents and results in the literature for analogous reactions of glutamic acid and glutaminyl peptides[92] suggest products similar to those for diazoamino acid esters.

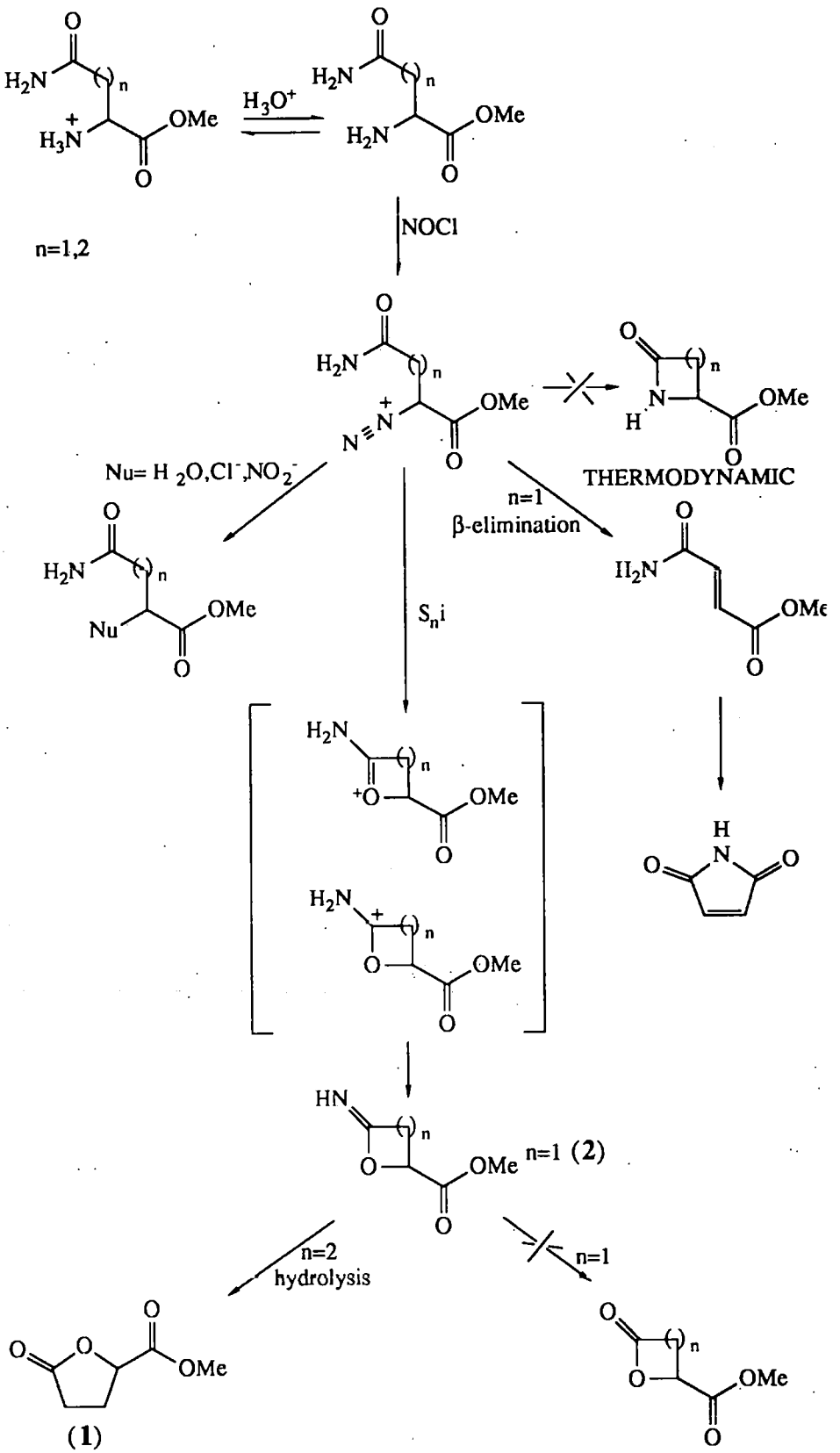

Figure 6.2 Reactions of diazoamino acids in protic solvents.

6.3 Thermal decomposition in aprotic media

In aprotic solvents the major observed thermolytic decomposition pathway involved intramolecular cyclisation on the O-atom of the carboxamide side chain to initially form cyclic imidates. Subsequent tautomerisation of these imidates was observed, together with some adventitious hydrolysis to the β-and γ-lactones (Figure 6.3). Further products, resulting from the decomposition of the β-lactone (2) derived from hydrolysis of the cyclic imidate, were observed in the reaction mixture of N_2AsnPheOMe after thermolysis.

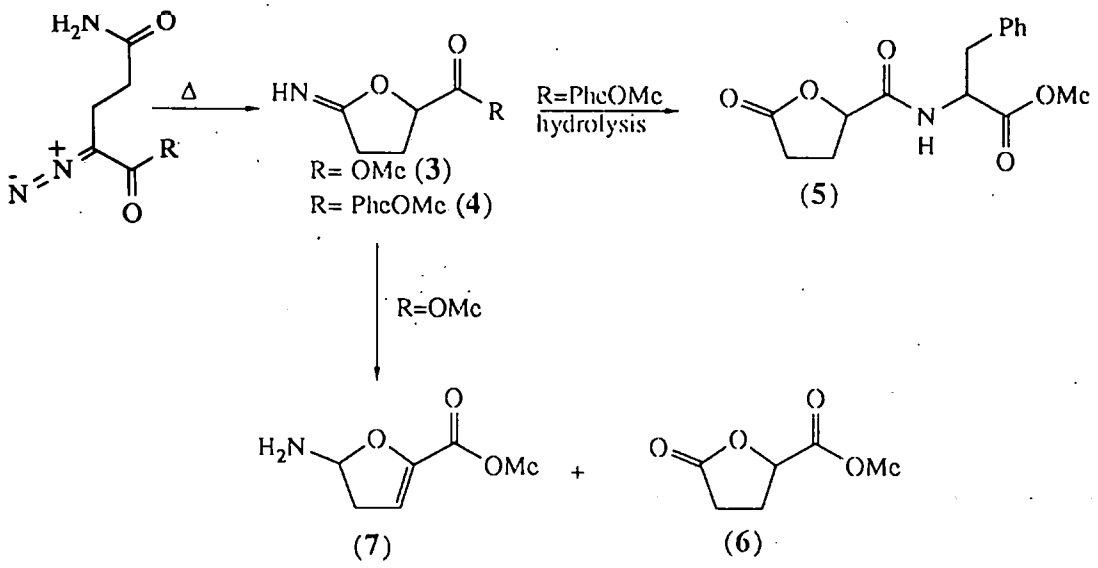

Figure 6.3 Thermal reaction of N_2GlnOMe and N_2GlnPheOMe in EtOAc

N-Acetylphenylalanine methyl ester and the N-substituted maleimide were observed. Proposed mechanisms for their formation are shown in Figure 6.4. A third component was also observed, but its structure could not be completely elucidated.

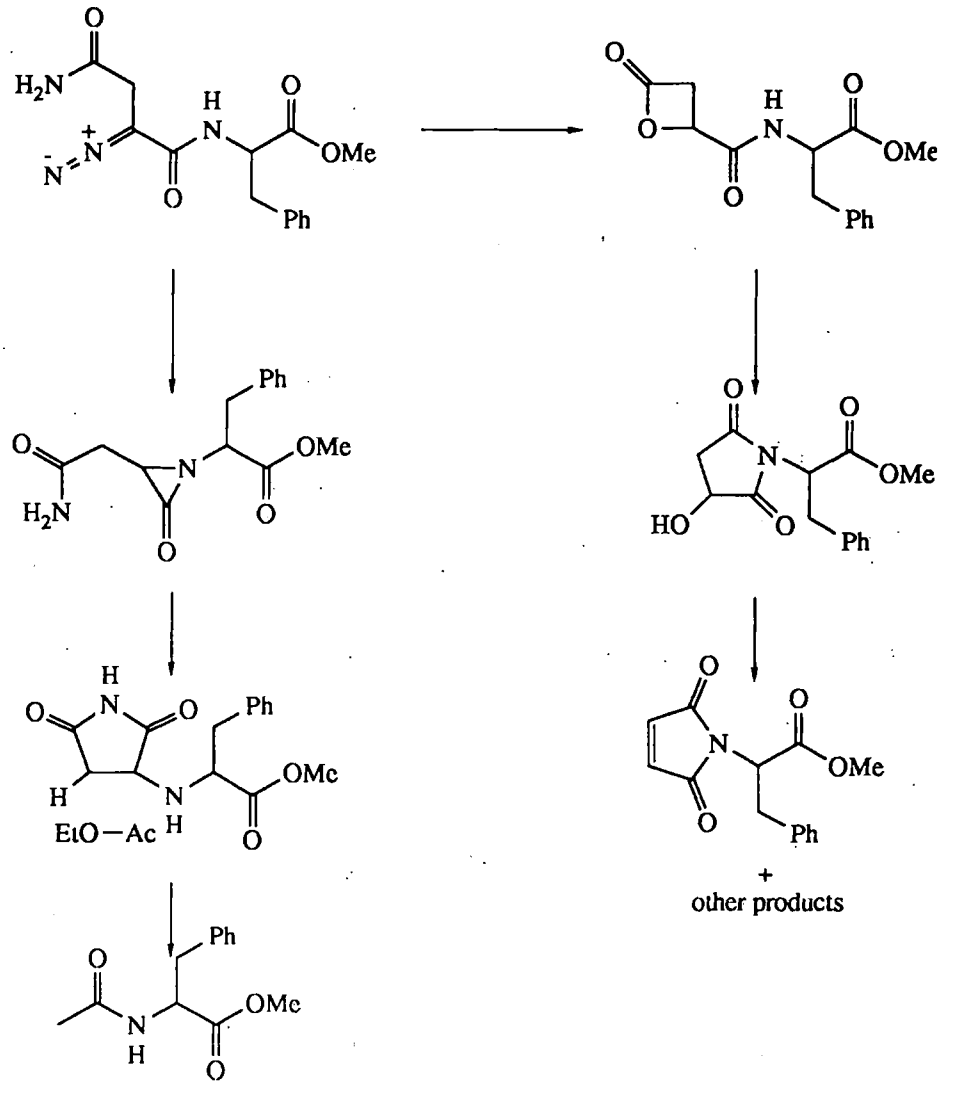

Figure 6.4 Decomposition of N_2AsnPheOMe in EtOAC

β-Lactams and γ-lactams resulting from N-alkylation, alkenes derived from β-elimination (including maleimide) and products resulting from the possible reactions of a carbene intermediate (including the Wolff rearrangement) were not observed, although in some instances these cannot be discounted since standards were not available for all possible reaction products.

Several mechanisms can be proposed for the formation of the observed products.

1. Water, absorbed by the diazocompounds, particularly the hygroscopic peptides, acts as the proton source to generate the diazonium ion. This may be discounted since

it is unlikely that there would be sufficient water present in the organic phase to bring about rapid protonation.

2. Reaction *via* a singlet carbene negates the need for a proton source (Figure 6.5).

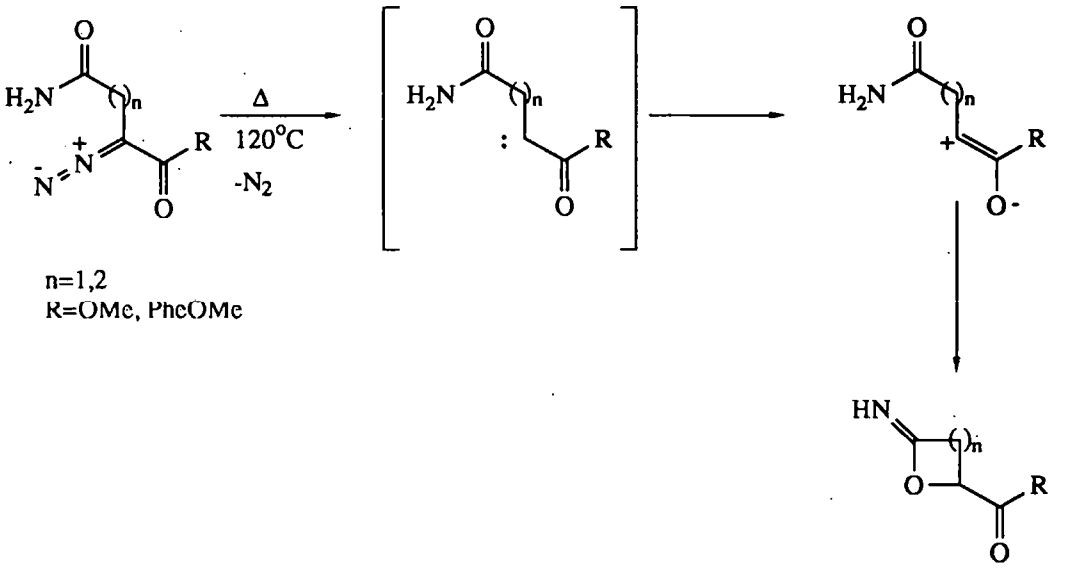

Figure 6.5 Carbene pathway for imidate formation.

However, there is no evidence of other reaction products which may be expected from the highly reactive carbene intermediate (eg. products arising from the Wolff rearrangement which is well documented for diazo esters and ketones[23,60,61]) and this mechanism is considered unlikely.

3. Another pathway overcoming the need for a proton source would involve the initial formation of the triazene structure (12) (Figure 6.6) with subsequent extrusion of nitrogen to form the amide anion and carbonium ion, which then cyclise. Triazene formation is known for the nitrosation of arylamines bearing an ortho carbamoyl group, but their subsequent decomposition is usually acid catalysed and therefore this mechanism was not favoured.

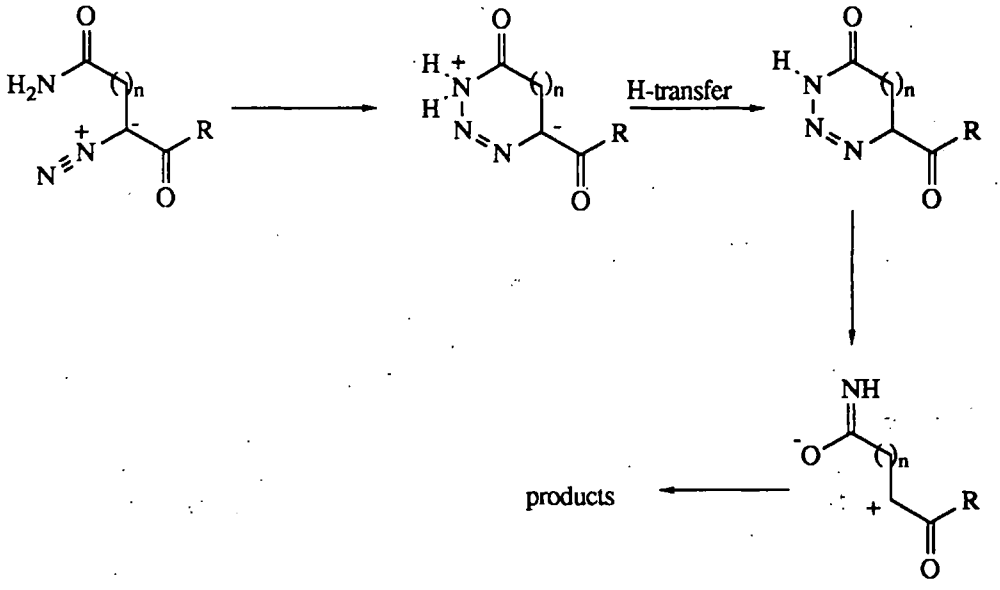

Figure 6.6 *Cyclisation of diazoasparaginyl and diazoglutaminyl compounds via a triazene.*

4. An intramolecular proton transfer from the carboxamide side chain to the α-C-atom, generating both the amide anion and diazonium ion with subsequent reaction on the amide O-atom under charge controlled conditions (Figure 6.7), is a fourth possible pathway by which the reaction may occur. It is reported that the O-atom of an amide anion carries the greatest negative charge[157] and the diazo moiety is sufficiently basic to abstract a proton from water, hence the spontaneous hydrolysis reaction. The pK_a of the carboxamide groups of glutamine and asparagine are not known but may be expected not to differ greatly from that of acetamide ($pK_a \sim 15$). Therefore such a reaction would appear likely and this mechanism is considered to be the most appropriate for the decomposition of the diazocompounds in aprotic solvents.

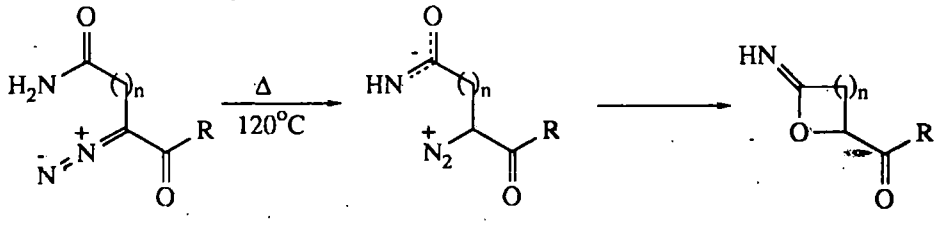

n=1,2
R–OMe, PheOMe

Figure 6.7 *Cyclisation via an amide anion.*

6.4 Toxicity

Very little is known about the mutagenicity of diazo amino acids and peptides other than glycyl compounds, which have proved to be powerful mutagens.[15,16,107] There is currently insufficient data available to draw any conclusions about structure activity relationships in the toxicity of diazo amino acids and peptides. This work has shown that diazo asparaginyl and glutaminyl compounds decompose to give cyclic products, which in the case of asparagine may prove to be mutagenic since this too can also act as an alkylating agent. Further work in trying to elucidate the potential risk posed by *in vivo* nitrosation of peptides should not only include thorough biological testing of the diazocompounds themselves but also any decomposition products which may act as stabilised alkylating agents. A full risk evaluation must also consider the quantities of these products formed under gastric conditions.

CHAPTER 7 EXPERIMENTAL

7 EXPERIMENTAL

7.1 General reagents and instrumentation

Regular laboratory reagents were obtained from commercial sources and where necessary purified using standard procedures. HPLC grade solvents (May and Baker) and amino acids and peptides (Aldrich Chemical Company Ltd and Sigma Chemical Company Ltd) were used as supplied. Dinitrogen tetroxide or nitrogen dioxide was obtained from BOSG and was also used without purification.

Stock buffer solutions were prepared gravimetrically in distilled water from Analar grade reagents. Working buffer solutions were then prepared by volumetric dilution of the stock solutions and where necessary, their ionic strength was adjusted with Analar $NaClO_4$.

Standard $HClO_4$ solutions were prepared from Analar reagent (either 60 or 70% w/w) by volumetric dilution and were assayed by titration against aqueous NaOH, itself standardised against AVS HCl using a phenyl red indicator. Deuterio perchloric acids were prepared from concentrated $HClO_4$ (70% w/w) by dilution with D_2O (n_D=0.999). The solutions were then standardised as for $HClO_4$ and stored in tightly stoppered flasks. The diluted $DClO_4$ solutions contained n_D>0.990.

The physical properties of compounds were evaluated on the following instruments. ^1H- and ^{13}C-nmr spectra were recorded on a Jeol FX-90Q 90 MHz multinuclear spectrometer using Me_4Si as the internal reference. ^1H-400MHz nmr spectra were recorded at the SERC nmr centre, University of Warwick.

Mass spectra were recorded on a VG20-250 quadrupole instrument equipped with an Ion Tech fast atom bombardment (FAB) gun, and a Hewlett Packard 5900A gas chromatograph. FAB ionization, with argon gas, was used for the analysis of amino acids, peptides and their derivatives. Usually, dry glycerol was used as the matrix although less nucleophilic matrices (eg. tetraethyleneglycoldiethyl ether (TEGDE)) were

used for labile compounds. Electron impact (EI) and chemical ionization (CI) (with NH_3) techniques were employed where compounds gave poor FAB spectra and for GLC separations. FAB accurate mass measurements were made on a Kratos MS 80 RFA spectrometer with a resolving power of 3000: ionization was by a xenon ion beam and polyethylene glycol (200) was used both as the matrix and for the calibration.

Infra red spectra were recorded on either a Perkin Elmer 1710 fourier transform (FT) spectrometer with a deuterated triglycine sulphate (TGS) detector or a Perkin Elmer 1420 dispersion spectrometer. The FT-IR data was processed on a Perkin Elmer 7500 professional computer with DS-3 applications software.

UV/Visible spectra were obtained on a Kontron Uvikon 810p spectrophotometer fitted with a Grant thermostated circulator. The cell temperature was better than $\pm$ 0.1°C.

Elemental microanalyses were provided by Medac Ltd, Brunel. pH Measurements were made on a PTI-6 universal digital pH meter fitted with a Sensorex sealed reference combination electrode, calibrated with two standard buffer solutions. Melting points were measured on an Electrothermal Digital Melting Point apparatus and are uncorrected.

7.2 Kinetic measurements

7.2.1 Decomposition of N-(1'-methoxycarbonyl-2'-phenyl)ethyl-oxetan-2-one-4-carboxamide (1) in dilute acid and aqueous buffers

The rates of decomposition at (1) in dilute acid and aqueous buffers (pH<7.5) at 37±0.2°C were determined by following changes in the concentration of (1) by HPLC. The HPLC system comprised of LDC constametric 3000 pump, an LDC spectromonitor 3010 variable wavelength UV detector set at λ=220nm, coupled to an LDC C110B computing integrator. The assay was carried out on a Jones Apex II ODS (25cm x 4.0mm) column using 35% (v/v) acetonitrile in 0.01M KH_2PO_4 buffer

(pH4.5). At a flow rate of 1.0cm^3/min. eluted at 9.5 ± 0.5 mins. A custom injection system, designed and built by The Open University Interfaculty Electronics Unit and shown schematically in Figure 7.1, allowed aliquots (10μl) to be taken automatically from the reaction solution at timed intervals and injected onto the column.

Solutions of (1) (ca. 1mM, 25cm^3) were prepared in the appropriate buffer solution at constant ionic strengths μ=0.2 ($NaClO_4$) in a volumetric flask and allowed to thermally equilibrate at 37°C in a robust reaction flask (25ml). At timed intervals the reaction vessel was pressurised to flush the reaction solution through the 10μl sample loop of the HPLC equipment. The solution was pressurised sufficiently to ensure that the loop was thoroughly flushed with fresh reaction solution and to allow automatic loading of an aliquot (10μl) onto the column. The pressure in the reaction vessel was then released and the integrator automatically started recording the time of sample injection. The chromatogram was recorded for sufficient time to allow the elution of the β-lactone (ca. 12mins). Most reactions were followed until all the lactone had reacted but for slow reactions ($t_{1/2}$> ca. 9h) infinity values were assumed to be zero on the basis of the faster reactions.

The concentration of (1) was shown to be directly proportional to both peak height and peak area over at least the range 10^{-3}M to 5 x 10^{-5}M. Typical chromatograms are shown in Figure 2.20. Values of k_{obs} (Rate=k_{obs}(1)) were determined from the rate of loss of the peak due to (1) (Rf=9.5 ± 0.5min) using plots of ln (peak area $_t$/peak area $_{t=0}$) versus time. Typical ln plots for the decomposition of (I) in 2M$HClO_4$ and formic acid buffer at pH 3.32 at 37°C are shown in Figures 2.8 and 2.6 respectively. Values of k_{obs} were reproducible to ± 10%.

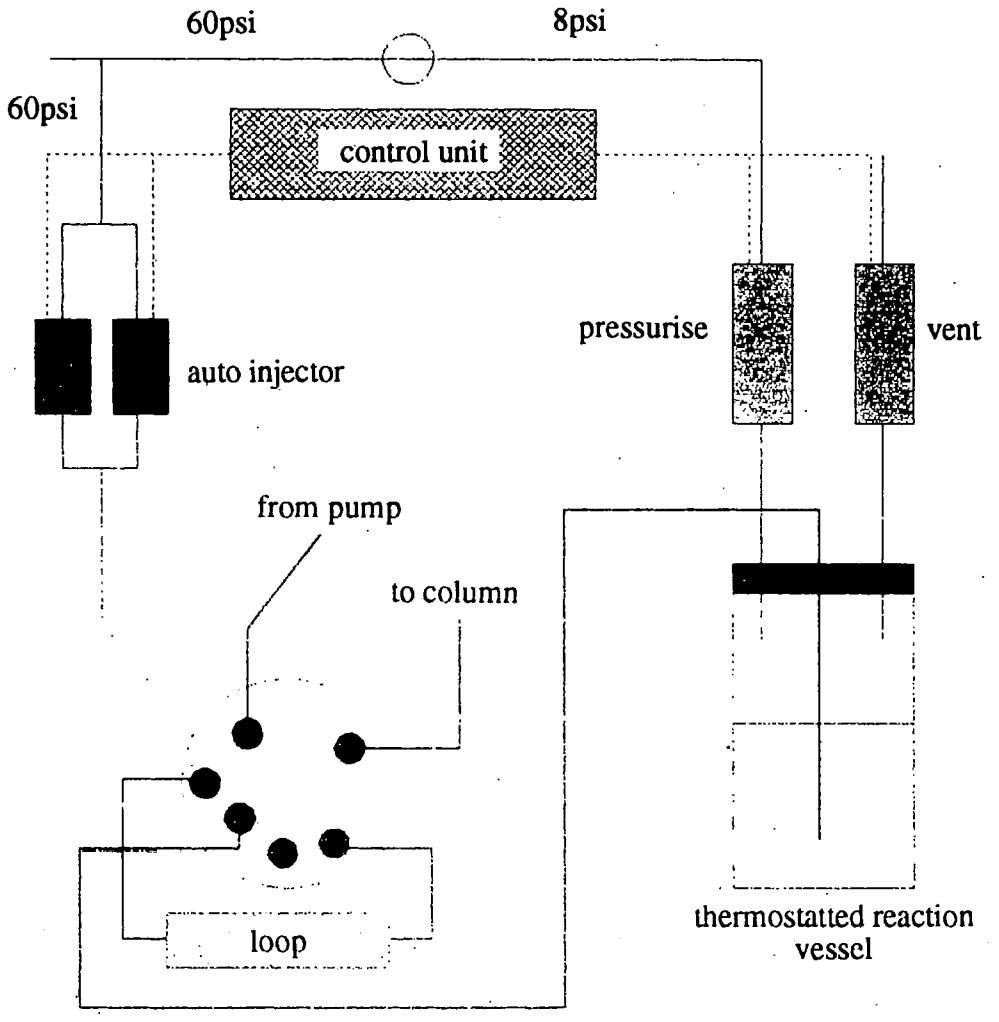

Figure 7.1 *Schematic representation of HPLC custom injection system*

7.2.2 Decomposition of aspartame in dilute acid (pH<O) at 37°C

The hydrolysis of the terminal methyl ester group of aspartame was determined using the same automatic procedure as for the decomposition of the β-lactone (1). The HPLC eluent was modified to consist of 15% (v/v) acetonitrile in 0.01M KH_2PO_4. Using a Jones Apex II ODS (25cm x 4.0mm) column and a flow rate of 1.0cm^3/min aspartame gave a retention time of 8.5 ± 0.3mins.

Reactions were studied using 1mM aspartame in dilute $HClO_4$ (25ml) at 37 ± 0.1°C. Values of k_O (rate = k_O[aspartame]) were determined from the rate of loss of the aspartame peak using plots of ln ((peak area $_t$ - peak area $_\infty$)/peak area t=o - peak area $_\infty$)) versus time. The infinity values were usually zero. Values of k_O were reproducible to ± 10%.

7.2.3 Decomposition of (1) in dilute NaOH at 37°C

Reactions in dilute NaOH (pH>8) were too fast to monitor using the HPLC assay. Decomposition of (1) in aqueous NaOH (pH 8-10) was therefore determined by assay of the carboxylic acid product using an automated titrator configured to maintain a constant pH in the reaction solution by the addition of small amounts of base (pH-stat). This equipment comprised a Radiometer TTT80 titrator with ABU80 autoburette, coupled to a PHM82 pH meter and REA270 pH-stat. The pH sensor was a glass electrode and a calomel reference electrode (calibrated against standard buffers), placed in a thermostated reaction vessel with an efficient stirrer. The titrant was 10mM NaOH, protected with a soda-lime guard tube to minimise absorption of atmospheric CO_2.

In a typical experiment, 10mM NaOH (ca. 0.15cm^3) was added by means of the autoburette to distilled water (20cm^3) in the jacketed reaction vessel until the desired pH was reached. The contents of the reaction vessel were efficiently stirred and maintained at 37 ± 0.2°C and the space above the reaction solution was continually purged with nitrogen to prevent CO_2 absorption. Once pH and thermal equilibrium had been

established, an aliquot (100-300μl) of the β-lactone (1) (ca. 10^{-5} mole) in methanol was added by autopipette to the reaction solution. NaOH titrant was automatically added to the reaction solution to maintain the pH and the volume added was recorded with respect to time. The reactions were monitored until the pH remained constant without addition of NaOH titrant and the final volume was taken as the ∞ reading. The number of moles of sodium hydroxide titrant added was plotted against time and the initial rate of decomposition of (1) was determined from the gradient of this plot drawn over the initial 5% reaction. Values of k_o (rate = k_o[I]) were obtained by dividing the initial rate by the initial number of moles of (1) and were reproducible to ± 10%.

7.2.4 Nitrosation of amino acids and their derivatives

The rates of nitrosation of amino acids in dilute HCl were usually measured from the uptake of nitrite using excess substrate. The substrate (0.1M) was prepared in 0.2M HCl from the free base or in 0.1M HCl from the HCl salt. The reaction solution was prepared by the addition of 0.01M $NaNO_2$ (0.25 cm^3) to the substrate solution (25cm^3). It was then loaded into several screw top vials which were sealed tightly without dead volume above the solution. The vials were immersed in a thermostatted water bath at 37 ± 0.1°C to start the reaction and removed at appropriate timed intervals for nitrite determination by the Shinn's method.[2] This involved the addition of an aliquot (2cm^3) of the reaction solution to a 1% (w/v) solution of sulphanilamide in 5M HCl (2cm^3). This mixture was left at ambient temperature for 2min to form the diazosulphonamide derivative. Then, a 0.1% (w/v) solution of N-1-naphthyl-ethylenediamine (2cm^3) in 0.1M HCl was added and the mixture was left for 15min to allow the violet azo dye (λ_{max} 541nm ε 51000 $dm^3cm^{-1}mol^{-1}$)[62] to fully develop. The solution was then diluted in a volumetric flask to 10cm^3 with distilled water and the uv absorbance was determined at 541nm. The absorbance of the azo dye is directly proportional to the nitrite concentration. The *pseudo* first order rate constants k_o, (rate = k_o[HNO_2] were determined directly from plots of ln (A_t-A_∞/A_o-A_∞) time. Control reactions without substrate were carried out to assess the rate of spontaneous

decomposition of nitrite in aqueous acid. The spontaneous decomposition of nitrite was always less than 3.5% of the rate of nitrite uptake in the presence of substrate provided the dead volume in the reaction vial was zero. Therefore no correction of k_0 for spontaneous nitrite decomposition was made. Values of k_0 were reproducible to ± 10%. Typical plots of ln $(A_t-A_\infty/A_0-A_\infty)$ versus time are shown in Figure 4.1 for the nitrosation of 0.1M L-glutamine, L-asparagine glycine ethyl ester and L-glutamine methyl ester in 0.1M HCl with 1mM $NaNO_2$ at 37°C.

7.2.5 Formation of methyl (S) 5-oxo-2-tetrahydrofuran carboxylate (2) from L-glutamine methyl ester

These reactions were followed by quantitation of the γ-lactone product (2) by capillary GLC.

Typically the reaction mixture was prepared by the addition of an aliquot ($0.2cm^3$) of $NaNO_2$ (3M) to glutamine methyl ester HCl salt ($25cm^3$, 3mM) in 0.1M HCl. Aliquots of the reaction mixture were placed in screw cap vials ($2cm^3$) with zero dead volume above the solution and all were then incubated at 37° ± 0.1°C in a thermostated tank. At timed intervals vials were removed from the bath, cooled and an aliquot ($1cm^3$) of the contents were extracted with ethyl acetate (2 x 1 cm^3) containing 0.005% (v/v) undecane as an internal standard. After separation, the combined organic extracts were adjusted to $2cm^3$ with ethyl acetate containing the internal standard, then dried over magnesium sulphate (ca. 20mg) prior to quantitation by GLC.

The GLC assay was carried out on a Perkin Elmer 8410 instrument with an FID detector using an SGE BP5 column (25m x 0.32 ; 0.5μ film thickness), and hydrogen carrier gas at a linear velocity of $40cms^{-1}$. The instrument was operated in the splitless mode with the injector at 200°C and an oven programme of 78°C for 1min, 10°C/min ramp to 140°C then 30°C/min ramp to 200°C. The injection volume was 1μL and the injection port was purged after 1.4min to reduce solvent front tailing. Under these

conditions, the γ-lactone (2) gave Rf=6.04min, and undecane Rf=4.08min and the limit of detection of (2) was ca. 10ng/μl.

In preliminary experiments, the extraction efficiency of ethyl acetate was determined for 10^{-3}M (2) in water. Aliquots ($1cm^3$) extracted with ethyl acetate ($2cm^3$) containing 0.005% (v/v) undecane gave an extraction efficiency of 96 ± 11%.

For each reaction sample, concentrations of the γ-lactone (2) were determined from a calibration graph of (peak area (2)/peak area undecane) against [(2)], which was linear over the range 8 x 10^{-5}M to 10^{-3}M (2). The error in estimating γ-lactone (2) concentrations is ca. ± 5%. For each kinetic experiment, the variation in γ-lactone (2) concentration was plotted against time, and the initial rate of formation of (2) was determined from the gradient drawn over the initial 5% reaction. Values of k_o (rate = k_o[glutamine methyl ester]) were obtained by dividing the initial rate by the [glutamine methyl ester] and they are reproducible to ± 15%. Typical results for the reaction of 3mM glutamine methyl ester with 30mM $NaNO_2$ in 0.1M HCl at 37°C are shown in Figure 4.22 These generate $k_o = 2.7 \times 10^{-5}\ s^{-1}$.

7.2.6 Decomposition of (2) in nitrous acid

The rates of decomposition of (2) in 0.1M hydrochloric acid containing sodium nitrite (ca. 30mM) at 37°C were determined by following changes in the concentration of (2) by HPLC.

The reaction mixture was prepared by the addition of an aliquot (100μL) of 3M $NaNO_2$ to a solution of (2) ($10cm^3$ 5mM) in 0.1M HCl. Aliquots of the reaction mixture were placed in screw cap vials ($2cm^3$) with zero volume above the solution and all were placed in a thermostatted bath at 37 ± 0.1°C. At timed intervals, vials were removed from the bath, cooled and an aliquot (10μL) was analysed by HPLC assay. The assay was carried out on a Varian 5060 ternary gradient liquid chromatograph with a Jones Apex II ODS (25cm x 4.6mm) column using 5% (v/v) acetonitrile in 0.075M KH_2PO_4

(pH 4.5) at a flow rate of 1.0cm^3/min. The column eluent was monitored with a Kratos SF757 variable wavelength uv detector at λ=215nm, coupled to an LDC C11OB computing integrator. Under these conditions the γ-lactone eluted at 12.8 ± 2min.

Reactions were monitored for at least 4 half lives and were then left for a further 24h to obtain an ∞ value which was usually zero. Peak areas were shown to be proportional to concentration of (2) over at least the range 10mM to 0.1mM (2) and values of k_o (rate=k_o[(2)]) were determined from the rate of loss of (2) using plots of ln (A_t-A_∞/A_o-A_∞) versus time. Values of k_o were reproducible to ± 10%. A typical plot is shown in Figure 4.24.

7.2.7 Decomposition of diazoamino acid methyl esters and diazodipeptide methyl esters

The diazoamino acid and diazodipeptide esters were decomposed in aqueous buffers and dilute acid at 25°C. These reactions were followed by the decrease in the uv absorbance of the diazo group of the substrate (λ_{max} ca. 260nm; log ε ca. 4) with respect to time. Two slightly different procedures were followed depending on the rapidity of the reaction.

Slow reactions ($t_{1/2}$>40s)

Serial dilutions of the appropriate stock buffer solutions were adjusted to a constant ionic strength (μ = 0.5) by the addition of 1.0M $NaClO_4$. An aliquot (3cm^3) of the buffer solution was thermally equilibrated to 37 ± 0.1°C in stoppered uv cuvettes within the thermostatted cell block of the uv visible spectrophotometer and then an aliquot (typically 20-100μl) of the diazocompound in 95% ethanol was added to start the decomposition reaction. The uv absorbance was monitored until constant or in the case of very slow reactions, over at least 4 half lives before adding a drop of conc. HCl to the cuvette to obtain the infinity value (usually < 0.02AU for the amino acids

N_2GlnOMe and N_2AsnOMe and ca.0.04AU for the dipeptides N_2GlnPheOMe and N_2AsnPheOMe). Values of the *pseudo* first order rate coefficient k_0 (rate= k_0[substrate]) were determined from plots of ln $(A_t-A_\infty/A_0-A_\infty)$ versus time. The k_0 values were reproducible to ± 5%. A typical plot for the reaction of N_2GlnOMe in 0.1M, 1:1 HOAc: NaOAc at pH 3.88 is shown in Figure 4.8

Linear plots of k_0 against buffer acid concentration were extrapolated to zero buffer acid concentration to determine intercept values (k_0^i) which, at low pH, approximate to $k_{H_3O^+}[H_3O^+]$. These intercept values were reproducible to ± 10%. A typical plot for the reaction of N_2GlnOMe in 1:1 AcOH:NaOAc buffers at pH 4.47 and 25°C is shown in Figure 4.9.

Fast reactions ($2.5<t_{1/2}<40s$)

The acid catalysed decomposition of some diazo-compounds was too fast to be measured accurately in the cuvette of the uv spectrophometer and a stopped-flow technique was therefore used. This utilized the Hi-Tech model SFA-11 stopped-flow accessory, with an 80µl cell volume and a dead volume of 700µl/reagent, fitted into the cell compartment of a Pye Unicam SP8-500 spectrophotometer with the reactant solutions and cell block thermostatted at 25 ± 0.1°C. An aqueous solution of the diazocompound (ca. 0.2mM) and dil. $HClO_4$ (0.001-1.0M) were placed separately into each reactant reservoir of the stopped-flow accessory and allowed to equilibrate thermally. The $HClO_4$ solutions were not adjusted to constant ionic strength. In a single operation, equal volumes of the two reactant solutions were passed manually through the mixing chamber and into the uv cuvette. After passage of ca. 0.5cm^3 of each reaction solution the liquid flow is stopped mechanically and the absorbance of the reaction solution is recorded with respect to time. Values of k_0 (rate=k_0[substrate]) were determined from plots of ln $(A_t-A_\infty/A_0-A_\infty)$ versus time. The k_0 values were reproducible to ± 5%. A typical plot for the hydrolysis of N_2GlnOMe in 0.01M $HClO_4$ at 25°C is shown in Figure 4.7.

The stopped-flow technique was also used to determine the solvent deuterium isotope effects for the decomposition of the diazocompounds by using $DClO_4$ in place of $HClO_4$ and dissolving the diazocompound in D_2O (n_D=0.999). The n_D>0.990 in the final reaction solution.

The mixing ratio of the stopped-flow accessory was checked periodically by titration of the reaction solution after mixing and complete reaction, against standardised NaOH. The mixing ratio was found to be 1:1 (v/v) ± 5%.

7.3 Product analysis

7.3.1 Reaction of N-(1′-methoxycarbonyl-2′-phenyl)ethyloxetan-2-one-4-carboxamide (1) with SCN^- and morpholine

Reaction with SCN^-

The β-lactone (1) (19mg, 6.8 x 10^{-5} mole) was dissolved in a solution of 0.1M KSCN (40cm^3) in acetonitrile. The reaction mixture was held at 37°C for 12h before concentrating to ca. 10cm^3 by evaporation in vacuo. The product was purified by semi-preparative HPLC using a Waters Delta Prep 3000 preparative chromatography system consisting of a quaternary pump, Waters 600E system controller, Waters 484 tunable absorbance detector (set λ=215nm) and Waters 745B data module. The sample (1-2cm^3) was chromatographed on a Phase Separations Spherisorb S5 ODS 2 (25cm x 20mm) column using 0.01M heptafluorobutyric acid containing 35% (v/v) acetonitrile as the eluent at a flow rate of 25cm^3/min. The solvent was removed from the combined fractions containing the product (Rf=ca. 6-9min) by freeze drying. The product was analysed by mass spectrometry.

Reaction with morpholine

The β-lactone (1) (20mg, 7.2 x 10^{-5}mole) was dissolved in 7.2mM morpholine in acetonitrile (10cm^3). The reaction solution was incubated at 37°C until no β-lactone (1) remained (as determined by HPLC, Section 7.2.1). The solvent was

evaporated under vacuum and the product, a semicrystalline oil was analysed by mass spectrometry.

7.3.2 Reaction of 3-hydroxybutyric acid β-lactone with nucleophiles

3-Hydroxybutyric acid β-lactone was reacted with a number of nucleophiles in either CD_3CN or CD_3CN/D_2O and the products analysed by ^{13}C nmr. Thus, in a typical experiment 3-hydroxybutyric acid β-lactone (0.5cm ^{3}, 6.1mmole) in CD_3CN (1cm^3) was cooled to 0°C and treated with 1 molar equivalent of the nucleophile. If the nucleophile was insoluble in CD_3CN, it was dissolved in D_2O (0.5cm^3) prior to the addition. The reaction solution was allowed to warm to room temperature and the decoupled 90MHz ^{13}C spectra were recorded.

7.3.3 Deamination of glutamine and asparagine methyl esters in dilute HNO_2

The two amino acid esters were treated with HNO_2 at 0°C in a biphasic system containing CH_2Cl_2. The products that partitioned into the organic phase, were analysed using a capillary GLC MS technique.

Thus, 1M $NaNO_2$ (ca. 0.9cm^3, 0.9mmole) was added to a pre-cooled bi-phasic solution of the amino acid HCl salt (ca. 0.3mmole) in 0.1M HCl (12cm^3) and CH_2Cl_2 (10cm^3) at 0°C. The mixture was stirred rapidly for 5h at 0°C after which the organic phase was separated. The aqueous phase was extracted with CH_2Cl_2 (2 x 10cm^3) and the combined organic phases were washed with water (2 x 5cm^3) and dried over Na_2SO_4. The organic phase was concentrated, by evaporation in vacuo, to ca. 2cm^3 prior to analysis.

GLC-MS analysis

The mass spectrometer was coupled to a Hewlett-Packard 5890A gas chromatograph. Samples (1μl) were introduced through a heated injection port (160°C) and were

chromatographed on an SGE 12m BP5 column (0.25μ film thickness) using helium carrier gas at 4psi. The mass spectrometer was operated with a source temperature of 200°C and electron impact was used as the ionization technique. The following GC oven conditions were used:

Initial T	40°C isothermal time 0min
Ramp	10°C/min to 160°C isothermal time 2min

A typical chromatogram is shown in Figure 4.25 for the products from the decomposition of AsnOMe in dilute HNO_2

7.3.4 Nitrosation of amino acid and peptide substrates with gaseous NO_2

These reactions were investigated to assess the possibility of forming and isolating the corresponding diazocompounds. Although these compounds usually show a strong absorbance at λ ca. 260nm, simple assay by uv spectroscopy was unsuitable because of strong absorbance by nitrite ions and nitrous acid (generated by the hydrolysis of NO_2) in this region. Therefore the reaction solutions were analysed by HPLC using a diode array detector. The following is a typical procedure. Glutamine methyl ester HCl salt (1.7×10^{-2}g, 0.086mM) dissolved in 0.1M borax ($10cm^3$) was placed in a $50cm^3$ conical flask fitted with a silicone rubber Suba-seal stopper. Gaseous NO_2 ($0.5cm^3$) obtained from above a reservoir containing liquid N_2O_4 in equilibrium with gaseous NO_2 at 25°C, by means of a gas syringe (Pressure Lok $1cm^3$), was injected into the conical flask. The contents of the flask were then shaken vigorously for ca. 20s. Reaction was evident from the appearance of white fumes in the flask and a yellow orange colouration of the solution.

The reaction solution was then analysed for the presence of diazo derivatives by HPLC with diode array detection using the conditions described below. Subsequently a sample ($2cm^3$) of the reaction solution was acidified with conc. HCl (pH<4) and then

reanalysed. Since diazoderivatives are very unstable in dilute acid (pH<4), the disappearance of eluted peaks was regarded as evidence for the presence of these products in the reaction solution. The sample was then made alkaline by the addition of 4M NaOH and reanalysed by HPLC assay.

A further sample of the reaction solution was kept at room temperature for ca. 8h and analysed by HPLC to obtain preliminary information on the stability of the diazo product in borax buffer.

7.3.5 HPLC assay of diazoamino acid esters and diazodipeptide esters

The HPLC analysis of the diazocompounds was carried out on a Varian 5060 ternary gradient liquid chromatograph, using a Hamilton PRP1 column (15cm x 4.1mm) and acetonitrile in 0.01M borax buffer eluent at a flow rate of $1cm^3$/min. The column eluent was monitored by either a Kratos SF 757 variable wavelength uv detector at 260nm or a Varian 9060 Polychrom diode array detector with a wavelength range of 190-370nm, coupled to a Spectraphysics SP40400 Chromjet integrator. The eluents and retention times for each diazo product are summarised in Table 7.1. Solutions of 0.1mM diazo compound (10µl) could easily be detected using this assay and peak areas were reproducible to ± 5%. The assay was used qualitatively only, attempts at quantitation of diazocompound were not made.

Table 7.1 Retention times of authentic diazoamino acid esters and diazodipeptide esters

Compound	%(v/v)AcN in 0.01M borax	R.T./mins ± 0.1
N_2GlnOMe	5	10.8
N_2GlnOMe	10	5.0
N_2AsnOMe	5	5.0
N_2AsnOMe	10	3.0
N_2GlnPheOMe	25	4.6
N_2AsnPheOMe	25	4.4

7.3.6 Thermolysis of diazoamino acid methyl esters and diazodipeptide methyl esters

Solutions of diazoglutamine methyl ester (13mM), diazoasparagine methyl ester (10mM), diazoglutaminylphenylalanine methyl ester (16mM) and diazo-asparaginyl phenylalaninemethyl ester (17mM) were prepared in dry ethyl acetate, free of AcOH. Aliquots (0.5cm^3) of the above solutions in sealed Pierce Reacti vials (Pierce, 0.5cm^3) were heated to 120°C in a thermostatted reaction block until no diazocompound remained by HPLC (see Section 7.3.4). The resulting solution was analysed by GLC and GLC MS as described in Section 7.3.8.

7.3.7 Hydrolysis of diazoamino acid methyl esters and diazodipeptide methyl esters after thermolysis

Aliquots (2-300µl) of the solutions containing thermolysed diazo substrates (see above) were evaporated under a stream of nitrogen to remove the solvent. The residue was

dissolved in 0.01M NaOH (200µl) and held at room temperature for 30min before freeze drying to remove the water. The resulting residue was redissolved in ethyl acetate (2-300µl) and analysed by GLC and GLC MS as described in Section 7.3.8.

7.3.8 Product analysis from thermal decomposition of diazosubstrates

GLC procedure

The GLC assay was carried out on a Perkin Elmer 8410 instrument with an FID detector using an SGE BP5 column (25m x 0.32mm); 0.5µ film thickness), and hydrogen carrier gas at a linear velocity of 40cms^{-1}. The instrument was operated in splitless mode using the oven conditions given below. The injection volume was 1µl and the injection port was purged after 1.4min to reduce solvent front tailing.

GLC conditions for analysis of diazoamino acid esters

Injector	200°C	
Initial T	78°C	isothermal time 1min.
Ramp 1	10°C/min to 140°C	isothermal time 0min.
Ramp 2	30°C/min to 200°C	

The retention times of the analytes are given in Table 7.2.

Table 7.2 Retention times of authentic cyclic compounds

Compound	RT ± .1/min.
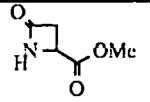	6.0
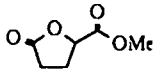	5.9
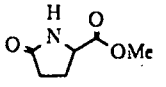	8.3

Typical chromatograms are shown in Figures 4.34 and 4.44 for the thermolysis of diazoglutamine methyl ester and diazoasparagine methyl ester respectively.

GLC conditions for analysis of diazodipeptide esters

Injector	250°C	
Initial T	90°C	isothermal time 0min.
Ramp	15°C/min to 250°C	isothermal time 10min.

N-(1′-methyoxycarbonyl-2′-phenyl)ethyloxetan-2-one-4-carboxamide had a retention time of 10.5 ± 1min.

GLC-MS procedure

The mass spectrometer was coupled to a Hewlett Packard 5890A gas chromatograph. Helium at a linear gas velocity of ca. 30cms^{-1} was used as the carrier gas. Samples were introduced through a heated injector port or using an on-column injection technique. The injection technique had little bearing on the subsequent chromatography, although the on-column technique was more sensitive. The MS was operated using a source temperature of 200°C and two different ionization techniques. Thus electron impact was used to generate fragment ions, but to detect molecular ions the milder chemical ionization technique with ammonia as the reactant gas was used.

Diazoamino acid esters

The reaction solutions were chromatographed on an SGE 12m BP1 capillary column (0.25μ film thickness). Typical sample volumes of 0.5μl were injected using the on-column technique and the following gc oven conditions.

Initial T	50°C	isothermal time 0min.
Ramp 1	30°C/min to 78°C	isothermal time 0min.
Ramp 2	5°C/min to 140°C	isothermal time 0min.
Ramp 3	30°C/min to 200°C	isothermal time 10min.

A typical GC chromatogram is shown in Figure 4.37 for the analysis of the reaction mixture of the thermolysis of diazoglutamine methyl ester. Typical EI spectra are shown in Figures 4.38 and 4.45.

Diazodipeptide methyl esters

These reaction solutions were analysed on an SGE BP5 capillary column (25m x 0.22mm, 0.25μ film thickness). Samples (1μl) were introduced via the heated vaporizing injector port (275°C) and eluted using the following temperature program.

Initial T	80°C	isothermal time 0min.
Ramp 1	30°C/min to 250°C	isothermal time 10min.

Typical GC chromatograms are shown in Figures 5.17 and 5.22 for thermolysis mixtures of diazoglutaminephenylalanine methyl ester and diazoasparaginyl-phenylalanine methyl ester respectively and typical EI spectra in Figures 5.18 and 5.23.

7.4 Preparation of reagents

7.4.1 Diazomethane

This was prepared by the method of Vogel.[159] Thus, 0.1M KOH (8cm^3), diethylether (16cm^3) and 2(2′-ethoxyethoxyethanol) (28cm^3) were stirred and heated to 65°C in a flask contained in a water bath. N-Methyl-N-nitroso-p-toluene sulphonamide (10g, 4.6mmole) in diethyl ether (100cm^3) was then added dropwise with stirring to affect gentle distillation of ethereal diazomethane. Once all the solution of nitrosoamide had been added, Et_2O (30cm^3) was added slowly until the distillate was colourless. The ethereal diazomethane was stored at -30°C.

The concentration of diazomethane in the ether solution was determined by titration. Thus, an aliquot (1cm^3) was quenched with 0.2M ethereal benzoic acid (3cm^3), water (10cm^3) was added, and the biphasic solution was titrated against 0.1M NaOH using phenyl red indicator. Typically the ethereal diazomethane was 0.15-0.20M.

7.4.2 Palladium black

Palladium black was prepared from the method described by Elvidge and Sammes.[160] Thus, palladium chloride (1g) was heated to 80°C in water (200cm^3) and 20% (w/v) NaOH was added until the suspension gave pH7, 2.6% (v/v) formic acid (5cm^3) and, after 2min, a further aliquot of 20% NaOH (10cm^3), followed by more 2.6% formic acid (10cm^3) were added ensuring that the solution remained alkaline throughout. The reaction mixture was boiled for 2h, after which the precipitated palladium black was filtered-off under argon, washed with water and finally dried in vacuo over $CaCl_2$.

7.5 Synthesis

7.5.1 N-(1′-Methoxycarbonyl-2′-phenyl)ethyloxetan-2-one 4-carboxamide(1)

L-Aspartyl-L-phenylalanine methyl ester (0.147g, 0.5mmole) was stirred in CH_2Cl_2 (10cm^3), 0.6M $NaNO_2$ (2.5cm^3, 1.5mmole) and thiourea (0.01g) were added, and the rapidly stirred solution was warmed to 37°C. 1M HCl (2.5cm^3, 2.5mmole) was then added and the flask was stoppered securely. After 90min with rapid stirring, the CH_2Cl_2 layer was separated, the aqueous phase was washed with CH_2Cl_2 (2 x 20cm^3) and the combined organic phases were washed with water (2 x 10cm^3), 5% $NaHCO_3$ (2 x 10cm^3), and finally saturated NaCl (10cm^3). The organic extract was dried over anhyd. $MgSO_4$, and after filtration the CH_2Cl_2 was removed at the pump to give an off-white, crystalline solid. This was purified by column chromatography on silica using Et_2O as the eluent. N-(1-Methoxycarbonyl-2'-phenyl)ethyloxetan-2-one-4-carboxamide crystallised from ethereal solution as a white solid (38mg, 27%), m.p. 107.0-107.6°C (lit.[97] 105°C) (Found: C, 60.6; H, 5.4; N, 5.0; calc. for $C_{14}H_{15}NO_5$: C, 60.65; H, 5.45; N, 5.05%) ν_{max} (KBr) 3315 (amide NH), 3080, 3060, and 3032 (aromatic CH), 2951 (CH_3), 1841 (β-lactone CO), 1742 (ester CO), 1662 (amide CO), 1558cm^{-1} (amide II); δ_H (400MHz;CD_2Cl_2) 7.33 (3H, m, aromatic CH), 7.16 (2H, aromatic CH); 6.73 (1H, br d, NH), 4.81 (1H, ddd, J5.66, 6.88, J_{NH} 8.07Hz, NCH),

4.87 (1H, dd, J_{cis} 4.66, J_{trans} 6.88Hz, OCH), 3.84 (1H, dd, J_{trans} 6.89, J_{gem} 16.80Hz, ring CH(H)), 3.76 (3H, s, OCH_3), 3.53 (1H, dd, J_{cis} 4.67, J_{gem} 16.81Hz, ring C(H)H), 3.24 (1H, dd, J5.64, J_{gem} 13.97Hz, CH(H)Ph), and 3.12 (1H, dd, J6.86, J_{gem} 13.97Hz, C(H)HPh).

7.5.2 Methyl 2-pyrrolidine-5-carboxylate

L-2-Pyrrolidone-5-carboxylic acid (0.25g, 1.9mmole) dissolved in dry MeOH ($5cm^3$) and cooled to 0°C was treated with a slight excess of diazomethane (ca. 15ml) until a permanent yellow colour remained. After 20min at 0°C, excess diazomethane was quenched with AcOH (ca. 50μl) and the solvents removed under vacuum to yield a colourless oil. This was purified by silica column chromatography (eluent 2:3 (v/v) EtOH:EtOAc to 3:2 (v/v) EtOH:EtOAc) to give 5-methyl-2-pyrrolidone-5-carboxylate as a colourless oil (0.27g, 98%) ν_{max} (neat) 3352, 3255 (β-lactam N-H H-bonded), 2957 (CH_3), 1741 (ester C=O), 1699 (γ-lactam C=O), 1459 (amide II), 1215cm^{-1} (ester C-O); δ_H (90MHz; $CDCl_3$) 7.6 (1H, s, NH), 4.2 (1H, dd, J4.4, J6.3Hz, CH), 3.8 (3H, s, CH_3), 2.4 (4H, m, CH_2CH_2); δ_C (22.5MHz; $CDCl_3$) 178.2 (ester CO), 173.1 (amide CO), 55.7 (CH), 52.4(OCH_3), 29.4 ($COCH_2$), 24.9 ($CHCH_2$); m/z (FAB+ve (glycerol)) 144 ($M+H^+$), 84 ($M+H^+$- CO-MeOH), 430 (M_3+H^+), 287 (M_2+H^+), 236 (M+glycerol+H^+); m/z (FAB-ve (glycerol)) 142 ($M-H^+$), 128 ($M-CH_3^+$), 82 (M-CO-MeOH-H^+); m/z (EI+ve) 28 ($CO^{+\bullet}$; 100%), 84 ($M^{+\bullet}$-$\dot{C}O_2Me$; 82), 56 ($M^{\bullet+}$-CO_2-HNCO; 45), 99 ($M^{\bullet+}$-CO_2 ;42), 41 ($M^{\bullet+}$-$\dot{C}O_2Me$-HNCO; 27), 143 ($M^{\bullet+}$; 6).

7.5.3 Methyl (S)-azetidin-2-one-4-carboxylate

7.5.3.1 Dibenzyl (S)-aspartate-p-toluene sulponic acid salt (3)

Compound (3) was prepared using the method of Zervas, Winitz and Greenstein.[147] Thus aspartic acid (16.6g, 0.125mole) was slurried in benzyl alcohol (50cm^3, 0.48mole) together with p-toluenesulphonic acid (24.2g, 0.14mole) and benzene (25cm^3). The mixture was heated under reflux for 18h and water formed in the reaction was removed azeotropically by a Dean Stark trap. The mixture was cooled to room temperature and then diluted with benzene (175cm^3). Dry diethyl ether (200cm^3) was added and the product slowly crystalised at 0°C over a period of 5h. The solid was filtered off, washed with diethyl ether and recrystallised from methanol:ether to give the dibenzyl-(S)-aspartate-p-toluenesulphonic acid salt as a white crystalline solid (38g, 63%), m.p. 129.5-130.4°C (lit.[147] 158-160°C), ν_{max} (KBr) 3140 ($\overset{+}{H_3N}$), 3033 (aromatic CH), 1761 (ester CO), 1596 (aromatic C=C) 1529 ($\overset{+}{H_3N}$), 1498 and 1456 (aromatic C=C), 1186 (S-O), 1164 (C-O), 1035cm^{-1} (S-O); δ_H (90MHz: d^{4}MeOH) 7.4 (14H, m, aromatic CH), 5.1 (2H, s, CH_2Ph), 5.0 (2H, s, CH_2Ph), 4.3 (1H, t, J5.3Hz, CH), 2.9 (2H, d, J5.4Hz, CH_2), 2.2 (3H, s, CH_3); δ_C (22.5MHz; d^{4}MeOH) 172.3 (α-benzyl ester CO), 170.6 (β-benzylester CO), 145 (aromatic C-SO_3^-), 143.2 (aromatic C-Me), 138.3 (aromatic α-benzylester C-CH_2O); 137.7 (aromatic β-benzylester C-CH_2O), 131.2, 130.7 and 128.5 (remaining aromatic CH), 71.0 (α-benzylester CH_2Ph), 69.9 (β-benzylester CH_2Ph), 52.0 (CH), 36.6 (CH_2), 22.9(CH_3); m/z (FAB+ve(glycerol)) 91 (CH_2Ph^+), 314 ($M+H^+$)

7.5.3.2 Benzyl 4-(S)-azetidin-2-one-4-carboxylate (4)

Compound (4) was prepared using the method of Salzmann et.al.[146] To dibenzyl (S)-aspartate-p-toluene sulphonic acid (19.75g, 0.04mole) in ice cold diethyl ether (120cm^3) in a separating funnel were added cold water (40cm^3) and sat. K_2CO_3 (20.5cm^3) and the mixture was shaken vigorously. The layers were separated, the aqueous phase was extracted with diethyl ether (2 x 40cm^3) and the combined ether

extracts were washed with sat. NaCl and then dried over $MgSO_4$. Removal of the solvent under vacuum yielded dibenzylaspartate as a colourless oil. This was dissolved in dry diethyl ether ($80cm^3$) at 0°C under argon. Trimethylsilylchloride ($5.16cm^3$, 0.041mole) was added to the solution to give a white precipitate, followed by Et_3N ($5.16cm^3$, 0.04mole), the mixture was allowed to warm to room temperature and to stand for 2h. The mixture was filtered under a positive pressure of argon to remove triethylammonium chloride, and then stripped under vacuum to give dibenzyl-N-trimethylsilyl-aspartate as a colourless oil. Ether ($100cm^3$) was added to the oil contained, under argon, in a flask equipped with an overhead stirrer. After cooling to 0°C an ethereal solution of 2M -butylmagnesium chloride ($20.3cm^3$, 0.04mole) was added dropwise over 30min to give a yellow precipitate. The mixture was allowed to warm to room temperature, stirred overnight, and after cooling in an ice-methanol bath, 2M HCl saturated with NH_4Cl ($40cm^3$) was added slowly. The mixture was diluted with water ($40cm^3$) before extraction with EtOAc ($40cm^3$). The aqueous phase was separated and washed with EtOAc ($3x10cm^3$). The combined organic extracts were washed with water ($80cm^3$); 5% $NaHCO_3$ ($40cm^3$); water ($40cm^3$); and finally with sat. NaCl ($40cm^3$) before drying over $MgSO_4$. Filtration followed by removal of the solvent under vacuum, gave a brown oil, which after crystallisation from chloroform:hexane (3:5 v/v), gave benzyl-4-(s)-azetidin-2-one-4-carboxylate as a pale yellow solid (3.41g, 41%) m.p. 112.0-112.2°C (lit.[146] 136-139°C) (Found: C, 64.4; H, 5.4; N, 6.8; calculated for $C_{11}H_{17}NO_3$ C, 64.4; H, 5.4; N, 6.7%) ν_{max} (KBr) 3447 (lactam NH), 3033 (aromatic CH), 1770 (β-lactam CO), 1734 (ester CO), 1499 and 1458 (aromatic C=C), 1285 (ester C-O), $1098cm^{-1}$ (ester C-O); δ_H (90MHz, $CDCl_3$) 7.3 (5H, s, aromatic CH), 6.2 (1H, br, s, NH), 5.2 (2H, s, CH_2Ph), 4.2(1H, dd, J_{cis} 3.1, J_{trans} 5.5 Hz, CH), 3.4 (1H, ddd, J_{NH} 1.5, J_{trans} 5.6, J_{gem} 14.9 Hz, CH(H)), 3.1 (1H, ddd, J_{NH} 2.01, J_{cis} 3.2, J_{gem} 14.9Hz, C(H)H); δ_C (22.5MHz, $CDCl_3$)170.7 (ester CO), 166.2 (β-lactam CO); 134.8 (C-CH_2), 128.6, 128.3, and 126.8 (aromatic CH), 67.3 (CH_2Ph), 47.2(CH), 43.4 (CH_2); m/z (FAB+ve(glycerol))

91 (CH_2Ph^+), 206($M+H^+$), 178 ($M+H^+$-CO), 298 (M+glycerol+H^+); m/z (FAB-ve(glycerol)) 114 ($M-CH_2Ph^+$); 204 ($M-H^+$).

7.5.3.3 Methyl 4-(s)-azetidin-2-one-4-carboxylate (5)

Benzyl-4-(s)-azetidinone-4-carboxylate (0.5g, 2.5mmole) and 10% Pd/C (0.1g) in dry methanol (20cm^3) were sparged with hydrogen at room temperature. The reaction was monitored by TLC (silica, Et_2O, Rf(5)=0.4). After 1h, the reaction was complete and the catalyst was filtered-off and washed with MeOH. The combined filtrates were evaporated under vacuum to give a colourless oil. This was dissolved in dry MeOH (5cm^3) and cooled to 0°C. Ethereal diazomethane (ca. 20cm^3) was added until the solution became pale yellow. After 2h at 0°C, the excess diazomethane was quenched with glacial AcOH and the solvents were removed under vacuum to give a pale yellow oil. This was purified by silica column chromatography (1:9 (v/v) hexane:ether to 100% ether) to give methyl 4-(s)-azetidine-2-one-4-carboxylate as a colourless oil (0.18g, 53%) (Found: C, 46.25; H, 5.5; N, 10.7, $C_5H_7NO_3$ requires: C, 46.5; H, 5.5; N,10.85%) ν_{max} (neat) 3294 (β-lactam NH), 2959 (CH_3), 1750 (β-lactam C=O), 1742 (ester C=O), 1440 (amide II), 1369 (CH_3), 1186 cm^{-1} (ester C-O); δ_H (90MHz; $CDCl_3$) 7.2 (1H, brs, NH), 4.2 (1H, dd, J_{cis} 2.9, J_{trans} 5.4Hz, CH), 3.8 (3H, s, CH_3), 3.3 (6H, dd, CH(H)), 3.1 (6H, br dd, CHCH)); δ_C (22.5MHz; $CDCl_3$) 171.9 (ester CO), 167.3 (β-lactone CO), 52.6 (CH), 47.2 (CH_3), 43.2 (CH_2); m/z (EI+ve GLC MS) (conditions as 7.3.5(6) Rf=7.15min.) 28 ($CO^{\bullet+}$ 100%), 43 ($HNCO^{\bullet+}$; 71), 55 ($M^{\bullet+}$-HNCO-$^{\bullet}$OMe, 59), 70 ($M^{\bullet+}$-$CO_2Me^{\bullet}$; 42) 101 ($M^{\bullet+}$-CO; 32), 42 ($CH_2CO^{\bullet+}$; 32), 129 ($M^{\bullet+}$ 20), 86 ($M^{\bullet+}$-HNCO; 10), 59 (CO_2Me^+; 9).

7.5.4 Methyl 5-(S)-oxo-tetrahydrofuran carboxylate

5-(S)-Oxo-2-tetrahydrofuran carboxylic acid (0.50g, 3.85mmole) dissolved in dry MeOH (3cm^3) was treated with a slight excess of ethereal diazomethane (ca. 30cm^3) at 0°C. The reaction was held at 0°C for 30min before quenching the excess diazomethane with glacial AcOH (ca. 50μl). Vacuum evaporation of the solvent gave a

yellow oil which was purified by silica chromatography using diethyl ether. Methyl 5-(S)-oxo-tetrahydrofuran carboxylate crystallised from the ethereal solution on cooling (0.42g, 74%) m.p. 58.1-58.9°C (Found: C, 50.0; H, 5.6; $C_6H_8O_4$ requires: C, 50.0; H, 5.6%) ν_{max} (KBr) 2964 (CH_3), 1780 (γ-lactone CO), 1747 (ester CO), 1434, 1384, 1222 (γ-lactone C-O), 1205 (ester C-O), 1161, 1149cm^{-1}, δ_H (90MHz, $CDCl_3$) 4.9 (1H, m, CH), 3.8 (3H, s, OCH_3), 2.5 (4H, m, CH_2CH_2); δ_C (22.5MHz, $CDCl_3$) 175.7 (γ-lactone CO), 169.8 (ester CO), 75.0 (CH), 51.8 (OCH_3), 26.0 ($COCH_2$), 24.9 ($CHCH_2$); m/z (FAB+ve(glycerol)) 145 ($M+H^+$), 85 ($M+H^+-HCO_2Me$), 117 ($M+H^+-CO$), 237 (M+glycerol+H^+), 251 (M_2+H^+); m/z (EI+ve) 85 ($M^{\bullet+}-\overset{\bullet}{C})O_2Me$, 100%), 29 ($HNCO^{\bullet+}$, 52), 28 ($CO^+$, 40), 57 ($M^{\bullet+}-\overset{\bullet}{C})O_2Me-CO$, 11), 59 ($CO_2Me^{\bullet+}$, 5), 144 ($M^{\bullet+}$, 1.5).

7.5.5 N-Acetylphenylalanine methyl ester

N-Acetylphenylalanine (0.5g, 2.4mmole) in dry MeOH (1cm^3) was treated with a slight excess of ethereal diazomethane (ca. 20ml) at 0°C. After 30min. at 0°C the excess diazomethane was quenched with glacial AcOH (ca. 50μl). Vacuum evaporation of the solvent gave N-acetylphenylalanine as a white crystalline solid (0.52g, 98%) δ_H (90MHz, $CDCl_3$) 7.2 (6H, m, aromatic CH and NH), 4.8 (1H, br, dd, CH), 3.6 (3H, s, OCH_3), 3.1 (2H, dd, J_{syn} 2.4Hz, J_{anti} 5.85Hz, CH_2), 1.91 (3H, s, CH_3CO); m/z (EI+ve) 162 ($C_6H_5CH=CHCO_2Me^{\bullet+}$; 100%), 88 ($M^{\bullet+}-C_7H_3^{\bullet}-CH_2=C=O$, 94), 43 ($CH_3\overset{+}{C}O$; 59); 120 ($H_2N=CHCH_2Ph^+$, 48), 91 ($C_7H_3^{\bullet+}$, 41), 131 (162-OMe$^{\bullet}$, 36), 221 ($M^{\bullet+}$, 0.5).

7.5.6 L-Aspartic acid α methyl ester

7.5.6.1 N-α-Carbobenzyloxy-L-aspartic acid (6)

Compound (6) was prepared using the Schotten-Bowmann[161] procedure. Thus benzylchloroformate (12.8cm^3, 9.0mmole) and 4M NaOH (19.8cm^3) were added simultaneously, dropwise to a stirred solution of L-aspartic acid (10g, 76mmole) in 2M

NaOH (77cm^3) at 0°C. The mixture was held at 0°C for 3h before washing with ether and neutralizing to pH 1.5 with conc. HCl to give a white gelatinous precipitate. The precipitate was extracted from the solution with EtOAc (3 x 40cm^3), the organic extracts were combined, dried over $MgSO_4$ and after removal of the solvent under vacuum gave N-α-carbobenzyloxy-l-aspartic acid as a white solid (14.5g, 72%).

7.5.6.2 N-α-Carbobenzyloxy-L-aspartic acid α-methyl ester

Compound (6) (10g, 37mmole) was dissolved in Ac_2O (50cm^3) and stirred for 18h at room temperature. The Ac_2O was removed under reduced pressure to give a colourless oil, which was then dissolved in dry MeOH (50cm^3) and held at room temperature overnight. Removal of the MeOH under vacuum yielded a colourless oil containing a mixture of both mono and dimethyl esters. The N-α-carbo-benzyloxy-L-aspartic acid α methyl ester was isolated by silica column chromatography using 10% (v/v) hexane in ether as the eluent and then further purified by recrystallization from chloroform/hexane to give N-α-carbobenzyloxy-L-aspartic acid α–methyl ester as a white solid (3.95g, 38%) m.p. 89.7-90.3°C (Found: C, 55.4, H, 5.4, N, 4.9; calc. for $C_{13}H_{15}NO_6$: C, 55.5; H, 5.4; N, 5.0%) ν_{max} (KBr) 3394 (carbamate NH), 3277 (acid OH), 3066 (aromatic CH), 2960 (CH_3), 1734 (ester CO), 1678 (carbamate CO), 1525 (carbamate NH), 1440 (CO_2H), 1353; 1224 (CO_2H), 1163 (ester CO), 1082cm^{-1}; δ_H (90MHz; $CDCl_3$) 11.2 (1H, s,OH), 7.2(5H, s, aromatic CH), 5.8 (1H, br d, J8.3Hz NH), 5.0 (2H, s, CH_2Ph), 4.5 (1H, m, CH), 3.6 (3H, s, OCH_3), 2.9, (2H, m, CH_2); δ_C (22.5MHz; $CDCl_3$), 176 (acid CO), 171 (ester CO), 156 (carbamate CO), 136 (aromatic C-), 128 (aromatic CH), 67 (CH_2Ph), 52 (OCH_3), 50 (CH), 36 (CH_2); m/z (FAB+ve (glycerol)) 91 (CH_2Ph^+), 45 ($COOH^+$), 73, 117, 238 ($M+H^+-CO_2$), 282 ($M+H^+$).

7.5.6.3 L-Aspartic acid α–methyl ester

N-α-Carbobenzyloxy-L-aspartic acid monomethyl ester (0.5g, 2.0mmole) and palladium black (0.1g) in MeOH (10cm^3) and 1M HCl (2cm^3) were sparged with

hydrogen. The reaction was followed by silica TLC (Et_2O). After 1h the reaction was complete and the catalyst was removed by filtration before stripping the solvent under vacuum to give L-aspartic acid α methyl ester as an off white hygroscopic solid. (0.30g, 82%) m/z (FAB+ve(glycerol)) 148 ($M+H^+$), 102 ($M+H^+$-CO-H_2O), 88 ($M+H^+$-MeOH-CO), 117, 130 ($M+H^+$-H_2O), 45 (HCO_2^+).

7.5.7 Hydroxysuccinic acid dimethyl ester

Dry HCl gas was bubbled through MeOH to give ca. 6M HCl. To this HCl solution ($30cm^3$) was added hydroxysuccinic acid (1g, 7.46mmole). The solution was warmed to 40°C and held at this temperature overnight with stirring. The methanol was removed under reduced pressure to give hydroxysuccinic acid dimethyl ester as a colourless oil. (1.22g, 96%) δ_H (90MHz; $CDCl_3$) 5.3 (6H, br, s, OH), 4.3 (1H, t, J5.6Hz, CH), 3.6 (3H, s, OCH_3), 3.5 (3H, s, OCH_3), 2.6 (2H, d, CH_2 J4.9Hz); δ_C (22.5MHz, $CDCl_3$) 172.5 (α ester CO), 170.0 (β ester CO), 66.2 (CHOH), 52.2 (OCH_3), 51.4 (OCH_3), 37.6 (CH_2).

7.5.8 Methyl-2-diazo-4-carbamoyl butanoate (N_2GlnOMe)

7.5.8.1 N-α-Carbobenzyloxy-L-glutamine methyl ester (7)

Compound (7) was prepared using the method of Sondheimer and Holley.[137] N-α-Carbo-benzyloxy-L-glutamine (1g, 7.14mmole) in dry EtOH ($10cm^3$) was cooled to 0°C. A slight excess of ethereal diazomethane (ca. $40cm^3$) was added with stirring so that the solution retained a permanent yellow colour. The mixture was held at 0°C for 1h during which time the product precipitated out of solution and then the excess diazomethane was quenched with glacial HOAc (ca. 50μl). The mixture was stored at 0-5°C overnight. The solid was filtered off, washed with diethyl ether (2 x $10cm^3$) and recrystallised from methanol to give N-α-carbobenzyl oxy-L-glutamine methyl ester as a white solid (0.90g, 86%) m.p. 137.2-137.5°C (lit.[137] 139-140°C) (Found: C, 57.0; H, 6.1; N, 9.4; calc. for $C_{14}H_{18}N_2O_5$: C, 57.1; H, 6.2; N, 9.5%) ν_{max} (KBr) 3376,

3327 and 3202 (H-bonded amide N-H), 3064 and 3036 (aromatic CH), 2952 (CH_3), 1743 (ester CO), 1694, 1680 (carbamate ester CO), 1653 (amide CO), 1613 (amide II), 1542cm^{-1} (carbamate ester NH); δ_H (90MHz, $CDCl_3$) 7.2 (5H, s, aromatic CH), 6.1 (1H, brs, CONH(H)), 6.0 (1H, brs, CON(H)H), 5.8 (1H, brs, CONH), 4.9 (2H, s, CH_2Ph), 4.2 (1H, m, CH), 3.55 (3H, s, OCH_3), 2.1 (4H, m, CH_2CH_2); δ_C (22.5MHz, $CDCl_3$) 177.4 (ester CO), 174.1 (amide CO), 158.5 (carbamate ester CO), 138.0 (aromatic CH), 129.4 129.0 and 128.7 (aromatic CH), 67.7 (CH_2Ph), 55.0 (CH), 52.7 (OCH_3), 32.4 (CH_2CONH_2), 28.3 ($CHCH_2$).

7.5.8.2 L-Glutamine methyl ester hydrochloride salt

N-α-Carbobenzyloxy-L-glutamine methyl ester (6) was deprotected using a similar method to that described by Sondheimer and Holley.[138] Thus, N-α-carbobenzyloxy-L-glutamine methyl ester (1.16g, 3.94mmole) in MeOH (30cm^3) containing 5M HCl (0.8cm^3, 4mmole) and 10% Pd/C (0.25g) was hydrogenated at room temperature by sparging hydrogen gas through a fine teflon sinter into the stirred solution. The hydrogenolysis reaction was followed by TLC (1:1 (v/v) acetone:acetonitrile on silica, developed with dil. $KMnO_4$ Rf(7) ca. 0.6). The reaction usually required 30-60min for completion. The catalyst was filtered off and the solvent removed under vacuum to give a sticky solid. This was dissolved in distilled water (10cm^3) and filtered through a cotton wool plug to remove any unreacted starting material. The solution was freeze dried to give L-glutamine methyl ester HCl salt as a white hygroscopic solid (0.76g, 98%). The compound was generally used without further purification. Recrystallisation from methanol:ethyl acetate gave a microanalytically pure fine white crystalline solid m.p. 140.9-141.9°C (lit.[138] 145-147°C) (Found: C, 36.3; H, 6.6; N, 14.1; Cl, 18.5; calc. for $C_6H_{13}N_2O_3Cl$: C, 36.65; H, 6.7; N, 14.3; Cl 18.0%) ν_{max} (KBr) 3419 (amide NH), 3187 ($H_3\overset{+}{N}$-NH), 2958 (CH_3), 1746 (ester CO), 1665 (amide CO), 1615 (amide II), 1306 (N-H bond C-N str combination), 1244cm^{-1} (ester C-O); δ_H (90MHz; D_2O), 4.2 (1H, m, CH), 3.8 (3H, s, OCH_3), 2.5 (2H, m, CH_2CONH_2), 2.2 (2H, m, $C(H)CH_2$); δ_C (22.5MHz; D_2O) 178.9 (ester CO), 172.4

(amide CO), 56.0 (OCH_3), 54.6 (CH), 32.7 (CH_2CONH_2), 27.6 ($CHCH_2$); m/z (FAB+ve(glycerol)) 161 ($M+H^+$), 144 ($M+H^+-NH_3$) 84 ($M+H^+-NH_3$-CO-MeOH), 101 ($M+H^+$-CO-MeOH), 321 (M_2+H^+).

7.5.8.3 Methyl-2-diazo-4-carbamoylbutanoate

In the synthesis of diazocompounds it was necessary to carry out the reactions and subsequent purifications in the dark.

L-Glutamine methyl ester HCl salt (0.01g, 0.5mmole) was slurried in freshly distilled, dry CH_2Cl_2 ($2cm^3$). Et_3N ($0.36cm^3$, 2.5mmole) was added and once all the HCl salt had dissolved anhydrous Na_2SO_4 (0.1g) was also added. After cooling the mixture to -40°C N_2O_4 ($0.05cm^3$, 0.79mmole) in dry CH_2Cl_2 ($2cm^3$), pre-cooled with liquid nitrogen in a jacketed pressure-equalised dropping funnel, was added slowly to the stirred solution over 10min. The mixture was allowed to warm to room temperature (ca. 15min) then concentrated under vacuum to ca.$1cm^3$. The diazo product was purified by alumina chromatography (Woelm, neutral, activity 1) with gradient elution using i) $CHCl_3$; ii) 25% (v/v) EtOH in $CHCl_3$; and iii) 40% (v/v) EtOH in $CHCl_3$. After removal of the solvent under vacuum methyl 2-diazo-4-carbamoylbutanoate was obtained as a yellow solid (35.2mg, 41%) m.p. 75.1-75.9°C decomp. (Found: C, 42.5; H, 5.6; N, 23.3; $C_6H_9N_3O_3$ requires: C, 42.1; H, 5.3, N, 24.55%) λ_{max} (EtOH) 261nm (ε 12787 $dm^3mol^{-1}cm^{-1}$) λ_{max} (KBr) 3430, 3295, and 3202 (amide NH), 2957, and 2927 (CH skeletal), 2105 ($C=\overset{+}{N}=\overset{-}{N}$), 1678 (amide CO), 1626 (amide II), 1193cm^{-1} (ester C-O); δ_H (90MHz; $CDCl_3$) 6.2 (2H, br, s, NH_2), 3.8 (3H, s, OCH_3), 2.5 (4H, m, CH_2CH_2); δ_C (22.5MHz; $CDCl_3$) 174.2 (ester CO), 168.0 (amide CO), 55.4 ($C=\overset{+}{N}=\overset{-}{N}$), 51.9 ($OCH_3$), 33.4 ($CH_2CONH_2$), 19.7 ($CH_2C=\overset{+}{N}=\overset{-}{N}$; m/z (FAB+ve(glycerol)) 144 ($M+H^+-N_2$), 112 ($M+H^+$-MeOH-N_2), 172 ($M+H^+$), 84 ($M+H^+$-MeOH-CO-N_2), 100 ($M+H^+-NH_3$-CO), 127 ($M+H^+-N_2-NH_3$), 264 (M+glycerol+H^+), 343 (M_2+H^+), 194 ($M+Na^+$); m/z (FAB+ve accurate mass ($M+H^+-N_2$) (polyethyleneglycol)) Found: 144.0587; $C_6H_{10}NO_3$ requires 144.0661.

7.5.9 Methyl-2-diazo-3-carbamoylpropanoate (N_2AsnOMe)

7.5.9.1 N-α-Carbobenzyloxy-L-asparagine methyl ester

N-α-Carbobenzyloxy-L-asparagine (2g, 7.5mmole) in dry EtOH (40cm^3) at 0°C was treated with excess ethereal diazomethane (ca. 50cm^3) until a permanent yellow colour remained. The reaction was worked-up and purified by recrystallisation from methanol as for carbobenzyloxy-L-glutamine methyl ester to give N-α-carbobenzyloxy-L-asparagine methyl ester as a white solid (1.45g, 69%) m.p. 147.8-148.2°C (Found: C, 55.6; H, 5.7); N,10.0; $C_{13}H_{16}N_2O_5$ requires C, 55.7; H, 5.75; N, 10.0%) ν_{max} (KBr) 3403, 3349, 3300 and 3211 (H-bonded amide NH), 3066 and 3031 (aromatic CH), 2951 (CH_3), 1741 (ester CO), 1681 (carbamate ester CO), 1666 (amide CO), 1611 (amide II), 1550 (carbamate NH), 1198cm^{-1} (ester C-O); δ_H (90MHz; $CDCl_3$) 7.3 (5H, s, aromatic CH), 6.1 (1H, d, NH), 5.7 (2H, s, NH_2), 5.1 (2H, s, CH_2Ph), 4.6 (1H, m, CH), 3.7 (3H, s, OCH_3), 2.8 (2H, m, CH_2CONH_2); δ_C (22.5MHz, $CDCl_3$), 172.0 (ester CO), 171.5 (amide CO), 156.0 (carbamate ester CO), 136.1 (aromatic C), 128.4, 128.1, 127.9 (aromatic CH), 67.0 (CH_2Ph), 52.7 (CH), 50.7 (OCH_3), 37.2 (CH_2CONH_2).

7.5.9.2 L-Asparagine methyl ester hydrochloride salt

N-α-Carbobenzyloxy-L-asparagine methyl ester (1.2g, 4.3mmole) was deprotected using the same procedure described above for L-glutamine methyl ester. After freeze drying, L-asparagine methyl ester hydrochloride salt was obtained as a white hygroscopic salt and was used without further purification (0.78g, 100%) m.p. 72.7-74.1°C (Found: C, 31.5; H, 6.3; N, 14.5; Cl, 18.9; $C_5H_{10}N_2O_3$1HCl $^1/_2$ H_2O requires: C, 31.3; H, 6.3; N, 14.6; Cl, 18.5 %) ν_{max} (KBr) 3429 (amide NH) 3182 ($H_3\overset{+}{N}$ NH), 2960 (CH_3), 1748 (ester CO), 1675 (amide CO), 1615cm^{-1} (amide II); δ_H (90MHz, D_2O) 4.6 (1H, m, CH), 4.0 (3H, s, CH_3), 3.2 (2H, d, CH_2); δ_C (22.5MHz, D_2O), 175.3 (ester CO), 172.0 (amide CO), 56.3 (OCH_3), 51.9 (CH), 36.1 (CH_2); m/z (FAB+ve(glycerol)) 147 ($M+H^+$), 130 ($M+H^+-NH_3$), 115 ($M+H^+$-

MeOH), 87 ($M+H^+$-MeOH-CO), 166 ($M+Na^+$), 293, (M_2+H^+), 331 ($M+(glycerol)_2+H^+$), 239, ($M+glycerol+H^+$).

7.5.9.3 Methyl-2-diazo-3-carbamoylpropanoate

This was prepared by the procedure described for diazoglutamine methyl ester. Thus, asparagine methyl ester HCl salt (0.18g, 0.99mmole) was slurried in dry CH_2Cl_2 ($3cm^3$). Triethylamine ($0.68cm^3$, 4.93mmole) and anhydrous Na_2SO_4 (0.2g) were added. After cooling to -40°C pre-cooled N_2O_4 ($0.1cm^3$, 1.6mmole) in CH_2Cl_2 ($3cm^3$) was added slowly. After warming to room temperature the solution was concentrated and purified by alumina column chromatography (Woelm, neutral, activity 1) using an elution gradient of i) $CHCl_3$; ii) 25% (v/v) EtOH in $CHCl_3$ and iii) 50% (v/v) EtOH in $CHCl_3$. Removal of the solvent under vacuum gave methyl-2-diazo-3-carbamoylpropanoate as a yellow crystalline solid (63mg, 41%) m.p. 78.6-78.5°C (decomp.) (Found: C, 39.0; H, 4.6; N, 26.0; $C_5H_7N_3O_3$ requires C, 38.2; H, 4.5; N, 26.7%), λ_{max} (EtOH) 259nm (ε 12671 $dm^3mol^{-1}cm^{-1}$); λ_{max} (KBr) 3394, 3316, and 3185 (H bonded amide NH), 2955 (CH_3), 2095 ($C=\overset{+}{N}=\overset{-}{N}$), 1703 (ester CO), 1668 (amide CO), 1637 (amide II), 1202cm^{-1} (ester C-O); δ_H (90MHz, $CDCl_3$) 6.6 (2H, br, s, NH_2), 3.8 (3H, s, OCH_3), 3.2 (2H, s, CH_2); δ_C (22.5MHz, $CDCl_3$) 172.1 (ester CO), 167.8 (amide CO), 53.5 ($C=\overset{+}{N}=\overset{-}{N}$), 52.3 ($OCH_3$), 30.1 ($CH_2$); m/z (FAB+ve(glycerol)) 130 ($M+H^+-N_2$), 158($M+H^+$), 98 ($M+H^+$-MeOH-N_2), 113 ($M+H^+-N_2-NH_3$), 70 $M+H^+$-CO-MeOH-N_2), 315 (M_2+H^+), 250 ($M+glycerol+H^+$), 287 ($M_2+H^+-N_2$); m/z (FAB-ve(glycerol)), 156 ($M-H^+$), 128($M-H^+-N_2$), 59 (CO_2Me^-), m/z (FAB+ve accurate mass ($M+H^+-N_2$) (polyethyleneglycol)) Found: 130.0373; $C_5H_8NO_3$ requires 130.0502.

7.5.10 N-α-Carbobenzyloxy-L-asparaginyl-L-leucine methyl ester (8)

Dipeptide (8) was prepared using the procedure described by Sondheimer and Holley.[138]

7.5.10.1 N-α-carbobenzyloxy-L-asparagine hydrazide

A solution of N-α-carbobenzyloxy-L-asparagine methyl ester (0.5g, 1.78mmole) in warm MeOH (7cm^3) was cooled rapidly to 0°C and 99% hydrazine hydrate (0.6cm^3) was added with stirring. The reaction mixture was held at 0-5°C overnight before filtering-off the white hydrazide. The solid was washed with MeOH (ca. 5cm^3) and water (ca. 10cm^3) and dried over P_2O_5 in vacuo to give N-α-carbobenzyloxy-asparagine hydrazide (0.51g, 100%) m.p. 160.6-161.0°C, δ_H (90MHz; CD_3OD) 7.2 (5H, m, aromatic CH), 5.0 (2H, s, CH_2Ph), 4.4 (1H, t, J6.4Hz, CH), 2.5 (2H, d, J6.15Hz, CH_2CONH_2).

7.5.10.2 N-α-carbobenzyloxy-L-asparaginyl azide

2M $NaNO_2$ (0.5cm^3) was added to a solution of N-α-carbobenzyloxy-L-asparagine hydrazide (0.28g, 1.0mmole) in 0.5M HCl (4cm^3) at 0°C. After 15min at 0°C, the white, precipitated azide was filtered-off and washed with 3% $NaHCO_3$ (2 x 1cm^3) and water (2 x 2cm^3), before drying in vacuo over P_2O_5. It was used below without further purification.

7.5.10.3 N-α-Carbobenzyloxy-L-asparaginyl-L-leucine methyl ester

Free leucine methyl ester was prepared by treating a stirred solution of the corresponding HCl salt (0.22g, 1mmole) in Et_2O (6cm^3) with 50% (w/v) K_2CO_3 (1cm^3) at 0°C. After 30min the ether phase was separated, and dried over Na_2SO_4 before being added to a solution of the N-α-carbobenzyloxy-L-asparaginyl azide in DMF (2cm^3). The ether was removed under vacuum at 0°C. The solution was held at 0-5°C for 24h and then at room temperature for a further 24h. Water (3cm^3) was added, to give a fine white precipitate. After stirring for 90min a further aliquot (5cm^3)

of water was added and the solution was held at 0°C for 20min. The precipitated N-α-carbobenzyloxy-L-asparaginyl-L-leucine methyl ester was filtered, washed with water (2 x 10cm^3) and dried in vacuo over P_2O_5 (0.18g, 48%) δ_H (90MHz, CD_3OD), 7.2 (5H, s, aromatic CH), 5.0 (2H, s, CH_2Ph), 4.4 (2H, m, 2 x CH), 3.6 (3H, s, OCH_3), 2.4 (2H, m, CH_2CONH_2), 1.5 (3Hm, $CHCH_2$), 0.8(6H, m, C $(CH_3)_2$); m/z (FAB+ve(glycerol)) 91 (CH_2Ph), 394 ($M+H^+$), 146 (Leu OMe+H^+), 260 (AsnLeuOMe+H^+), 377 ($M+H^+-NH_3$), 185, 177, 249 ($PhCH_2OCONHCH(CH_2CONH_2)CO^+$).

7.5.11 N-α-Carbobenzyloxy-L-asparaginylglycine ethyl ester (9)

N-α-Carbobenzyloxy-L-asparaginylglycine ethyl ester was prepared via two separate synthetic pathways.

7.5.11.1 N-α-Carbobenzyloxy-L-asparaginylglycine ethyl ester (9)

Dipeptide (9) was prepared from asparagine methyl ester and glycine ethyl ester HCl salt (0.37g, 2.6mmole) using the method described for N-α-carbobenzyloxy-L-asparaginyl-L-leucine methyl ester. This gave N-α-carbobenzyloxy-L-asparaginylglycine ethyl ester as a white solid (0.36g, 39%) m.p. (water) 153.1-153.6°C (lit.[162] 184-185°C); δ_H (90MHz, CD_3OD), 7.2 (5H, m, aromatic CH), 5.0 (2H, s, CH_2Ph), 4.0 (2H, q, J7.2Hz, CH_2Me), 3.7 (2H, d, CH_2NH), 2.6 (2H, d, J6.15Hz, CH_2CONH_2) 1.1 (3H, t, J7.2Hz CH_3CH_2); m/z (FAB+ve(glycerol)) 91 (CH_2Ph^+), 352 ($M+H^+$), 87, 335 ($M+H^+-NH_3$), 104 ($H_3NCH_2CO_2Et^+$), 367 ($M+H^+-NH_3$-MeOH).

7.5.11.2 N-α-Carbobenzyloxy-L-asparaginylglycine ethyl ester

1-Hydroxybenzotriazole (0.51g, 3.8mmole) and dicyclohexylcarbodiimide (DCC) (0.77g, 3.8mmole) in dry DMF (10cm^3) were heated under reflux and argon for 90min to give an orange solution. The solution was cooled to 0°C and N-α-carbobenzyloxy-L-asparagine (0.5g, 1.9mmole) and DCC (0.39g, 1.9mmole) were added. The mixture

was stirred at 0°C for 45min and at room temperature for a further 15min. Free glycine ethyl ester, prepared from the appropriate HCl salt (0.262g, 1.1mmole) and Et_3N (0.19g, 1.9mmole) in dry DMF (2cm^3), was added to the N-α-carbobenzyloxy-L-asparagine solution and the mixture stirred at room temperature under argon for 60h. The precipitated urea was filtered-off and washed with DMF (2 x 2cm^3). The DMF was removed from the combined filtrates under vacuum to give a brown oil. The oil was dissolved in EtOAc (40cm^3) and the white solid, which precipitated from the solution on trituration, was filtered off. The ethylacetate filtrate was washed with 2% (w/v) citric acid (2 x 20cm^3), 10% (w/v) Na_2CO_3 (2 x 20cm^3) and finally with water (2 x 20cm^3). It was then dried over Na_2SO_4, removing the solvent under vacuum to give N-α-carbobenzyloxy-L-asparaginylglycine ethyl ester as an off white solid (0.23g, 34%) m.p. (water) 148.2-149.6°C (lit.[162] 184-185°C) δ_H (90MHz, $CDCl_3$), 7.3 (5H, s, aromatic CH), 5.13 (2H, s, CH_2Ph), 4.1 (3H, m, CH, CH_2COEt), 1.8-1.3 (25H, br, m, CH_2, CH_2CH_3+DCC+urea); m/z 91 (CH_2Ph^+), 225 (dicyclohexyl urea +H^+), 75, 57, 61, 352 (M+H^+), 104 ($H_3NCH_2CO_2Et^+$), 335 (M+H^+-NH_3), 249 (M+H^+-H_2N-CH_2CO_2Et), 219 (M+H^+-$PhCH_2OH$-CO).

7.5.12 N-α-Carbobenzyloxy-L-glutaminyl-L-leucine methyl ester (10)

Compound (10) was prepared using the same method as for N-α-carbobenzyl-oxy-L-asparaginyl leucine methyl ester.

7.5.12.1 N-α-Carbobenzyloxy-L-glutamine hydrazide (11)

Hydrazide (11) was prepared from N-α-carbobenzyloxy-L-glutamine methyl ester (1.00g, 3.4mmole). N-α-Carbobenzyloxy-L-glutamine hydrazide was obtained as a white crystalline solid (1.0g, 94%) m.p. 173.8-174.2°C (lit.[138] 173-176°C) δ_H (90MHz; CD_3OD) 7.2 (5H, m, aromatic CH), 4.9 (2H, s, CH_2Ph) 4.0 (m, 1H, CH), 1.8-2.2 (4H, m, $CH_2CH_2CONH_2$).

7.5.12.2 N-α-Carbobenzyloxy-L-glutaminyl-L-leucine methyl ester

Compound (11) (0.31g, 1.0mmole) in 0.5M HCl ($4cm^3$) was converted to N-α-carbobenzyloxy-L-glutaminyl azide upon treatment with 2M $NaNO_2$ ($0.5cm^3$). A solution of the azide in DMF was treated with L-leucine methyl ester, prepared from the corresponding hydrochloride salt (0.22g, 1.2mmole). The mixture was held at 0°C for 12h and at room temperature for 24h. On the addition of water ($3cm^3$) a white solid precipitated from the solution. After 3h at room temperature a second aliquot of water ($4cm^3$) was added and the mixture was held at 0-5°C for 3h. N-α-Carbobenzyloxy-L-glutaminyl-L-leucine methyl ester was recrystallised from DMF:water (ca. 1:1 v/v) (0.27g, 66%) m.p. 162.4-163.1°C (lit.[138] 163-164°C) δ_H (90MHz; CD_3OD) 7.2 (5H, s, aromatic CH), 4.9 (2H, s, CH_2Ph), 4.3 (1H, m, CH), 4.1 (1H, m, CH), 3.6 (3H, s, OCH_3), 2.2 (2H, t, CH_2CONH_2) 1.9 (2H, m, CH_2-(CH_2CONH_2)), 1.4 (3H, m, $CH_2CH(Me)_2$), 0.8 (6H, m, $C(CH_3)_2$); m/z (FAB+ve (glycerol)) 91 (CH_2Ph^+), 146 (LeuOMe+H^+), 274 (GlnLeuOMe+H^+), 408 (M+H^+), 174, 257, 129 ($H_2NCH(CO)CH_2)_2CONH_2^+$).

7.5.13 N-α-Carbobenzyloxy-L-glutaminylglycine ethyl ester (12)

The dipeptide (12) was prepared from N-α-carbobenzyloxy-L-glutamine hydrazide (1.25g 4.7mmole) and glycine ethyl ester HCl salt (0.50g, 3.58mmole) as described for N α-carbobenzyloxy asparaginyl-L-leucine methyl ester. N-α-Carbobenzyloxy-L-glutaminylglycine ethyl ester was obtained as a white solid (0.65g, 38%) δ_H (90MHz, CD_3OD), 7.2 (5H, m, aromatic CH), 5.0 (2H, s, CH_2Ph), 4.1 (1H, m, CH), 4.0 (2H, q, J7.2 Hz, CH_2Me), 3.8 (2H, s, CH_2), 2.2 (2H, m, CH_2CONH_2), 1.9 (2H, m, $CH_2CH_2CONH_2$), 1.1 (3H, t, J7.2Hz, CH_3).

7.5.14 N(2-Diazo-4-carbamoylbutanoyl)phenylalanine methyl ester (N_2GlnPheOMe)

7.5.14.1 N-α-Carbobenzyloxy-L-glutamine-p-nitrophenyl ester

Method 1

The method of Bodanszky and DuVigneaud[157] was used to prepare the activated ester. Thus to a solution of N-α-carbobenzyloxy-L-glutamine (1g, 3.6mmole) in DMF (9cm^3) at 0°C were added dicyclohexylcarbodiimide (0.74g, 3.6mmole) and p-nitrophenol (0.6g, 4.3mmole). The solution was held at 0°C for 1h and then allowed to warm to room temperature. The precipitated urea was removed by filtration and water (ca. 20cm^3) was added to the filtrate to precipitate the product. The white solid was filtered-off and washed with water (100cm^3) before drying in vacuo. The N-α-carbobenzyloxy-L-glutamine p-nitrophenyl ester was purified by redissolving in DMF, filtering and re-precipitating with water (0.76g, 53%) m.p. 151.5-151.8°C (lit.[157] 155-156°C).

Method 2

An alternative synthesis of N-α-carbobenzyloxy-L-glutamine p-nitrophenyl ester involved using ethyl 3(3-dimethylaminopropyl)carbodiimide hydrochloride instead of DCC. Thus to N-α-carbobenzyloxy-L-glutamine (1g, 3.6mmole) in DMF (9cm^3) at 0°C were added p-nitrophenol (0.6g, 4.3mmole) and ethyl 3(3-dimethylaminopropyl) carbodiimide hydrochloride (0.68g, 3.6mmole). After 2h 0°C and a further 2h at room temperature the mixture was poured into water (50cm^3). The white precipitate was removed by filtration, washed with water (100cm^3) and dried in vacuo over $CaCl_2$. N-α-Carbobenzyloxy-L-glutamine p-nitrophenyl ester was recrystallised from acetonitrile (0.72g, 50%) m.p. 152.6-153.3°C (lit.[157] 155-156°C) δ_H (90MHz, $(CD_3)_2CO$) 8.4 (1H, s, NH(H)), 8.3 (1H, s, N(H)H), 7.4 (9H, m, aromatic CH), 5.1 (2H, s, CH_2Ph), 4.5 (1H, m, CH), 2.4

(4H, m, $CH_2CH_2CONH_2$); m/z (FAB+ve(thiodimethanol)), 91 (CH_2Ph^+), 87, 75, 402 ($M+H^+$), 263 ($M+H^+$-$HOPhNO_2$), 358.

7.5.14.2 N-α-Carbobenzyloxy-L-glutaminyl-L-phenylalanine methyl ester (13)

Method 1

Et_3N (0.96cm^3) was added to N-α-carbobenzyloxyglutamine p-nitrophenyl ester (2.0g, 5.00mmole) and phenylalanine methyl ester HCl salt (1.08g, 5.01mmole) in dry DMF (5cm^3) at 0°C. The reaction was held at room temperature overnight during which time a solid was precipitated. The mixture was slurried in water (150cm^3) before filtering and washing with water (100cm^3) and drying in vacuo over $CaCl_2$. It was purified by silica column chromatography using an eluent gradient from 100% EtOAc to 100% CH_3CN to give N-α-carbobenzyloxy-L-glutaminyl-L-phenylalanine methyl ester as a white solid (1.64g, 75%) m.p. 173.6-174.5°C.

Method 2

A more efficient synthesis of (13) was carried out using the method of Yamada et al.[154] N-α-carbobenzyloxy-L-glutamine (5g, 18mmole) and phenylalanine methyl ester HCl salt (4.6g, 21mmole) in DMF (50cm^3) were cooled at 0°C and diphenylphosphoryl-azide (5.38g, 20mmole) in DMF (50cm^3) was added dropwise. After this addition Et_3N (5.4cm^3, 39mmole) was added and the solution was held at 0°C overnight. The volume of the mixture was then reduced (ca. 30cm^3) and distilled water (ca. 20cm^3) was added to precipitate the product. The mixture was held at 0°C for 5h before filtering off the product. The N-α-carbobenzyloxy-L-glutaminylphenylalanine methyl ester was washed with water and dried in vacuo over silica gel (7.30g, 93%) m.p. 174.1-174.4°C. (Found: C, 62.7; H, 6.2; N, 9.4; $C_{23}H_{27}N_3O_6$ requires: C, 62.6; H, 6.2; N, 9.5%) ν_{max} (KBr) 3414 (amide NH), 3303 (carbamate ester NH), 3067 (aromatic CH), 2956 (CH_3), 1746 (ester CO), 1684 (carbamate ester CO), 1654 (amide CO), 1538 (amide II carbamate), 1184cm^{-1} (ester C-O); δ_H (90MHz; $(CD_3)_2SO$) 8.3

(1H, d, J7.08Hz, NH), 7.4 and 7.2 (12H, 2 x 5 aromatic CH+NH+NH(H)), 6.8 (1H, s, N(H)H), 5.0 (2H, s, OCH_2Ph), 4.5 (1H, m, CH), 4.0 (1H, m, CH), 3.6 (3H, s, OCH_3), 3.0 (2H, d, J7.08Hz, CH_2Ph), 2.1 (2H, m, CH_2), 1.8 (2H, m, CH_2); δ_C (22.5MHz, $CDCl_3$) 179.3 (ester CO), 175.8 (amide CO), 174.9 (amide CO), 159.9 (carbamate CO), 139.5 (CBZ, aromatic C), 131.9 ($PhCH_2CH$ aromatic C), 131.1, 130.6, 130.5 and 129.5 (aromatic CH), 69.4 ($PhCH_2O$), 57.4 ($CHCO_2Me$), 56.8 (CH), 54.3 (OCH_3), 39.9 (CH_2Ph), 34.0 (CH_2CONH_2), 30.7 (CH_2).

7.5.14.3 L-Glutaminyl-L-phenylalanine methyl ester HCl salt

N-α-Carbobenzyloxy-L-glutaminyl-L-phenylalanine methyl ester (8g, 18mmole) was dissolved in MeOH ($400cm^3$) containing 1.0M HCl ($18cm^3$). After addition of 10% Pd/C (1.6g) hydrogen was sparged through the stirred solution at room temperature. The reaction was monitored by silica TLC (eluent 3:2 (v/v) $(CH_3)_2CO$:CH_3CN) and required ca. 90min. Once complete, the catalyst was removed by filtration and washed with methanol (2 x $10cm^3$). The solvent was removed from the combined filtrates, under vacuum to give a sticky white solid. This was dissolved in water (ca. $30cm^3$) and filtered through a cotton wool plug before freeze drying. L-Glutaminyl-L-phenylalanine methyl ester HCl salt was obtained as a white hygroscopic solid (6.23g, 100%) m.p. 91.0-91.7°C (Found: C, 51.7; H, 6.6; N, 11.85; $C_{15}H_{21}N_3O_4$ HCl $^1/_4$ H_2O requires: C, 51.7; H, 6.5; N,12.1%) ν_{max} (KBr), 3412 (amide NH), 3202 ($-\overset{+}{N}H_3$ NH), 3061 (aromatic CH), 2953(CH_3), 1740 (ester CO), 1667 (amide CO), 1606 (aromatic C=C), 1552cm^{-1} (amide II); δ_H (90MHz; $(CD_3)_2SO$) 9.2(1H, d, J7.08Hz, NH), 8.4(3H, brs, $\overset{+}{N}H_3$), 7.6(1H, s, NH(H)), 7.3(5H, s, aromatic CH), 7.0(1H, s, N(H)H), 4.5(1H, m, J_{NHCH} 7.08Hz, $CHCO_2Me$), 3.9(1H, brm, $CH\overset{+}{N}H_3$), 3.6(3H, s, OCH_3), 3.0(2H, d, J7.57Hz, CH_2Ph); 2.2 (2H, m, CH_2CONH_2), 2.0(2H, m, CH_2CH); δ_C (100MHz; D_2O) 177.44 (ester CO), 173.56 (s amide CO), 169.77 (p amide CO), 136.98 (aromatic -C) 129.92, 129.56 and 128.04 (aromatic CH), 55.27($CHCO_2Me$), 53.71(OCH_3), 53.14($CHNH_3^+$), 37.11(CH_2Ph), 30.83(CH_2CONH_2), 27.35(CH_2); m/z (FAB+ve (glycerol)) 308($N+H^+$),

84($C_4H_6NO^+$), 120($H_2N{=}CHCH_2Ph$), 180(PheOMe+H^+) 231(M+H^+-NH_3-MeOH), 291 (M+H^+-NH_3), 101 ($H_2N{=}CHCH_2CH_2CONH_2^+$).

7.5.14.4 N-(2-Diazo-4-carbamoylbutanoyl)phenylalanine methyl ester

As with N_2GlnOMe and N_2AsnOMe precautions were taken to exclude light during the synthesis and purification of diazoglutaminylphenylalanine methyl ester.

L-Glutaminyl-L-phenylalanine methyl ester HCl salt (1.04g, 3.0mmole) was slurried in dry CH_2Cl_2 ($10cm^3$) under argon. Et_3N (1.26ml, 9.0mmole) was added and, once all the HCl salt had dissolved, more CH_2Cl_2 ($40cm^3$) and anhydrous Na_2SO_4 (5g) were added. The reaction solution was cooled to -78°C with stirring. N_2O_4 ($0.28cm^3$, 4.4mmole) in dry CH_2Cl_2 ($40cm^3$) pre-cooled to -78°C in a jacketed pressure-equalised dropping funnel was then added slowly over ca. 15min. Once the addition was complete, the mixture was allowed to warm to room temperature before filtration to remove the Na_2SO_4. The solvent was removed under vacuum and the residue was taken up in dry acetone ($1cm^3$). Precipitated $Et_3\overset{+}{N}HCl^-$ was filtered-off and the filtrate was worked-up by silica column chromatography using a gradient eluent of ether to 75% (v/v) acetone in ether. After evaporation of the solvent N(2-diazo-4-carbamoylbutamoyl)phenylalanine methyl ester was isolated as a highly hygroscopic yellow solid, (0.25g, 26%) m.p. 76.8-77.8°C decomp. λ_{max} (EtOH) 289nm (ε10516 $dm^3\ mol^{-1}cm^{-1}$); (KBr) 3401 (amide NH), 3063 and 3031 (aromatic CH), 2953 (CH_3), 2085 ($C{=}\overset{+}{N}{=}\overset{-}{N}$), 1741 (ester CO), 1667 (amide CO), 1620 (amide II), 1206cm^{-1} (ester C-O); δ_H (90MHz, $CDCl_3$), 7.2 (5H, m, aromatic CH), 6.9 (1H, d, J7.8Hz, NH), 6.3 (1H, br, s, NH(H)), 6.1 (1H, br, s, N(H)H), 4.8 (1H, m, CH), 3.7 (3H, s, OCH_3), 3.1 (2H, m, CH_2Ph), 2.5 (4H, m, CH_2CH_2); δ_C (22.5MHz; $CDCl_3$), 174.5 (ester CO), 172.8 (s amide CO), 166.6 (p amide CO), 136.6 (aromatic-C), 129.1 128.6 and 127.0 (aromatic CH), 57.6 ($C{=}\overset{+}{N}{=}\overset{-}{N}$), 54.2 (CH), 52.3 ($OCH_3$), 37.8 ($CH_2Ph$), 33.6 ($CH_2CONH_2$), 19.4 ($CH_2C{=}\overset{+}{N}{=}\overset{-}{N}$); m/z (FAB=ve(glycerol)) 120 ($H_2N{=}CHCH_2Ph^+$), 91 (CH_2Ph^+), 84 (C_4H_6NO), 291 (M+H^+-N_2), 180

(PheOMe+H^+), 231 (M+H^+-N_2-HCO_2Me), 112 (N=N=$CCH_2CH_2CO_2NH_2^+$); m/z (FAB+ve(tetraethyleneglycoldiethylether (TEGDE))) 291 (M+H^+-N_2), 319 (M+H^+); (m/z (FAB-ve (TEGDE)) 317 (M-H^+); m/z (FAB+ve accurate mass (M+H^+) and (M+H^+-N_2) (polyethylene glycol)) Found: 319.1500 $C_{15}H_{19}N_4O_4$ requires 319.1406, Found: 291.1420 $C_{15}H_{19}N_2O_4$ requires 291.1344.

7.5.15 N(2-Diazo-3-carbamoylpropanoyl)phenylalanine methyl ester (N_2AsnPheOMe)

7.5.15.1 N-α-Carbobenzyloxy-L-asparaginyl-L-phenylalanine methyl ester

This was prepared from N-α-carbobenzyloxy-L-asparagine (4.75g, 18mmole) and phenylalanine methyl ester HCl salt (4.6g, 21mmole) using the Yamada[154] procedure described for N-α-carbobenzyloxy-L-glutaminylphenylalanine methyl ester. N-α-carbobenzyloxy-L-glutaminylphenylalanine methyl ester was obtained as a white solid (6.87g, 90%) m.p. 190.5-190.8°C (Found: C, 61.5; H, 5.9; N, 9.9; calc. for $C_{22}H_{25}N_3O_6$ C, 61.8; H, 5.9; N, 9.8%) ν_{max} (KBr) 3436 (amide NH), 3301 (carbamate ester NH), 3063 (aromatic CH), 2952 (CH_3), 1739 (ester CO) 1698 (carbamate ester CO), 1661 (amide CO), 1640 (amide II), 1540cm^{-1} (amide II carbamate); δ_H (90MHz; $(CD_3)_2SO$) 8.3 (1H, d, NH), 7.3 and 7.2 (12H, 2 x s, aromatic CH+NH+NH(H)); 6.9 (1H, s, N(H)H), 5.0 (2H, s, $PhCH_2O$), 4.4 (2H, m, CH, CH), 3.6 (3H, s, OCH_3), 3.0 (2H, s, J7.08Hz, CH_2Ph), 2.4 (2H, m, CH_2).

7.5.15.2 L-Asparaginyl-L-phenylalanine methyl ester HCl salt (14)

The dipeptide (14) was prepared in a similar manner to the L-glutaminyl analogue. Thus N-α-carbobenzyloxy-L-asparaginyl-L-phenylalanine methyl ester (1.75g, 4.1mmole) was dissolved in MeOH (200cm^3) containing 1.0M HCl (4.1cm^3) and 10% Pd/C (0.5g). After hydrogenolysis and work-up as previously described L-asparaginyl-L-phenylalanine methyl ester hydrochloride was obtained as a white

hygroscopic solid (1.32g, 98%) m.p. 89.7-90.7°C (Found: C, 49.1; H, 6.1; N, 12.45; Cl, 11.3; $C_{14}H_{19}N_3O_4$ $1HCl^3/_4$ H_2O requires: C, 48.95; H, 6.4; N, 12.2; Cl, 10.3%) ν_{max} (KBr) 3411 (amide NH), 3196 ($H_3\overset{+}{N}$-NH), 3063 (aromatic CH), 2954 (CH_3), 1740 (ester CO), 1675 (amide CO), 1605 (aromatic C=C), 1556cm^{-1} (amide II); δ_H (90MHz; $(CD_3)_2SO$) 9.2 (1H, d, J7.08Hz, NH), 8.4 (3H, br, s, -$\overset{+}{N}H_3$), 7.9 (1H, s, NH(H)), 7.3 (6H, s+sh, aromatic CH+N(H)H), 4.5 (1H, m, $CHCO_2Me$), 4.1 (1H, m, $CH\overset{+}{N}H_3$), 3.6 (3H, s, OCH_3), 3.0 (2H, d, J5.37Hz, CH_2Ph), 2.8 (2H, m, CH_2CONH_2); δ_C (22.5MHz; $(CD_3)_2SO$) 171.2 (ester CO), 170.7 (s amide CO), 168.3 (p amide CO), 136.8 (aromatic-C) 129.0, 128.3 and 126.6 (aromatic CH), 54.1 ($CHCO_2Me$), 51.9 (OCH_3), 48.9 ($CH\overset{+}{N}H_3$), 36.2 (CH_2Ph), 35.3 (CH_2CONH_2); m/z (FAB+ve(glycerol)) 120 ($H_2N{=}CHCH_2\overset{+}{P}h$), 87 ($H_2N{=}CHCH_2CONH_2^+$), 294 ($M+H^+$), 91 ($CH_2Ph^+$), 180 (PheOMe+$H^+$), 44 ($H_2NCO^+$), 70 ($C_3H_4N\overset{+}{O}$), 277 ($M+H^+$-$NH_3$), 260 ($M+H^+$-$NH_3$-$NH_3$), 235 ($M+H^+$-$H_2NCOCH_3$), 200 ($M+H^{+-NH_3}$-$NH_3$-$HCO_2Me$).

7.5.15.3 N-(2-Diazo-3-carbamoylpropanoyl)phenylalanine methyl ester

This was synthesised by a similar procedure to that for diazoglutaminyl-L-phenylalanine methyl ester from L-asparaginyl-L-phenylalanine methyl ester HCl salt (0.50g, 1.5mmole) and N_2O_4 (0.144ml, 2.27mmole). After filtration and removal of the organic solvent under vacuum the residue was taken up in EtOAc (1cm^3) and the precipitated $Et_3\overset{+}{N}HCl^-$ was removed by filtration. The filtrate was chromatographed on silica using ethyl acetate as the eluent to give N-(2-diazo-3-carbamoylpropanoyl)phenylalanine methyl ester as a yellow hygroscopic solid (65mg (14%)) m.p. 44.9-47.8 °C decomp. λ_{max} (EtOH) 260nm (ε 5754 dm^{3}mol^{-1}cm^{-1}) ν_{max} (KBr) 3415 (amide NH), 3063 and 3030 (aromatic OH), 2954 (CH_3), 2092 ($C{=}\overset{+}{N}{=}\overset{-}{N}$), 1741 (ester CO), 1673 (amide CO), 1625 (amide II) 1207cm^{-1} (ester C-O); δ_H (90MHz, $CDCl_3$) 7.2 (5H, m, aromatic CH), 7.0 (1H, d, J8.05Hz, NH), 6.8 (1H, brs, NH(H)), 6.2 (1H, brs, N(H)H), 4.8 (1H, m, CH), 3.7 (3H, s, OCH_3), 3.1 (4H, m, CH_2Ph+CH_2CONH_2); δ_C (22.5MHz, $CDCl_3$) 172.8 (ester CO), 172.4 (s amide

CO), 166.2 (p amide CO), 136.1 (aromatic-C), 129.2, 128.6 and 127.1 (aromatic CH), 54.6 ($C=\overset{+}{N}=\overset{-}{N}$) 54.2 (CH), 52.4 (OCH3), 37.8 (CH_2Ph), 30.4 (CH_2CONH_2); m/z (FAB+ve(TEGDE)) 305 ($M+H^+$), 277 ($M+H^+-N_2$); m/z (FAB-ve(TEGDE)) 303 ($M-H^+$); m/z (FAB+ve accurate mass ($M+H^+-N_2$) (polyethyleneglycol) Found: 277.1198 $C_{14}H_{17}N_2O_4$ requires 277.1188.

CHAPTER 8 REFERENCES

1. P. N. Magee & J. M. Barnes, *Adv. Cancer Res.*, 1976, **10**, 163.

2. P. N. Magee , R. Montesano & R. Preussmann, "Chemical Carcinogens" ed. C. E. Searle, ACS Monograph 173, American Chemical Society, Washington D. C., 1976, p.491.

3. S. S. Mirvish, *Toxicol. Appl. Pharmacol.*, 1975, **31**, 325.

4. C. L. Walters, M. J. Hill & W. S. J. Ruddel, "Environmental Aspects of N-Nitroso Compounds", Eds., E. A. Walker, M. Castegnaro, L. Griciute & R. E. Lyle, IARC, Scient. Publ. Nº **19**, IARC, Lyon, France 1977, p.279.

5. S. R. Tannenbaum, M. Weisman & D. Fett, *Food Cosmet. Toxicol.*, 1976, **14**, 549.

6. P. I. Reed, P. L. R. Smith, K. Haines, F. R. House & C. L. Walters, *Lancet*, 1981, ii 550.

7. S. R. Tannenbaum , "Relevance of N-nitrosocompounds to Human Cancer: and Mechanisms' Eds. H. Bartsch, I. K. O'Neill & R. Schultz-Hermann, IARC Scient Publ Nº 84, IARC, Lyon, France,1987, p.292.

8. W. Kubacka, L. M. Libbey & R. A. Scanlan, *J. Agric. Food Chem.*, 1984, **32**, 401.

9. W. Kubacka & R. A. Scanlan, *Ibid*, 404.

10. S. E. Shephard, C. H. Schlatter & W. K. Lutz, *Fd. Chem. Toxicol.*, **25**, 91, 1987.

11. S. E. Shephard, C. H. Schlatter & W. K. Lutz, in ref 7 p.328.

12. B. C. Challis, B. R. Glover & J. R. A. Pollock, in ref 7 p.345.

13. B. C. Challis, J. R. Milligan & R. C. Mitchell, *J. Chem. Soc. Chem. Common.*, 1984, 1050

14. B. C. Challis, A. R. Hopkins & J. R. Milligan R. C. Massey, D. Anderson & S. D. Blowers, *Toxicol. Lett.*, 1985, **26**, 89.

15. C. Monti-Bragadin, M. Tamaro & E. Banfi, *Antimicrob. Agents and Chemotherapy*, 1974, **6**, 655.

16. E. Banfi, M. Tamaro, B. Pani & C. Monti-Bragadin, *Boll. Inst. Sieroter. Milan*, 1974, **531**, 632.

17. J. H. Ridd, *Quart. Review*, 1961, **15**, 418.

18. B. C. Challis & A. R. Butler, "The Chemistry of the Amino Group" Ed. S. Patai, *Interscience*, John Wiley and Sons, London, 1968, p.305.

19. B. C. Challis, "Safety Evaluation of Nitrosable Drugs and Chemicals", Eds. G. G. Gibson & C. Loannides, Taylor and Francis Ltd, London, 1981, p.16.

20. A. F. Hegarty, "The Chemistry of the Diazonium and Diazo Groups", Ed. S. Patai, John Wiley and Sons Ltd, Chichester, 1978, p.511.

21. K. Bott , *Angew. Chem. Int. Edn.*, 1979, **18**, 259.

22. H. Zollinger, "Azo and Diazo Chemistry", *Interscience*, N. Y. 1961.

23. For a comprehensive review, see "The Chemistry of the Diazonium and Diazo Groups", Ed. S. Patai, Chichester, 1978.

24. G. W. Cowell & A. Ledwith, *Quart. Rev.*, 1970, **24**, 119.

25. W. Rundell, *Angew. Chem.*, 1962, **74**, 469.

26. T. Curtius, *Ber.*, 1889, **22**, 2161.

27. W. R. Bamford & T. S. Stevens, *J. Chem. Soc.*, 1952, 4735.

28. S. M. Hecht & J. W. Kozarich, *Tetrahedron Lett.*, 1972, **50**, 5147.

29. D. A. Ben-Etraim, in ref 20, p149

30. F. C. Whitmore & D. P. Langelois, *J. Am. Chem. Soc.*, 1932, **54**, 3441

31. A. Streitweiser Jr. & W.D. Schaeffer, *J. Am. Chem. Soc* ,1957, **79**, 2888.

32. D. J. Cram & J. E. McCanty, *J. Am. Chem. Soc.*, 1957, **79**, 2866.

33. D. Semenow, C. L. Shih & W. G. Young, *J. Am. Chem. Soc.*, 1958, **80**, 5472.

34. D. D. Van-Slyke, A. Hiller, R. A. Phillips, P. B. Hamilton, V. P. Dole, R. M. Archibald & H. A. Eder *J. Biol. Chem.* 1950, 331.

35. P. A. Morris & D. L. H. Williams, *J. Chem. Soc. Perkin Trans. II*, 1988, 513.

36. D. L. H. Williams, *Chem. Rev.*, 1985, **14**, 171.

37. R. Bonnett & P. Nicolaidou, *Heterocycles*, 1977, **7**, 637.

38. S. S. Mirvish, J. Sams, T. Y. Fan & S. R. Tannenbaum, *J. Natl. Cancer Inst.*, 1973, **51**, 1833.

39. K. Hildrum, J. L. Williams & R. A. Scanlan, *J. Agric. Food Chem.*, 1975, **23**, 439.

40. T. A. Meyer & D. L. H. Williams, *J. Chem. Soc. Perkin Trans. II*, 1988, 517.

41. C. Janzowski, R. Klein, P. Preussmann & G. Eisenbrand, *Fd. Chem. Toxicol.*, 1982, **20**, 595.

42. A. Kurosky & T. Hoffmann, *Can. J. Biochem.*, 1972, **50**, 1282.

43. J. Casado, A. Castro, J. R. Leis, M. Mosquera & M. E. Pena, *J. Chem. Soc. Perkin Trans. II*, 1985, 1859.

44. T. Curtius, *Ber.*, 1904, **37**, 1285.

45. T. Curtius & A. Darapsky, *Ber.*, 1906, **39**, 1373.

46. T. Curtius & J. Thompson, *Ber.*, 1906, **39**, 1379.

47. T. Curtius & T. Callan, *Ber.*, 1910, **43** 2447.

48. J. H. Looker & J. W. Carpenter, *Canad. J. Chem.*, 1967, **45**, 1727.

49. T. Curtius & E. Miller, *Ber.*, 1904, **37**, 1261.

50. H. Reimlinger & L. Skatteböl, *Ber.*, 1960, **93**, 2162.

51. E. H. White & R. J. Baumgarten, *J. Org. Chem.*, 1964, **29**, 2070.

52. R. J. Baumgarten, *J. Org. Chem.*, 1967, **32**, 484.

53. N. Takamura, T. Mizoguchi, K. Koga & S. Yamada, *Tetrahedron Lett.*, 1971, **47**, 4495.

54. N. Takamura, T. Mizoguchi, K. Koga & S. Yamada, *Tetrahedron*, 1975, **31**, 227.

55. J. F. McGarrity, *J. Chem. Soc. Chem. Commun.*, 1974, 558.

56. G. N. Okafo, Ph.D Thesis, London, 1989.

57. B. C. Challis & S. Shuja current work.

58. B. C. Challis, M. H. R. Fernandes, B. G. Glover & F. Latif, ref 7 p.308.

59. B. C. Challis & F. Latif, *J. Chem. Soc. Perkin Trans. I*, 1990, 1005.

60. W. J. Baron, M. R. DeCamp, M. E. Hendrick, M. Jones Jr., R. H. Levin & M. B. Sohn, "Carbenes" Volume I., Eds. M. Jones Jr., R. A. Moss, John Wiley and Sons, N. Y. 1973, p.1.

61. H. Chaimovich, R. J. Vaughan & F. H. Westheimer, *J. Am. Chem. Soc.*, 1968, **90**, 4088.

62. T. Curtius & J. Thompson, *Ber.*, 1906, **39**, 4140.

63. B. G. Glover, Ph.D Thesis, London, 1985

64. W. J. Albery, A. N. Campbell-Crawford & K. S. Hobbs, *J. Chem. Soc. Perkin Trans. II.*, 1972, 2180.

65. W. J. Albery & R. P. Bell, *Trans. Faraday Soc.*, 1961, **LVII**, 1942.

66. W. J. Albery & M. H. Davies, *Trans. Faraday Soc.*, 1969, **LXV**, 1066.

67. W. J. Albery, J. E. C. Hutchins, R. M. Hyde & R. H. Johnson, *J. Chem. Soc. B.*, 1968, 219.

68. M. M. Kreevoy & D. E. Konasewich, *J. Phys. Chem.*, 1970, **74**, 4464.

69. F. Latif, Ph.D Thesis, University of London 1986

70. R. Piria, *Ann. Chem. Phys.*, 1848, **22**, 160.

71. G. A. Olah & J. Welch, *Synthesis*, 1974, 652.

72. J. P. Gouesnard, *Boll. Soc. Chem. Fr.*, 1989, 88.

73. P. Brewser, F. Hiron, E. D. Hughes, C. K. Ingold & P. A. D. S. Rao, *Nature*, 1950, **166**, 178.

74. C. K. Ingold, "Structure and Mechanism in Organic Chemistry", G. Bell and Sons Ltd., London, 1963, p381.

75. M. Larcheveque & Y. Petit , *Tetrahedron Lett.*, 1984, **25**, 3705.

76. "Asymmetric Synthesis - Construction of Chiral Molecules using Amine Acids" Eds. G. M. Coppola & H. F. Schoster, John Wiley and Sons Inc., N. Y., 1987.

77. S. Henrot, M. Larcheveque & Y. Petit, *Synth. Commun.*, 1986, **16**, 183.

78. M. B. Takeo & A. Eiichi, see *Chem. Abs.*, 83 (23) 193732 K.

79. S. G. Cohen & S. Y. Weinstein, *J. Am. Chem. Soc.*, 1964, **86**, 5326.

80. K. Koga, C. C. Wu & S. Yamada *Tetrahedron Lett.*, 1971 **25**, 2287.

81. A. T. Austin, *J. Chem. Soc.*, 1950, 149.

82. J. R. A. Pollock, "N-Nitrosocompounds: Occurrence and Biological Effects" Eds. H. Bartsch, I. K. O'Neill & M. Castegnaro, IARC, Scient.Publ Nº 41, p.81.

83. A. R. Tricker & R. Preussmann, *Carcinogenisis*, 1986, **7**, 1523.

84. J. R. A. Pollock ,*Fd. Chem. Toxicol.*, 1985 **23** 701.

85. A. T. Austin & J. Howard, *J. Chem. Soc.*, 1961, 3278.

86. J. H. Markgraf & H. A. Davis, *J. Chem. Ed.*, 1990, **67**, 173.

87. A. T. Austin & J. Howard, *J. Chem. Soc.*, 1961, 3284.

88. Ref 76 p.237

89. S. Yamada, N. Oh-Hashi & K. A. Achiwa, *Tetrahedron Lett.*, 1976, **29**, 2557.

90. L. R. Smith & H. J. Williams, *J. Chem. Ed.*, 1979, **56**, 696.

91. R. E. Doolittle & R. R. Heath, *J. Org. Chem.*, 1984, **49**, 5041.

92. H. Sachs & E. Brand *J. Am. Chem. Soc.*, 1954, 76, 3601.

93. N. Lichtenstein, *J. Am. Chem. Soc.*, 1942, **64**, 1021.

94. A. T. Austin & J. Howard, *J. Chem. Soc.*, 1961, 3593.

95. A. T. Austin & J. Howard, *Chem. Ind.*, 1959, 1413.

96. E. Testa, L. Fontanella, G. F. Cristiani & L. Mariani, *Ann. Chem.*, 1961, **639**, 166.

97. B. C. Challis & J. Sandhu unpublished work.

98. C. D. Maycock & R. J. Stoodley, *J. Chem. Soc. Chem. Commun.*, 1976, 234.

99. C. D. Maycock & R. J. Stoodley, *J. Chem. Soc. Perkin Trans.I.*, 1979, 1852.

100. T. Ishibashi & T. Kawabata, *J. Agric. Food Chem.*, 1981, **29**, 1098.

101. P. D. Lawley in ref 2 p.183.

102. A. R. Olsen & R. J. Miller, *J. Am. Chem. Soc.*, 1938, **60**, 2687.

103. A. R. Olsen & J. L. Hyde, *J. Am. Chem. Soc.*, 1941, **63**, 2459.

104. F. A. Long & M. Purchase, *J. Am. Chem. Soc.*, 1950, **72** , 3267.

105. H. T. Liang & P. D. Bartlett, *J. Am. Chem. Soc.*, 1958, **80**, 3585.

106 T. L. Gresham, J. E. Jansen & F. W. Shaver, *J. Am. Chem. Soc.*, 1948, **70**, 998, 1001, 1003.

T. L. Gresham, J. E. Jansen, F. W. Shaver & J. T. Gregory, *Ibid*, 1948, **70**, 999.

T. L. Gresham, J. E. Jansen, F. W. Shaver, J. T. Gregory & W. L. Beears, *Ibid*, 1948, **70**, 1004.

T. L. Gresham, J. E. Jansen, F. W. Shaver, R. A. Bankert , W. L. Beears & M. G. Prendergast, *Ibid*, 1949, **71**, 661.

T. L. Gresham, J. E. Jansen, F. W. Shaver & R. A. Bankert, *Ibid*, 1949, **71**, 2807.

T. L. Gresham, J. E. Jansen & F. W. Shaver, *Ibid*, 1950, **72**, 72.

107. B. Pani, N. Baburdi, F. Bartoli-Klugmann, S. Venturini & I di Fant, *Mut. Res.*, 1980, **78**, 375.

108. S. Parodi, M. Picca, C. Bolognesi, M. Cavanna, P. Carlo, R. Finollo & G. Brambilla, *Pharmacol. Res. Commun.*, 1977, **9**, 621.

109. G. Brambilla, M. Cavanna, P. Carlo, R. Finollo, L. Sciaba, S. Parodi & C. Bolognesi, *J. Cancer Res. Clin. Oncol.*, 1979, **94**, 7.

110. G. Brambilla, M. Cavanna, S. Parodi & C. F. Caraceni, *Boll. Soc. Ital. Biol.* Sper., 1970, **46**, 227.

111 G.Brambilla, M. Cavanna, S. Parodi & L. Baldini, *Eur. J. Cancer* 1972, **8**, 127.

112. L. Baldini & G. Brambilla, *Cancer Res.*, 1966, **26**, 1754.

113. T. Giraldi, A. M. Guarino, C. Nisi & L. Baldini, *Eur. J. Cancer*, 1979, **15**, 603.

114. R. Catane, D. D. Von Hoff, D. L. Glaubiger & F. M. Muggia, *Cancer Treat. Rep.*, 1979, **63**, 1033.

115. Colburn & R. K. Boutwell, *Cancer Res.*, 1966, **26**, 1701.

116. F. Dickens & H. E. H. Jones, *Brit. J. Cancer*, 1961, **15**, 85.

117. P.J.C.M. Janssen & C.A. van der Heijden, *Toxicol.*, 1988, **50**, 1

118. The Guardian, Friday 20th July 1990.

119. I. Meier, S. E. Shephard & W. K. Lutz, *Mut. Res.*, 1990, **238**, 193.

120. S. E. Shephard, M. E. Hegi & W. K. Lutz, in ref 7 p.232.

121. D. L. H. Williams, *J. Chem. Soc. Perkin Trans. II*, 128, 1977.

122. R. A. Robinson & R. H. Stokes, "Electrolyte Solutions", 2nd Edn. Butterworths, 1968.

123. M. A. Paul & F. A. Long, *Chem. Rev.*, 1957, **57**, 1.

124. D. E. Nitecki, B. Halpern & J. W. Westley, *J. Org. Chem.*, 1968, **33**, 864.

125. P. B. Dews, *Fd. Chem. Toxicol.*, 1987, **25**, 549.

126. A. A. Frost & R. G. Pearson, "Kinetics and Mechanism. The Study of Homogenous Chemical Reactions." 2nd Edn.,J. Wiley and Sons, London, 1961, p170

127. D. D. Perrin, "Dissociation Constants of Organic Bases in Aqueous Solution " Butterworths, London, 1965

128. C. G. Swain & C. B. Scott, *J. Am. Chem. Soc.*, 1953, **75**, 141.

129. P. D. Bartlett & G. Small Jr., *J. Am. Chem. Soc.*, 1950, **72**, 4867.

130. A. A. van Zealand, *Mutagenesis*, 1988, **3**, 179.

131. J. A. Oppermann, "Aspartame Physiology and Biochemistry", Eds. L. D. Steginh & L. T. Filer Jr., Marcel Dekker , N.Y. 1984, p.141.

132. D. M. Matthews in Ref 131 p.43.

133. H. Bartsch, B. Terracini, C. Malaveille, L. Tomatis, J. Wahrendorf, G. Brun & B. Dodet, *Mut. Res.*, 1983, **110**, 187.

134. A. Barbin & H. Bartsch, *Mut. Res.*, 1989, **215**, 95.

135. G. W. Vogel, *Carcinogenesis*, 1989, **10**, 2093.

136. A. J. Kirby,"Comprehensive Chemical Kinetics", Volume10, Eds. C. H. Bamford & C. F. H. Tipper, Elsevier, London, 1972, p153

137. E. Sondheimer & R. W. Holley, *J. Am. Chem. Soc.*, 1954, **76**, 2467.

138. E. Sondheimer & R. W. Holley, *J. Am. Chem. Soc.*, 1954, **76**, 2816.

139. M. B. Shinn, *Ind. Eng. Chem. Analyt.*, 1941, **13**, 33.

140. "C. R. C. Handbook of Biochemistry", 3rd Edition, Cleveland Rubber Co., Ohio

141. W. J. Albery, A. N. Campbell-Crawford & K. S. Hobbs, *J. Chem. Soc., Perkin Trans. II*, 1972, 2180.

142. H. Dahn & M. Ballenegger, *Helv. Chim. Acta.*, 1969, **52**, 2417.

143. W. J. Albery, J. S. Corran & A. N. Campbell-Crawford, *J. Chem. Soc. Perkin Trans. II*, 1972, 2185.

144. L. Birkofer & J. Schramm, *Ann. Chem.*, 1975, 2195.

145. T. N. Salzmann, R. W. Ratcliffe, B.G. Christensen & F. A. Booffard, *J. Am. Chem. Soc.*, 1980, **102**, 6161.

146. B. G. Christensen, T. N. Salzmann & R. W. Ratcliffe, *Eurpat 0 007 973.*

147. L. Zervas, M. Winitz & J. P. Greenstein, *J. Org. Chem.*, 1957, **22**, 1515.

148. Ref. 126, p166

149. S. J. Leach & H. Lindley, *Trans. Faraday Soc.*, 1953, **49**, 915.

150. F. J. Kezdy, J. Jaz & A. Bruylants, *Bull. Soc. Chim. Belg.*, 1958, **67**, 687.

151. B. C. Challis, J. N. Iley, H. S. Rzepa, *J. Chem. Soc., Perkin Trans II*, 1983, 1037.

152. N. Kornblum & G. P. Coffey, *J. Org. Chem.*, 1966, **31**, 3447.

153. 'For a comprehnsive review see The Peptides Analysis, Synthesis, Biology' Volume I, Ed. C. Gross & J. Meienhofer, Academic Press Inc. 1979.

154. T. Shioik, K. Ninomiya & S. Yamada, *J. Am. Chem. Soc.*, 1972, **94**, 6203.

155. F. Latif, PhD Thesis, London, 1986.

156. D. H. Rich & J. Singh, Ref. 153, p251.

157. M. Bodanszky & V. du Vigneaud, *J. Am. Chem. Soc.*, 1959, **81**, 5688.

158. D. E. Nitecki, B. Halpern & J. W. Westley, *J. Org. Chem.* 1968, **33**, 864.

159. A. I. Vogel, "A Textbook of Practical Organic Chemistry Including Qualitative Organic Analysis", 3rd Edn., Longman, London, 1970, p971

160. J. A. Elvidge & P. G. Sammes, "A Course in Modern Techniques of Organic Chemistry", 2nd Edn., Butterworths, London, 1966, p138

161. J. P. Greenstein & M. Winitz, "Chemistry of the Amino Acids", Volume 2, R. E. Kreiger, Florida, 1984, p890

162. S. J. Leach & H. Lindley, *Austral. J. Chem.*, 1954, **7**, 173.